5-2015

An Optimization-Based Approach to Decoupling Fluid-Structure Interaction

Paul Allen Kuberry
Clemson University

An Optimization-Based Approach to Decoupling Fluid-Structure Interaction

---

A Dissertation
Presented to
the Graduate School of
Clemson University

In Partial Fulfillment
of the Requirements for the Degree
Doctor of Philosophy
Mathematical Sciences

---

by
Paul Allen Kuberry
May 2015

Accepted by:
Dr. Hyesuk Lee, Committee Chair
Dr. Leo Rebholz
Dr. Eleanor Jenkins
Dr. Timo Heister

Abstract

Fluid-structure interaction (FSI) is ubiquitous in both manufacturing and nature. At the same time, models describing this phenomenon are highly sensitive and nonlinear. Providing an analytical solution to these models for a realistic set of initial and boundary conditions has proven to be intractable.

Within the domain of computational simulation, significant effort has been invested in developing numerical methods to approximate solutions using these models. Current efforts to date have included monolithic and partitioned schemes.

In this dissertation, a novel partitioned approach is detailed in the context of Galerkin finite elements using body fitted meshes. It capitalizes upon the continuity of traction force on the interface shared between fluid and structure subdomains. Introducing a Neumann control in lieu of this shared traction force, the problem is decoupled and permits solving fluid and structure subproblems both independently and simultaneously.

Analytical results are provided which uniformly bound and demonstrate the existence of an optimal virtual control for the decoupled weak form of the fluid-structure interaction model. The existence of Lagrange multipliers is proven using the derivation of the Fréchet derivative of the operator occurring in the state equations. Discrete solutions to the resulting optimality system are proven to converge over a single time step using the theory from Brezzi, Rappaz, and Raviart. A steepest descent method is applied to the discrete system of equations and proven to converge under certain conditions.

This work provides a theoretical foundation for the application of optimization-based decoupling to fluid-structure interaction. For problems with moderate domain deformation, this method has been demonstrated to converge at optimal rates and to be competitive against state of the art methods for numerically solving fluid-structure interaction.

Table of Contents

List of Tables

List of Figures

Chapter 1

INTRODUCTION

Modeling fluid-structure interaction (FSI) problems is of great practical importance for many applications in manufacturing, energy, aeroelasticity, defense, and biology [10, 16, 20, 22, 40, 43, 48, 51, 57, 61, 64]. A few concrete examples in which fluid-structure interactions play an important role are piezoelastic print heads used in some models of inkjet printers, the design of blades for wind turbines, wing design for airplanes, combustion chambers in engines, offshore oil rigs, and blood flow through vessels or arteries.

Fluid-structure interaction problems are multiphysics problems with governing equations that are coupled through the condition of continuity of traction force and velocity on the interface. For all but the strongest assumptions, namely negligible displacement, and most basic initial and boundary conditions, the FSI operators are too complex to admit tractable analytical solutions. However, in recent decades there has been success in simulating FSI numerically [11]. Numerical simulation of this phenomenon is not without difficulty. There is a tight coupling between the fluid and structure subsystems, which makes numerical simulations difficult to perform. As the fluid exerts force onto the structure, the traction forces must balance on the shared interface, which generally results in some movement of the structure. Again, this exerts force on the fluid. The result is that the computational domains are deforming in time and in a way that is implicitly determined by the fluid and structure states.

The limitations of computational simulation are most evident in the simulating of the flow of blood through an artery. In order to correctly capture the flow, it is necessary to use a patient's own geometry, which requires three dimensional modeling. In order to reduce the computational workload needed, it is of particular importance that methods for solving FSI problems significantly reduce the number of iterations as well as the complexity of solves at each time step.

There are a wide variety of methods for simulating the coupled FSI system, but each is limited by factors including computational complexity and stability. One class of approaches are monolithic formulations enforcing the interface conditions while simultaneously solving both subproblems in a single matrix system [6, 42, 45, 67]. The other class of approaches are partitioned methods, solving each subproblem separately while finding and transferring boundary conditions. Fluid-structure interaction is multidisciplinary in the sense that the governing equations in the fluid subdomain involve the domain knowledge of experts in computational fluid dynamics, while the governing equations in the structure subdomain involve the domain knowledge of experts in continuum mechanics. Partitioned approaches permit the use of specialized fluid and structure solvers utilizing domain specific knowledge, which is attractive because they are generally easier to implement and allow the use of legacy codes [21, 25].

Solving an FSI problem using a monolithic formulation of the problem [67] is computationally complex due to requiring many large matrix solves to converge on a solution to the nonlinear system. Additional difficulties with this method include the development of efficient and appropriate preconditioners for the matrix resulting from the discretized system, although this is currently an active area of research [9, 33, 68].

The most common approaches decouple the fluid and structure subsystems, which allows for operations on a smaller matrix for each subsystem solve. In order to use existing fluid or structure solvers as-is or slightly modified to solve each subproblem, an effective approach must cleverly enforce the interface conditions so as to quickly converge upon an accurate solution. How and which interface conditions are enforced will have wide-

ranging effects on stability, speed, and accuracy of the algorithm. For a partitioned method, there are many options for how to transmit boundary condition information back and forth between the two subsystems. A strategy for the transmission of boundary conditions, such as Dirichlet–Neumann [62] (see Figure 1.1), can be either explicit or implicit, depending on the condition for proceeding to the next time step. If only a few iterations between subsystems are allowed, then the method is explicit. If the approach iterates between subsystems until the interface conditions are satisfied to within some tolerance, then the method is said to be implicit. The Dirichlet–Neumann iterations [49] will be used for comparison in the numerical results sections of this thesis.

Explicit decoupling approaches have the potential to be computationally efficient, particularly in cases where the densities between the fluid and structure differ greatly. For areas where there are large differences in densities of the subsystems, such as aerospace engineering, there has been much success applying explicit methods to numerical simulation of FSI. Two possible trade-offs are accuracy and stability. It has been shown that when densities of the subsystems are close, explicit sequentially staggered approaches fail outright and even implicit staggered methods may become unstable [54] due to the added mass effect [21,30,34]. One stabilized explicit method uses a formulation based on Nitsche's method and penalizes spurious pressure oscillations through the time penalty term on the fluid pressure fluctuations [19]. Counterintuitively, this added mass effect is only exacerbated by decreasing the time step size. For blood flow modeling, often the density of the vessel and fluid are nearly identical and the added mass effect is significant.

Implicit decoupling approaches vary widely in how they attempt to enforce interface conditions. The most common approaches are sequentially staggered in that they pass boundary conditions back and forth between subproblems. Generally, many nonlinear subsystem solves are required and even then stability can not be guaranteed [54]. By relaxing the update to the structure solve in each implicit iteration [21, 49], stability can be achieved. There are methods for dynamically changing the relaxation parameter in order to speed up convergence [34]. The largest problem with using relaxation schemes is that

the closer the two densities are in magnitude, the greater the increase in computational complexity because of the additional nonlinear subsystem solves needed. However, this is still an improvement over the divergence of the algorithm.

As a strong competitor among implicit methods, modified Robin-type boundary conditions have recently been used to increase stability and decrease iterations between subsystems [5].

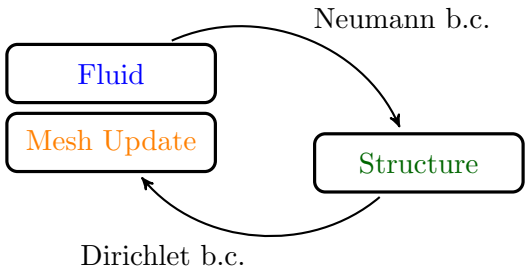

Figure 1.1: Dirichlet–Neumann coupling

All methods presented thus far were designed with finite elements in mind, although there may be extensions to finite volume or finite difference methods possible. However, the Immersed Boundary Method (IBM) [60], the Immersed Interface Method (IIM) [53], and variants of these make use of finite differences for solving FSI problems on a fixed uniform cartesian grid with an immersed interface that uses Dirac delta functions to integrate the force exerted by the structure on the fluid. As this family of methods are based on finite differences, their order of convergence is low. The IBM is first order accurate and the IIM is second order accurate. Recently, an adaptation of the IBM has been made so that finite elements may be used instead of finite differences [14]. These methods are not as general, since both the IBM or IIM treat the immersed structure as a fiber, rather than a multidimensional object. Advantages exist for these methods in applications where the forcing terms are derived from particle methods, since the Cartesian fluid domain is fully Eulerian and does not move, making the mapping of particles to cells particularly straight forward.

We are additionally motivated to develop algorithms for finite elements since en-

gineering disciplines are familiar with using finite element methods for solving structural mechanics problems from a Lagrangian framework. This is largely due to its ability to handle complex geometry with high order accuracy. Also, the finite element method lends itself well to analyzing stability and convergence.

A partitioned approach based on optimization is introduced in this thesis that provides a stable, accurate, and efficient method for decoupling fluid-structure interaction problems in the finite element setting. It is not specific to any particular fluid and structure combination, but will allow for solving the fluid and structure subproblems in parallel. The algorithm will be presented in the context of solving a Newtonian incompressible fluid coupled with a linear and nonlinear elastic solid.

The method works by treating the FSI system as a constrained optimal control problem in which the objective is to minimize the difference between the fluid velocity and the structure velocity on the interface. Minimizing the objective is equivalent to enforcing continuity between these velocities. Two different definitions of this control will be used. The definition used in Chapters 4–5 will nearly enforce continuity of stress along the interface and will enforce it for an optimal solution but also will allow for additional analytic properties needed to show the existence of an optimal solution. The one found in Chapter 3 and 6 will enforce continuity of stress for any choice of the control.

Although this method uses partitioned solves, it is implicit and stable. It *avoids* the large number of iterations generally required in other partitioned methods, since a single control is used for both subsystems simultaneously (see Figure 1.2), rather than iterating back and forth between subsystems.

Our approach is inspired by domain decomposition methods that have been explored by Gunzburger and Lee in [39] for solving the Navier–Stokes equations. In their approach, the computational domain is split into two subdomains using an artificial interface and a subproblem of the same governing equations is solved on each subdomain. The stress between the two subsystems is prescribed and updated through Gauss–Newton iterations so that it minimizes the discontinuity of the fluid velocity on the artificial interface. Similarly,

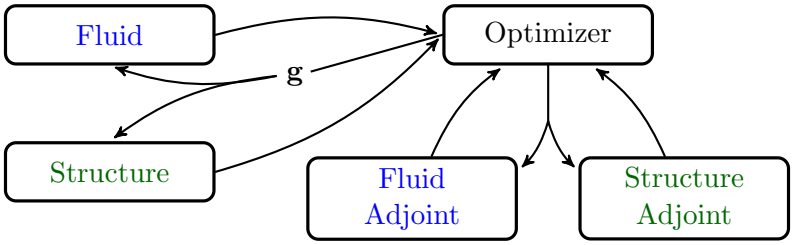

Figure 1.2: Optimization-based approach

in [28], this idea was used for the Stokes–Darcy equations. Because the stress is prescribed for the fluid and structure subsystem as a Neumann boundary condition, both subsystem solves may be made in parallel. In our adaptation of the algorithm, the interface will no longer be artificial, but rather the natural interface between the two subdomains, each having their own respective governing equations.

The use of constrained optimization for FSI has been implemented by Murea and Sy [54] for both a linear and nonlinear elastic formulation for the structure. However, in their approach for the linear formulation, they expand a function along the interface by its eigenfunctions and solve for coefficients to the inner product by use of optimization. This allows them to optimize a smaller number of unknowns. They use the stress on the interface as a Neumann control for solving the structure subsystem. Then, enforcing continuity of velocity through a Dirichlet boundary condition for the fluid subsystem, they update the control and repeat the process until the stress discontinuity on the interface is sufficiently small. This process requires that the subsystem solves must be made in serial and is still sequentially staggered. In their implementation, the Broyden–Fletcher–Goldfarb–Shanno (BFGS) algorithm is used to numerically optimize over the control space.

Our method differs from that of Murea and Sy in several important ways. First and foremost, our method is not sequentially staggered and both of our subsystems may be solved for simultaneously in the state, linearized, and adjoint equations. Second, we use the analytically linearized form of the state subsystem operators that would appear in solving the nonlinear state equations using Newton's method, rather than building a Hessian

numerically. This allows us to update our control by repeatedly solving linear problems. Lastly, by using Gauss–Newton iterations, few nonlinear state solves are necessary at each time step.

There is an impetus to provide a mathematical framework for non-Newtonian fluid interaction with an elastic medium, both having domains of the same dimension. The progress made in this thesis towards providing this framework for Newtonian fluids can be used as a template for non-Newtonian fluids. We intend to use the approach by constrained optimization to provide a robust foundation for numerical approximation of these problems. Improved numerical algorithms with a firm mathematical basis will benefit biomedical and polymer industries and help to improve health care outcomes.

This thesis is organized as follows. Part 1 deals with a fluid modeled by Navier–Stokes in contact with a linear elastic structure. In Chapter 2, the FSI model equations for a Newtonian fluid with linear elasticity are introduced in their strong form. After defining the notation that will be used throughout the rest of this thesis as well as some important properties of operators that are later referenced, the Arbitrary Lagrangian–Eulerian framework is introduced. The fully continuous variational formulation of the FSI problem is recast in the Arbitrary Lagrangian–Eulerian framework, and then discretized in time. This chapter will provide a starting point for the application of an optimization-based decoupling algorithm.

Chapter 3 begins by introducing a control into the semi-discretized weak form of the FSI problem, and then reformulating the monolithic FSI as a constrained optimization problem. The jump in velocities of the two substructures is minimized by a Neumann control enforcing the continuity of stress on the interface. A decoupling optimization algorithm is discussed, which requires few nonlinear solves at each time step. Numerical results are presented for a haemodynamic problem with parameters congruous with blood flow in a human artery. Additionally, results are given for a manufactured solution on a fixed domain with nonnegligible velocities on the interface.

In Chapter 4, a control is again introduced to the semi-discretized weak form of the

FSI problem, but two additional terms are absorbed by the control. Through the introduction of the augmented control, stability analysis for the fluid and structure subproblems becomes possible. Proofs for the stability and existence of optimal solutions for the previously presented functional minimizing the jump in velocities on the interface are given. A proof is given showing that as the Tikhonov regularization parameter goes to zero, the sequence of optimal controls converge on a solution to the fully coupled problem with interface conditions satisfied within a tolerance dependent on time step. Lagrange multipliers are shown to exist and an optimality system is derived. Using the necessary condition from the optimality system to update the control, the steepest descent approach is used to provide numerical results using the augmented control.

The Brezzi–Rappaz–Raviart theorem is applied in Chapter 5 to prove the convergence of solutions of the discrete optimality system to a solution of the continuous optimality system over a single time step. The approximation error due to spatial discretization is rigorously proven. Attention is again focused on the steepest descent method, and a proof is given outlining certain assumptions that must be satisfied to ensure convergence of the algorithm. The manufactured solution from Chapter 3 is again revisited with a view to demonstrating the theoretical convergence rate over a single time step. Next, the Gauss–Newton with conjugate gradient algorithm described in Chapter 3 is applied to the same problem over many time steps.

With a view to applying the optimization-based decoupling algorithm to more challenging and realistic applications, Part 2, Chapter 6 introduces the nonlinear elastic St. Venant–Kirchhoff model for the structure in contact with a Newtonian fluid again modeled by the Navier–Stokes equations. The strong form of the FSI equations are presented along with a derivation of the nonlinear elastic operator on a fixed domain using the Piola transform. The fluid is recast in the Arbitrary Lagrangian–Eulerian framework and discretized in time. The semi-discretized weak form of the FSI problem is then linearized. This linearization of the state operators are then applied to Gauss–Newton outer optimization loops with BiCGstab and GMRES performing the inner optimization loops. Numerical solutions are

presented to a haemodynamic problem having the same parameters as in Chapter 3, but with more realistic physics modeling the structure. A conclusion is given summarizing the results of this thesis and detailing areas that still need attention.

Part I

Navier–Stokes / Linear Elasticity

Chapter 2

MODEL EQUATIONS, NOTATION, AND FRAMEWORK

2.1 Model Equations

2.1.1 Navier–Stokes / Linear Elastic Model

The fluid-structure interaction that we will consider in the first part of this work is an incompressible Newtonian fluid and an isotropic linear elastic structure.

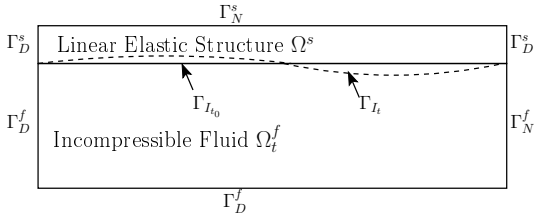

Figure 2.1: Fluid-structure interaction domain

Let Ω^f_t be a bounded moving fluid domain at time t in $\mathbb{R}^2$ with the boundary Γ^f_t such that $\Gamma^f_t = \Gamma^f_N \cup \Gamma^f_D \cup \Gamma_{I_t}$, where Γ_{I_t} is a moving boundary. Also let Ω^s be a fixed

structure domain with the boundary Γ^s such that $\Gamma^s = \Gamma^s_N \cup \Gamma^s_D \cup \Gamma_{I_{t_0}}$, where $\Gamma_{I_{t_0}}$ is the movable fluid boundary at time t_0. Consider the system of fluid and structure equations

$$\rho_f \left[\frac{\partial \mathbf{u}}{\partial t} + \mathbf{u} \cdot \nabla \mathbf{u} \right] - 2\nu_f \nabla \cdot D(\mathbf{u}) + \nabla p = \mathbf{f}_f \quad \text{in } \Omega^f_t \,, \tag{2.1}$$

$$\nabla \cdot \mathbf{u} = 0 \quad \text{in } \Omega^f_t \,, \tag{2.2}$$

$$\rho_s \frac{\partial^2 \boldsymbol{\eta}}{\partial t^2} - 2\nu_s \nabla \cdot D(\boldsymbol{\eta}) - \lambda \nabla (\nabla \cdot \boldsymbol{\eta}) = \mathbf{f}_s \quad \text{in } \Omega^s \,, \tag{2.3}$$

where $\mathbf{u}$ denotes the velocity vector of fluid, p the pressure of fluid, ρ_f the density of the fluid, ν_f the fluid viscosity, $\boldsymbol{\eta}$ the displacement of structure, and ρ_s the structure density. In (2.1) and (2.3), $D(\cdot)$ is the rate of the strain tensor, i.e., $D(\mathbf{v}) := (\nabla \mathbf{v} + \nabla \mathbf{v}^T)/2$. The Lam*é* parameters are denoted by ν_s and λ, and the body forces are denoted by $\mathbf{f}_f$ and $\mathbf{f}_s$. Initial and boundary conditions for $\mathbf{u}$ and $\boldsymbol{\eta}$ are given as follows:

$$2\nu_f D(\mathbf{u})\mathbf{n}_f - p\mathbf{n}_f = \mathbf{u}_N \quad \text{on } \Gamma^f_N \,, \tag{2.4}$$

$$\mathbf{u} = \mathbf{u}_D \quad \text{on } \Gamma^f_D \,, \tag{2.5}$$

$$2\nu_s D(\boldsymbol{\eta})\mathbf{n}_s + \lambda(\nabla \cdot \boldsymbol{\eta})\mathbf{n}_s = \boldsymbol{\eta}_N \quad \text{on } \Gamma^s_N \,, \tag{2.6}$$

$$\boldsymbol{\eta} = \mathbf{0} \quad \text{on } \Gamma^s_D \,, \tag{2.7}$$

$$\mathbf{u}(\mathbf{x}, t_0) = \mathbf{u}^0 \quad \text{in } \Omega^f_{t_0} \,, \tag{2.8}$$

$$\boldsymbol{\eta}(\mathbf{x}, t_0) = \boldsymbol{\eta}^0 \quad \text{in } \Omega^s \,, \tag{2.9}$$

$$\boldsymbol{\eta}_t(\mathbf{x}, t_0) = \dot{\boldsymbol{\eta}}^0 \quad \text{in } \Omega^s \,, \tag{2.10}$$

where $\dot{\boldsymbol{\eta}}^0 = \mathbf{u}^0$ on $\Gamma_{I_{t_0}}$. For brevity, we use $\mathbf{u} = \mathbf{0}$ on Γ^f_D, but all of our results hold for the case where $\mathbf{u} = \mathbf{u}_D \neq \mathbf{0}$ on Γ^f_D with a simple modification. The moving boundary Γ_{I_t} is determined by the displacement $\boldsymbol{\eta}$ at time t (Fig. 2.1). The interface conditions between the fluid and the structure are obtained by enforcing continuity of the velocity and the

stress force:

$$\frac{\partial \boldsymbol{\eta}}{\partial t} = \mathbf{u} \quad \text{on } \Gamma_{I_t}\,, \tag{2.11}$$

$$[2\nu_f D(\mathbf{u}) - p\,\mathbf{I}]\cdot \mathbf{n}_f = -[2\nu_s D(\boldsymbol{\eta}) + \lambda(\nabla\cdot\boldsymbol{\eta})]\cdot \mathbf{n}_s \quad \text{on } \Gamma_{I_t}\,. \tag{2.12}$$

2.2 Notation

We use the Sobolev spaces $W^{m,p}(D)$ with norms $\|\cdot\|_{m,p,D}$ if $p<\infty$, $\|\cdot\|_{m,\infty,D}$ if $p=\infty$. Denote the Sobolev space $W^{m,2}$ by H^m with the norm $\|\cdot\|_{m,D}$. The corresponding space of vector-valued or tensor-valued functions is denoted by $\mathbf{H}^m$.

For the variational formulation of the flow equations (2.26)–(2.27) in the ALE framework, described in section 2.3, we define the function space for the reference domain:

$$\boldsymbol{H}^1_D(\Omega^f_{t_0}) := \{\mathbf{v}\in \mathbf{H}^1(\Omega^f_{t_0}) : \mathbf{v}=\mathbf{0} \text{ on } \Gamma^f_D\}\,.$$

The function spaces for Ω^f_t are then defined as

$$\boldsymbol{H}^1_D(\Omega^f_t) := \{\mathbf{v}:\Omega^f_t\times[t_0,T]\to\mathbb{R}^2,\ \mathbf{v}=\overline{\mathbf{v}}\circ\Psi_t^{-1} \text{ for } \overline{\mathbf{v}}\in \boldsymbol{H}^1_D(\Omega^f_{t_0})\}\,,$$
$$L^2(\Omega^f_t) := \{q:\Omega^f_t\times[t_0,T]\to\mathbb{R}\,,\ q=\overline{q}\circ\Psi_t^{-1} \text{ for } \overline{p}\in L^2(\Omega^f_{t_0})\}\,.$$

where Ψ_t^{-1} is the inverse ALE mapping described in section 2.3.
For the structure displacement $\boldsymbol{\eta}$, define the function space

$$\boldsymbol{H}^1_D(\Omega^s) := \{\boldsymbol{\xi}\in \mathbf{H}^1(\Omega^s) : \boldsymbol{\xi}=\mathbf{0} \text{ on } \Gamma^s_D\}\,.$$

We use $(\cdot,\cdot)_{\Omega^f_t}$, $(\cdot,\cdot)_{\Gamma_{I_t}}$, $(\cdot,\cdot)_{\Omega^s}$, and $(\cdot,\cdot)_{\Gamma_{I_{t_0}}}$ to denote the L^2 inner product over Ω^f_t, Γ_{I_t}, Ω^s, and $\Gamma_{I_{t_0}}$, respectively.

In the moving fluid domain, we define the bilinear and trilinear forms

$$a(\mathbf{u},\mathbf{v})_{\Omega_t^f} := \frac{1}{4}\int_{\Omega_t^f}(\nabla\mathbf{u}+(\nabla\mathbf{u})^T):(\nabla\mathbf{v}+(\nabla\mathbf{v})^T)\,d\Omega_t^f \quad \forall\,\mathbf{u},\mathbf{v}\in \boldsymbol{H}_D^1(\Omega_t^f),$$
$$b(\mathbf{v},q)_{\Omega_t^f} := -\int_{\Omega_t^f} q(\nabla\cdot\mathbf{v})\,d\Omega_t^f \quad \forall\,\mathbf{v}\in \boldsymbol{H}_D^1(\Omega_t^f),\ q\in L^2(\Omega_t^f),$$

and

$$c(\mathbf{u},\mathbf{v},\mathbf{w})_{\Omega_t^f} := \frac{1}{2}\int_{\Omega_t^f}\mathbf{u}\cdot\nabla\mathbf{v}\cdot\mathbf{w}-\mathbf{u}\cdot\nabla\mathbf{w}\cdot\mathbf{v}\quad d\Omega_t^f.$$

For the stationary structure domain, we define the bilinear forms

$$d(\boldsymbol{\eta},\boldsymbol{\gamma})_{\Omega^s} := \frac{1}{4}\int_{\Omega^s}(\nabla\boldsymbol{\eta}+(\nabla\boldsymbol{\eta})^T):(\nabla\boldsymbol{\gamma}+(\nabla\boldsymbol{\gamma})^T)\,d\Omega^s \quad \forall\,\boldsymbol{\eta},\boldsymbol{\gamma}\in \boldsymbol{H}_D^1(\Omega^s),$$

and

$$e(\boldsymbol{\eta},\boldsymbol{\gamma})_{\Omega^s} := \int_{\Omega^s}(\nabla\cdot\boldsymbol{\eta})(\nabla\cdot\boldsymbol{\gamma})\,d\Omega^s \quad \forall\,\boldsymbol{\eta},\boldsymbol{\gamma}\in \boldsymbol{H}_D^1(\Omega^s).$$

It is noteworthy that

$$c(\mathbf{u},\mathbf{v},\mathbf{v})_{\Omega_t^f}=0\ \ \forall\mathbf{u},\mathbf{v}\in\boldsymbol{H}_D^1(\Omega_t^f). \tag{2.13}$$

Throughout this thesis, C represents a positive constant independent of time. As is well known, $a(\cdot,\cdot)$, $b(\cdot,\cdot)$, $c(\cdot,\cdot,\cdot)$, and $d(\cdot,\cdot)$ are continuous and there exist constants

C_1, C_2, C_3, C_4 and C_5 such that

$$|a(\mathbf{u},\mathbf{v})_{\Omega_t^f}| \leq C_1 \|\mathbf{u}\|_{1,\Omega_t^f} \|\mathbf{v}\|_{1,\Omega_t^f} \quad \forall \mathbf{u},\mathbf{v} \in \boldsymbol{H}_D^1(\Omega_t^f), \tag{2.14}$$

$$|b(\mathbf{v},q)_{\Omega_t^f}| \leq C_2 \|\mathbf{v}\|_{1,\Omega_t^f} \|q\|_{0,\Omega_t^f} \quad \forall \mathbf{v} \in \boldsymbol{H}_D^1(\Omega_t^f),\ \ \forall q \in L^2(\Omega_{t_n}^f), \tag{2.15}$$

$$|c(\mathbf{u},\mathbf{v},\mathbf{w})_{\Omega_t^f}| \leq C_3 \|\mathbf{u}\|_{1,\Omega_t^f} \|\mathbf{v}\|_{1,\Omega_t^f} \|\mathbf{w}\|_{1,\Omega_t^f} \quad \forall \mathbf{u},\mathbf{v},\mathbf{w} \in \boldsymbol{H}_D^1(\Omega_t^f), \tag{2.16}$$

$$|d(\boldsymbol{\eta},\boldsymbol{\gamma})_{\Omega^s}| \leq C_4 \|\boldsymbol{\eta}\|_{1,\Omega^s} \|\boldsymbol{\gamma}\|_{1,\Omega^s} \quad \forall \boldsymbol{\eta},\boldsymbol{\gamma} \in \boldsymbol{H}_D^1(\Omega^s), \tag{2.17}$$

and

$$|e(\boldsymbol{\eta},\boldsymbol{\gamma})_{\Omega^s}| \leq C_5 \|\boldsymbol{\eta}\|_{1,\Omega^s} \|\boldsymbol{\gamma}\|_{1,\Omega^s} \quad \forall \boldsymbol{\eta},\boldsymbol{\gamma} \in \boldsymbol{H}_D^1(\Omega^s). \tag{2.18}$$

There exist positive coercivity constants C_6 and C_7 such that

$$a(\mathbf{u},\mathbf{u})_{\Omega_t^f} \geq C_6 \|\mathbf{u}\|_{1,\Omega_t^f}^2 \quad \forall \mathbf{u} \in \boldsymbol{H}_D^1(\Omega_t^f), \tag{2.19}$$

$$d(\boldsymbol{\eta},\boldsymbol{\eta})_{\Omega^s} \geq C_7 \|\boldsymbol{\eta}\|_{1,\Omega^s}^2 \quad \forall \boldsymbol{\eta} \in \boldsymbol{H}_D^1(\Omega^s), \tag{2.20}$$

and $b(\cdot,\cdot)$ has the inf-sup condition

$$\sup_{\mathbf{0}\neq\mathbf{v}\in\boldsymbol{H}_D^1(\Omega_t^f)} \frac{b(\mathbf{v},q)_{\Omega_t^f}}{\|\mathbf{v}\|_{1,\Omega_t^f}} \geq C_8 \|q\|_{0,\Omega_t^f} \quad \forall q \in L^2(\Omega_t^f) \tag{2.21}$$

where C_8 is a positive constant.

2.3 Arbitrary Lagrangian–Eulerian Framework

The Arbitrary Lagrangian–Eulerian (ALE) [26, 46] framework is the most widely used description of the fluid subproblem in finite element FSI simulation. In the ALE formulation, a one-to-one coordinate transformation is introduced for the fluid domain, and the fluid equations can be rewritten with respect to a moving domain which is Lagrangian on its boundaries and in between Lagrangian and Eulerian on its interior. Specifically, we define the time-dependent bijective mapping Ψ_t which maps the reference domain $\Omega_{t_0}^f$ to

the physical domain Ω_t^f:

$$\Psi_t : \Omega_{t_0}^f \to \Omega_t^f, \qquad \Psi_t(\mathbf{y}) = \mathbf{x}(\mathbf{y}, t)\,, \tag{2.22}$$

where $\mathbf{y}$ and $\mathbf{x}$ are the spatial coordinates in $\Omega_{t_0}^f$ and Ω_t^f, respectively.

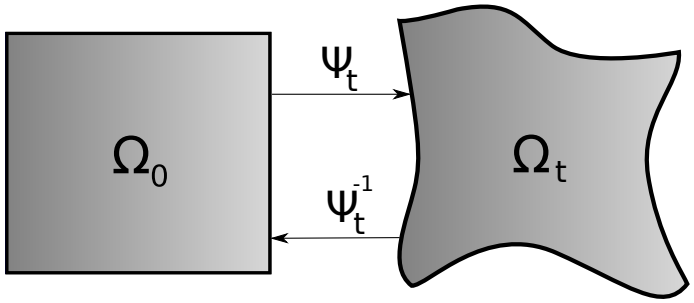

Figure 2.2: ALE coordinate transformation

The coordinate $\mathbf{y}$ is often called the *ALE coordinate*. Using Ψ_t, the weak formulation of the flow equations in Ω_t^f can be recast into a weak formulation defined in the reference domain $\Omega_{t_0}^f$. Thus, the model equations in the reference domain can be considered for numerical simulation and the transformation function Ψ_t needs to be determined at each time step as a part of computation.

For a function $\phi : \Omega_t^f \times [t_0, T] \to \mathbb{R}$, its corresponding function $\overline{\phi} = \phi \circ \Psi_t$ in the ALE setting is defined as

$$\overline{\phi} : \Omega_{t_0}^f \to \mathbb{R}, \qquad \overline{\phi}(\mathbf{y}, t) = \phi(\Psi_t(\mathbf{y}), t). \tag{2.23}$$

The time derivative in the ALE frame is also given as

$$\frac{\partial \phi}{\partial t}\,|_{\mathbf{y}} \colon \Omega_t^f \times [t_0, T] \to \mathbb{R}, \qquad \frac{\partial \phi}{\partial t}\,|_{\mathbf{y}}\,(\mathbf{x}, t) = \frac{\partial \overline{\phi}}{\partial t}(\mathbf{y}, t). \tag{2.24}$$

Using the chain rule, we have

$$\frac{\partial \phi}{\partial t}\,|_{\mathbf{y}} = \frac{\partial \phi}{\partial t}\,|_{\mathbf{x}} + \mathbf{z}\cdot\nabla_{\mathbf{x}}\phi, \tag{2.25}$$

where $\mathbf{z} := \frac{\partial \mathbf{x}}{\partial t}\,|_{\mathbf{y}}$ is the domain velocity. In (2.25) $\frac{\partial \phi}{\partial t}\,|_{\mathbf{y}}$ is the so-called *ALE derivative* of ϕ. The flow equations (2.1)–(2.2) can then be written in ALE formulation as

$$\rho_f\left[\frac{\partial \mathbf{u}}{\partial t}\,|_{\mathbf{y}} + (\mathbf{u}-\mathbf{z})\cdot\nabla_{\mathbf{x}}\mathbf{u}\right] - 2\nu_f\,\nabla_{\mathbf{x}}\cdot D_{\mathbf{x}}(\mathbf{u}) + \nabla_{\mathbf{x}}p = \mathbf{f}_f \quad \text{in } \Omega_t^f\,, \tag{2.26}$$

$$\nabla_{\mathbf{x}}\cdot\mathbf{u} = 0 \quad \text{in } \Omega_t^f\,, \tag{2.27}$$

where $D_{\mathbf{x}}(\mathbf{u}) = (\nabla_{\mathbf{x}}\mathbf{u} + \nabla_{\mathbf{x}}\mathbf{u}^T)/2$. Note that all spatial derivatives involved in (2.26)–(2.27), including the divergence operator, are with respect to $\mathbf{x}$. Throughout this thesis we will use $D_{\mathbf{x}}(\cdot)$ and $\nabla_{\mathbf{x}}$ only when they need to be clearly specified. Otherwise, $D(\cdot)$, ∇ will be used as $D_{\mathbf{x}}(\cdot)$, $\nabla_{\mathbf{x}}$, respectively.

The variational formulation for $(\mathbf{u}, p, \boldsymbol{\eta})$ in ALE framework is given by: for almost every $t \in [t_0, T]$, find $t \to \mathbf{u}(t) \in \boldsymbol{H}^1_D(\Omega_t^f)$, $t \to p(t) \in L^2(\Omega_t^f)$, and $t \to \boldsymbol{\eta}(t) \in \boldsymbol{H}^1_D(\Omega^s)$ such that

$$\begin{aligned}
&\rho_f\left(\frac{\partial \mathbf{u}}{\partial t}\,|_{\mathbf{y}} + (\mathbf{u}-\mathbf{z})\cdot\nabla\mathbf{u},\,\mathbf{v}\right)_{\Omega_t^f} + 2\nu_f a(\mathbf{u},\mathbf{v})_{\Omega_t^f} + b(\mathbf{v},p)_{\Omega_t^f} \\
&\qquad - (2\nu_f D(\mathbf{u})\cdot\mathbf{n}_f - p\mathbf{n}_f, \mathbf{v})_{\Gamma_{I_t}} \\
&\qquad = (\mathbf{f}_f,\mathbf{v})_{\Omega_t^f} + (\mathbf{u}_N,\mathbf{v})_{\Gamma_N^f}\ \forall \mathbf{v} \in \boldsymbol{H}^1_D(\Omega_t^f)\,, \qquad (2.28)\\
&b(\mathbf{u},q)_{\Omega_t^f} = 0 \quad \forall q \in L^2(\Omega_t^f)\,. \qquad (2.29)
\end{aligned}$$

and

$$\begin{aligned}
&\rho_s\left(\frac{\partial^2 \boldsymbol{\eta}}{\partial t^2},\,\boldsymbol{\xi}\right)_{\Omega^s} + 2\nu_s d(\boldsymbol{\eta},\boldsymbol{\xi})_{\Omega^s} + \lambda e(\boldsymbol{\eta},\boldsymbol{\xi})_{\Omega^s} \\
&\quad - (2\nu_s D(\boldsymbol{\eta})\cdot\mathbf{n}_s + \lambda(\nabla\cdot\boldsymbol{\eta})\mathbf{n}_s, \boldsymbol{\xi})_{\Gamma_{I_{t_0}}} = (\mathbf{f}_s,\boldsymbol{\xi})_{\Omega^s} + (\boldsymbol{\eta}_N,\boldsymbol{\xi})_{\Gamma_N^s}\ \forall \boldsymbol{\xi} \in \boldsymbol{H}^1_D(\Omega^s)\,, \qquad (2.30)
\end{aligned}$$

where the interface conditions (2.11)–(2.12) are imposed.

In order to define the ALE mapping Ψ_t, we consider the boundary position function $\mathbf{h} : \Gamma_{I_{t_0}} \times [t_0, T] \to \Gamma_{I_t}$. The ALE mapping can then determined by solving the Laplace equation

$$\begin{aligned} \Delta_{\mathbf{y}} \mathbf{x}(\mathbf{y}) &= 0 \qquad && \text{in } \Omega^f_{t_0}, \\ \mathbf{x}(\mathbf{y}) &= \mathbf{h}(\mathbf{y}, t) && \text{on } \Gamma_{I_{t_0}}, \\ \mathbf{x}(\mathbf{y}) &= 0 && \text{on } \Gamma^f_{t_0}/\Gamma_{I_{t_0}}. \end{aligned} \tag{2.31}$$

This method is called the *harmonic extension technique*, where the boundary position function $\mathbf{h}$ is extended onto the whole domain [56]. For a comparison of the harmonic extension with other extensions of $\mathbf{h}$ onto $\Omega^f_{t_0}$, see [66].

The Reynolds Transport formula is given by

$$\frac{d}{dt} \int_{V(t)} \boldsymbol{\phi}(\mathbf{x}, t)\, dV = \int_{V(t)} \frac{\partial \boldsymbol{\phi}}{\partial t} \,|_{\mathbf{y}} + \boldsymbol{\phi} \nabla_{\mathbf{x}} \cdot \mathbf{z}\, dV \tag{2.32}$$

for a function $\boldsymbol{\phi} : V(t) \to \mathbb{R}$, where $V(t) \subset \Omega^f_t$ such that $V(t) = \Psi_t(V_0)$ with $V_0 \subset \Omega^f_{t_0}$ [58]. Applying the Reynold's Transport formula with $\boldsymbol{\phi} = \mathbf{v}$, noting that $\mathbf{v}$ is a function from Ω^f_t to $\mathbb{R}$, and $\mathbf{v} = \overline{\mathbf{v}} \circ \Psi_t^{-1}$ for $\overline{\mathbf{v}} : \Omega^f_{t_0} \to \mathbb{R}$, we have that $\frac{\partial \mathbf{v}}{\partial t}|_{\mathbf{y}} = 0$ and therefore

$$\frac{d}{dt} \int_{\Omega^f_t} \boldsymbol{\phi} \mathbf{v}\, d\Omega = \int_{\Omega^f_t} \left[\frac{\partial \boldsymbol{\phi}}{\partial t} \,|_{\mathbf{y}} + \boldsymbol{\phi} \nabla_{\mathbf{x}} \cdot \mathbf{z} \right] \mathbf{v}\, d\Omega. \tag{2.33}$$

Using (2.33), (2.28)–(2.29) become

$$\begin{aligned} \rho_f \left[\frac{d}{dt} (\mathbf{u},\, \mathbf{v})_{\Omega^f_t} + ((\mathbf{u} - \mathbf{z}) \cdot \nabla \mathbf{u},\, \mathbf{v})_{\Omega^f_t} - ((\nabla \cdot \mathbf{z})\mathbf{u}, \mathbf{v})_{\Omega^f_t} \right] + 2\nu_f a(\mathbf{u}, \mathbf{v})_{\Omega^f_t} \\ + b(\mathbf{v}, p)_{\Omega^f_t} - (2\nu_f D(\mathbf{u}) \cdot \mathbf{n}_f - p\mathbf{n}_f, \mathbf{v})_{\Gamma_{I_t}} \\ = (\mathbf{f}_f, \mathbf{v})_{\Omega^f_t} + (\mathbf{u}_N, \mathbf{v})_{\Gamma^f_N} \ \forall \mathbf{v} \in \boldsymbol{H}^1_D(\Omega^f_t)\,, \end{aligned} \tag{2.34}$$

$$b(\mathbf{u}, q)_{\Omega^f_t} = 0 \quad \forall q \in L^2(\Omega^f_t)\,. \tag{2.35}$$

2.4 Semidiscrete Weak Formulations

We will implicitly define $\mathcal{V}(\cdot)$ in the following way:

$$(\mathbf{f}, \mathcal{V}(\mathbf{v}))_{\Omega^f_{t_j}} = (\mathbf{f}, \mathbf{v} \circ \Psi_{t_i} \circ \Psi^{-1}_{t_j})_{\Omega^f_{t_j}}, \ (\mathbf{f}, \mathcal{V}(\mathbf{v}))_{\Gamma_{I_{t_j}}} = (\mathbf{f}, \mathbf{v} \circ \Psi_{t_i} \circ \Psi^{-1}_{t_j})_{\Gamma_{I_{t_j}}},$$

where $\mathbf{f}$ is a function defined on the domain $\Omega^f_{t_j}$ (or $\Gamma_{I_{t_j}}$) and $\mathbf{v}$ is a function defined on the domain $\Omega^f_{t_i}$ (or $\Gamma_{I_{t_i}}$).

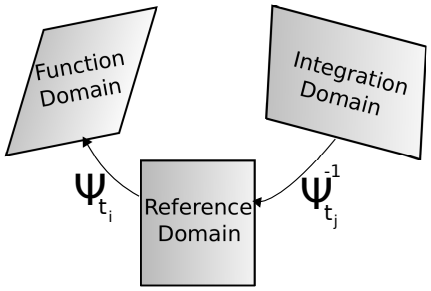

Figure 2.3: Action of the $\mathcal{V}(\cdot)$ operator

In order to semidiscretize the continuous weak form of the FSI problem, let us first define

$$\Psi_t(\mathbf{y}) = \frac{t - t_{n-1}}{\Delta t}\Psi_{t_n}(\mathbf{y}) + \frac{t_n - t}{\Delta t}\Psi_{t_{n-1}}(\mathbf{y}) \ \forall t \in [t_{n-1}, t_n]. \tag{2.36}$$

as in [15], where $\Psi_{t_{n-1}}$ and Ψ_{t_n} are the harmonic extensions onto $\Omega^f_{t_0}$ of $\boldsymbol{\eta}^{n-1}|_{\Gamma_{I_{t_0}}}$ and $\boldsymbol{\eta}^n|_{\Gamma_{I_{t_0}}}$, respectively. Here, $\boldsymbol{\eta}^{n-1}$ and $\boldsymbol{\eta}^n$ are the time discretized displacement solutions to (2.38)–(2.41). Also, note that as a consequence of (2.36),

$$\mathbf{z} := \frac{\partial \Psi_t}{\partial t} \circ \Psi_t^{-1} = \left[\frac{\Psi_{t_n} - \Psi_{t_{n-1}}}{\Delta t}\right] \circ \Psi_t^{-1} \ \forall \ t \in]t_{n-1}, t_n]. \tag{2.37}$$

In other words, $\mathbf{z}^n = \mathbf{z}(t_n)$ is the mesh velocity at time step t_n and for all times $t \in]t_{n-1}, t_n]$. Let us denote $J_t(\mathbf{y}) := \det[\frac{\partial}{\partial \mathbf{y}}\Psi_t(\mathbf{y})]$. In Chapter 4, we will make assumptions (4.14) and (4.15), as in [15], that gives J_t bounded below by a positive constant κ_{min} and above by a constant κ_{max}, for all $t \in [t_0, T]$. For further information on the mapping regularity

condition, see [55, pp. 19–21].

The mesh velocity $\mathbf{z}^n$, the two domain displacements Ψ_{t_n} and $\Psi_{t_{n-1}}$, and the deformation gradient of the moving fluid domain are all at least implicitly defined by $\boldsymbol{\eta}^n$ and $\boldsymbol{\eta}^{n-1}$. While $\boldsymbol{\eta}^n$ is an unknown we are solving for at time t_n, we will treat all of its descendants as fixed and known in order to make analysis of the problem tractable.

Temporal discretization of the fluid subsystem (2.34)–(2.35) by implicit Euler and of the structure subsystem (2.30) by a second order midpoint scheme yields: find $(\mathbf{u}^n, p^n, \boldsymbol{\eta}^n, \dot{\boldsymbol{\eta}}^n) \in \boldsymbol{H}^1_D(\Omega^f_{t_n}) \times L^2(\Omega^f_{t_n}) \times \boldsymbol{H}^1_D(\Omega^s) \times \mathbf{L}^2(\Omega^s)$ such that

$$\begin{aligned}\rho_f \left[(\mathbf{u}^n, \mathbf{v})_{\Omega^f_{t_n}} - (\mathbf{u}^{n-1}, \mathcal{V}(\mathbf{v}))_{\Omega^f_{t_{n-1}}}\right] &+ \Delta t\, \rho_f \left[((\mathbf{u}^n - \mathbf{z}^n)\cdot\nabla\mathbf{u}^n, \mathbf{v})_{\Omega^f_{t_n}} - ((\nabla\cdot\mathbf{z}^n)\mathbf{u}^n, \mathbf{v})_{\Omega^f_{t_n}}\right] \\ &+ \Delta t \left[2\nu_f a(\mathbf{u}^n, \mathbf{v})_{\Omega^f_{t_n}} + b(\mathbf{v}, p^n)_{\Omega^f_{t_n}}\right] \\ &- \Delta t\, (2\nu_f D(\mathbf{u}^n)\cdot\mathbf{n}_f - p^n\mathbf{n}_f, \mathbf{v})_{\Gamma_{I_t}} \\ &= \Delta t \left[(\mathbf{f}^n_f, \mathbf{v})_{\Omega^f_{t_n}} + (\mathbf{u}^n_N, \mathbf{v})_{\Gamma^f_N}\right] \;\; \forall \mathbf{v} \in \boldsymbol{H}^1_D(\Omega^f_{t_n})\,, \end{aligned} \tag{2.38}$$

$$b(\mathbf{u}^n, q)_{\Omega^f_{t_n}} = 0 \quad \forall q \in L^2(\Omega^f_{t_n})\,, \tag{2.39}$$

and

$$\begin{aligned}\rho_s \left(\dot{\boldsymbol{\eta}}^n - \dot{\boldsymbol{\eta}}^{n-1}, \boldsymbol{\xi}\right)_{\Omega^s} &\\ + \Delta t \left[\nu_s d\left(\boldsymbol{\eta}^n + \boldsymbol{\eta}^{n-1}, \boldsymbol{\xi}\right)_{\Omega^s} + \frac{\lambda}{2} e\left(\boldsymbol{\eta}^n + \boldsymbol{\eta}^{n-1}, \boldsymbol{\xi}\right)_{\Omega^s}\right] &\\ - \Delta t \left(\nu_s \left(D(\boldsymbol{\eta}^n + \boldsymbol{\eta}^{n-1})\cdot\mathbf{n}_s\right) + \frac{\lambda}{2}\left(\nabla\cdot\left(\boldsymbol{\eta}^n + \boldsymbol{\eta}^{n-1}\right)\right)\mathbf{n}_s, \boldsymbol{\xi}\right)_{\Gamma_{I_{t_0}}} &\\ = \frac{\Delta t}{2}\left[\left(\mathbf{f}^n_s + \mathbf{f}^{n-1}_s, \boldsymbol{\xi}\right)_{\Omega^s} + \left(\boldsymbol{\eta}^n_N + \boldsymbol{\eta}^{n-1}_N, \boldsymbol{\xi}\right)_{\Gamma^s_N}\right] \forall \boldsymbol{\xi} \in \boldsymbol{H}^1_D(\Omega^s)\,, \end{aligned} \tag{2.40}$$

$$\frac{\Delta t}{2}\left(\dot{\boldsymbol{\eta}}^n + \dot{\boldsymbol{\eta}}^{n-1}, \boldsymbol{\gamma}\right)_{\Omega^s} = \left(\boldsymbol{\eta}^n - \boldsymbol{\eta}^{n-1}, \boldsymbol{\gamma}\right)_{\Omega^s} \;\forall \boldsymbol{\gamma} \in \boldsymbol{L}^2(\Omega^s)\,. \tag{2.41}$$

This formulation will be considered in Chapters 3, 4, and 5.

Also, a first order time discretization of the structure problem is given by

$$\begin{aligned}
\rho_s \left(\boldsymbol{\eta}^n \right. & -2\boldsymbol{\eta}^{n-1} + \boldsymbol{\eta}^{n-2}, \boldsymbol{\xi}\big)_{\Omega^s} + \Delta t^2 \left[2\nu_s d\left(\boldsymbol{\eta}^n, \boldsymbol{\xi}\right)_{\Omega^s} + \lambda e\left(\boldsymbol{\eta}^n, \boldsymbol{\xi}\right)_{\Omega^s}\right] \\
& - \Delta t^2 \left(2\nu_s D(\boldsymbol{\eta}^n) \cdot \mathbf{n}_s + \lambda(\nabla \cdot \boldsymbol{\eta}^n)\mathbf{n}_s, \boldsymbol{\xi}\right)_{\Gamma_{I_0}} \\
& = \Delta t^2 \left[(\mathbf{f}_s^n, \boldsymbol{\xi})_{\Omega^s} + (\boldsymbol{\eta}_N^n, \boldsymbol{\xi})_{\Gamma_N^s}\right] \ \forall \boldsymbol{\xi} \in \boldsymbol{H}_D^1(\Omega^s)
\end{aligned} \tag{2.42}$$

and will be considered in Chapter 3.

The overall order of the time discretization is only first order accurate because of using implicit Euler for the fluid discretization. However, the analytical results can be easily extended to use the Crank–Nicolson time discretization scheme for the fluid instead of implicit Euler, but this was not done in order to keep the fluid equations simpler. Analysis for the structure subsystem will be developed using the second order time discretization due to a necessity for higher order accuracy, which will be needed later and is explained in Remark 4.6.

Chapter 3

OPTIMIZATION-BASED DECOUPLING

3.1 Introduction

In this chapter, we introduce a control into the semi-discretized weak form of the FSI equations which decouples the fluid and structure subproblems. The control that we use enforces the continuity of traction force on the interfaces for every choice of control. Our goal in optimization will be to find an optimal control which minimizes violations of the continuity of velocity on the interface.

A nonlinear function is defined whose norm is equivalent with the penalized functional which minimizes velocity mismatches between fluid and structure on the interface. Using Gauss–Newton iterations based on a Taylor series truncation, updates to the control can be performed by solving a linear least squares problem. The Fréchet derivative of the nonlinear function is presented for both first and second order time discretizations of the structure that were given in Chapter 2. A proof is furnished to prove that the adjoint of the linearized operators are correct as given.

A Newton–Krylov method is introduced to minimize the norm of the nonlinear function describing the velocity jump on the interface. There are many solver choices

available for minimizing the linear least squares problem occurring within each Gauss–Newton iteration. We choose to present the conjugate gradient for least squares algorithm, which does not require explicitly forming the normal equations in order to minimize the linear least squares problem.

A numerical study is included for a haemodynamic problem having clamped artery ends which was previously simulated by Murea and Sy [54]. Because the densities of the fluid and structure are similar, this problem suffers from the added mass effect and is too sensitive to be computed by iterative implicit partitioned schemes unless they contain sufficient relaxation. First, progressively refined meshes are used to demonstrate that the solution at the mesh resolution given in [54] is not mesh independent. Next, we compare the solution using our optimization-based approach against the result in [54]. After this, another series of tests were performed to compare the solutions gathered from an implicit relaxed partitioned scheme against the solution provided by our method.

3.2 Substitution of Traction Terms with a Control

It is desirable that an algorithm for solving FSI problems be able to stably decouple the subsystems and solve each subsystem in parallel. Stably decoupling the subsystems is of particular importance in the case when the added mass effect is present. With this in mind, we seek to exploit the shared traction (2.12) force between the coupled subsystems.

We set $\mathbf{g}^n = 2\nu_f D(\mathbf{u}^n) \cdot \mathbf{n}_f - p\mathbf{n}_f$ as our control for the stress on the interface for the fluid subproblem. Therefore $2\nu_s D(\boldsymbol{\eta}^n) \cdot \mathbf{n}_s + \lambda(\nabla \cdot \boldsymbol{\eta}^n)\mathbf{n}_s|_{I_0}$ can be replaced by $-(\mathbf{g}^n \circ \Psi_n^{-1})J_{t_n}$ in the structure subproblem because of interface condition (2.12), ensuring continuity of stress along the interface between the two subsystems for any choice of $\mathbf{g}^n$.

Making this substitution, the fluid subproblem (2.38)–(2.39) becomes

$$\rho_f \left[(\mathbf{u}^n, \mathbf{v})_{\Omega^f_{t_n}} - (\mathbf{u}^{n-1}, \mathbf{v})_{\Omega^f_{t_{n-1}}}\right] + \Delta t\, \rho_f \left[((\mathbf{u}^n - \mathbf{z}^n) \cdot \nabla \mathbf{u}^n, \mathbf{v})_{\Omega^f_{t_n}} - (\mathbf{u}^n (\nabla \cdot \mathbf{z}^n), \mathbf{v})_{\Omega^f_{t_n}}\right]$$
$$+ \Delta t \left[2\nu_f a(\mathbf{u}^n, \mathbf{v})_{\Omega^f_{t_n}} + b(\mathbf{v}, p^n)_{\Omega^f_{t_n}}\right]$$
$$= \Delta t \left[(\mathbf{f}^n_f, \mathbf{v})_{\Omega^f_{t_n}} + (\mathbf{u}^n_N, \mathbf{v})_{\Gamma^f_N} + (\mathbf{g}^n, \mathbf{v})_{\Gamma_{I_{t_n}}}\right] \ \forall \mathbf{v} \in \boldsymbol{H}^1_D(\Omega^f_{t_n}), \tag{3.1}$$

$$b(\mathbf{u}^n, q)_{\Omega^f_{t_n}} = 0 \quad \forall q \in L^2(\Omega^f_{t_n}), \tag{3.2}$$

the first order structure subproblem (2.42) becomes

$$\rho_s \left(\boldsymbol{\eta}^n - 2\boldsymbol{\eta}^{n-1} + \boldsymbol{\eta}^{n-2}, \boldsymbol{\xi}\right)_{\Omega^s} + \Delta t^2 \left[2\nu_s d\left(\boldsymbol{\eta}^n, \boldsymbol{\xi}\right)_{\Omega^s} + \lambda e\left(\boldsymbol{\eta}^n, \boldsymbol{\xi}\right)_{\Omega^s}\right]$$
$$= \Delta t^2 \left[(\mathbf{f}^n_s, \boldsymbol{\xi})_{\Omega^s} + (\boldsymbol{\eta}^n_N, \boldsymbol{\xi})_{\Gamma^s_N} - (\mathbf{g}^n, \mathcal{V}(\boldsymbol{\xi}))_{\Gamma_{I_{t_n}}}\right] \ \forall \boldsymbol{\xi} \in \boldsymbol{H}^1_D(\Omega^s), \tag{3.3}$$

and the second order structure subproblem (2.40)–(2.41) becomes

$$\rho_s \left(\dot{\boldsymbol{\eta}}^n - \dot{\boldsymbol{\eta}}^{n-1}, \boldsymbol{\xi}\right)_{\Omega^s}$$
$$+ \Delta t \left[2\,\nu_s d\left(\frac{\boldsymbol{\eta}^n + \boldsymbol{\eta}^{n-1}}{2}, \boldsymbol{\xi}\right)_{\Omega^s} + \lambda e\left(\frac{\boldsymbol{\eta}^n + \boldsymbol{\eta}^{n-1}}{2}, \boldsymbol{\xi}\right)_{\Omega^s}\right]$$
$$= \Delta t \left[\left(\frac{\mathbf{f}^n_s + \mathbf{f}^{n-1}_s}{2}, \boldsymbol{\xi}\right)_{\Omega^s} + \left(\frac{\boldsymbol{\eta}^n_N + \boldsymbol{\eta}^{n-1}_N}{2}, \boldsymbol{\xi}\right)_{\Gamma^s_N} + (\mathbf{g}^n, \mathcal{V}(\boldsymbol{\xi}))_{\Gamma_{I_{t_n}}}\right] \ \forall \boldsymbol{\xi} \in \boldsymbol{H}^1_D(\Omega^s), \tag{3.4}$$

$$\left(\boldsymbol{\eta}^n - \boldsymbol{\eta}^{n-1}, \boldsymbol{\gamma}\right)_{\Omega^s} - \Delta t \left(\frac{\dot{\boldsymbol{\eta}}^n + \dot{\boldsymbol{\eta}}^{n-1}}{2}, \boldsymbol{\gamma}\right)_{\Omega^s} = 0 \ \forall \boldsymbol{\gamma} \in \boldsymbol{H}^1_D(\Omega^s). \tag{3.5}$$

3.2.1 The Formal Optimization Problem

Now that we see a control can be introduced which will decouple the fluid and structure subsystems, we shall proceed to define the formal optimization problem. We seek a $\mathbf{g}^n$ in (3.1) and (3.3) or (3.4) to be chosen as a control in each time step to enforce the

continuity of velocity (2.11), i.e., we wish to minimize the penalized functional

$$\mathcal{J}_n(\mathbf{u}^n, \dot{\boldsymbol{\eta}}^n, \mathbf{g}^n) = \frac{1}{2}\int_{\Gamma_{I_{t_n}}} |\mathbf{u}^n - \mathcal{V}(\dot{\boldsymbol{\eta}}^n)|^2 \, d\Gamma + \frac{\epsilon}{2}\int_{\Gamma_{I_{t_n}}} |\mathbf{g}^n|^2 \, d\Gamma \,, \tag{3.6}$$

subject to (3.1)–(3.2) and (3.3) or (3.1)–(3.2) and (3.4)–(3.5), depending on the structure formulation used. If using the first order discretization of the structure subsystem (3.3), $\dot{\boldsymbol{\eta}}^n$ in (3.6) can be approximated by

$$\dot{\boldsymbol{\eta}}^n \approx \frac{\boldsymbol{\eta}^n - \boldsymbol{\eta}^{n-1}}{\Delta t}.$$

In (3.6), ϵ is the penalty parameter which gives relative weight to the latter term and $\Gamma_{I_{t_n}}$ denotes the interface at time step n, to be determined by the solution to (3.3) or (3.1)–(3.2) using Gauss–Newton iterations described later in Algorithm 3.3. Our approach is an implicit algorithm for the fluid-structure interaction problem.

We use nonlinear least squares to develop a computational algorithm for the constrained optimal control problem.

Define the nonlinear operator $N_n : \mathbf{L}^2(\Gamma_{I_{t_n}}) \to \mathbf{L}^2(\Gamma_{I_{t_n}}) \times \mathbf{L}^2(\Gamma_{I_{t_n}})$ by

$$N_n(\mathbf{g}^n) = \begin{pmatrix} (\mathbf{u}^n - \mathcal{V}(\dot{\boldsymbol{\eta}}^n)) \mid_{\Gamma_{I_{t_n}}} \\ \\ \sqrt{\epsilon}\, \mathbf{g}^n \end{pmatrix},$$

where $\mathbf{u}^n$, $\dot{\boldsymbol{\eta}}^n$ are the fluid and structure velocities satisfying (3.1)–(3.5) when $\mathbf{g}^n$ is the stress function on the interface. Then, (3.6) can be written as

$$\mathcal{J}_n(\mathbf{g}^n) = \frac{1}{2}\|N_n(\mathbf{g}^n)\|^2_{\mathbf{L}^2(\Gamma_{I_{t_n}})\times\mathbf{L}^2(\Gamma_{I_{t_n}})} \tag{3.7}$$

and the nonlinear least squares problem we consider is to

$$\textit{seek } \mathbf{g}^n \in \mathbf{L}^2(\Gamma_{I_{t_n}}) \textit{ such that } (3.7) \textit{ is minimized.} \tag{3.8}$$

We can linearize $N_n(\mathbf{g}^n)$ using the Fréchet derivative of $N_n(\cdot)$ at $\overline{\mathbf{g}}^n$, $N_n'(\overline{\mathbf{g}}^n)$, by

$$N_n(\mathbf{g}) = N_n(\overline{\mathbf{g}}^n) + N'(\overline{\mathbf{g}}_n)(\mathbf{g}^n - \overline{\mathbf{g}}^n) + O(\|\mathbf{g}^n - \overline{\mathbf{g}}^n\|^2_{\mathbf{L}^2(\Gamma_{I_{t_n}})\times\mathbf{L}^2(\Gamma_{I_{t_n}})})$$

so that solutions of the nonlinear least squares problem can be obtained by repeatedly solving the linear least squares problem

$$\min_{\mathbf{h}^n\in\mathbf{L}^2(\Gamma_{I_{t_n}})} \frac{1}{2}\|N(\overline{\mathbf{g}}^n) + N_n'(\overline{\mathbf{g}}^n)\mathbf{h}^n\|^2_{\mathbf{L}^2(\Gamma_{I_{t_n}})\times\mathbf{L}^2(\Gamma_{I_{t_n}})}\,, \tag{3.9}$$

where $\mathbf{h}^n = \mathbf{g}^n - \overline{\mathbf{g}}^n$. Hence, starting with arbitrary $\mathbf{g}^n_{(0)}$, we can find a sequence $\{\mathbf{g}^n_{(k)}\}$ obtained by $\mathbf{g}^n_{(k)} = \mathbf{g}^n_{(k-1)} + \mathbf{h}^n_{(k)}$, where $\mathbf{h}^n_{(k)}$ is a solution of the linear least squares problem (3.9).

Following is the definition of the linearized and linear adjoint problems that are to be solved in the use of the conjugate gradient algorithm and Algorithm 3.3. The linearized and linear adjoint problems are presented along with a proof of the definition of the adjoint for the first and second order structure formulations in sections 3.3 and 3.4, respectively.

3.3 First Order Time Discretization of the Structure Subsystem

For $\overline{\mathbf{g}}^n \in \mathbf{L}^2(\Gamma_{I_{t_n}})$, the Fréchet derivative $N'(\overline{\mathbf{g}}^n)(\cdot) : \mathbf{L}^2(\Gamma_{I_{t_n}}) \to \mathbf{L}^2(\Gamma_{I_{t_n}})\times\mathbf{L}^2(\Gamma_{I_{t_n}})$ is defined by

$$N_n'(\overline{\mathbf{g}}^n)(\mathbf{h}^n) = \begin{pmatrix} \left(\mathbf{w}^n - \frac{\mathcal{V}(\boldsymbol{\phi}^n)}{\Delta t}\right)\Big|_{\Gamma_{I_{t_n}}} \\ \sqrt{\epsilon}\,\mathbf{h}^n \end{pmatrix},$$

where $\mathbf{w}^n$, $\boldsymbol{\phi}^n$ are the solutions of

$$\begin{aligned}\rho_f(\mathbf{w}^n,\mathbf{v})_{\Omega^f_{t_n}} &+ \Delta t\,\rho_f\Big[(\mathbf{w}^n\cdot\nabla\overline{\mathbf{u}}^n,\mathbf{v})_{\Omega^f_{t_n}}+((\overline{\mathbf{u}}^n-\mathbf{z}^n)\cdot\nabla\mathbf{w}^n,\mathbf{v})_{\Omega^f_{t_n}}\\ &\qquad -(\mathbf{w}^n(\nabla\cdot\mathbf{z}^n),\mathbf{v})_{\Omega^f_{t_n}}\Big]+\Delta t\left[2\nu_f a(\mathbf{w}^n,\mathbf{v})_{\Omega^f_{t_n}}+b(\mathbf{v},\psi^n)_{\Omega^f_{t_n}}\right]\\ &= \Delta t\,(\mathbf{h}^n,\mathbf{v})_{\Gamma_{I_{t_n}}}\ \forall\mathbf{v}\in\boldsymbol{H}^1_D(\Omega^f_{t_n}),\end{aligned}\tag{3.10}$$

$$b(\mathbf{w}^n,q)_{\Omega^f_{t_n}} = 0\quad\forall q\in L^2(\Omega^f_{t_n}),\tag{3.11}$$

and

$$\begin{aligned}\rho_s\,(\boldsymbol{\phi}^n,\boldsymbol{\xi})_{\Omega^s}+\Delta t^2\,[2\,\nu_s d\,(\boldsymbol{\phi}^n,\boldsymbol{\xi})_{\Omega^s}+\lambda e\,(\boldsymbol{\phi}^n,\boldsymbol{\xi})_{\Omega^s}]&\\ = -\Delta t^2(\mathbf{h}^n,\mathcal{V}(\boldsymbol{\xi}))_{\Gamma_{I_{t_n}}}\ \forall\boldsymbol{\xi}\in\boldsymbol{H}^1_D(\Omega^s),&\end{aligned}\tag{3.12}$$

where $\overline{\mathbf{u}}^n$ is the solution of (3.1)–(3.2) with $\mathbf{g}^n$ replaced by $\overline{\mathbf{g}}^n$.

It is necessary to define the adjoint operator of $N_n'(\overline{\mathbf{g}}^n)$ in order to solve the linear least squares problem (3.9).

Theorem 3.1. *The adjoint of* $(N_n'(\overline{\mathbf{g}}^n))(\cdot)$ *is* $(N_n'(\overline{\mathbf{g}}^n))^*(\cdot):\mathbf{L}^2(\Gamma_{I_{t_n}})\times\mathbf{L}^2(\Gamma_{I_{t_n}})\to\mathbf{L}^2(\Gamma_{I_{t_n}})$, *given by*

$$(N_n'(\overline{\mathbf{g}}_n))^*\begin{pmatrix}\mathbf{r}^n\\ \mathbf{s}^n\end{pmatrix}=\left(\boldsymbol{\beta}^n-\frac{\mathcal{V}(\boldsymbol{\varphi}^n)}{\Delta t}\right)\Big|_{\mathbf{L}^2(\Gamma_{I_{t_n}})}+\sqrt{\epsilon}\,\mathbf{s}^n,$$

where $\boldsymbol{\beta}^n$, $\boldsymbol{\varphi}^n$ *are the solutions of*

$$\begin{aligned}\rho_f(\boldsymbol{\beta}^n,\mathbf{v})_{\Omega^f_{t_n}} &+ \Delta t\,\rho_f\Big[(\mathbf{v}\cdot\nabla\overline{\mathbf{u}}^n,\boldsymbol{\beta}^n)_{\Omega^f_{t_n}}+((\overline{\mathbf{u}}^n-\mathbf{z}^n)\cdot\nabla\mathbf{v},\boldsymbol{\beta}^n)_{\Omega^f_{t_n}}\\ &\qquad -(\boldsymbol{\beta}^n(\nabla\cdot\mathbf{z}^n),\mathbf{v})_{\Omega^f_{t_n}}\Big]+\Delta t\left[2\nu_f a(\boldsymbol{\beta}^n,\mathbf{v})_{\Omega^f_{t_n}}+b(\mathbf{v},\alpha^n)_{\Omega^f_{t_n}}\right]\\ &= \Delta t\,(\mathbf{r}^n,\mathbf{v})_{\Gamma_{I_{t_n}}}\ \forall\mathbf{v}\in\boldsymbol{H}^1_D(\Omega^f_{t_n}),\end{aligned}\tag{3.13}$$

$$b(\boldsymbol{\beta}^n,q)_{\Omega^f_{t_n}} = 0\quad\forall q\in L^2(\Omega^f_{t_n}),\tag{3.14}$$

and

$$\rho_s\left(\boldsymbol{\varphi}^n, \boldsymbol{\xi}\right)_{\Omega^s} + \Delta t^2\left[2\,\nu_s d\left(\boldsymbol{\varphi}^n, \boldsymbol{\xi}\right)_{\Omega^s} + \lambda e\left(\boldsymbol{\varphi}^n, \boldsymbol{\xi}\right)_{\Omega^s}\right]$$
$$= -\Delta t^2\left(\mathbf{r}^n, \mathcal{V}(\boldsymbol{\xi})\right)_{\Gamma_{I_{t_n}}} \;\forall \boldsymbol{\xi} \in \boldsymbol{H}_D^1(\Omega^s)\,. \tag{3.15}$$

Note that the linearized structure subsystem is self-adjoint. Again, $\overline{\mathbf{u}}^n$ in (3.13) is the solution of (3.1)–(3.2) with the replacement of $\mathbf{g}^n$ by $\overline{\mathbf{g}}^n$.

Proof. Let $(\mathbf{v}, q) = (\boldsymbol{\beta}^n, \alpha^n)$ and $\boldsymbol{\xi} = \boldsymbol{\varphi}^n$ in (3.10)–(3.12). Also, let $(\mathbf{v}, q) = (\mathbf{w}^n, \psi^n)$ and $\boldsymbol{\xi} = \boldsymbol{\phi}^n$ in (3.13)–(3.15). From this, we obtain that $(\mathbf{h}^n, \mathcal{V}(\boldsymbol{\varphi}^n))_{\Gamma_{I_{t_n}}} = (\mathbf{r}^n, \mathcal{V}(\boldsymbol{\phi}^n))_{\Gamma_{I_{t_n}}}$ and $(\mathbf{h}^n, \boldsymbol{\beta}^n)_{\Gamma_{I_{t_n}}} = (\mathbf{r}^n, \mathbf{w}^n)_{\Gamma_{I_{t_n}}}$. Therefore,

$$\begin{aligned}
\left(N_n'(\overline{\mathbf{g}}^n)\mathbf{h}^n, \begin{bmatrix}\mathbf{r}^n\\ \mathbf{s}^n\end{bmatrix}\right) &= (\mathbf{w}^n - \frac{\mathcal{V}(\boldsymbol{\phi}^n)}{\Delta t}, \mathbf{r}^n)_{\Gamma_{I_{t_n}}} + \sqrt{\epsilon}(\mathbf{h}^n, \mathbf{s}^n)_{\Gamma_{I_{t_n}}} \\
&= (\mathbf{h}^n, \boldsymbol{\beta}^n - \frac{\mathcal{V}(\boldsymbol{\varphi}^n)}{\Delta t})_{\Gamma_{I_{t_n}}} + \sqrt{\epsilon}(\mathbf{h}^n, \mathbf{s}^n)_{\Gamma_{I_{t_n}}} \\
&= \left(\mathbf{h}^n, N_n'(\overline{\mathbf{g}}^n)^*\left(\begin{bmatrix}\mathbf{r}^n\\ \mathbf{s}^n\end{bmatrix}\right)\right)\,.
\end{aligned}$$

□

3.4 Second Order Time Discretization of the Structure Subsystem

For $\overline{\mathbf{g}}^n \in \mathbf{L}^2(\Gamma_{I_{t_n}})$, the Fréchet derivative $N'(\overline{\mathbf{g}}^n)(\cdot) : \mathbf{L}^2(\Gamma_{I_{t_n}}) \to \mathbf{L}^2(\Gamma_{I_{t_n}}) \times \mathbf{L}^2(\Gamma_{I_{t_n}})$ is defined by

$$N_n'(\overline{\mathbf{g}}^n)(\mathbf{h}^n) = \begin{pmatrix} (\mathbf{w}^n - \mathcal{V}(\dot{\boldsymbol{\phi}}^n))\,|_{\Gamma_{I_{t_n}}} \\ \sqrt{\epsilon}\,\mathbf{h}^n \end{pmatrix},$$

where $\mathbf{w}^n$ is the solution of (3.10)–(3.11), and $\boldsymbol{\phi}^n$ is the solution of

$$\begin{aligned} \rho_s \left(\dot{\boldsymbol{\phi}}^n, \boldsymbol{\xi}\right)_{\Omega^s} &+ \Delta t \left[\nu_s d\left(\boldsymbol{\phi}^n, \boldsymbol{\xi}\right)_{\Omega^s} + \frac{\lambda}{2} e\left(\boldsymbol{\phi}^n, \boldsymbol{\xi}\right)_{\Omega^s}\right] \\ &= -\Delta t (\mathbf{h}^n, \mathcal{V}(\boldsymbol{\xi}))_{\Gamma_{I_{t_n}}} \ \forall \boldsymbol{\xi} \in \boldsymbol{H}_D^1(\Omega^s), \end{aligned} \tag{3.16}$$

$$(\boldsymbol{\phi}^n, \boldsymbol{\gamma})_{\Omega^s} - \frac{\Delta t}{2} \left(\dot{\boldsymbol{\phi}}^n, \boldsymbol{\gamma}\right)_{\Omega^s} = 0 \ \forall \boldsymbol{\gamma} \in \boldsymbol{H}_D^1(\Omega^s). \tag{3.17}$$

We now define the adjoint operator of $N_n'(\overline{\mathbf{g}}^n)$ needed in order to solve the linear least squares problem (3.9).

Theorem 3.2. *The adjoint of* $(N_n'(\overline{\mathbf{g}}^n))(\cdot)$ *is* $(N_n'(\overline{\mathbf{g}}^n))^*(\cdot) : \mathbf{L}^2(\Gamma_{I_{t_n}}) \times \mathbf{L}^2(\Gamma_{I_{t_n}}) \to \mathbf{L}^2(\Gamma_{I_{t_n}})$, *given by*

$$(N_n'(\overline{\mathbf{g}}_n))^* \begin{pmatrix} \mathbf{r}^n \\ \\ \mathbf{s}^n \end{pmatrix} = (\boldsymbol{\beta}^n - \mathcal{V}(\boldsymbol{\varphi}^n))|_{\mathbf{L}^2(\Gamma_{I_{t_n}})} + \sqrt{\epsilon}\, \mathbf{s}^n,$$

where $\boldsymbol{\beta}^n$ *is the solution of (3.13)–(3.14) and* $\boldsymbol{\varphi}^n$ *is the solution of*

$$(\dot{\boldsymbol{\varphi}}^n, \boldsymbol{\xi})_{\Omega^s} + \Delta t \left[\nu_s d\left(\boldsymbol{\varphi}^n, \boldsymbol{\xi}\right)_{\Omega^s} + \frac{\lambda}{2} e\left(\boldsymbol{\varphi}^n, \boldsymbol{\xi}\right)_{\Omega^s}\right] \tag{3.18}$$

$$= 0 \ \forall \boldsymbol{\xi} \in \boldsymbol{H}_D^1(\Omega^s), \tag{3.19}$$

$$\rho_s \left(\boldsymbol{\varphi}^n, \boldsymbol{\gamma}\right)_{\Omega^s} - \frac{\Delta t}{2} \left(\dot{\boldsymbol{\varphi}}^n, \boldsymbol{\gamma}\right)_{\Omega^s} = -\Delta t \left(\mathbf{r}^n, \mathcal{V}(\boldsymbol{\gamma})\right)_{\Gamma_{I_{t_n}}} \ \forall \boldsymbol{\gamma} \in \boldsymbol{H}_D^1(\Omega^s). \tag{3.20}$$

Proof. Let $(\mathbf{v}, q) = (\boldsymbol{\beta}^n, \alpha^n)$ and $(\boldsymbol{\xi}, \boldsymbol{\gamma}) = (\boldsymbol{\varphi}^n, \dot{\boldsymbol{\varphi}^n})$ in (3.10)–(3.11) and (3.16)–(3.17). Also, let $(\mathbf{v}, q) = (\mathbf{w}^n, \psi^n)$ and $(\boldsymbol{\xi}, \boldsymbol{\gamma}) = (\boldsymbol{\phi}^n, \dot{\boldsymbol{\phi}^n})$ in (3.13)–(3.14) and (3.19)–(3.20). From this, we obtain that $(\mathbf{h}^n, \mathcal{V}(\boldsymbol{\varphi}^n))_{\Gamma_{I_{t_n}}} = (\mathbf{r}^n, \mathcal{V}(\dot{\boldsymbol{\phi}^n}))_{\Gamma_{I_{t_n}}}$ and $(\mathbf{h}^n, \boldsymbol{\beta}^n)_{\Gamma_{I_{t_n}}} = (\mathbf{r}^n, \mathbf{w}^n)_{\Gamma_{I_{t_n}}}$.

Therefore,

$$\begin{aligned}\left(N_n'(\overline{\mathbf{g}}^n)\mathbf{h}^n, \begin{bmatrix}\mathbf{r}^n\\ \mathbf{s}^n\end{bmatrix}\right) &= (\mathbf{w}^n - \mathcal{V}(\dot{\boldsymbol{\phi}}^n), \mathbf{r}^n)_{\Gamma_{I_{t_n}}} + \sqrt{\epsilon}(\mathbf{h}^n, \mathbf{s}^n)_{\Gamma_{I_{t_n}}} \\ &= (\mathbf{h}^n, \boldsymbol{\beta}^n - \mathcal{V}(\boldsymbol{\varphi}^n))_{\Gamma_{I_{t_n}}} + \sqrt{\epsilon}(\mathbf{h}^n, \mathbf{s}^n)_{\Gamma_{I_{t_n}}} \\ &= \left(\mathbf{h}^n, N_n'(\overline{\mathbf{g}}^n)^* \left(\begin{bmatrix}\mathbf{r}^n\\ \mathbf{s}^n\end{bmatrix}\right)\right).\end{aligned}$$

□

3.5 Gauss–Newton Algorithm

For problem (3.9), we adopt the conjugate gradient method for least squares (CGLS) [59]. This method is mathematically equivalent to solving the normal equations, but does not require explicitly forming them. This is a variant of the conjugate gradient method which can be found in many references [37–39]. For the algorithm, we use the notation $A = N_n'(\overline{\mathbf{g}}^n)$, $A^* = (N_n'(\overline{\mathbf{g}}^n))^*$, $b = -N_n(\overline{\mathbf{g}}^n)$, and $x = \mathbf{h}^n$.

The nonlinear least squares problem (3.8) can be solved using the following Gauss–Newton algorithm.

Algorithm 3.3.

1. Choose $\mathbf{g}_{(0)}^n$.
2. For $k = 1, 2, 3, \ldots$,
   a. computable in parallel:
      i. find $\mathbf{u}_{(k)}^n$ and $p_{(k)}^n$ on $\Omega_{t_n,(k-1)}^f$ using $\mathbf{z}_{(k-1)}^n$ and $\mathbf{g}_{(k-1)}^n$,
      ii. find $\boldsymbol{\eta}_{(k)}^n$ and $\dot{\boldsymbol{\eta}}_{(k)}^n$ using $\mathbf{g}_{(k-1)}^n$,
   b. update $\Gamma_{I_n^{(k)}}$, $\mathbf{z}_{(k)}^n$, $\Psi_n^{(k)}$, and $\Omega_{t_n,(k)}^f$ using $\boldsymbol{\eta}_{(k)}^n$,
   c. if $\frac{1}{2}\int_{\Gamma_{I_{t_n}^{(k-1)}}} |\mathbf{u}_{(k)}^n - \mathcal{V}(\dot{\boldsymbol{\eta}}_{(k)}^n)|^2 \, d\Gamma < \epsilon_{tol}$, break,

d. compute $\mathbf{h}^n_{(k)}$ using CGLS to solve the least squares problem, minimizing $\frac{1}{2}\|Ax-b\|^2$,

e. set $\mathbf{g}^n_{(k)} = \mathbf{g}^n_{(k-1)} + \mathbf{h}^n_{(k)}$.

Remark 3.4. *Our choice of $\mathbf{g}^n_{(0)}$ in step 1. of Algorithm 3.3 is the final value of $\mathbf{g}^{n-1}$ determined in the previous time step.*

Remark 3.5. *In step 2.d. of Algorithm 3.3, determining $\mathbf{h}^n_{(k)}$ by means of the conjugate gradient algorithm is accomplished on the moving fluid domain determined by the structure problem using the control $\mathbf{g}^n_{(k-1)}$. Therefore, the moving fluid domain must only be updated for each Gauss–Newton iteration of Algorithm 3.3.*

3.6 Numerical Results

3.6.0.1 Haemodynamic Experiment

The first of two numerical tests is an FSI problem using the ALE formulation for the moving fluid domain, reported in [54], using parameters that are consistent with blood flow in a human body. The problem is heavily affected by the added mass effect, since the densities of the fluid and structure are very close, and is therefore an excellent test candidate. This effect causes explicit decoupling without relaxation to fail, as was observed by experimentation and also reported in [54].

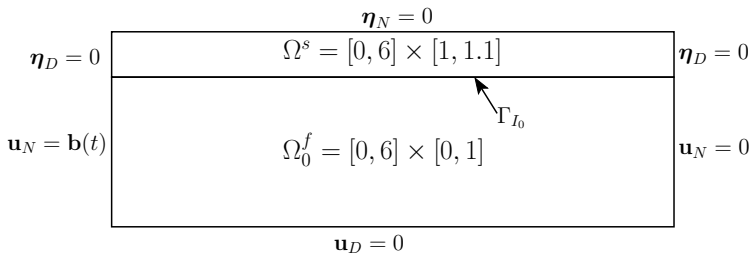

Figure 3.1: Domain and boundary conditions for numerical experiment

A force $\mathbf{b}(t)$ is applied to the left fluid boundary (Fig. 3.1) at t s where

$$\mathbf{b}(t) = \begin{cases} (-10^3(1-\cos\frac{2\pi t}{.025}),0) \ \text{ dyne/cm}^2, & t \leq 0.025 \\ (0,0), & 0.025 < t < T. \end{cases}$$

The function $\mathbf{b}(t)$ defines the stress on the inlet denoted by $\mathbf{u}_N$ in (2.4). The volume force for the fluid and structure are $\mathbf{f}(t) = (0,0)$ dyne/cm^2. The other boundary conditions on the domain configuration are homogeneous Dirichlet or Neumann (Fig. 3.1), and the simulation begins at rest.

The reference domain for the fluid subsystem has height 1 cm and length 6 cm. The density of the fluid, ρ_f, is 1 g/cm^3 and the viscosity of the fluid, ν_f, is 0.035 g/cm·s. The structure domain has height 0.1 cm and length 6 cm. The density of the structure, ρ_s, is 1.1 g/cm^3. The Young's Modulus of the structure, E, is 3×10^6 dyne/cm^2 and its Poisson ratio, ν, is 0.3. The Lamé parameters λ and ν_s are defined as follows:

$$\lambda = \frac{\nu E}{(1-2\nu)(1+\nu)} \text{ dyne/cm}^2, \quad \nu_s = \frac{E}{2(1+\nu)} \text{ dyne/cm}^2.$$

The fluid and structure reference domains were spatially discretized using a uniform mesh. Let h_x and h_y represent the spatial discretization in the x and y direction, respectively. We used the triangular $(\mathbb{P}_1 + bubble, \mathbb{P}_1)$ pair for the finite element solution to (3.1)–(3.2) on the fluid domain and $\mathbb{P}_1$ finite elements for the solution to (3.3) or (3.4)–(3.5) on the structure domain for all computations that will be presented. Additionally, all computations performed used a time step of $\Delta t = 10^{-4}$ s and were from $T = 0$ s to $T = 0.1$ s. All computations were performed using FreeFEM++ [41].

The first sequence of simulations (Fig. 3.2) demonstrates the strong dependence of the solution on the spatial discretization. The plots of the vertical displacement on the interface are computed using Algorithm 3.3. It is worth noting that using a spatial discretization with $h_x = 0.1$ cm and allowing h_y to range from 0.1 cm to $\frac{1}{30}$ cm for both computational domains gives significantly different results. There is much more agreement

using the two finer spatial discretizations which indicates that the solution is sensitive to having degrees of freedom on the interior of the structure FEM space.

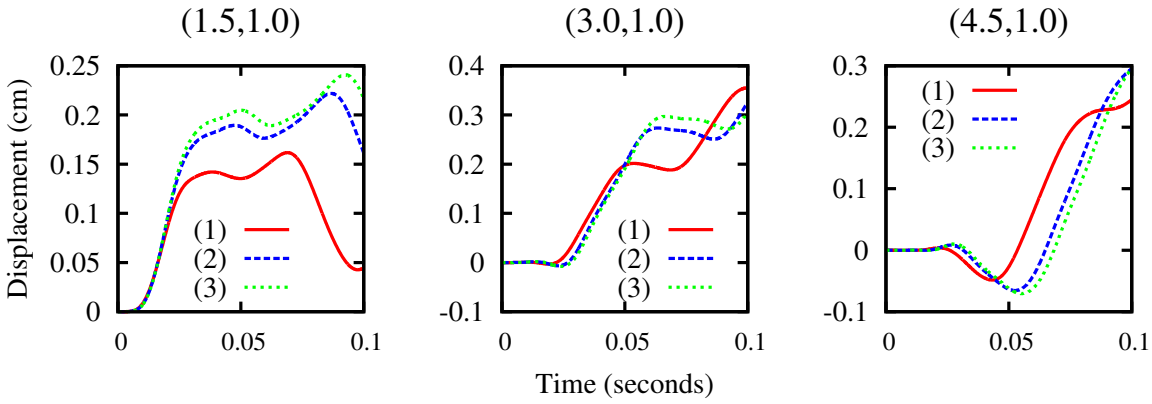

Figure 3.2: Vertical displacement at three points on the interface using the first order structure formulation with: (1) $h_x = 0.1$ cm, $h_y = 0.1$ cm, (2) $h_x = 0.1$ cm, $h_y = 0.05$ cm, and (3) $h_x = 0.1$ cm, $h_y = \frac{1}{30}$ cm

The solution to the FSI problem computed by Murea and Sy [54] is on a mesh with $h_x \approx 0.2$ cm and $h_y \approx 0.1$ cm for the structure domain, $h_x \approx 0.1$ cm and $h_y \approx 0.1$ cm for the fluid domain. We have seen that the solution depends heavily on the spatial discretization with a mesh as coarse as is used for this comparison, so it is not reasonable for us to expect an exact match with their results. Particularly because, in Murea and Sy's work, a truncated eigenfunction basis for the solution on the structure domain was used. Additionally, the uniqueness of the optimal solution is not guaranteed theoretically for Algorithm 3.3 in its continuous form, so the numerical solution may be determined by the initial choice of the control. Regardless, we have compared our solution with Murea and Sy's (Fig. 3.3) and note that, while they differ in amplitude, they both have similar wavelike features. Our computation was made using $h_x = 0.2$ cm and $h_y = 0.1$ cm for the structure domain, $h_x = 0.1$ cm and $h_y = 0.1$ cm for the fluid domain, $\epsilon = 0$, and $\epsilon_{tol} = 10^{-6}$ for Algorithm 3.3.

Table 3.1 contains the norm of the jump in velocities on the interface at three time steps for the computation made using $h_x = 0.05$ cm and $h_y = 0.05$ cm as the spatial

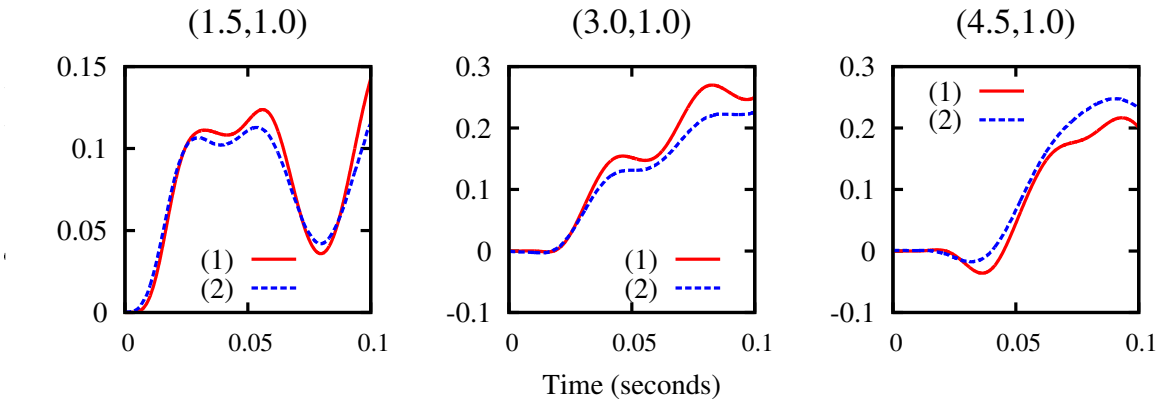

Figure 3.3: Vertical displacement at three points on the interface using (1) Algorithm 3.3 with the first order formulation for the structure beside the vertical displacement from (2) Murea and Sy

discretization, $\epsilon = 0$, and $\epsilon_{tol} = 10^{-6}$. Observe the fast convergence of the Gauss–Newton iterations. Figure 3.4 contains pressure profiles of the same solution at the same three time steps.

Interface Velocity Error $\mathcal{J}_n(\cdot)$

Time (s)	Iter. 1	Iter. 2	Iter. 3
0.010	4.1781e-04	5.7408e-05	6.2945e-08
0.025	1.4958e-04	1.4712e-04	2.6601e-08
0.035	2.3213e-04	1.0033e-04	1.4864e-09

Table 3.1: Error in the continuity of velocity between subsystems for each Gauss–Newton iteration at three representative time steps

We now verify that the solutions found by Algorithm 3.3 for the first and second order formulations of the linear elastic structure closely match the solution found with Aitken's relaxation [21], using the same finite elements and with the same spatial discretization. Aitken's relaxation is an implicit scheme that is applied to the structure update. It works by relaxing the update to $\boldsymbol{\eta}^n$ at each iteration of an implicit scheme. For instance, suppose $\tilde{\boldsymbol{\eta}}^n_{(k)}$ is the solution to the structure subproblem for implicit iteration k. Then, $\boldsymbol{\eta}^n_{(k)}$ is updated as

$$\boldsymbol{\eta}^n_{(k)} = \omega\, \tilde{\boldsymbol{\eta}}^n_{(k)} + (1-\omega)\, \boldsymbol{\eta}^n_{(k-1)},\ \omega \in]0,1]. \tag{3.21}$$

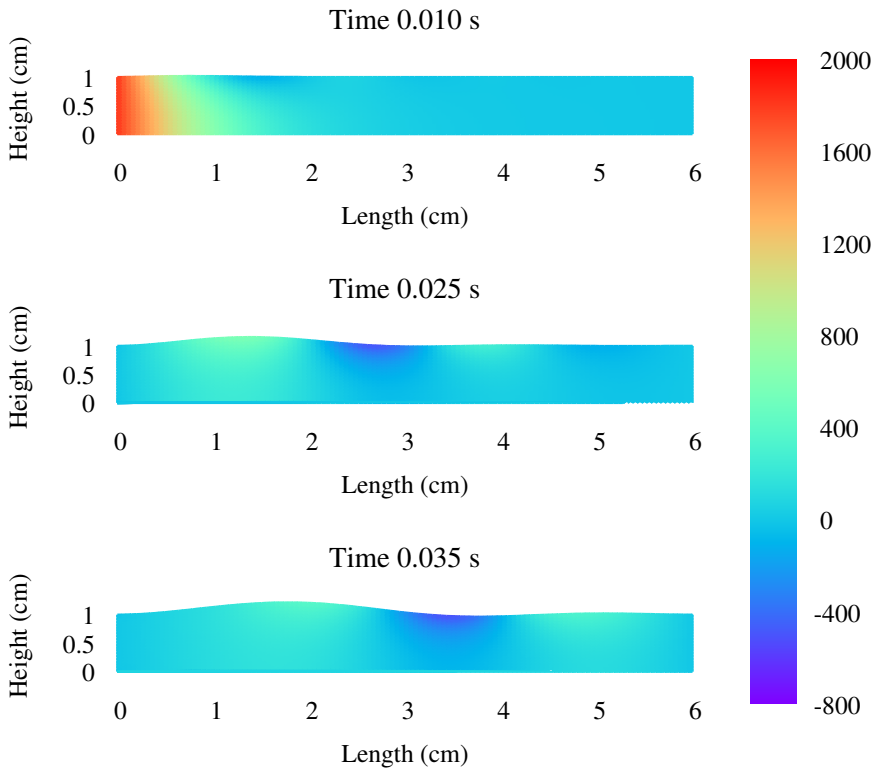

Figure 3.4: Fluid pressure profiles [dyne/cm^2] at three time steps

See [21] for more details on Aitken's relaxation.

While easy to implement, this is an incredibly expensive method to use because ω must be very small in order the system to remain stable and converge. The smaller the value of ω, the more iterations are needed at each time step, requiring many nonlinear solves on the fluid domain. Using $\omega = 0.025$, the result is reliable and useful as a reference solution with which to compare (Fig. 3.5). Spatial discretization was made with $h_x = 0.2$ cm and $h_y = 0.1$ cm for both fluid and structure domains. The stopping criteria used for Aitken's relaxation was $\left(\int_{\Gamma_{I_0}} (\boldsymbol{\eta}^n_{(k)} - \boldsymbol{\eta}^n_{(k-1)})^2 \, d\Gamma\right)^{\frac{1}{2}} < 10^{-7}$, while $\epsilon = 0$ and $\epsilon_{tol} = 10^{-6}$ for Algorithm 3.3.

It was observed that the first and second order formulation for the structure made no significant difference on the solution found. Both solutions matched well the reference result using Aitken's relaxation, and as expected, Algorithm 3.3 significantly reduced com-

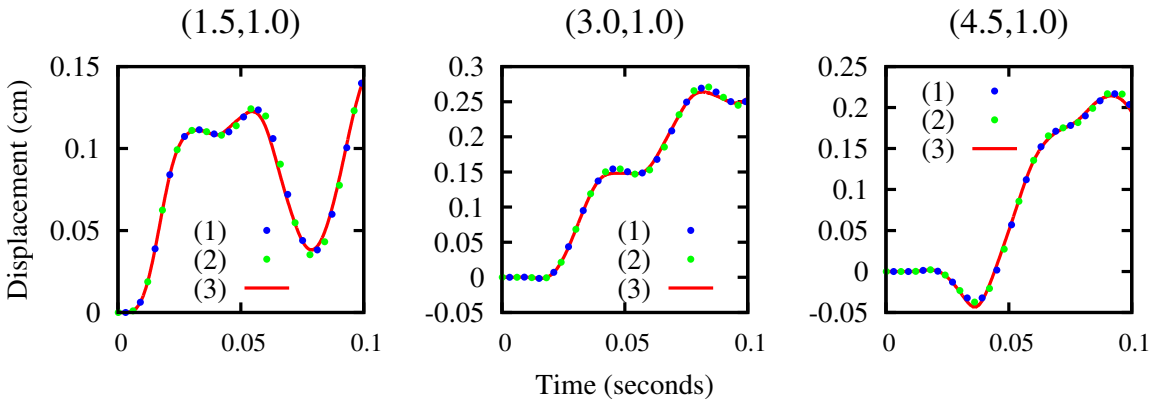

Figure 3.5: Vertical displacement at three points on the interface using (1) first and (2) second order formulations with the optimal control algorithm beside vertical displacement using (3) Aitken's relaxation

putation times. The first order formulation using Algorithm 3.3 ran for 135 minutes before completion, while the Aitken's relaxation ran for 1,624 minutes with a tolerance of 10^{-6} on each time step and 2,701 minutes using a tolerance of 10^{-7} on each time step. We do not expect a 90% reduction in run time compared with other state-of-the-art implicit methods, but Aitken's relaxation is a benchmark against which many implicit algorithms can be compared.

3.6.0.2 Comparison with an Analytical Solution

In order to observe the convergence and accuracy of our method, we have compared it with the analytical solution for the FSI problem presented by Astorino and Grandmont [3]. The fluid governing equations are for Stokes flow on a stationary fluid domain, but still have the same challenge of solving an FSI problem with similar densities between the fluid and structure [2,5,19]. This problem also provides support that our optimal control approach is applicable for solving a broad range of FSI problems. Solving the Stokes flow on a stationary domain means that when we solve (3.1)–(3.2), the equations will not have the nonlinear term $(\mathbf{u}^n \cdot \nabla \mathbf{u}^n, \mathbf{v})_{\Omega^f_{t_n}}$ and we will drop all terms including $\mathbf{z}$, since $\mathbf{z} = 0$ and $\nabla \cdot \mathbf{z} = 0$ in the Eulerian framework. The corresponding terms are removed from the linearized and adjoint

problems defined in sections 3.3 and 3.4.

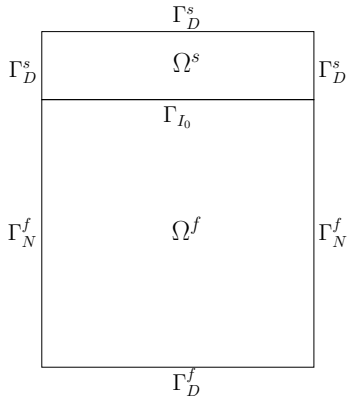

Figure 3.6: Computational domain for a manufactured solution

Parameters for the problem are: $\rho_f = 1.0$ g/cm^3, $\nu_f = 0.0013$ g/cm·s, $\rho_s = 1.9$ g/cm^3, $\nu_s = 3$ dyne/cm^2, and $\lambda = 4.5$ dyne/cm^2. Initial conditions, body forces, and boundary conditions are determined by the analytical solution according to the method of manufactured solutions:

On $\Omega_t^f = \Omega^f = [0,1] \times [0,1]$ and $\Omega^s = [0,1] \times [1,1.25]$ (Fig. 3.6),

$$\begin{aligned}
\mathbf{u}_1 &= \cos(x+t)\sin(y+t) + \sin(x+t)\cos(y+t), \\
\mathbf{u}_2 &= -\sin(x+t)\cos(y+t) - \cos(x+t)\sin(y+t), \\
p &= 2\nu_f(\sin(x+t)\sin(y+t) - \cos(x+t)\cos(y+t)) + 2\nu_s\cos(x+t)\sin(y+t), \\
\boldsymbol{\eta}_1 &= \sin(x+t)\sin(y+t), \\
\boldsymbol{\eta}_2 &= \cos(x+t)\cos(y+t).
\end{aligned} \tag{3.22}$$

As in [3], we used a uniform mesh with a spatial discretization of $h = 0.05$ cm. The Taylor–Hood finite element pair, $(\mathbb{P}_2, \mathbb{P}_1)$, were used for solutions on the fluid domain, while $\mathbb{P}_2$ finite elements were used to approximate the structure displacement. The FSI

problem was repeatedly solved by Algorithm 3.3 using decreasing time steps ($\Delta t = 6.25 \cdot 10^{-2}, 3.125 \cdot 10^{-2}, 1.5625 \cdot 10^{-2}, 7.8125 \cdot 10^{-3}$ s) and compared with the exact solution (3.22). For Algorithm 3.3, $\epsilon = 0$ and $\epsilon_{tol} = 10^{-6}$ were used. Norms used to compute the error between the solution found by means of our optimal control algorithm and the exact solution are as follows: for $\mathbf{u}$ and p, $\mathbf{L}^{\infty}(0.5, 1; \mathbf{L}^2(\Omega^f))$; for $\boldsymbol{\eta}$, $\mathbf{L}^{\infty}(0.5, 1; \mathbf{H}^1(\Omega^s))$. Results are plotted in logarithmic scale format as a function of Δt in Figure 3.7 and are approximately linear. The results indicate that our algorithm for solving the FSI problem converges upon the exact solution. Providing error estimation for the optimal control algorithm will be the focus of Chapter 5.

3.7 Conclusion

The monolithic fluid-structure interaction problem was reformulated as an optimal control problem where violation of continuity of velocity on the interface of two subsystems is minimized using a control on the interface representing the shared traction force. A nonlinear function was defined whose norm is the nonnegative Tikhonov regularized functional. The Gauss–Newton outer optimization loop was detailed using the nonlinear function as well as its Fréchet derivative. Linearized versions for the fluid and both time discretized versions of the structure along with their adjoints were derived in sections 3.3 and 3.4 and proofs were furnished showing that the adjoint was as defined. Steps for the Gauss–Newton algorithm were outlined along with the related roles of the Fréchet derivative and adjoint of the nonlinear function.

The problems described in 3.6.0.1 and 3.6.0.2 were implemented in FreeFEM++ using the optimal control algorithm described in section 3.5 and computations were performed on the Palmetto cluster.

The presented algorithm successfully decoupled the FSI problem into two subproblems. Very few nonlinear solves were needed for each time step because of the fast convergence of the Gauss–Newton algorithm in determining the optimal virtual control. It was

not necessary to introduce relaxation parameters for updating either the structure or fluid subsystems. Additionally, all problems including the linearized and adjoint problems for the fluid and structure subsystem can be solved in parallel, which is increasingly important as more effort is being expended on building large computational clusters for distributed computing.

Although Figure 3.2 indicates that the solution to the first FSI problem tested was very sensitive to spatial discretization and finite element choice, our algorithm was able to find solutions that enforced continuity of stress always and continuity of velocity within a specified tolerance. Further, Figure 3.5 indicates that the solution of the optimization algorithm matched the results of using a much more computationally expensive implicit method and also shows very strong agreement between both first and second order formulations for the structure subproblem. Computation time was reduced by over 90% when compared with a naive but easy to implement Aitken's relaxation method.

Using a Stokes-linear elastic structure FSI problem on a fixed domain with an analytical solution, we were able to show nearly linear convergence in the very strict $||\cdot||_{\mathbf{L}^\infty}$ norm with respect to time. This gives us confidence that the algorithm by optimization is converging upon the true solution.

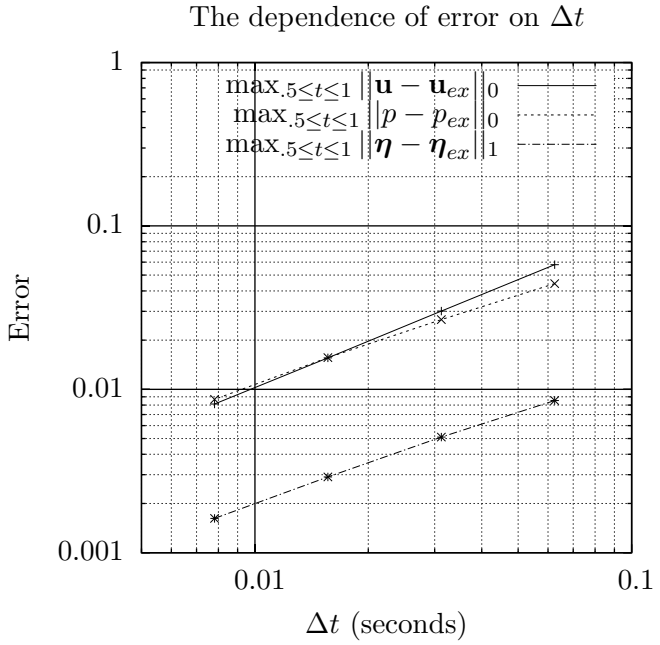

Figure 3.7: Convergence results for the analytic problem

Chapter 4

EXISTENCE PROOFS

4.1 Introduction

A new and alternative implicit decoupling approach to recast the FSI problem as an optimal control problem is presented in this chapter. It is similar in form to the approach in Chapter 3, using each subsystem as a constraint. The control introduced in this chapter differs in that it has additional terms included and approximately and progressively enforces the continuity of stress on the interface while minimizing any violation of the continuity of velocity on the interface. This is opposed to constantly enforcing continuity of traction force for any choice of control, as was the case with the control from Chapter 3. The two subsystems are again decoupled and this allows for them to be solved simultaneously and independently, but also allows for additional analysis to be performed on the optimization problem.

Using a penalized functional with Tikhonov regularization and some a priori stability estimates proved in Section 4.4, the existence of an optimal solution is shown to exist. A proof is given that with some strong assumptions on the regularity of the strong form of the FSI problem, the limit of the sequence of optimal solutions formed by taking the limit as the Tikhonov parameter approaches zero exists and satisfies the continuity of velocity condition to within a specified tolerance. The existence of Lagrange multipliers, and the

derivation of an optimality system are presented next.

A steepest descent algorithm is detailed in Section 4.9 followed by a numerical experiment in Section 4.10. The algorithm is applied to a haemodynamic numerical experiment, which demonstrates that the approach by optimization is faster than a Dirichlet–Neumann implicit decoupled approach augmented by Aitken's relaxation. A parameter study is also included to show the effects of the Tikhonov regularization parameter on the optimal solution found.

4.2 Weak Formulation of the Constraints

Assuming $\mathbf{f}_f^n, \mathbf{f}_s^{n-1}, \mathbf{f}_s^n \in \mathbf{L}^2(\Omega_{t_n}^f)$, $\mathbf{g}^n \in \mathbf{L}^2(\Gamma_{I_{t_n}})$, $\mathbf{u}_N^n \in \mathbf{L}^2(\Gamma_N^f)$, $\boldsymbol{\eta}_N^n \in \mathbf{L}^2(\Gamma_N^s)$, $\mathbf{u}^{n-1} \in \boldsymbol{H}_D^1(\Omega_{t_{n-1}}^f)$, and $\boldsymbol{\eta}^{n-1} \in \boldsymbol{H}_D^1(\Omega^s)$, (2.38)–(2.39) can be rewritten as

$$\begin{aligned}
\rho^f[(\mathbf{u}^n,\mathbf{v})_{\Omega_{t_n}^f} &- (\mathbf{u}^{n-1},\mathcal{V}(\mathbf{v}))_{\Omega_{t_{n-1}}^f}] + \Delta t\ \rho^f[c(\mathbf{u}^n,\mathbf{u}^n,\mathbf{v})_{\Omega_{t_n}^f} + \frac{1}{2}((\mathbf{u}^n\cdot\mathbf{n}_f)\mathbf{u}^n,\mathbf{v})_{\Gamma_{I_{t_n}}} \\
&+ \frac{1}{2}((\mathbf{u}^n\cdot\mathbf{n}_f)\mathbf{u}^n,\mathbf{v})_{\Gamma_N^f} - \frac{1}{2}((\mathbf{z}^n\cdot\mathbf{n}_f)\mathbf{u}^n,\mathbf{v})_{\Gamma_{I_{t_n}}} - \frac{1}{2}((\nabla\cdot\mathbf{z}^n)\mathbf{u}^n,\mathbf{v})_{\Omega_{t_n}^f} \\
&- c(\mathbf{z}^n,\mathbf{u}^n,\mathbf{v})_{\Omega_{t_n}^f}] + \Delta t\ 2\nu_f a(\mathbf{u}^n,\mathbf{v})_{\Omega_{t_n}^f} + \Delta t\ b(\mathbf{v},p^n)_{\Omega_{t_n}^f} \\
&= \Delta t\ (\mathbf{f}_f^n,\mathbf{v})_{\Omega_{t_n}^f} + \Delta t\ (\mathbf{u}_N^n,\mathbf{v})_{\Gamma_N^f} \qquad (4.1)\\
&\quad + \Delta t\ (2\nu_f D(\mathbf{u}^n)\cdot\mathbf{n}_f - p\mathbf{n}_f,\mathbf{v})_{\Gamma_{I_{t_n}}} \quad \forall\mathbf{v}\in\boldsymbol{H}_D^1(\Omega_{t_n}^f),
\end{aligned}$$

$$b(\mathbf{u}^n,q)_{\Omega_{t_n}^f} = 0 \quad q\in L^2(\Omega_{t_n}^f), \qquad (4.2)$$

using

$$\begin{aligned}
(\mathbf{u}^n\cdot\nabla\mathbf{u}^n,\mathbf{v})_{\Omega_{t_n}^f} &= -(\mathbf{u}^n\cdot\nabla\mathbf{v},\mathbf{u}^n)_{\Omega_{t_n}^f} - ((\nabla\cdot\mathbf{u}^n)\mathbf{v},\mathbf{u}^n)_{\Omega_{t_n}^f} + ((\mathbf{u}^n\cdot\mathbf{n}_f)\mathbf{v},\mathbf{u}^n)_{\Gamma_{I_{t_n}}\cup\Gamma_N^f},\\
(\mathbf{z}^n\cdot\nabla\mathbf{u}^n,\mathbf{v})_{\Omega_{t_n}^f} &= -(\mathbf{z}^n\cdot\nabla\mathbf{v},\mathbf{u}^n)_{\Omega_{t_n}^f} - ((\nabla\cdot\mathbf{z}^n)\mathbf{v},\mathbf{u}^n)_{\Omega_{t_n}^f} + ((\mathbf{z}^n\cdot\mathbf{n}_f)\mathbf{v},\mathbf{u}^n)_{\Gamma_{I_{t_n}}\cup\Gamma_N^f},
\end{aligned}$$

by Green's Theorem and $((\mathbf{z}^n\cdot\mathbf{n}_f)\mathbf{v},\mathbf{u}^n)_{\Gamma_N^f} = 0$ since $\mathbf{z}^n|_{\Gamma_N^f} = 0$ because Γ_N^f is fixed.

On the interface, we replace

$$(2\nu_f D(\mathbf{u}^n)\cdot\mathbf{n}_f - p\mathbf{n}_f - \frac{1}{2}((\mathbf{u}^n-\mathbf{z}^n)\cdot\mathbf{n}_f)\mathbf{u}^n,\mathbf{v})_{\Gamma_{I_{t_n}}} \tag{4.3}$$

with $(\mathbf{g}^n,\mathbf{v})_{\Gamma_{I_{t_n}}}$ where $\mathbf{g}^n|_{\Gamma_{I_{t_n}}}$ will become our control. We similarly replace $(2\nu_s D(\boldsymbol{\eta}^n)\cdot\mathbf{n}_s + \lambda(\nabla\cdot\boldsymbol{\eta}^n)\mathbf{n}_s,\boldsymbol{\xi})$ with $-(\mathcal{V}(\mathbf{g}^n)J_{t_n},\boldsymbol{\xi})_{\Gamma_{I_{t_0}}}$. The terms replaced by the control differ from the terms selected in Chapter 3. The purpose in adding terms to the control is to make analysis of the problem possible. A detailed explanation of the justification for this substitution is given in Section 4.3.

Making these substitutions, (4.1) and (4.2) become

$$\begin{aligned}\rho^f[(\mathbf{u}^n,\mathbf{v})_{\Omega^f_{t_n}} - (\mathbf{u}^{n-1},\mathcal{V}(\mathbf{v}))_{\Omega^f_{t_{n-1}}}] + \Delta t\ \rho^f[c(\mathbf{u}^n,\mathbf{u}^n,\mathbf{v})_{\Omega^f_{t_n}} + \frac{1}{2}((\mathbf{u}^n\cdot\mathbf{n}_f)\mathbf{u}^n,\mathbf{v})_{\Gamma^f_N}\\ - \frac{1}{2}((\nabla\cdot\mathbf{z}^n)\mathbf{u}^n,\mathbf{v})_{\Omega^f_{t_n}} - c(\mathbf{z}^n,\mathbf{u}^n,\mathbf{v})_{\Omega^f_{t_n}}]\\ + \Delta t\ 2\nu_f a(\mathbf{u}^n,\mathbf{v})_{\Omega^f_{t_n}} + \Delta t\ b(\mathbf{v},p^n)_{\Omega^f_{t_n}}\\ = \Delta t\ (\mathbf{f}^n_f,\mathbf{v})_{\Omega^f_{t_n}} + \Delta t\ (\mathbf{u}^n_N,\mathbf{v})_{\Gamma^f_N} + \Delta t\ (\mathbf{g}^n,\mathbf{v})_{\Gamma_{I_{t_n}}} \quad \forall\mathbf{v}\in\boldsymbol{H}^1_D(\Omega^f_{t_n}),\end{aligned} \tag{4.4}$$

$$b(\mathbf{u}^n,q)_{\Omega^f_{t_n}} = 0 \quad q\in L^2(\Omega^f_{t_n}). \tag{4.5}$$

Also, (2.40) and (2.41) can be rewritten as

$$\begin{aligned}\rho^s[(\dot{\boldsymbol{\eta}}^n,\boldsymbol{\xi})_{\Omega^s} - (\dot{\boldsymbol{\eta}}^{n-1},\boldsymbol{\xi})_{\Omega^s}] + \Delta t\ \nu_s d(\boldsymbol{\eta}^n+\boldsymbol{\eta}^{n-1},\boldsymbol{\xi})_{\Omega^s} + \frac{\Delta t}{2}\ \lambda e(\boldsymbol{\eta}^n+\boldsymbol{\eta}^{n-1},\boldsymbol{\xi})_{\Omega^s}\\ = \frac{\Delta t}{2}\ (\mathbf{f}^n_s+\mathbf{f}^{n-1}_s,\boldsymbol{\xi})_{\Omega^s} + \frac{\Delta t}{2}\ (\boldsymbol{\eta}^n_N+\boldsymbol{\eta}^{n-1}_N,\boldsymbol{\xi})_{\Gamma^s_N}\\ - \frac{\Delta t}{2}\ (\mathcal{V}(\mathbf{g}^n)J_{t_n}+\mathcal{V}(\mathbf{g}^{n-1})J_{t_{n-1}},\boldsymbol{\xi})_{\Gamma_{I_{t_0}}} \quad \forall\boldsymbol{\xi}\in\boldsymbol{H}^1_D(\Omega^s),\end{aligned} \tag{4.6}$$

$$\frac{\Delta t}{2}[(\dot{\boldsymbol{\eta}}^n,\boldsymbol{\gamma})_{\Omega^s} + (\dot{\boldsymbol{\eta}}^{n-1},\boldsymbol{\gamma})_{\Omega^s}] = (\boldsymbol{\eta}^n,\boldsymbol{\gamma})_{\Omega^s} - (\boldsymbol{\eta}^{n-1},\boldsymbol{\gamma})_{\Omega^s} \quad \forall\boldsymbol{\gamma}\in\boldsymbol{L}^2(\Omega^s). \tag{4.7}$$

4.3 Description of the Optimization Problem

For any choice of $\mathbf{g}^n$, (4.4)–(4.5) and (4.6)–(4.7) can be solved independently. Therefore, using $\mathbf{g}^n$ as a control at each time step permits the fluid and structure subsystems to

be solved simultaneously using partitioned solvers. For any $\mathbf{g}^n$ chosen arbitrarily, we should not expect that the solution will satisfy the interface conditions (2.11)–(2.12), which are necessary to satisfy the system (2.38)–(2.39) and (2.40)–(2.41).

In order to attempt to enforce the continuity of velocity (2.11) and continuity of stress (2.12) along the interface, we wish to minimize the penalized functional

$$\mathcal{J}_n^\delta(\mathbf{u}^n, p^n, \boldsymbol{\eta}^n, \dot{\boldsymbol{\eta}}^n, \mathbf{g}^n) = \frac{1}{2}\int_{\Gamma_{I_{t_n}}} |\mathbf{u}^n - \mathcal{V}(\dot{\boldsymbol{\eta}}^n)|^2 \, d\Gamma_{I_{t_n}} + \frac{\delta}{2}\int_{\Gamma_{I_{t_n}}} |\mathbf{g}^n|^2 \, d\Gamma_{I_{t_n}} , \tag{4.8}$$

subject to (4.4)–(4.5) and (4.6)–(4.7), where $\Gamma_{I_{t_n}}$ denotes the interface in the n-th time step and δ is a positive constant penalty parameter that is chosen to dictate the importance of the last term in (4.8). This optimal control problem is to be solved at each time step.

We anticipate that it will not be possible to get a stability estimate for $\dot{\boldsymbol{\eta}}^n$ in $\boldsymbol{H}^1_D(\Omega^s)$ and the existence of an optimal $\hat{\dot{\boldsymbol{\eta}}}^n$ can be shown only in $\mathbf{L}^2(\Omega^s)$. In this case, the functional (4.8) is not well-defined since the trace of an optimal $\dot{\boldsymbol{\eta}}^n$ on $\Gamma_{I_{t_n}}$ is not well-defined. In order to avoid this difficulty, we will replace $\dot{\boldsymbol{\eta}}^n$ with its first order approximation, $\frac{\boldsymbol{\eta}^n - \boldsymbol{\eta}^{n-1}}{\Delta t}$. As will be seen in Remark 4.6, using a first order approximation in the functional will cause no greater loss in accuracy than using a higher order approximation. With $\mathbf{u}^{n-1}$, $\boldsymbol{\eta}^{n-1}$, and $\dot{\boldsymbol{\eta}}^{n-1}$ as known data obtained at the previous time step, we wish to minimize

$$\mathcal{J}_n^\delta(\mathbf{u}^n, p^n, \boldsymbol{\eta}^n, \dot{\boldsymbol{\eta}}^n, \mathbf{g}^n) = \frac{1}{2}\int_{\Gamma_{I_{t_n}}} \left|\mathbf{u}^n - \frac{\mathcal{V}(\boldsymbol{\eta}^n) - \mathcal{V}(\boldsymbol{\eta}^{n-1})}{\Delta t}\right|^2 \, d\Gamma_{I_{t_n}} + \frac{\delta}{2}\int_{\Gamma_{I_{t_n}}} |\mathbf{g}^n|^2 \, d\Gamma_{I_{t_n}} , \tag{4.9}$$

subject to (4.4)–(4.5) and (4.6)–(4.7), which will enforce continuity of velocity and stress along the interface (2.11)–(2.12).

The optimization problem to be solved is

find $\mathbf{u}^n, p^n, \boldsymbol{\eta}^n, \dot{\boldsymbol{\eta}}^n,$ and $\mathbf{g}^n$ such that (4.9) is minimized

subject to (4.4)–(4.5) and (4.6)–(4.7) for a given $\mathbf{u}^{n-1}$, $\boldsymbol{\eta}^{n-1}$, and $\dot{\boldsymbol{\eta}}^{n-1}$, (4.10)

and our admissibility set is

$$S := \{(\mathbf{u}^n, p^n, \boldsymbol{\eta}^n, \dot{\boldsymbol{\eta}}^n, \mathbf{g}^n) \in \boldsymbol{H}^1_D(\Omega^f_{t_n}) \times L^2(\Omega^f_{t_n}) \times \boldsymbol{H}^1_D(\Omega^s) \times \boldsymbol{L}^2(\Omega^s) \times \mathbf{L}^2(\Gamma_{I_{t_n}}) : \\ \mathcal{J}^\delta_n(\mathbf{u}^n, p^n, \boldsymbol{\eta}^n, \dot{\boldsymbol{\eta}}^n, \mathbf{g}^n) < \infty \text{ and (4.4)–(4.5) and (4.6)–(4.7) are satisfied.}\} \tag{4.11}$$

Then $(\hat{\mathbf{u}}^n, \hat{p}^n, \hat{\boldsymbol{\eta}}^n, \hat{\dot{\boldsymbol{\eta}}}^n, \hat{\mathbf{g}}^n) \in S$ is called an optimal solution if there exists $\epsilon > 0$ such that

$$\begin{aligned} \mathcal{J}^\delta_n(\hat{\mathbf{u}}^n, \hat{p}^n, \hat{\boldsymbol{\eta}}^n, \hat{\dot{\boldsymbol{\eta}}}^n, \hat{\mathbf{g}}^n) \quad &\leq \quad \mathcal{J}^\delta_n(\mathbf{u}^n, p^n, \boldsymbol{\eta}^n, \dot{\boldsymbol{\eta}}^n, \mathbf{g}^n) \\ \forall (\mathbf{u}^n, p^n, \boldsymbol{\eta}^n, \dot{\boldsymbol{\eta}}^n, \mathbf{g}^n) \in S \quad &\text{satisfying} \quad \|\mathbf{g}^n - \hat{\mathbf{g}}^n\|_{0,\Gamma_{I_{t_n}}} \leq \epsilon. \end{aligned} \tag{4.12}$$

Now that we have an objective to minimize, we can explain the rationale for our substitution of the control into the semidiscrete weak formulation of the FSI problem. When replacing terms with the control in the fluid equations, $\frac{1}{2}((\mathbf{u}^n - \mathbf{z}^n) \cdot \mathbf{n}_f)\mathbf{u}^n|_{\Gamma_{I_{t_n}}}$ was added to (4.3) in order to make a stability result for the resulting weak form of the partial differential equation possible. If we choose a $\mathbf{g}^n$ which results in a solution that satisfies $\mathbf{u}^n|_{\Gamma_{I_{t_n}}} \approx (\frac{\boldsymbol{\eta}^n - \boldsymbol{\eta}^{n-1}}{\Delta t}) \circ \Psi^{-1}_{t_n}|_{\Gamma_{I_{t_n}}}$, then $\mathbf{u}^n|_{\Gamma_{I_{t_n}}} \approx \mathbf{z}^n|_{\Gamma_{I_{t_n}}}$ by the definition of $\mathbf{z}^n$ in (2.37). This means that $\frac{1}{2}((\mathbf{u}^n - \mathbf{z}^n) \cdot \mathbf{n}_f)\mathbf{u}^n|_{\Gamma_{I_{t_n}}}$ will be almost zero and therefore the control $\mathbf{g}^n$ will represent $2\nu_f D(\mathbf{u}^n) \cdot \mathbf{n}_f - p\mathbf{n}_f|_{\Gamma_{I_{t_n}}}$ in the fluid equations and $-(\mathbf{g}^n \circ \Psi_n)J_{t_n}$ will represent $2\nu_s D(\boldsymbol{\eta}^n) \cdot \mathbf{n}_s + \lambda(\nabla \cdot \boldsymbol{\eta}^n)\mathbf{n}_s|_{\Gamma_{I_{t_0}}}$ in the structure equations. Since $\mathbf{g}^n$ then holds the place of the interfacial stress common to both subsystems, the continuity of stress on the interface (2.12) will be satisfied. While many solutions may exist such that $\frac{1}{2}((\mathbf{u}^n - \mathbf{z}^n) \cdot \mathbf{n}_f)\mathbf{u}^n|_{\Gamma_{I_{t_n}}}$ will be approximately zero, this will certainly be the case at an optimal solution.

4.4 A Priori Estimates

We make the following assumptions to obtain a priori bounds for solutions to the weak formulations (4.4)–(4.7) and for analysis throughout the rest of this chapter:

- the Neumann boundary Γ_N^f is an outflow boundary, (4.13)
- $\Omega_t^f = \Psi_t(\Omega_{t_0}^f)$ is a Lipschitz domain, (4.14)
- $\Psi_t \in \mathbf{W}^{1,\infty}(\Omega_{t_0}^f)$ and $\Psi_t^{-1} \in \mathbf{W}^{1,\infty}(\Omega_t^f)\ \forall t \in [t_0, T]$, (4.15)
- $\mathbf{z}, \dfrac{\partial \mathbf{z}}{\partial t} \in \mathbf{W}^{1,\infty}(\Omega_t^f)\ \forall t \in [t_0, T]$. (4.16)

Assumption (4.13) is necessary for stability of any Navier–Stokes flow with nonhomogeneous Neumann boundary conditions. Assumptions (4.14)–(4.16) are reasonable for the movement and shape of the moving domain [32, 56].

As a result of (4.14) and (4.15), proposition 2.1 of [56] further gives

$$\exists \kappa_{min}, \kappa_{max} \in \mathbb{R}^+ \text{ such that } \ 0 < \kappa_{min} \leq J_t \leq \kappa_{max} < \infty \ \forall\ t \in [t_0, T]. \tag{4.17}$$

The following estimates will be used for analysis of the optimal control problem.

Theorem 4.1. *Stability of* $\mathbf{u}^n$

If $\Delta t^2\ C_9 \left\|\nabla \cdot \mathbf{z}^i\right\|_{L^\infty, \Omega_{t_i}^f} < 1$ *for* $i = 1, \ldots, n$ *where*
$C_9 = \left\|\nabla_{\mathbf{y}} \mathcal{V}(\mathbf{z}^i)\right\|_{L^\infty, \Omega_{t_0}^f} \left\|\nabla_{\mathbf{y}} \Psi_t\right\|_{L^\infty, \Omega_{t_0}^f}$, *then*

$$\begin{aligned} &\rho^f \left\|\mathbf{u}^n\right\|_{0,\Omega_{t_n}^f}^2 + 2\Delta t \sum_{i=1}^{n} \nu_f C_6 \left\|\mathbf{u}^i\right\|_{1,\Omega_{t_i}^f}^2 \\ &\qquad \leq C \left[\Delta t \sum_{i=0}^{n} \left[\left\|\mathbf{f}_f^i\right\|_{0,\Omega_{t_i}^f}^2 + \left\|\mathbf{u}_N^i\right\|_{0,\Gamma_N^f}^2 + \left\|\mathbf{g}^i\right\|_{0,\Gamma_{I_{t_i}}}^2\right] + \rho^f \left\|\mathbf{u}^0\right\|_{0,\Omega_{t_0}^f}^2\right]. \end{aligned} \tag{4.18}$$

Proof. Let $(\mathbf{v}, q) = (\mathbf{u}^n, p^n)$ in (4.4)–(4.5). From this,

$$\begin{aligned}
\rho^f \Big[\|\mathbf{u}^n\|^2_{0,\Omega^f_{t_n}} \; & -(\mathbf{u}^{n-1}, \mathcal{V}(\mathbf{u}^n))_{\Omega^f_{t_{n-1}}} \Big] \\
& + \Delta t \; \rho^f \Big[c(\mathbf{u}^n, \mathbf{u}^n, \mathbf{u}^n)_{\Omega^f_{t_n}} + \frac{1}{2}((\mathbf{u}^n \cdot \mathbf{n}_f), |\mathbf{u}^n|^2)_{\Gamma^f_N} - \frac{1}{2}((\nabla \cdot \mathbf{z}^n), |\mathbf{u}^n|^2)_{\Omega^f_{t_n}} \\
& - c(\mathbf{z}^n, \mathbf{u}^n, \mathbf{u}^n)_{\Omega^f_{t_n}} \Big] + \Delta t \; 2\nu_f a(\mathbf{u}^n, \mathbf{u}^n)_{\Omega^f_{t_n}} + \Delta t \; b(\mathbf{u}^n, p^n)_{\Omega^f_{t_n}} \\
& = \Delta t \; (\mathbf{f}^n_f, \mathbf{u}^n)_{\Omega^f_{t_n}} + \Delta t \; (\mathbf{u}^n_N, \mathbf{u}^n)_{\Gamma^f_N} + \Delta t \; (\mathbf{g}^n, \mathbf{u}^n)_{\Gamma_{I_{t_n}}}, \qquad (4.19) \\
b(\mathbf{u}^n, p^n)_{\Omega^f_{t_n}} & = 0. \qquad (4.20)
\end{aligned}$$

Using $c(\mathbf{u}^n, \mathbf{u}^n, \mathbf{u}^n)_{\Omega^f_{t_n}} = 0$, $c(\mathbf{z}^n, \mathbf{u}^n, \mathbf{u}^n)_{\Omega^f_{t_n}} = 0$, dropping $\frac{1}{2}((\mathbf{u}^n \cdot \mathbf{n}_f), |\mathbf{u}^n|^2)_{\Gamma^f_N}$ by the assumption $\mathbf{u}^n \cdot \mathbf{n}_f > 0$ (4.13), and also using $b(\mathbf{u}^n, p^n)_{\Omega^f_{t_n}} = 0$ in (4.19) gives

$$\begin{aligned}
\rho^f \|\mathbf{u}^n\|^2_{0,\Omega^f_{t_n}} & - \Delta t \; \frac{\rho^f}{2}((\nabla \cdot \mathbf{z}^n), |\mathbf{u}^n|^2)_{\Omega^f_{t_n}} + \Delta t \; 2\nu_f a(\mathbf{u}^n, \mathbf{u}^n)_{\Omega^f_{t_n}} \\
& \leq \Delta t \; (\mathbf{f}^n_f, \mathbf{u}^n)_{\Omega^f_{t_n}} + \Delta t \; (\mathbf{u}^n_N, \mathbf{u}^n)_{\Gamma^f_N} + \Delta t \; (\mathbf{g}^n, \mathbf{u}^n)_{\Gamma_{I_{t_n}}} + \rho^f (\mathbf{u}^{n-1}, \mathcal{V}(\mathbf{u}^n))_{\Omega^f_{t_{n-1}}}. \qquad (4.21)
\end{aligned}$$

Combining terms and using (2.19) and Cauchy-Schwarz inequality in (4.21) yields

$$\begin{aligned}
\rho^f \|\mathbf{u}^n\|^2_{0,\Omega^f_{t_n}} & - \Delta t \; \frac{\rho^f}{2} \; ((\nabla \cdot \mathbf{z}^n), |\mathbf{u}^n|^2)_{\Omega^f_{t_n}} + \Delta t \; 2\nu_f C_6 \, \|\mathbf{u}^n\|^2_{1,\Omega^f_{t_n}} \\
& \leq \Delta t \; \left\|\mathbf{f}^n_f\right\|_{-1,\Omega^f_{t_n}} \|\mathbf{u}^n\|_{1,\Omega^f_{t_n}} + \Delta t \; \|\mathbf{u}^n_N\|_{0,\Gamma^f_N} \|\mathbf{u}^n\|_{0,\Gamma^f_N} + \Delta t \; \|\mathbf{g}^n\|_{0,\Gamma_{I_{t_n}}} \|\mathbf{u}^n\|_{0,\Gamma_{I_{t_n}}} \\
& \quad + \rho^f \left\|\mathbf{u}^{n-1}\right\|_{0,\Omega^f_{t_{n-1}}} \|\mathcal{V}(\mathbf{u}^n)\|_{0,\Omega^f_{t_{n-1}}}. \qquad (4.22)
\end{aligned}$$

The trace theorem followed by Young's inequality with an appropriate choice of parameters

gives

$$\begin{aligned}\rho^f \left\|\mathbf{u}^n\right\|^2_{0,\Omega^f_{t_n}} &- \Delta t\, \frac{\rho^f}{2}\left((\nabla\cdot\mathbf{z}^n), |\mathbf{u}^n|^2\right)_{\Omega^f_{t_n}} + \Delta t\; 2\nu_f C_6 \left\|\mathbf{u}^n\right\|^2_{1,\Omega^f_{t_n}} \\ &\leq C\Delta t\, \left[\left\|\mathbf{f}^n_f\right\|^2_{-1,\Omega^f_{t_n}} + \left\|\mathbf{u}^n_N\right\|^2_{0,\Gamma^f_N} + \left\|\mathbf{g}^n\right\|^2_{0,\Gamma_{I_{t_n}}}\right] + \Delta t\; \nu_f C_6 \left\|\mathbf{u}^n\right\|^2_{1,\Omega^f_{t_n}} \\ &+ \rho^f \left[\frac{1}{2}\left\|\mathbf{u}^{n-1}\right\|^2_{0,\Omega^f_{t_{n-1}}} + \frac{1}{2}\left\|\mathcal{V}(\mathbf{u}^n)\right\|^2_{0,\Omega^f_{t_{n-1}}}\right]. \end{aligned} \tag{4.23}$$

We rewrite and combine like terms in (4.23) to get

$$\begin{aligned}\frac{\rho^f}{2}\left[\left\|\mathbf{u}^n\right\|^2_{0,\Omega^f_{t_n}} - \left\|\mathbf{u}^{n-1}\right\|^2_{0,\Omega^f_{t_{n-1}}}\right] &+ \frac{\rho^f}{2}\left[\left\|\mathbf{u}^n\right\|^2_{0,\Omega^f_{t_n}} - \left\|\mathcal{V}(\mathbf{u}^n)\right\|^2_{0,\Omega^f_{t_{n-1}}}\right] \\ &- \Delta t\, \frac{\rho^f}{2}\left((\nabla\cdot\mathbf{z}^n), |\mathbf{u}^n|^2\right)_{\Omega^f_{t_n}} + \Delta t\; \nu_f C_6 \left\|\mathbf{u}^n\right\|^2_{1,\Omega^f_{t_n}} \\ &\leq C\Delta t\, \left[\left\|\mathbf{f}^n_f\right\|^2_{0,\Omega^f_{t_n}} + \left\|\mathbf{u}^n_N\right\|^2_{0,\Gamma^f_N} + \left\|\mathbf{g}^n\right\|^2_{0,\Gamma_{I_{t_n}}}\right]. \end{aligned} \tag{4.24}$$

Since $\mathbf{u}^n$ is not time dependent, we can integrate both sides of (2.32) from t_{n-1} to t_n where $\boldsymbol{\phi}(\mathbf{x},t) = (\mathbf{u}^n(\mathbf{x}))^2$ as in [15], using

$$\int_{t_{n-1}}^{t_n} \frac{d}{dt}\int_{\Omega^f_t} |\mathbf{u}^n|^2\, d\Omega^f_t\; dt = \int_{t_{n-1}}^{t_n}\int_{\Omega^f_t} \frac{\partial \mathcal{V}((\mathbf{u}^n)^2)}{\partial t}|_{\mathbf{y}} + (\nabla_{\mathbf{x}}\cdot\mathbf{z}(\mathbf{x},t))|\mathcal{V}(\mathbf{u}^n)|^2\, d\Omega^f_t\; dt$$

with $\mathbf{z}(\mathbf{x},t) = \mathbf{z}^n(\mathbf{x})\ \forall t \in [t_{n-1}, t_n]$ by (2.37) and $\frac{\partial \mathcal{V}((\mathbf{u}^n)^2)}{\partial t}|_{\mathbf{y}} = 0$, to get

$$\begin{aligned}\left\|\mathbf{u}^n\right\|^2_{0,\Omega^f_{t_n}} &- \left\|\mathcal{V}(\mathbf{u}^n)\right\|^2_{0,\Omega^f_{t_{n-1}}} - \Delta t\, \left((\nabla_{\mathbf{x}}\cdot\mathbf{z}^n), |\mathbf{u}^n|^2\right)_{0,\Omega^f_{t_n}} \\ &= \int_{t_{n-1}}^{t_n} \left((\nabla_{\mathbf{x}}\cdot\mathbf{z}^n), |\mathcal{V}(\mathbf{u}^n)|^2\right)_{0,\Omega^f_t}\, dt - \Delta t\, \left((\nabla_{\mathbf{x}}\cdot\mathbf{z}^n), |\mathbf{u}^n|^2\right)_{0,\Omega^f_{t_n}}. \end{aligned}$$

Because $\mathbf{u}^n$ and $\mathcal{V}(\mathbf{u}^n)$ have the same values for corresponding points on the moving domain, and $|J_t - J_{t_n}| \leq \Delta t\; C_9$ where $C_9 = C\left\|\nabla_{\mathbf{y}}\mathcal{V}(\mathbf{z}^n)\right\|_{L^\infty,\Omega^f_{t_0}} \left\|\nabla_{\mathbf{y}}\Psi_t\right\|_{L^\infty,\Omega^f_{t_0}}$ and C is a positive

constant that does not depend on Δt or the ALE mapping (see [15]),

$$\begin{aligned}
\|\mathbf{u}^n\|^2_{0,\Omega^f_{t_n}} - \|\mathcal{V}(\mathbf{u}^n)\|^2_{0,\Omega^f_{t_{n-1}}} - \Delta t\ ((\nabla_{\mathbf{x}}\cdot\mathbf{z}^n), |\mathbf{u}^n|^2)_{0,\Omega^f_{t_n}} \\
&\leq \int_{t_{n-1}}^{t_n} ((\nabla_{\mathbf{x}}\cdot\mathbf{z}^n), |\mathcal{V}(\mathbf{u}^n)|^2(J_t - J_{t_n}))_{\Omega^f_{t_0}}\ dt \\
&\leq \Delta t^2\ C_9\ (|\nabla\cdot\mathbf{z}^n|, |\mathbf{u}^n|^2)_{0,\Omega^f_{t_n}} \\
&\leq \Delta t^2\ C_9\ \|\nabla\cdot\mathbf{z}^n\|_{L^\infty,\Omega^f_{t_n}}\ \|\mathbf{u}^n\|^2_{0,\Omega^f_{t_n}} \qquad (4.25)
\end{aligned}$$

Substituting (4.25) into (4.24),

$$\begin{aligned}
&\frac{\rho^f}{2}\left[\ \|\mathbf{u}^n\|^2_{0,\Omega^f_{t_n}} - \left\|\mathbf{u}^{n-1}\right\|^2_{0,\Omega^f_{t_{n-1}}}\right] + \Delta t\ \nu_f C_6\ \|\mathbf{u}^n\|^2_{1,\Omega^f_{t_n}} \\
&\quad\leq C\Delta t\ \left[\left\|\mathbf{f}^n_f\right\|^2_{0,\Omega^f_{t_n}} + \|\mathbf{u}^n_N\|^2_{0,\Gamma^f_N} + \|\mathbf{g}^n\|^2_{0,\Gamma_{I_{t_n}}}\right] + \Delta t^2\ \frac{\rho^f C_9}{2}\ \|\nabla\cdot\mathbf{z}^n\|_{L^\infty,\Omega^f_{t_n}}\ \|\mathbf{u}^n\|^2_{0,\Omega^f_{t_n}}\ .
\end{aligned}$$

Observe that with $\nabla\cdot\mathbf{z}^n \in L^\infty(\Omega^f_{t_n})$, an implication of (4.16), we can derive two stability results. The first is for boundedness at a single time step:

$$\begin{aligned}
&\frac{\rho^f}{2}\left[1\ -\Delta t^2\ C_9\ \|\nabla\cdot\mathbf{z}^n\|_{L^\infty,\Omega^f_{t_n}}\right]\|\mathbf{u}^n\|^2_{0,\Omega^f_{t_n}} + \Delta t\ \nu_f C_6\ \|\mathbf{u}^n\|^2_{1,\Omega^f_{t_n}} \\
&\quad\leq C\Delta t\ \left[\left\|\mathbf{f}^n_f\right\|^2_{0,\Omega^f_{t_n}} + \|\mathbf{u}^n_N\|^2_{0,\Gamma^f_N} + \|\mathbf{g}^n\|^2_{0,\Gamma_{I_{t_n}}}\right] + \left\|\mathbf{u}^{n-1}\right\|^2_{0,\Omega^f_{t_{n-1}}}\ .
\end{aligned}$$

The second is for boundedness over all time steps using a discrete Gronwall lemma after

first multiplying by 2 and summing over time steps.

$$\begin{aligned}\rho^f \left\|\mathbf{u}^n\right\|^2_{0,\Omega^f_{t_n}} &+ 2\Delta t \sum_{i=1}^{n} \nu_f C_6 \left\|\mathbf{u}^i\right\|^2_{1,\Omega^f_{t_i}} \\ &\leq C\Delta t \sum_{i=0}^{n} \left[\left\|\mathbf{f}^i_f\right\|^2_{0,\Omega^f_{t_i}} + \left\|\mathbf{u}^i_N\right\|^2_{0,\Gamma^f_N} + \left\|\mathbf{g}^i\right\|^2_{0,\Gamma_{I_{t_i}}} \right] \\ &+ \Delta t \sum_{i=0}^{n} \Delta t\, C_9 \left\|\nabla\cdot\mathbf{z}^i\right\|_{L^\infty,\Omega^f_{t_i}} \rho^f \left\|\mathbf{u}^i\right\|^2_{0,\Omega^f_{t_i}} + \rho^f \left\|\mathbf{u}^0\right\|^2_{0,\Omega^f_{t_0}}.\end{aligned}$$

This yields

$$\begin{aligned}\rho^f \left\|\mathbf{u}^n\right\|^2_{0,\Omega^f_{t_n}} &+ 2\Delta t \sum_{i=1}^{n} \nu_f C_6 \left\|\mathbf{u}^i\right\|^2_{1,\Omega^f_{t_i}} \\ &\leq C \left[\Delta t \sum_{i=0}^{n} \left[\left\|\mathbf{f}^i_f\right\|^2_{0,\Omega^f_{t_i}} + \left\|\mathbf{u}^i_N\right\|^2_{0,\Gamma^f_N} + \left\|\mathbf{g}^i\right\|^2_{0,\Gamma_{I_{t_i}}} \right] + \rho^f \left\|\mathbf{u}^0\right\|^2_{0,\Omega^f_{t_0}} \right]\end{aligned}$$

when $\Delta t^2\ C_9 \left\|\nabla\cdot\mathbf{z}^i\right\|_{L^\infty,\Omega^f_{t_i}} < 1$ for $i = 1,\ldots,n$, according to the discrete Gronwall lemma [44]. Therefore, Δt must be chosen sufficiently small. □

Theorem 4.2. *Stability of p^n*

If $\Delta t^2\ C_9 \left\|\nabla\cdot\mathbf{z}^i\right\|_{L^\infty,\Omega^f_{t_i}} < 1$ for $i = 1,\ldots,n$, then

$$\left\|p^n\right\|_{0,\Omega^f_{t_n}} \leq C\ P(\left\|\mathbf{f}^0_f\right\|_{0,\Omega^f_{t_0}}, \left\|\mathbf{g}^0\right\|_{0,\Gamma_{I_{t_0}}}, \left\|\mathbf{u}^0_N\right\|_{0,\Gamma^f_N}, \ldots, \left\|\mathbf{f}^n_f\right\|_{0,\Omega^f_{t_n}}, \left\|\mathbf{g}^n\right\|_{0,\Gamma_{I_{t_n}}}, \left\|\mathbf{u}^n_N\right\|_{0,\Gamma^f_N}), \tag{4.26}$$

where $P(\cdot,\ldots,\cdot)$ is a quadratic polynomial.

Proof. Rearranging (4.4), we get

$$\begin{aligned}b(\mathbf{v},p^n)_{\Omega^f_{t_n}} = &-\frac{\rho^f}{\Delta t}\left[(\mathbf{u}^n,\mathbf{v})_{\Omega^f_{t_n}} - (\mathbf{u}^{n-1},\mathcal{V}(\mathbf{v}))_{\Omega^f_{t_{n-1}}}\right] + \rho^f\left[-c(\mathbf{u}^n,\mathbf{u}^n,\mathbf{v})_{\Omega^f_{t_n}} + c(\mathbf{z}^n,\mathbf{u}^n,\mathbf{v})_{\Omega^f_{t_n}}\right. \\ &\left.+\frac{1}{2}((\nabla\cdot\mathbf{z}^n)\mathbf{u}^n,\mathbf{v})_{\Omega^f_{t_n}} - \frac{1}{2}((\mathbf{u}^n\cdot\mathbf{n}_f)\mathbf{u}^n,\mathbf{v})_{\Gamma^f_N}\right] - 2\nu_f a(\mathbf{u}^n,\mathbf{v})_{\Omega^f_{t_n}} + (\mathbf{f}^n_f,\mathbf{v})_{\Omega^f_{t_n}} \\ &+ (\mathbf{u}^n_N,\mathbf{v})_{\Gamma^f_N} + (\mathbf{g}^n,\mathbf{v})_{\Gamma_{I_{t_n}}} \quad \forall\mathbf{v}\in\boldsymbol{H}^1_D(\Omega^f_{t_n}).\end{aligned} \tag{4.27}$$

In (4.27),

$$
\begin{aligned}
\left(\mathbf{u}^{n-1}, \mathcal{V}(\mathbf{v})\right)_{\Omega^f_{t_{n-1}}} &= \int_{\Omega^f_{t_{n-1}}} \mathbf{u}^{n-1} \cdot \mathcal{V}(\mathbf{v})\, d\Omega^f_{t_{n-1}} \\
&= \int_{\Omega^f_{t_0}} J_{t_{n-1}} \mathcal{V}(\mathbf{u}^{n-1}) \cdot \mathcal{V}(\mathbf{v})\, d\Omega^f_{t_0} \\
&\leq \int_{\Omega^f_{t_0}} J_{t_{n-1}} \mathcal{V}(\mathbf{u}^{n-1}) \cdot \mathcal{V}(\mathbf{v}) \frac{J_{t_n}}{\kappa_{min}}\, d\Omega^f_{t_0} \\
&\leq \frac{1}{\kappa_{min}} \left\| J^{\frac{1}{2}}_{t_n} \right\|_{L^\infty, \Omega^f_{t_0}} \left\| J^{\frac{1}{2}}_{t_{n-1}} \right\|_{L^\infty, \Omega^f_{t_0}} \\
&\quad * \left(\int_{\Omega^f_{t_0}} J_{t_{n-1}} (\mathcal{V}(\mathbf{u}^{n-1}))^2\, d\Omega^f_{t_0} \right)^{\frac{1}{2}} \left(\int_{\Omega^f_{t_0}} J_{t_n} \mathcal{V}(\mathbf{v})^2\, d\Omega^f_{t_0} \right)^{\frac{1}{2}} \\
&\leq \frac{1}{\kappa_{min}} \left\| J^{\frac{1}{2}}_{t_n} \right\|_{L^\infty, \Omega^f_{t_0}} \left\| J^{\frac{1}{2}}_{t_{n-1}} \right\|_{L^\infty, \Omega^f_{t_0}} \left\| \mathbf{u}^{n-1} \right\|_{0, \Omega^f_{t_{n-1}}} \left\| \mathbf{v} \right\|_{0, \Omega^f_{t_n}} \\
&\leq \frac{\kappa_{max}}{\kappa_{min}} \left\| \mathbf{u}^{n-1} \right\|_{0, \Omega^f_{t_{n-1}}} \left\| \mathbf{v} \right\|_{1, \Omega^f_{t_n}} \\
&\leq C \left\| \mathbf{u}^{n-1} \right\|_{0, \Omega^f_{t_{n-1}}} \left\| \mathbf{v} \right\|_{1, \Omega^f_{t_n}} . \qquad (4.28)
\end{aligned}
$$

Applying Hölder's inequality, the Sobolev imbedding of $\mathbf{W}^{\frac{1}{2},2}(\Gamma_{I_{t_n}}) \subseteq \mathbf{W}^{0,4}(\Gamma_{I_{t_n}})$ [1, p. 85], and then the trace theorem,

$$
\begin{aligned}
\left((\mathbf{u}^n \cdot \mathbf{n}_f)\mathbf{u}^n, \mathbf{v}\right)_{\Gamma^f_N} &\leq C \left\| \mathbf{u}^n \right\|_{\mathbf{L}^4, \Gamma^f_N} \left\| \mathbf{u}^n \right\|_{0, \Gamma^f_N} \left\| \mathbf{v} \right\|_{\mathbf{L}^4, \Gamma^f_N} \\
&\leq C \left\| \mathbf{u}^n \right\|_{\frac{1}{2}, \Gamma^f_N} \left\| \mathbf{u}^n \right\|_{0, \Gamma^f_N} \left\| \mathbf{v} \right\|_{\frac{1}{2}, \Gamma^f_N} \\
&\leq C \left\| \mathbf{u}^n \right\|^{\frac{3}{2}}_{1, \Omega^f_{t_n}} \left\| \mathbf{u}^n \right\|^{\frac{1}{2}}_{0, \Omega^f_{t_n}} \left\| \mathbf{v} \right\|_{1, \Omega^f_{t_n}} \qquad (4.29)
\end{aligned}
$$

Applying Cauchy–Schwarz, using (2.14)–(2.16) and (4.28)–(4.29) in (4.27),

$$
\begin{aligned}
\frac{b(\mathbf{v}, p^n)_{\Omega^f_{t_n}}}{\left\| \mathbf{v} \right\|_{1, \Omega^f_{t_n}}} \leq \frac{C}{\Delta t} \left[\left\| \mathbf{u}^n \right\|_{1, \Omega^f_{t_n}} + \left\| \mathbf{u}^{n-1} \right\|_{0, \Omega^f_{t_{n-1}}} \right] + \rho^f \left\| \mathbf{u}^n \right\|_{1, \Omega^f_{t_n}} \Bigg[C_3 \left\| \mathbf{u}^n \right\|_{1, \Omega^f_{t_n}} + C_3 \left\| \mathbf{z}^n \right\|_{1, \Omega^f_{t_n}} \\
+ \frac{1}{2} \left\| \nabla \cdot \mathbf{z}^n \right\|_{L^\infty, \Omega^f_{t_n}} + \frac{C}{2} \left\| \mathbf{u}^n \right\|^{\frac{1}{2}}_{0, \Omega^f_{t_n}} \left\| \mathbf{u}^n \right\|^{\frac{1}{2}}_{1, \Omega^f_{t_n}} \Bigg] + 2\nu_f C_1 \left\| \mathbf{u}^n \right\|_{1, \Omega^f_{t_n}} + \left\| \mathbf{f}^n_f \right\|_{0, \Omega^f_{t_n}} \\
+ \left\| \mathbf{u}^n_N \right\|_{0, \Gamma^f_N} + \left\| \mathbf{g}^n \right\|_{0, \Gamma_{I_{t_n}}} \quad \forall \mathbf{v} \in \boldsymbol{H}^1_D(\Omega^f_{t_n}). \qquad (4.30)
\end{aligned}
$$

Therefore, using (4.18) with Δt sufficiently small, the inf-sup condition (2.21), and $\mathbf{z}^n \in \boldsymbol{H}^1_D(\Omega^f_{t_n})$ by (4.16),

$$\begin{aligned}\|p^n\|_{0,\Omega^f_{t_n}} &\leq \sup_{0\neq\mathbf{v}\in\Omega^f_{t_n}} \frac{b(\mathbf{v},p^n)}{\|\mathbf{v}\|_{1,\Omega^f_{t_n}}} \\ &\leq C\ P(\left\|\mathbf{f}^0_f\right\|_{0,\Omega^f_{t_0}}, \left\|\mathbf{g}^0\right\|_{0,\Gamma_{I_{t_0}}}, \left\|\mathbf{u}^0_N\right\|_{0,\Gamma^f_N}, \ldots, \left\|\mathbf{f}^n_f\right\|_{0,\Omega^f_{t_n}}, \|\mathbf{g}^n\|_{0,\Gamma_{I_{t_n}}}, \|\mathbf{u}^n_N\|_{0,\Gamma^f_N}),\end{aligned}$$

where $P(\cdot,\ldots,\cdot)$ is a quadratic polynomial. □

Theorem 4.3. *Stability of $\boldsymbol{\eta}^n$ and $\dot{\boldsymbol{\eta}}^n$*

$$\begin{aligned}&\left\|\frac{\dot{\boldsymbol{\eta}}^n+\dot{\boldsymbol{\eta}}^{n-1}}{2}\right\|^2_{0,\Omega^s} + \left\|\frac{\boldsymbol{\eta}^n+\boldsymbol{\eta}^{n-1}}{2}\right\|^2_{1,\Omega^s} \\ &\leq C\left[\left(\|\mathbf{f}^n_s\|^2_{-1,\Omega^s} + \left\|\mathbf{f}^{n-1}_s\right\|^2_{-1,\Omega^s}\right) + \left(\|\boldsymbol{\eta}^n_N\|^2_{0,\Gamma^s_N} + \left\|\boldsymbol{\eta}^{n-1}_N\right\|^2_{0,\Gamma^s_N}\right)\right. \\ &\quad\left. + \left(\|\mathbf{g}^n\|^2_{0,\Gamma_{I_{t_n}}} + \left\|\mathbf{g}^{n-1}\right\|^2_{0,\Gamma_{I_{t_{n-1}}}}\right) + \left\|\dot{\boldsymbol{\eta}}^0\right\|^2_{0,\Omega^s} + \left\|\boldsymbol{\eta}^0\right\|^2_{1,\Omega^s}\right].\end{aligned} \tag{4.31}$$

Proof. Letting $\boldsymbol{\xi} = \frac{\boldsymbol{\eta}^n - \boldsymbol{\eta}^{n-1}}{\Delta t}$ in (4.6), $\boldsymbol{\gamma} = \frac{\dot{\boldsymbol{\eta}}^n - \dot{\boldsymbol{\eta}}^{n-1}}{\Delta t}$ in (4.7), and substituting,

$$\begin{aligned}&\rho^s\left(\frac{\dot{\boldsymbol{\eta}}^n-\dot{\boldsymbol{\eta}}^{n-1}}{\Delta t}, \frac{\dot{\boldsymbol{\eta}}^n+\dot{\boldsymbol{\eta}}^{n-1}}{2}\right)_{\Omega^s} \\ &\qquad + \nu_s d\left(\boldsymbol{\eta}^n+\boldsymbol{\eta}^{n-1}, \frac{\boldsymbol{\eta}^n-\boldsymbol{\eta}^{n-1}}{\Delta t}\right)_{\Omega^s} + \frac{\lambda}{2} e\left(\boldsymbol{\eta}^n+\boldsymbol{\eta}^{n-1}, \frac{\boldsymbol{\eta}^n-\boldsymbol{\eta}^{n-1}}{\Delta t}\right)_{\Omega^s} \\ &\qquad = \frac{1}{2}\left(\mathbf{f}^n_s+\mathbf{f}^{n-1}_s, \frac{\boldsymbol{\eta}^n-\boldsymbol{\eta}^{n-1}}{\Delta t}\right)_{\Omega^s} + \frac{1}{2}\left(\boldsymbol{\eta}^n_N+\boldsymbol{\eta}^{n-1}_N, \frac{\boldsymbol{\eta}^n-\boldsymbol{\eta}^{n-1}}{\Delta t}\right)_{\Gamma^s_N} \\ &\qquad\quad - \frac{1}{2}\left(\mathcal{V}(\mathbf{g}^n)J_{t_n} + \mathcal{V}(\mathbf{g}^{n-1})J_{t_{n-1}}, \frac{\boldsymbol{\eta}^n-\boldsymbol{\eta}^{n-1}}{\Delta t}\right)_{\Gamma_{I_{t_0}}}.\end{aligned} \tag{4.32}$$

Adding $\rho^s\left(\frac{2\dot{\boldsymbol{\eta}}^{n-1}}{\Delta t}, \frac{\dot{\boldsymbol{\eta}}^n+\dot{\boldsymbol{\eta}}^{n-1}}{2}\right)_{\Omega^s}$, $\nu_s d(\boldsymbol{\eta}^n+\boldsymbol{\eta}^{n-1}, \frac{2\boldsymbol{\eta}^{n-1}}{\Delta t})_{\Omega^s}$, and $\frac{\lambda}{2}e(\boldsymbol{\eta}^n+\boldsymbol{\eta}^{n-1}, \frac{2\boldsymbol{\eta}^{n-1}}{\Delta t})_{\Omega^s}$ to

both sides of the equation,

$$\begin{aligned}
\rho^s \left(\frac{\dot{\boldsymbol{\eta}}^n + \dot{\boldsymbol{\eta}}^{n-1}}{\Delta t} \, , \frac{\dot{\boldsymbol{\eta}}^n + \dot{\boldsymbol{\eta}}^{n-1}}{2} \right)_{\Omega^s} & \\
+ \nu_s d \left(\boldsymbol{\eta}^n + \boldsymbol{\eta}^{n-1}, \frac{\boldsymbol{\eta}^n + \boldsymbol{\eta}^{n-1}}{\Delta t} \right)_{\Omega^s} + \frac{\lambda}{2} e \left(\boldsymbol{\eta}^n + \boldsymbol{\eta}^{n-1}, \frac{\boldsymbol{\eta}^n + \boldsymbol{\eta}^{n-1}}{\Delta t} \right)_{\Omega^s} & \\
= \frac{1}{2} \left(\mathbf{f}_s^n + \mathbf{f}_s^{n-1}, \frac{\boldsymbol{\eta}^n - \boldsymbol{\eta}^{n-1}}{\Delta t} \right)_{\Omega^s} + \frac{1}{2} \left(\boldsymbol{\eta}_N^n + \boldsymbol{\eta}_N^{n-1}, \frac{\boldsymbol{\eta}^n - \boldsymbol{\eta}^{n-1}}{\Delta t} \right)_{\Gamma_N^s} & \\
- \frac{1}{2} \left(\mathcal{V}(\mathbf{g}^n) J_{t_n} + \mathcal{V}(\mathbf{g}^{n-1}) J_{t_{n-1}}, \frac{\boldsymbol{\eta}^n - \boldsymbol{\eta}^{n-1}}{\Delta t} \right)_{\Gamma_{I_{t_0}}} & \\
+ \rho^s \left(\frac{2\dot{\boldsymbol{\eta}}^{n-1}}{\Delta t}, \frac{\dot{\boldsymbol{\eta}}^n + \dot{\boldsymbol{\eta}}^{n-1}}{2} \right)_{\Omega^s} + \nu_s d \left(\boldsymbol{\eta}^n + \boldsymbol{\eta}^{n-1}, \frac{2\boldsymbol{\eta}^{n-1}}{\Delta t} \right)_{\Omega^s} & \\
+ \frac{\lambda}{2} e \left(\boldsymbol{\eta}^n + \boldsymbol{\eta}^{n-1}, \frac{2\boldsymbol{\eta}^{n-1}}{\Delta t} \right)_{\Omega^s} . & \qquad (4.33)
\end{aligned}$$

Using (2.20), dropping a positive term, multiplying by Δt, and simplifying, (4.33) becomes

$$\begin{aligned}
2\rho^s \left\| \frac{\dot{\boldsymbol{\eta}}^n + \dot{\boldsymbol{\eta}}^{n-1}}{2} \right\|_{0,\Omega^s}^2 + 4\nu_s C_7 \left\| \frac{\boldsymbol{\eta}^n + \boldsymbol{\eta}^{n-1}}{2} \right\|_{1,\Omega^s}^2 & \\
= \frac{1}{2} \Big[(\mathbf{f}_s^n + \mathbf{f}_s^{n-1}, \boldsymbol{\eta}^n - \boldsymbol{\eta}^{n-1})_{\Omega^s} + (\boldsymbol{\eta}_N^n + \boldsymbol{\eta}_N^{n-1}, \boldsymbol{\eta}^n - \boldsymbol{\eta}^{n-1})_{\Gamma_N^s} & \\
- (\mathcal{V}(\mathbf{g}^n) J_{t_n} + \mathcal{V}(\mathbf{g}^{n-1}) J_{t_{n-1}}, \boldsymbol{\eta}^n - \boldsymbol{\eta}^{n-1})_{\Gamma_{I_{t_0}}} \Big] & \\
+ \rho^s \left(\dot{\boldsymbol{\eta}}^{n-1}, \dot{\boldsymbol{\eta}}^n + \dot{\boldsymbol{\eta}}^{n-1} \right)_{\Omega^s} + 2\nu_s d(\boldsymbol{\eta}^n + \boldsymbol{\eta}^{n-1}, \boldsymbol{\eta}^{n-1})_{\Omega^s} & \\
+ \lambda e(\boldsymbol{\eta}^n + \boldsymbol{\eta}^{n-1}, \boldsymbol{\eta}^{n-1})_{\Omega^s} . &
\end{aligned}$$

Applying Cauchy–Schwarz inequality, the trace theorem, $0 < J_t < \kappa_{max} < \infty$, and then

Young's inequality,

$$
\begin{aligned}
&2\rho^s \left\| \frac{\dot{\boldsymbol{\eta}}^n + \dot{\boldsymbol{\eta}}^{n-1}}{2} \right\|_{0,\Omega^s}^2 + 4\nu_s C_7 \left\| \frac{\boldsymbol{\eta}^n + \boldsymbol{\eta}^{n-1}}{2} \right\|_{1,\Omega^s}^2 \\
&\quad \leq C \left[\left(\|\mathbf{f}_s^n\|_{-1,\Omega^s}^2 + \left\|\mathbf{f}_s^{n-1}\right\|_{-1,\Omega^s}^2 \right) + \left(\|\boldsymbol{\eta}_N^n\|_{-\frac{1}{2},\Gamma_N^s}^2 + \left\|\boldsymbol{\eta}_N^{n-1}\right\|_{-\frac{1}{2},\Gamma_N^s}^2 \right) \right. \\
&\qquad \left. + \left(\|\mathbf{g}^n\|_{-\frac{1}{2},\Gamma_{I_{t_n}}}^2 + \left\|\mathbf{g}^{n-1}\right\|_{-\frac{1}{2},\Gamma_{I_{t_{n-1}}}}^2 \right) \right] + \frac{\nu_s C_7}{4} \left\| \frac{\boldsymbol{\eta}^n - \boldsymbol{\eta}^{n-1}}{2} \right\|_{1,\Omega^s}^2 \\
&\qquad + \rho^s \left\| \frac{\dot{\boldsymbol{\eta}}^n + \dot{\boldsymbol{\eta}}^{n-1}}{2} \right\|_{0,\Omega^s}^2 + \rho^s \left\| \dot{\boldsymbol{\eta}}^{n-1} \right\|_{0,\Omega^s}^2 \\
&\qquad + 3\nu_s C_7 \left\| \frac{\boldsymbol{\eta}^n + \boldsymbol{\eta}^{n-1}}{2} \right\|_{1,\Omega^s}^2 + \left[\frac{2\nu_s C_4^2}{C_7} + \frac{\lambda^2 C_5^2}{\nu_s C_7} \right] \left\| \boldsymbol{\eta}^{n-1} \right\|_{1,\Omega^s}^2 . \qquad (4.34)
\end{aligned}
$$

Adding and subtracting terms with the triangle inequality for norms, Cauchy–Schwarz inequality, and combining like terms,

$$
\begin{aligned}
&\rho^s \left\| \frac{\dot{\boldsymbol{\eta}}^n + \dot{\boldsymbol{\eta}}^{n-1}}{2} \right\|_{0,\Omega^s}^2 + \frac{\nu_s C_7}{2} \left\| \frac{\boldsymbol{\eta}^n + \boldsymbol{\eta}^{n-1}}{2} \right\|_{1,\Omega^s}^2 \\
&\quad \leq C \left[\left(\|\mathbf{f}_s^n\|_{-1,\Omega^s}^2 + \left\|\mathbf{f}_s^{n-1}\right\|_{-1,\Omega^s}^2 \right) + \left(\|\boldsymbol{\eta}_N^n\|_{-\frac{1}{2},\Gamma_N^s}^2 + \left\|\boldsymbol{\eta}_N^{n-1}\right\|_{-\frac{1}{2},\Gamma_N^s}^2 \right) \right. \\
&\qquad \left. + \left(\|\mathbf{g}^n\|_{-\frac{1}{2},\Gamma_{I_{t_n}}}^2 + \left\|\mathbf{g}^{n-1}\right\|_{-\frac{1}{2},\Gamma_{I_{t_{n-1}}}}^2 \right) \right] + 4n\rho^s \sum_{j=1}^{n-1} \left\| \frac{\dot{\boldsymbol{\eta}}^j + \dot{\boldsymbol{\eta}}^{j-1}}{2} \right\|_{0,\Omega^s}^2 \\
&\qquad + 4n \left[\frac{\nu_s C_7}{2} + \frac{2\nu_s C_4^2}{C_7} + \frac{\lambda^2 C_5^2}{\nu_s C_7} \right] \sum_{j=1}^{n-1} \left\| \frac{\boldsymbol{\eta}^j + \boldsymbol{\eta}^{j-1}}{2} \right\|_{1,\Omega^s}^2 \\
&\qquad + C \left[\left\| \dot{\boldsymbol{\eta}}^0 \right\|_{0,\Omega^s}^2 + \left\| \boldsymbol{\eta}^0 \right\|_{1,\Omega^s}^2 \right] . \qquad (4.35)
\end{aligned}
$$

Let $\alpha = \min\{\rho^s, \frac{\nu_s C_7}{2}\}$ and $\beta = \max\{\rho^s, \frac{\nu_s C_7}{2} + \frac{2\nu_s C_4^2}{C_7} + \frac{\lambda^2 C_5^2}{\nu_s C_7}\}$. With the discrete Gronwall lemma [44] and no restriction on Δt, (4.35) is bounded by

$$
\begin{aligned}
&\left\| \frac{\dot{\boldsymbol{\eta}}^n + \dot{\boldsymbol{\eta}}^{n-1}}{2} \right\|_{0,\Omega^s}^2 + \left\| \frac{\boldsymbol{\eta}^n + \boldsymbol{\eta}^{n-1}}{2} \right\|_{1,\Omega^s}^2 \\
&\leq \frac{C}{\alpha} \exp\left(\frac{4n^2\beta}{\alpha} \right) \left[\left(\|\mathbf{f}_s^n\|_{-1,\Omega^s}^2 + \left\|\mathbf{f}_s^{n-1}\right\|_{-1,\Omega^s}^2 \right) + \left(\|\boldsymbol{\eta}_N^n\|_{-\frac{1}{2},\Gamma_N^s}^2 + \left\|\boldsymbol{\eta}_N^{n-1}\right\|_{-\frac{1}{2},\Gamma_N^s}^2 \right) \right. \\
&\quad \left. + \left(\|\mathbf{g}^n\|_{-\frac{1}{2},\Gamma_{I_{t_n}}}^2 + \left\|\mathbf{g}^{n-1}\right\|_{-\frac{1}{2},\Gamma_{I_{t_{n-1}}}}^2 \right) + \left\| \dot{\boldsymbol{\eta}}^0 \right\|_{0,\Omega^s}^2 + \left\| \boldsymbol{\eta}^0 \right\|_{1,\Omega^s}^2 \right] .
\end{aligned}
$$

Multiplying by Δt and summing (4.35) over time steps,

$$\Delta t \left[\sum_{i=1}^{n} \left\| \frac{\dot{\boldsymbol{\eta}}^i + \dot{\boldsymbol{\eta}}^{i-1}}{2} \right\|_{0,\Omega^s}^2 + \sum_{i=1}^{n} \left\| \frac{\boldsymbol{\eta}^i + \boldsymbol{\eta}^{i-1}}{2} \right\|_{1,\Omega^s}^2 \right]$$
$$\leq \Delta t\, C \sum_{i=0}^{n} \left[\left\| \mathbf{f}_s^i \right\|_{-1,\Omega^s}^2 + \left\| \boldsymbol{\eta}_N^i \right\|_{-\frac{1}{2},\Gamma_N^s}^2 + \left\| \mathbf{g}^i \right\|_{-\frac{1}{2},\Gamma_{I_{t_i}}}^2 + \left\| \dot{\boldsymbol{\eta}}^0 \right\|_{0,\Omega^s}^2 + \left\| \boldsymbol{\eta}^0 \right\|_{1,\Omega^s}^2 \right].$$

□

4.5 The Existence of an Optimal Solution

Theorem 4.4. *There exists a* $(\hat{\mathbf{u}}^n, \hat{p}^n, \hat{\boldsymbol{\eta}}^n, \hat{\dot{\boldsymbol{\eta}}}^n, \hat{\mathbf{g}}^n) \in S$ *such that (4.10) is minimized.*

Proof. Clearly, the set S is nonempty. Let $\{(\mathbf{u}_{(k)}^n, p_{(k)}^n, \boldsymbol{\eta}_{(k)}^n, \dot{\boldsymbol{\eta}}_{(k)}^n, \mathbf{g}_{(k)}^n)\}$ be a sequence in S such that

$$\lim_{k\to\infty} \mathcal{J}_n^\delta(\mathbf{u}_{(k)}^n, p_{(k)}^n, \boldsymbol{\eta}_{(k)}^n, \dot{\boldsymbol{\eta}}_{(k)}^n, \mathbf{g}_{(k)}^n) = \inf_{(\mathbf{u}^n, p^n, \boldsymbol{\eta}^n, \dot{\boldsymbol{\eta}}^n, \mathbf{g}^n) \in S} \mathcal{J}_n^\delta(\mathbf{u}^n, p^n, \boldsymbol{\eta}^n, \dot{\boldsymbol{\eta}}^n, \mathbf{g}^n).$$

By the definition of (4.11), $\mathbf{g}_{(k)}^n$ is uniformly bounded in $\mathbf{L}^2(\Gamma_{I_{t_n}})$.

From (4.18), (4.26), and (4.31), we have,

$$\rho^f \left\| \mathbf{u}_{(k)}^n \right\|_{0,\Omega_{t_n}^f}^2 + \Delta t\, \nu_f C_6 \left[\left\| \mathbf{u}_{(k)}^n \right\|_{1,\Omega_{t_n}^f}^2 + \sum_{i=1}^{n-1} \left\| \mathbf{u}^i \right\|_{1,\Omega_{t_n}^f}^2 \right]$$
$$\leq C \left[\Delta t \left[\left\| \mathbf{g}_{(k)}^n \right\|_{0,\Gamma_{I_{t_n}}}^2 + \sum_{i=0}^{n-1} \left\| \mathbf{g}^i \right\|_{0,\Gamma_{I_{t_i}}}^2 + \sum_{i=0}^{n} \left[\left\| \mathbf{f}_f^i \right\|_{0,\Omega_{t_n}^f}^2 + \left\| \mathbf{u}_N^i \right\|_{0,\Gamma_i^f}^2 \right] \right] \right.$$
$$\left. + \rho^f \left\| \mathbf{u}^0 \right\|_{0,\Omega_{t_0}^f}^2 \right],$$

$$\left\| p^n \right\|_{0,\Omega_{t_n}^f} \leq C\, P(\left\| \mathbf{f}_f^0 \right\|_{0,\Omega_{t_0}^f}, \left\| \mathbf{g}^0 \right\|_{0,\Gamma_{I_{t_0}}}, \left\| \mathbf{u}_N^0 \right\|_{0,\Gamma_N^f}, \ldots, \left\| \mathbf{f}_f^n \right\|_{0,\Omega_{t_n}^f}, \left\| \mathbf{g}_{(k)}^n \right\|_{0,\Gamma_{I_{t_n}}}, \left\| \mathbf{u}_N^n \right\|_{0,\Gamma_N^f}),$$

and

$$\begin{aligned}
&\left\|\dot{\boldsymbol{\eta}}^n_{(k)}\right\|^2_{0,\Omega^s} + \left\|\boldsymbol{\eta}^n_{(k)}\right\|^2_{1,\Omega^s} \\
&\qquad \le C\left[\left(\|\mathbf{f}^n_s\|^2_{-1,\Omega^s} + \left\|\mathbf{f}^{n-1}_s\right\|^2_{-1,\Omega^s}\right) + \left(\|\boldsymbol{\eta}^n_N\|^2_{0,\Gamma^s_N} + \left\|\boldsymbol{\eta}^{n-1}_N\right\|^2_{0,\Gamma^s_N}\right)\right. \\
&\qquad\quad + \left(\left\|\mathbf{g}^n_{(k)}\right\|^2_{0,\Gamma_{I_{t_n}}} + \left\|\mathbf{g}^{n-1}\right\|^2_{0,\Gamma_{I_{t_{n-1}}}}\right) + \left\|\dot{\boldsymbol{\eta}}^0\right\|^2_{0,\Omega^s} + \left\|\boldsymbol{\eta}^0\right\|^2_{1,\Omega^s} \\
&\qquad\quad \left. + \left\|\dot{\boldsymbol{\eta}}^{n-1}\right\|^2_{0,\Omega^s} + \left\|\boldsymbol{\eta}^{n-1}\right\|^2_{1,\Omega^s}\right].
\end{aligned}$$

Therefore, $(\mathbf{u}^n_{(k)}, p^n_{(k)}, \boldsymbol{\eta}^n_{(k)}, \dot{\boldsymbol{\eta}}^n_{(k)}, \mathbf{g}^n_{(k)}) \in \boldsymbol{H}^1_D(\Omega^f_{t_n}) \times L^2(\Omega^f_{t_n}) \times \boldsymbol{H}^1_D(\Omega^s) \times \boldsymbol{L}^2(\Omega^s) \times \mathbf{L}^2(\Gamma_{I_{t_n}})$ is uniformly bounded. Then, there must exist subsequences such that

$$\begin{aligned}
\mathbf{u}^n_{(k_j)} &\rightharpoonup \hat{\mathbf{u}}^n \ \text{ in } \mathbf{H}^1(\Omega^f_{t_n}), \quad \boldsymbol{\eta}^n_{(k_j)} &&\rightharpoonup \hat{\boldsymbol{\eta}}^n \ \text{ in } \mathbf{H}^1(\Omega^s), \\
p^n_{(k_j)} &\rightharpoonup \hat{p}^n \ \text{ in } \mathbf{L}^2(\Omega^f_{t_n}), \quad \dot{\boldsymbol{\eta}}^n_{(k_j)} &&\rightharpoonup \hat{\dot{\boldsymbol{\eta}}}^n \ \text{ in } \mathbf{L}^2(\Omega^s), \\
\mathbf{u}^n_{(k_j)} &\to \hat{\mathbf{u}}^n \ \text{ in } \mathbf{L}^2(\Omega^f_{t_n}), \quad \mathbf{g}^n_{(k_j)} &&\rightharpoonup \hat{\mathbf{g}}^n \ \text{ in } \mathbf{L}^2(\Gamma_{I_{t_n}}), \\
&\text{and } \mathbf{u}^n_{(k_j)}|_{\Gamma^f_N \cup \Gamma_{I_{t_n}}} \to \hat{\mathbf{u}}^n \ \text{ in } \mathbf{L}^2(\Gamma^f_N \cup \Gamma_{I_{t_n}}),
\end{aligned}$$

for some $(\hat{\mathbf{u}}^n, \hat{p}^n, \hat{\boldsymbol{\eta}}^n, \hat{\dot{\boldsymbol{\eta}}}^n, \hat{\mathbf{g}}^n) \in S$.

The last two statements with strong convergence are a result of the compact imbeddings $\mathbf{H}^1(\Omega^f_{t_n}) \subset \mathbf{L}^2(\Omega^f_{t_n})$ and $\mathbf{H}^{\frac{1}{2}}(\Gamma^f_N \cup \Gamma_{I_{t_n}}) \subset \mathbf{L}^2(\Gamma^f_N \cup \Gamma_{I_{t_n}})$.

Now we wish to show that by passing to the limit, $(\hat{\mathbf{u}}^n, \hat{p}^n, \hat{\boldsymbol{\eta}}^n, \hat{\dot{\boldsymbol{\eta}}}^n, \hat{\mathbf{g}}^n)$ satisfies (4.4)–(4.7). Equations (4.4)–(4.7) are linear with the exception of $c(\mathbf{u}^n_{(k)}, \mathbf{u}^n_{(k)}, \mathbf{v})_{\Omega^f_{t_n}}$ and $\frac{1}{2}((\mathbf{u}^n_{(k)} \cdot \mathbf{n}_f)\mathbf{u}^n_{(k)}, \mathbf{v})_{\Gamma^f_N}$ in (4.4).

$$\begin{aligned}
&\lim_{k\to\infty} c(\mathbf{u}^n_{(k)}, \mathbf{u}^n_{(k)}, \mathbf{v})_{\Omega^f_{t_n}} + \frac{1}{2}((\mathbf{u}^n_{(k)} \cdot \mathbf{n}_f)\mathbf{u}^n_{(k)}, \mathbf{v})_{\Gamma^f_N} \\
&= \lim_{k\to\infty} -(\mathbf{u}^n_{(k)} \cdot \nabla\mathbf{v}, \mathbf{u}^n_{(k)})_{\Omega^f_{t_n}} + \frac{1}{2}((\mathbf{u}^n_{(k)} \cdot \mathbf{n}_f)\mathbf{u}^n_{(k)}, \mathbf{v})_{\Gamma^f_N \cup \Gamma_{I_{t_n}}} + \frac{1}{2}((\mathbf{u}^n_{(k)} \cdot \mathbf{n}_f)\mathbf{u}^n_{(k)}, \mathbf{v})_{\Gamma^f_N} \\
&= -(\hat{\mathbf{u}}^n \cdot \nabla\mathbf{v}, \hat{\mathbf{u}}^n)_{\Omega^f_{t_n}} + \frac{1}{2}((\hat{\mathbf{u}}^n \cdot \mathbf{n}_f)\hat{\mathbf{u}}^n, \mathbf{v})_{\Gamma^f_N \cup \Gamma_{I_{t_n}}} + \frac{1}{2}((\hat{\mathbf{u}}^n \cdot \mathbf{n}_f)\hat{\mathbf{u}}^n, \mathbf{v})_{\Gamma^f_N} \\
&= c(\hat{\mathbf{u}}^n, \hat{\mathbf{u}}^n, \mathbf{v})_{\Omega^f_{t_n}} + \frac{1}{2}((\hat{\mathbf{u}}^n \cdot \mathbf{n}_f)\hat{\mathbf{u}}^n, \mathbf{v})_{\Gamma^f_N} \ \ \forall \mathbf{v} \in \mathbf{C}^\infty(\overline{\Omega^f_{t_n}})
\end{aligned} \tag{4.36}$$

since $\mathbf{u}^n_{(k_j)} \to \hat{\mathbf{u}}$ in $\mathbf{L}^2(\Omega^f_{t_n})$ and $\mathbf{u}^n_{(k_j)} \to \hat{\mathbf{u}}|_{\Gamma_{I_{t_n}}}$ in $\mathbf{L}^2(\Gamma_{I_{t_n}})$. Then, because $\mathbf{C}^\infty(\overline{\Omega^f_{t_n}})$ is dense

in $\boldsymbol{H}^1_D(\Omega^f_{t_n})$,

$$\lim_{k\to\infty} c(\mathbf{u}^n_{(k)},\mathbf{u}^n_{(k)},\mathbf{v})_{\Omega^f_{t_n}} + \frac{1}{2}((\mathbf{u}^n_{(k)}\cdot\mathbf{n}_f)\mathbf{u}^n_{(k)},\mathbf{v})_{\Gamma^f_N} = c(\hat{\mathbf{u}}^n,\hat{\mathbf{u}}^n,\mathbf{v})_{\Omega^f_{t_n}} + \frac{1}{2}((\hat{\mathbf{u}}^n\cdot\mathbf{n}_f)\hat{\mathbf{u}}^n,\mathbf{v})_{\Gamma^f_N} \quad \forall \mathbf{v}\in\boldsymbol{H}^1_D(\Omega^f_{t_n}).$$

Additionally, since $\mathcal{J}^\delta_n$ is lower semicontinuous,

$$\mathcal{J}^\delta_n(\hat{\mathbf{u}^n},\hat{p^n},\hat{\boldsymbol{\eta}}^n,\hat{\dot{\boldsymbol{\eta}}}^n,\hat{\mathbf{g}}^n) = \inf_{(\mathbf{u}^n,p^n,\boldsymbol{\eta}^n,\dot{\boldsymbol{\eta}}^n,\mathbf{g}^n)\in S} \mathcal{J}^\delta_n(\mathbf{u}^n,p^n,\boldsymbol{\eta}^n,\dot{\boldsymbol{\eta}}^n,\mathbf{g}^n),$$

so there exists a solution to the optimal control problem, although we can not show in general that $(\hat{\mathbf{u}}^n,\hat{p}^n,\hat{\boldsymbol{\eta}}^n,\hat{\dot{\boldsymbol{\eta}}}^n,\hat{\mathbf{g}}^n)$ is unique. □

4.6 Convergence of Vanishing Penalty Parameter

In this section, we show that as $\delta\to 0$, the optimal solution to (4.10) converges to a solution that satisfies (2.38)–(2.39) and (2.40)–(2.41) and satisfies the interface conditions (2.11)–(2.12) within a tolerance on the order of $\Delta t^{\frac{3}{2}}$.

In addition to (4.13)–(4.16), we make the following assumptions on regularity of the strong solution satisfying (2.1)–(2.12) that are needed for the theorem that follows: $\mathbf{u}$, $\frac{d\mathbf{u}}{dt}\,|_{\mathbf{y}}\in L^2(t_0,t_n;\mathbf{H}^2(\Omega^f_t))$, p, $\frac{dp}{dt}\,|_{\mathbf{y}}\in L^2(t_0,t_n;\mathbf{H}^1(\Omega^f_t))$, $\boldsymbol{\eta}\in L^2(t_0,t_n;\mathbf{H}^2(\Omega^s))$, $\boldsymbol{\eta}_t\in L^\infty(t_0,t_n;\mathbf{H}^1(\Omega^s))$, $\boldsymbol{\eta}_{tt}\in L^\infty(t_0,t_n;\mathbf{H}^1(\Omega^s))$, the body forces and boundary conditions are sufficiently smooth, and Δt is sufficiently small.

We will assume no time discretization error of $\mathbf{g}^n$ in the L^2 sense. Future work will provide a detailed proof using the entire derived optimality system.

Theorem 4.5. *Let $(\mathbf{u}^n_\delta,p^n_\delta,\boldsymbol{\eta}^n_\delta,\dot{\boldsymbol{\eta}}^n_\delta,\mathbf{g}^n_\delta)$ denote an optimal solution satisfying (4.4)–(4.5) and (4.6)–(4.7) for $\delta>0$, where $\mathbf{u}^{n-1}=\mathbf{u}(t_{n-1})\in\boldsymbol{H}^1_D(\Omega^f_{t_{n-1}})$, $\boldsymbol{\eta}^{n-1}=\boldsymbol{\eta}(t_{n-1})\in\boldsymbol{H}^1_D(\Omega^s)$, and $\mathbf{u}(t_{n-1})$ and $\boldsymbol{\eta}(t_{n-1})$ are solutions to (2.1)–(2.12) at $t=t_{n-1}$.*

Then, the solution $(\tilde{\mathbf{u}}^n,\tilde{p}^n,\tilde{\boldsymbol{\eta}}^n,\tilde{\dot{\boldsymbol{\eta}}}^n)$ exists as a solution of (4.4)–(4.7) at $t=t_n$ such that $\|\mathbf{u}^n_\delta-\tilde{\mathbf{u}}^n\|_{1,\Omega^f_{t_n}}+\|p^n_\delta-\tilde{p}^n\|_{0,\Omega^f_{t_n}}+\|\boldsymbol{\eta}^n_\delta-\tilde{\boldsymbol{\eta}}^n\|_{1,\Omega^s}+\|\dot{\boldsymbol{\eta}}^n_\delta-\tilde{\dot{\boldsymbol{\eta}}}^n\|_{0,\Omega^s}\to 0$ as $\delta\to 0$. Also,

in the limit, $\mathcal{J}_n(\tilde{\mathbf{u}}^n, \tilde{p}^n, \tilde{\boldsymbol{\eta}}^n, \tilde{\dot{\boldsymbol{\eta}}}^n, \tilde{\mathbf{g}}^n) \leq C\Delta t^{\frac{3}{2}}$.

Proof. Consider the solution to the semidiscrete weak formulations (2.38)–(2.39) and (2.40)–(2.41) satisfying the boundary conditions (2.11)–(2.12), and denote this $(\mathbf{u}_{sd}^n, p_{sd}^n, \boldsymbol{\eta}_{sd}^n, \dot{\boldsymbol{\eta}}_{sd}^n)$. Letting $g_{sd}^n = [2\nu_f D(\mathbf{u}_{sd}^n)\cdot\mathbf{n}_f - p_{sd}^n\mathbf{n}_f - \frac{1}{2}((\mathbf{u}_{sd}^n - \mathbf{z}_{sd}^n)\cdot\mathbf{n}_f)\mathbf{u}_{sd}^n]|_{\Gamma_{I_{t_n}}}$, we see that $(\mathbf{u}_{sd}^n, p_{sd}^n, \boldsymbol{\eta}_{sd}^n, \dot{\boldsymbol{\eta}}_{sd}^n, \mathbf{g}_{sd}^n)$ is also a solution to (4.4)–(4.7). Also, $\mathbf{u}_{sd}^n$, $\boldsymbol{\eta}_{sd}^n$, and $\boldsymbol{\eta}^{n-1}$ are bounded in $\boldsymbol{H}_D^1(\Omega_{t_n}^f)$, $\boldsymbol{H}_D^1(\Omega^s)$, and $\boldsymbol{H}_D^1(\Omega^s)$, respectively, so

$$\begin{aligned}\mathcal{J}_n^\delta(\mathbf{u}_{sd}^n, p_{sd}^n, \boldsymbol{\eta}_{sd}^n, \dot{\boldsymbol{\eta}}_{sd}^n, \mathbf{g}^n) &= \frac{1}{2}\int_{\Gamma_{I_{t_n}}} \left|\mathbf{u}_{sd}^n - \frac{\mathcal{V}(\boldsymbol{\eta}_{sd}^n) - \mathcal{V}(\boldsymbol{\eta}^{n-1})}{\Delta t}\right|^2 d\Gamma_{I_{t_n}} + \frac{\delta}{2}\int_{\Gamma_{I_{t_n}}} |\mathbf{g}_{sd}^n|^2\, d\Gamma_{I_{t_n}} \\ &\leq C\left[\|\mathbf{u}_{sd}^n\|_{1,\Omega_{t_n}^f}^2 + \|\boldsymbol{\eta}_{sd}^n\|_{1,\Omega^s}^2 + \left\|\boldsymbol{\eta}^{n-1}\right\|_{1,\Omega^s}^2 + \delta\,\|\mathbf{g}_{sd}^n\|_{1,\Omega_{t_n}^f}^2\right] \\ &< \infty.\end{aligned}$$

Therefore, we can conclude that $(\mathbf{u}_{sd}^n, p_{sd}^n, \boldsymbol{\eta}_{sd}^n, \dot{\boldsymbol{\eta}}_{sd}^n, \mathbf{g}_{sd}^n) \in S$.

By the definition of an optimal solution in (4.12) and since $(\mathbf{u}_{sd}^n, p_{sd}^n, \boldsymbol{\eta}_{sd}^n, \dot{\boldsymbol{\eta}}_{sd}^n, \mathbf{g}_{sd}^n) \in S$,

$$\begin{aligned}\mathcal{J}_n^\delta(\mathbf{u}_\delta^n, p_\delta^n, \boldsymbol{\eta}_\delta^n, \dot{\boldsymbol{\eta}}_\delta^n, \mathbf{g}_\delta^n) &= \inf_{(\mathbf{u}^n, p^n, \boldsymbol{\eta}^n, \dot{\boldsymbol{\eta}}^n, \mathbf{g}^n)\in S} \mathcal{J}_n^\delta(\mathbf{u}^n, p^n, \boldsymbol{\eta}^n, \dot{\boldsymbol{\eta}}^n, \mathbf{g}^n) \\ &\leq \mathcal{J}_n^\delta(\mathbf{u}_{sd}^n, p_{sd}^n, \boldsymbol{\eta}_{sd}^n, \dot{\boldsymbol{\eta}}_{sd}^n, \mathbf{g}_{sd}^n). \end{aligned} \tag{4.37}$$

In (4.37),

$$\begin{aligned}\mathcal{J}_n^\delta(\mathbf{u}_{sd}^n, p_{sd}^n, \boldsymbol{\eta}_{sd}^n, \dot{\boldsymbol{\eta}}_{sd}^n, \mathbf{g}_{sd}^n) &= \frac{1}{2}\int_{\Gamma_{I_{t_n}}} \left|\mathbf{u}_{sd}^n - \frac{\mathcal{V}(\boldsymbol{\eta}_{sd}^n) - \mathcal{V}(\boldsymbol{\eta}^{n-1})}{\Delta t}\right|^2 d\Gamma_{I_{t_n}} + \frac{\delta}{2}\int_{\Gamma_{I_{t_n}}} |\mathbf{g}_{sd}^n|^2\, d\Gamma_{I_{t_n}} \\ &\leq C\left[\|\mathbf{u}_{sd}^n - \mathbf{u}(t_n)\|_{0,\Gamma_{I_{t_n}}}^2 + \|\mathbf{u}(t_n) - \mathcal{V}(\boldsymbol{\eta}_t(t_n))\|_{0,\Gamma_{I_{t_n}}}^2\right. \\ &\quad \left. + \left\|\boldsymbol{\eta}_t(t_n) - \frac{\boldsymbol{\eta}_{sd}^n - \boldsymbol{\eta}^{n-1}}{\Delta t}\right\|_{0,\Gamma_{I_{t_0}}}^2\right] + \frac{\delta}{2}\,\|\mathbf{g}_{sd}^n\|_{0,\Gamma_{I_{t_n}}}^2 \end{aligned} \tag{4.38}$$

where $\mathbf{u}(t_n)$ and $\boldsymbol{\eta}_t(t_n)$ are solutions to (2.1)–(2.12) at time $t = t_n$. Since $\mathbf{u}(t_n)$ and $\boldsymbol{\eta}_t(t_n)$ satisfy (2.11), $\|\mathbf{u}(t_n) - \mathcal{V}(\boldsymbol{\eta}_t(t_n))\|_{0,\Gamma_{I_{t_n}}}^2 = 0$.

By adding and subtracting $\frac{\boldsymbol{\eta}(t_n)}{\Delta t}$ to $\left\|\boldsymbol{\eta}_t(t_n) - \frac{\boldsymbol{\eta}^n_{sd}-\boldsymbol{\eta}^{n-1}}{\Delta t}\right\|^2_{0,\Gamma_{I_{t_0}}}$ in (4.38), recognizing that $\boldsymbol{\eta}^{n-1} = \boldsymbol{\eta}(t_{n-1})$, and using the triangle inequality for norms,

$$\begin{aligned}
&\mathcal{J}^{\delta}_n(\mathbf{u}^n_{sd}, p^n_{sd}, \boldsymbol{\eta}^n_{sd}, \dot{\boldsymbol{\eta}}^n_{sd}, \mathbf{g}^n_{sd}) \\
&\qquad \leq \frac{\delta}{2}\left\|\mathbf{g}^n_{sd}\right\|^2_{0,\Gamma_{I_{t_n}}} + C\left[\left\|\mathbf{u}^n_{sd} - \mathbf{u}(t_n)\right\|^2_{0,\Gamma_{I_{t_n}}}\right. \\
&\qquad\quad \left. + \left\|\boldsymbol{\eta}_t(t_n) - \frac{\boldsymbol{\eta}(t_n) - \boldsymbol{\eta}(t_{n-1})}{\Delta t}\right\|^2_{0,\Gamma_{I_{t_0}}} + \left\|\frac{\boldsymbol{\eta}(t_n) - \boldsymbol{\eta}^n_{sd}}{\Delta t}\right\|^2_{0,\Gamma_{I_{t_0}}}\right].
\end{aligned} \tag{4.39}$$

Since Ω^f_t is Lipschitz continuous by (4.14), we use the trace theorem to get

$$\left\|\mathbf{u}^n_{sd} - \mathbf{u}(t_n)\right\|^2_{0,\Gamma_{I_{t_n}}} \leq C\left\|\mathbf{u}^n_{sd} - \mathbf{u}(t_n)\right\|_{0,\Omega^f_{t_n}}\left\|\mathbf{u}^n_{sd} - \mathbf{u}(t_n)\right\|_{1,\Omega^f_{t_n}}. \tag{4.40}$$

We use a result similar to the error estimate derived in [52], except in our case it is continuous in space and has a constant viscosity. Along with this, we include the assumptions on $\mathbf{u}$, made in the statement of the theorem, to get

$$\left\|\mathbf{u}^n_{sd} - \mathbf{u}(t_n)\right\|^2_{0,\Gamma_{I_{t_n}}} \leq C\Delta t^{\frac{3}{2}}. \tag{4.41}$$

The second order time discretization [55, pp. 131–134] for the linear elasticity equations along with the assumptions on $\boldsymbol{\eta}$ and $\boldsymbol{\eta}_t$ gives

$$\left\|\boldsymbol{\eta}(t_n) - \boldsymbol{\eta}^n_{sd}\right\|^2_{0,\Gamma_{I_{t_0}}} \leq C\left\|\boldsymbol{\eta}(t_n) - \boldsymbol{\eta}^n_{sd}\right\|_{0,\Omega^s}\left\|\boldsymbol{\eta}(t_n) - \boldsymbol{\eta}^n_{sd}\right\|_{1,\Omega^s} \leq C\Delta t^{\frac{7}{2}}. \tag{4.42}$$

Using (4.42),

$$\left\|\frac{\boldsymbol{\eta}(t_n) - \boldsymbol{\eta}^n_{sd}}{\Delta t}\right\|^2_{0,\Gamma_{I_{t_0}}} \leq C\Delta t^{\frac{3}{2}}. \tag{4.43}$$

Substituting (4.41) and (4.43) into (4.39) gives

$$\mathcal{J}_n^\delta(\mathbf{u}_{sd}^n, p_{sd}^n, \boldsymbol{\eta}_{sd}^n, \dot{\boldsymbol{\eta}}_{sd}^n, \mathbf{g}_{sd}^n) \leq \frac{\delta}{2} \left\|\mathbf{g}_{sd}^n\right\|_{0,\Gamma_{I_{t_n}}}^2 + C\left[\Delta t^{\frac{3}{2}} + \left\|\boldsymbol{\eta}_t(t_n) - \frac{\boldsymbol{\eta}(t_n) - \boldsymbol{\eta}(t_{n-1})}{\Delta t}\right\|_{0,\Gamma_{I_{t_0}}}^2\right]. \tag{4.44}$$

Using Taylor series expansion along with $\|\boldsymbol{\eta}_{tt}\|_{\mathbf{L}^\infty(t_{n-1},t_n;\mathbf{H}^1(\Omega^s))} < \infty$ gives

$$\left\|\boldsymbol{\eta}_t(t_n) - \frac{\boldsymbol{\eta}(t_n) - \boldsymbol{\eta}(t_{n-1})}{\Delta t}\right\|_{0,\Gamma_{I_{t_0}}}^2 \leq C\Delta t^2 \left\|\boldsymbol{\eta}_{tt}\right\|_{\mathbf{L}^\infty(t_{n-1},t_n;\mathbf{H}^1(\Omega^s))} \leq C\Delta t^2. \tag{4.45}$$

We now substitute (4.45) into (4.44) and (4.44) into (4.37) to get

$$\begin{aligned}\mathcal{J}_n^\delta(\mathbf{u}_\delta^n, p_\delta^n, \boldsymbol{\eta}_\delta^n, \dot{\boldsymbol{\eta}}_\delta^n, \mathbf{g}_\delta^n) &\leq \mathcal{J}_n^\delta(\mathbf{u}_{sd}^n, p_{sd}^n, \boldsymbol{\eta}_{sd}^n, \dot{\boldsymbol{\eta}}_{sd}^n, \mathbf{g}_{sd}^n) \\ &\leq C\Delta t^{\frac{3}{2}} + \frac{\delta}{2}\left\|\mathbf{g}_{sd}^n\right\|_{0,\Gamma_{I_{t_n}}}^2. \end{aligned} \tag{4.46}$$

From (4.46), we can see that $\mathbf{g}_\delta^n$ is uniformly bounded. Combining this with (4.18), (4.26), and (4.31), we know that $\mathbf{u}_\delta^n, p_\delta^n, \boldsymbol{\eta}_\delta^n$, and $\dot{\boldsymbol{\eta}}_\delta^n$ are uniformly bounded as well.

Then, there must exist subsequences such that

$$\begin{aligned} \mathbf{u}_\delta^n &\rightharpoonup \tilde{\mathbf{u}}^n \ \text{ in } \mathbf{H}^1(\Omega_{t_n}^f), \quad \boldsymbol{\eta}_\delta^n &&\rightharpoonup \tilde{\boldsymbol{\eta}}^n \ \text{ in } \mathbf{H}^1(\Omega^s), \\ p_\delta^n &\rightharpoonup \tilde{p}^n \ \text{ in } \mathbf{L}^2(\Omega_{t_n}^f), \quad \dot{\boldsymbol{\eta}}_\delta^n &&\rightharpoonup \tilde{\dot{\boldsymbol{\eta}}}^n \ \text{ in } \mathbf{L}^2(\Omega^s), \\ \mathbf{u}_\delta^n &\to \tilde{\mathbf{u}}^n \ \text{ in } \mathbf{L}^2(\Omega_{t_n}^f), \quad \mathbf{g}_\delta^n &&\rightharpoonup \tilde{\mathbf{g}}^n \ \text{ in } \mathbf{L}^2(\Gamma_{I_{t_n}}), \\ &\text{and } \mathbf{u}_\delta^n|_{\Gamma_N^f \cup \Gamma_{I_{t_n}}} \to \tilde{\mathbf{u}}^n \ \text{ in } \mathbf{L}^2(\Gamma_N^f \cup \Gamma_{I_{t_n}}), \end{aligned}$$

as $\delta \to 0$ for some $(\tilde{\mathbf{u}}^n, \tilde{p}^n, \tilde{\boldsymbol{\eta}}^n, \tilde{\dot{\boldsymbol{\eta}}}^n, \tilde{\mathbf{g}}^n) \in S$, such that

$$\mathcal{J}_n(\tilde{\mathbf{u}}^n, \tilde{p}^n, \tilde{\boldsymbol{\eta}}^n, \tilde{\dot{\boldsymbol{\eta}}}^n, \tilde{\mathbf{g}}^n) = \left\|\tilde{\mathbf{u}}^n - \frac{\mathcal{V}(\tilde{\boldsymbol{\eta}}^n) - \mathcal{V}(\boldsymbol{\eta}(t_{n-1}))}{\Delta t}\right\|_{0,\Gamma_{I_{t_n}}}^2 \leq C\Delta t^{\frac{3}{2}}. \tag{4.47}$$

□

Remark 4.6. *For any choice of finite difference formula in the functional, note from (4.43) that we will lose two powers of Δt from (4.42). This is the reason that, from an analytical*

perspective, we should choose to use a second order time discretization for the structure despite only using a first order time-formula in the functional.

Additionally, with respect to (4.43), we see that by using a second order time discretization for the structure, there would be no improvement by increasing the order of the finite difference formula used in the functional.

4.7 The Existence of Lagrange Multipliers

We desire to change the optimization problem from constrained to unconstrained. This can be done by means of the Lagrange multiplier rule after proving the existence of Lagrange multipliers. We use the same approach to show the existence of Lagrange multipliers as was used in [27, 31].

Lemma 4.7. *Let* $\mathbf{X}$ *and* $\mathbf{Y}$ *be two real Banach spaces,* $\mathcal{J}$ *a functional on* $\mathbf{X}$*, and* M *a mapping from* $\mathbf{X}$ *to* $\mathbf{Y}$*. Assume* u *is a solution of the following constrained minimization problem:*

$$find\ u \in \mathbf{X}\ such\ that\ \mathcal{J}(u) = \inf\{\mathcal{J}(v) | v \in \mathbf{X},\ M(v) = y_0\},$$

where y_0 *is some fixed element of* $\mathbf{Y}$*. Additionally, assume the following three conditions are satisfied:*

1. M *is Fréchet-differentiable in an open neighborhood of* u *and its Fréchet derivative* M' *is continuous at* u*.*

2. $\mathcal{J} : Neighborhood(u) \subset \mathbf{X} \to \mathbb{R}$ *is Fréchet-differentiable at* u *with Fréchet derivative* $\mathcal{J}'$*.*

3. $M' : \mathbf{X} \to \mathbf{Y}$ *is onto.*

Then there exists a $\mu \in \mathbf{Y}^*$ *satisfying*

$$-\mathcal{J}'(u) \cdot w + \langle \mu, M'(u) \cdot w \rangle = 0 \ \ \forall\ w \in \mathbf{X}.$$

Proof. See [69]. □

In the following two theorems, we will verify the assumptions of Lemma 4.7. We begin by verifying the first part of Assumption 1 of Lemma 4.7 in Theorem 4.8, namely that M is Fréchet-differentiable in an open neighborhood of u.

Let $\mathbf{X} = \boldsymbol{H}^1_D(\Omega^f_{t_n}) \times L^2(\Omega^f_{t_n}) \times \boldsymbol{H}^1_D(\Omega^s) \times \boldsymbol{L}^2(\Omega^s) \times \mathbf{L}^2(\Gamma_{I_{t_n}})$, $\mathbf{Y} = \boldsymbol{H}^1_D(\Omega^f_{t_n})^* \times L^2(\Omega^f_{t_n}) \times \boldsymbol{H}^1_D(\Omega^s)^* \times \boldsymbol{L}^2(\Omega^s)$, $\mathcal{J} = \mathcal{J}^\delta_n$ defined in (4.9), and $M : \mathbf{X} \to \mathbf{Y}$ be the nonlinear mapping representing the generalized constraint equations: $M(\mathbf{u}^n, p^n, \boldsymbol{\eta}^n, \dot{\boldsymbol{\eta}}^n, \mathbf{g}^n) = (\mathbf{f}^n_f, \phi_1, \mathbf{f}^n_s, \boldsymbol{\phi}_2)$ for $(\mathbf{u}^n, p^n, \boldsymbol{\eta}^n, \dot{\boldsymbol{\eta}}^n, \mathbf{g}^n) \in \mathbf{X}$ and $(\mathbf{f}^n_f, \phi_1, \mathbf{f}^n_s, \boldsymbol{\phi}_2) \in \mathbf{Y}$, if and only if,

$$\begin{aligned}
\rho^f(\mathbf{u}^n, \mathbf{v})_{\Omega^f_{t_n}} + &\Delta t\ \rho^f[c(\mathbf{u}^n, \mathbf{u}^n, \mathbf{v})_{\Omega^f_{t_n}} + \frac{1}{2}((\mathbf{u}^n \cdot \mathbf{n}_f)\mathbf{u}^n, \mathbf{v})_{\Gamma^f_N} - c(\mathbf{z}^n, \mathbf{u}^n, \mathbf{v})_{\Omega^f_{t_n}}] \\
&+ \Delta t\ 2\nu_f a(\mathbf{u}^n, \mathbf{v})_{\Omega^f_{t_n}} + \Delta t\ b(\mathbf{v}, p^n)_{\Omega^f_{t_n}} - \Delta t\ (\mathbf{g}^n, \mathbf{v})_{\Gamma_{I_{t_n}}} \\
&= (\mathbf{f}^n_f, \mathbf{v})_{\Omega^f_{t_n}} \quad \forall \mathbf{v} \in \boldsymbol{H}^1_D(\Omega^f_{t_n}), \qquad (4.48) \\
b(\mathbf{u}^n, q)_{\Omega^f_{t_n}} &= (\phi_1, q)_{\Omega^f_{t_n}} \quad q \in L^2(\Omega^f_{t_n}), \qquad (4.49)
\end{aligned}$$

$$\begin{aligned}
\rho^s(\dot{\boldsymbol{\eta}}^n, \boldsymbol{\xi})_{\Omega^s} + \Delta t\ \nu_s d(\boldsymbol{\eta}^n + \boldsymbol{\eta}^{n-1}, \boldsymbol{\xi})_{\Omega^s} + \frac{\Delta t}{2}\ \lambda e(\boldsymbol{\eta}^n + \boldsymbol{\eta}^{n-1}, \boldsymbol{\xi})_{\Omega^s} + \frac{\Delta t}{2}\ (\mathcal{V}(\mathbf{g}^n) J_{t_n}, \boldsymbol{\xi})_{\Gamma_{I_{t_0}}} \\
= (\mathbf{f}^n_s, \boldsymbol{\xi})_{\Omega^s} \quad \forall \boldsymbol{\xi} \in \boldsymbol{H}^1_D(\Omega^s), \qquad (4.50) \\
\frac{\Delta t}{2}(\dot{\boldsymbol{\eta}}^n, \boldsymbol{\gamma})_{\Omega^s} - (\boldsymbol{\eta}^n, \boldsymbol{\gamma})_{\Omega^s} = (\boldsymbol{\phi}_2, \boldsymbol{\gamma})_{\Omega^s} \quad \forall \boldsymbol{\gamma} \in \boldsymbol{L}^2(\Omega^s). \qquad (4.51)
\end{aligned}$$

Theorem 4.8. *Let $(\mathbf{u}^n, p^n, \boldsymbol{\eta}^n, \dot{\boldsymbol{\eta}}^n, \mathbf{g}^n)$ be an optimal solution to Problem (4.10) and M be defined as in (4.48)–(4.51). The Fréchet derivative of M, denoted M', exists in an open neighborhood of $(\mathbf{u}^n, p^n, \boldsymbol{\eta}^n, \dot{\boldsymbol{\eta}}^n, \mathbf{g}^n)$. M' is defined by*
$M'(\mathbf{u}^n, p^n, \boldsymbol{\eta}^n, \dot{\boldsymbol{\eta}}^n, \mathbf{g}^n) \cdot (\mathbf{w}^n, r^n, \boldsymbol{\theta}^n, \boldsymbol{\varphi}^n, \mathbf{h}^n) = (\bar{\mathbf{f}^n_f}, \bar{\phi_1}, \bar{\mathbf{f}^n_s}, \bar{\boldsymbol{\phi}_2})$ *for* $(\mathbf{w}^n, r^n, \boldsymbol{\theta}^n, \boldsymbol{\varphi}^n, \mathbf{h}^n) \in \mathbf{X}$ *and* $(\bar{\mathbf{f}^n_f}, \bar{\phi^n_1}, \bar{\mathbf{f}^n_s}, \bar{\boldsymbol{\phi}^n_2}) \in \mathbf{Y}$*, if and only if*

$$\rho^f(\mathbf{w}^n,\mathbf{v})_{\Omega^f_{t_n}} + \Delta t\ \rho^f[c(\mathbf{u}^n,\mathbf{w}^n,\mathbf{v})_{\Omega^f_{t_n}} + c(\mathbf{w}^n,\mathbf{u}^n,\mathbf{v})_{\Omega^f_{t_n}} + \frac{1}{2}((\mathbf{u}^n\cdot\mathbf{n}_f)\mathbf{w}^n,\mathbf{v})_{\Gamma^f_N}$$
$$+\frac{1}{2}((\mathbf{w}^n\cdot\mathbf{n}_f)\mathbf{u}^n,\mathbf{v})_{\Gamma^f_N} - \frac{1}{2}((\nabla\cdot\mathbf{z}^n)\mathbf{w}^n,\mathbf{v})_{\Omega^f_{t_n}} - c(\mathbf{z}^n,\mathbf{w}^n,\mathbf{v})_{\Omega^f_{t_n}}]$$
$$+\Delta t\ 2\nu_f a(\mathbf{w}^n,\mathbf{v})_{\Omega^f_{t_n}} + \Delta t\ b(\mathbf{v},r^n)_{\Omega^f_{t_n}} - \Delta t\ (\mathbf{h}^n,\mathbf{v})_{\Gamma_{I_{t_n}}}$$
$$= (\bar{\mathbf{f}^n_f},\mathbf{v})_{\Omega^f_{t_n}} \quad \forall\mathbf{v}\in\boldsymbol{H}^1_D(\Omega^f_{t_n}), \tag{4.52}$$

$$b(\mathbf{w}^n,q)_{\Omega^f_{t_n}} = (\bar{\phi_1},q)_{\Omega^f_{t_n}} \quad q\in L^2(\Omega^f_{t_n}), \tag{4.53}$$

$$\rho^s(\boldsymbol{\varphi}^n,\boldsymbol{\xi})_{\Omega^s} + \Delta t\ \nu_s d(\boldsymbol{\theta}^n,\boldsymbol{\xi})_{\Omega^s} + \frac{\Delta t}{2}\ \lambda e(\boldsymbol{\theta}^n,\boldsymbol{\xi})_{\Omega^s} + \frac{\Delta t}{2}\ (\mathcal{V}(\mathbf{h}^n)J_{t_n},\boldsymbol{\xi})_{\Gamma_{I_{t_0}}}$$
$$= (\bar{\mathbf{f}^n_s},\boldsymbol{\xi})_{\Omega^s} \quad \forall\boldsymbol{\xi}\in\boldsymbol{H}^1_D(\Omega^s), \tag{4.54}$$

$$\frac{\Delta t}{2}(\boldsymbol{\varphi}^n,\boldsymbol{\gamma})_{\Omega^s} - (\boldsymbol{\theta}^n,\boldsymbol{\gamma})_{\Omega^s} = (\bar{\boldsymbol{\phi}_2},\boldsymbol{\gamma})_{\Omega^s} \quad \forall\boldsymbol{\gamma}\in\boldsymbol{L}^2(\Omega^s). \tag{4.55}$$

Proof. We begin by showing that for $\epsilon>0$, $\exists\ \delta>0$ such that if

$\|(\mathbf{u}^n_1-\mathbf{u}^n_2, p^n_1-p^n_2, \boldsymbol{\eta}^n_1-\boldsymbol{\eta}^n_2, \dot{\boldsymbol{\eta}}^n_1-\dot{\boldsymbol{\eta}}^n_2, \mathbf{g}^n_1-\mathbf{g}^n_2)\|_{\mathbf{X}} < \delta$, then

$\|M(\mathbf{u}^n_1, p^n_1, \boldsymbol{\eta}^n_1, \dot{\boldsymbol{\eta}}^n_1, \mathbf{g}^n_1) - M(\mathbf{u}^n_2, p^n_2, \boldsymbol{\eta}^n_2, \dot{\boldsymbol{\eta}}^n_2, \mathbf{g}^n_2)$

$$-M'(\mathbf{u}^n, p^n, \boldsymbol{\eta}^n, \dot{\boldsymbol{\eta}}^n, \mathbf{g}^n)\cdot(\mathbf{u}^n_1-\mathbf{u}^n_2, p^n_1-p^n_2, \boldsymbol{\eta}^n_1-\boldsymbol{\eta}^n_2, \dot{\boldsymbol{\eta}}^n_1-\dot{\boldsymbol{\eta}}^n_2, \mathbf{g}^n_1-\mathbf{g}^n_2)\|_{\mathbf{Y}} \le \epsilon.$$

Let $\epsilon > 0$. For any $(\mathbf{v}, q, \boldsymbol{\xi}, \boldsymbol{\gamma}) \in \mathbf{Y}^*$,

$$
\begin{aligned}
&\langle M(\mathbf{u}_1^n, p_1^n, \boldsymbol{\eta}_1^n, \dot{\boldsymbol{\eta}}_1^n, \mathbf{g}_1^n) - M(\mathbf{u}_2^n, p_2^n, \boldsymbol{\eta}_2^n, \dot{\boldsymbol{\eta}}_2^n, \mathbf{g}_2^n) \\
&\quad - M'(\mathbf{u}^n, p^n, \boldsymbol{\eta}^n, \dot{\boldsymbol{\eta}}^n, \mathbf{g}^n) \cdot (\mathbf{u}_1^n - \mathbf{u}_2^n, p_1^n - p_2^n, \boldsymbol{\eta}_1^n - \boldsymbol{\eta}_2^n, \dot{\boldsymbol{\eta}}_1^n - \dot{\boldsymbol{\eta}}_2^n, \mathbf{g}_1^n - \mathbf{g}_2^n), (\mathbf{v}, q, \boldsymbol{\xi}, \boldsymbol{\gamma})\rangle \\
&\quad = c(\mathbf{u}_1^n, \mathbf{u}_1^n, \mathbf{v})_{\Omega_{t_n}^f} + \frac{1}{2}((\mathbf{u}_1^n \cdot \mathbf{n}_f)\mathbf{u}_1^n, \mathbf{v})_{\Gamma_N^f} - c(\mathbf{u}_2^n, \mathbf{u}_2^n, \mathbf{v})_{\Omega_{t_n}^f} - \frac{1}{2}((\mathbf{u}_2^n \cdot \mathbf{n}_f)\mathbf{u}_2^n, \mathbf{v})_{\Gamma_N^f} \\
&\qquad - c(\mathbf{u}^n, \mathbf{u}_1^n - \mathbf{u}_2^n, \mathbf{v})_{\Omega_{t_n}^f} - c(\mathbf{u}_1^n - \mathbf{u}_2^n, \mathbf{u}^n, \mathbf{v})_{\Omega_{t_n}^f} - \frac{1}{2}((\mathbf{u}^n \cdot \mathbf{n}_f)(\mathbf{u}_1^n - \mathbf{u}_2^n), \mathbf{v})_{\Gamma_N^f} \\
&\qquad - \frac{1}{2}(((\mathbf{u}_1^n - \mathbf{u}_2^n) \cdot \mathbf{n}_f)\mathbf{u}^n, \mathbf{v})_{\Gamma_N^f} \\
&\quad = c(\mathbf{u}_1^n - \mathbf{u}_2^n, \mathbf{u}_1^n, \mathbf{v})_{\Omega_{t_n}^f} + \frac{1}{2}(((\mathbf{u}_1^n - \mathbf{u}_2^n) \cdot \mathbf{n}_f)\mathbf{u}_1^n, \mathbf{v})_{\Gamma_N^f} \\
&\qquad + c(\mathbf{u}_2^n, \mathbf{u}_1^n - \mathbf{u}_2^n, \mathbf{v})_{\Omega_{t_n}^f} + \frac{1}{2}((\mathbf{u}_2^n \cdot \mathbf{n}_f)(\mathbf{u}_1^n - \mathbf{u}_2^n), \mathbf{v})_{\Gamma_N^f} \\
&\qquad - c(\mathbf{u}^n, \mathbf{u}_1^n - \mathbf{u}_2^n, \mathbf{v})_{\Omega_{t_n}^f} - c(\mathbf{u}_1^n - \mathbf{u}_2^n, \mathbf{u}^n, \mathbf{v})_{\Omega_{t_n}^f} - \frac{1}{2}((\mathbf{u}^n \cdot \mathbf{n}_f)(\mathbf{u}_1^n - \mathbf{u}_2^n), \mathbf{v})_{\Gamma_N^f} \\
&\qquad - \frac{1}{2}(((\mathbf{u}_1^n - \mathbf{u}_2^n) \cdot \mathbf{n}_f)\mathbf{u}^n, \mathbf{v})_{\Gamma_N^f} \leq C \left\|\mathbf{u}_1^n - \mathbf{u}_2^n\right\|_{1,\Omega_{t_n}^f} \left\|\mathbf{v}\right\|_{1,\Omega_{t_n}^f}.
\end{aligned}
$$

Therefore, $\|M(\mathbf{u}_1^n, p_1^n, \boldsymbol{\eta}_1^n, \dot{\boldsymbol{\eta}}_1^n, \mathbf{g}_1^n) - M(\mathbf{u}_2^n, p_2^n, \boldsymbol{\eta}_2^n, \dot{\boldsymbol{\eta}}_2^n, \mathbf{g}_2^n)$
$-M'(\mathbf{u}^n, p^n, \boldsymbol{\eta}^n, \dot{\boldsymbol{\eta}}^n, \mathbf{g}^n) \cdot (\mathbf{u}_1^n - \mathbf{u}_2^n, p_1^n - p_2^n, \boldsymbol{\eta}_1^n - \boldsymbol{\eta}_2^n, \dot{\boldsymbol{\eta}}_1^n - \dot{\boldsymbol{\eta}}_2^n, \mathbf{g}_1^n - \mathbf{g}_2^n)\|_{\mathbf{Y}} \leq C \left\|\mathbf{u}_1^n - \mathbf{u}_2^n\right\|_{1,\Omega_{t_n}^f}$
$\leq \epsilon$ when $\|(\mathbf{u}_1^n - \mathbf{u}_2^n, p_1^n - p_2^n, \boldsymbol{\eta}_1^n - \boldsymbol{\eta}_2^n, \dot{\boldsymbol{\eta}}_1^n - \dot{\boldsymbol{\eta}}_2^n, \mathbf{g}_1^n - \mathbf{g}_2^n)\|_{\mathbf{X}}$ is sufficiently small.

□

It is straight forward to verify Assumption 2 of Lemma 4.7, showing that $\mathcal{J}_n^\delta$ is Fréchet differentiable at $(\mathbf{u}^n, p^n, \boldsymbol{\eta}^n, \dot{\boldsymbol{\eta}}^n, \mathbf{g}^n)$ with Fréchet derivative $(\mathcal{J}_n^\delta)'$. Next, we will prove Assumption 3 and the second part of Assumption 1 of Lemma 4.7.

Theorem 4.9. *The operator $M' : \mathbf{X} \to \mathbf{Y}$ is onto $\mathbf{Y}$ for a sufficiently small Δt and $\left\|\mathbf{u}^0\right\|_{0,\Omega_{t_n}^f}$, and M' is continuous at $(\mathbf{u}^n, p^n, \boldsymbol{\eta}^n, \dot{\boldsymbol{\eta}}^n, \mathbf{g}^n)$.*

Proof. In Theorem 4.8, it was shown that M' exists and maps $\mathbf{X} \to \mathbf{Y}$. With $\mathbf{h}^n = \mathbf{0}$ and $\mathbf{v} = \mathbf{w}^n$, (4.52)–(4.53) is a time-discretized linearized Navier–Stokes operator with four additional terms: $c(\mathbf{w}^n, \mathbf{u}^n, \mathbf{w}^n)_{\Omega_{t_n}^f}$, $((\nabla \cdot \mathbf{z}^n)\mathbf{w}^n, \mathbf{w}^n)_{\Omega_{t_n}^f}$, $((\mathbf{w}^n \cdot \mathbf{n}_f)\mathbf{u}^n, \mathbf{w}^n)_{\Gamma_N^f}$, and $((\mathbf{u}^n \cdot \mathbf{n}_f)\mathbf{w}^n, \mathbf{w}^n)_{\Gamma_N^f}$. Coercivity of the linearized Navier–Stokes operater can be proven without a time step restriction [65, p. 334], i.e, we are left with proving that for any

$\mathbf{w}^n \in \boldsymbol{H}^1_D(\Omega^f_{t_n})$,

$$\frac{\rho^f}{\Delta t}\left\|\mathbf{w}^n\right\|^2_{0,\Omega^f_{t_n}} + C_9\nu_f\left\|\mathbf{w}^n\right\|^2_{1,\Omega^f_{t_n}} + \rho^f c(\mathbf{w}^n,\mathbf{u}^n,\mathbf{w}^n)_{\Omega^f_{t_n}} - \frac{\rho^f}{2}((\nabla\cdot\mathbf{z}^n)\mathbf{w}^n,\mathbf{w}^n)_{\Omega^f_{t_n}} + \frac{\rho^f}{2}((\mathbf{u}^n\cdot\mathbf{n}_f)\mathbf{w}^n,\mathbf{w}^n)_{\Gamma^f_N} + \frac{\rho^f}{2}((\mathbf{w}^n\cdot\mathbf{n}_f)\mathbf{u}^n,\mathbf{w}^n)_{\Gamma^f_N} \geq C_{10}\left\|\mathbf{w}^n\right\|_{1,\Omega^f_{t_n}},$$

where C_9 and C_{10} are some positive constants.

Here, we show that $\rho^f c(\mathbf{w}^n,\mathbf{u}^n,\mathbf{w}^n)_{\Omega^f_{t_n}} \leq C_{11}\frac{\rho^{f4}\|\mathbf{u}^n\|^4_{1,\Omega^f_{t_n}}}{C_9^3\nu_f^3}\left\|\mathbf{w}^n\right\|^2_{0,\Omega^f_{t_n}} + \frac{C_9\nu_f}{4}\left\|\mathbf{w}^n\right\|^2_{1,\Omega^f_{t_n}}$.

$$\begin{aligned}\rho^f c(\mathbf{w}^n,\mathbf{u}^n,\mathbf{w}^n)_{\Omega^f_{t_n}} &= \frac{\rho^f}{2}\left[(\mathbf{w}^n\cdot\nabla\mathbf{u}^n,\mathbf{w}^n)_{\Omega^f_{t_n}} - (\mathbf{w}^n\cdot\nabla\mathbf{w}^n,\mathbf{u}^n)_{\Omega^f_{t_n}}\right]\\ &\leq \frac{C\rho^f}{2}\Big[\left\|\mathbf{w}^n\right\|_{\mathbf{L}^4,\Omega^f_{t_n}}\left\|\nabla\mathbf{u}^n\right\|_{0,\Omega^f_{t_n}}\left\|\mathbf{w}^n\right\|_{\mathbf{L}^4,\Omega^f_{t_n}}\\ &\qquad + \left\|\mathbf{w}^n\right\|_{\mathbf{L}^4,\Omega^f_{t_n}}\left\|\nabla\mathbf{w}^n\right\|_{0,\Omega^f_{t_n}}\left\|\mathbf{u}^n\right\|_{\mathbf{L}^4,\Omega^f_{t_n}}\Big]\end{aligned}$$

by applying Hölder's inequality with p=4, q=2, r=4,

$$\leq C\rho^f\left\|\mathbf{w}^n\right\|^{\frac{1}{2}}_{0,\Omega^f_{t_n}}\left\|\mathbf{w}^n\right\|^{\frac{3}{2}}_{1,\Omega^f_{t_n}}\left\|\mathbf{u}^n\right\|_{1,\Omega^f_{t_n}}$$

since $\Omega^f_{t_n} \in \mathbb{R}^2$ [50, p. 11],

$$\leq C\frac{\rho^f}{4}\left\|\mathbf{w}^n\right\|^2_{0,\Omega^f_{t_n}}\left\|\mathbf{u}^n\right\|^4_{1,\Omega^f_{t_n}}\frac{(3\rho^f)^3}{(C_9\nu_f)^3} + \frac{3C_9\nu_f}{3\cdot 4}\left\|\mathbf{w}^n\right\|^2_{1,\Omega^f_{t_n}}$$

applying Young's inequality with p=4 and q=$\frac{4}{3}$. Therefore,

$$\rho^f c(\mathbf{w}^n,\mathbf{u}^n,\mathbf{w}^n)_{\Omega^f_{t_n}} \leq C_{11}\frac{\rho^{f4}\left\|\mathbf{u}^n\right\|^4_{1,\Omega^f_{t_n}}}{C_9^3\nu_f^3}\left\|\mathbf{w}^n\right\|^2_{0,\Omega^f_{t_n}} + \frac{C_9\nu_f}{4}\left\|\mathbf{w}^n\right\|^2_{1,\Omega^f_{t_n}}.$$

The term $\mathbf{u}^n$ is uniformly bounded by (4.18) independent of Δt, if the additional assumption is made that $\left\|\mathbf{u}^0\right\|_{0,\Omega^f_{t_n}} < \Delta t^4$. This is a reasonable assumption to make if the simulation begins at rest. Because $\mathbf{z}^n \in \mathbf{W}^{1,\infty}(\Omega^f_{t_n})$ by assumption (4.16), we can bound $\rho^f((\nabla\cdot\mathbf{z}^n)\mathbf{w}^n,\mathbf{w}^n)_{\Omega^f_{t_n}} \leq C_{12}\rho^f\left\|\nabla\cdot\mathbf{z}^n\right\|_{\mathbf{L}^\infty,\Omega^f_{t_n}}\left\|\mathbf{w}^n\right\|^2_{0,\Omega^f_{t_n}}$ using Hölder's inequality with p=∞, q=2, and r=2. Applying the Sobolev imbedding of $\mathbf{W}^{\frac{1}{2},2}(\Gamma_{I_{t_n}}) \subseteq \mathbf{W}^{0,4}(\Gamma_{I_{t_n}})$ [1, p. 85] followed by Hölder's inequality and the trace theorem along with the boundedness of $\mathbf{u}^n$ from (4.18),

we get

$$\begin{aligned}
\rho^f((\mathbf{w}^n\cdot\mathbf{n}_f)\mathbf{u}^n,\mathbf{w}^n)_{\Gamma_N^f} &\leq C\rho^f\left\|\mathbf{n}_f\right\|_{\mathbf{L}^\infty,\Gamma_{I_{t_n}}}\left\|\mathbf{w}^n\right\|_{\mathbf{L}^4,\Gamma_{I_{t_n}}}\left\|\mathbf{u}^n\right\|_{\mathbf{L}^4,\Gamma_{I_{t_n}}}\left\|\mathbf{w}^n\right\|_{0,\Gamma_{I_{t_n}}}\\
&\leq C\rho^f\left\|\mathbf{w}^n\right\|_{\mathbf{W}^{\frac{1}{2},2},\Gamma_{I_{t_n}}}\left\|\mathbf{u}^n\right\|_{\mathbf{W}^{\frac{1}{2},2},\Gamma_{I_{t_n}}}\left\|\mathbf{w}^n\right\|^{\frac{1}{2}}_{0,\Omega^f_{t_n}}\left\|\mathbf{w}^n\right\|^{\frac{1}{2}}_{1,\Omega^f_{t_n}}\\
&\leq C\rho^f\left\|\mathbf{w}^n\right\|^{\frac{1}{2}}_{0,\Omega^f_{t_n}}\left\|\mathbf{w}^n\right\|^{\frac{3}{2}}_{1,\Omega^f_{t_n}}\left\|\mathbf{u}^n\right\|_{1,\Omega^f_{t_n}}\\
&\leq C_{13}\rho^f\left\|\mathbf{w}^n\right\|^2_{0,\Omega^f_{t_n}}\left\|\mathbf{u}^n\right\|^4_{1,\Omega^f_{t_n}}\frac{{\rho^f}^3}{C_9^3\nu_f^3}+\frac{C_9\nu_f}{2}\left\|\mathbf{w}^n\right\|^2_{1,\Omega^f_{t_n}}\\
&\leq \frac{C_{13}{\rho^f}^4}{C_9^3\nu_f^3}\left\|\mathbf{u}^n\right\|^4_{1,\Omega^f_{t_n}}\left\|\mathbf{w}^n\right\|^2_{0,\Omega^f_{t_n}}+\frac{C_9\nu_f}{2}\left\|\mathbf{w}^n\right\|^2_{1,\Omega^f_{t_n}}.
\end{aligned}$$

We apply the inequalities and imbeddings in the same way for $\rho^f((\mathbf{u}^n\cdot\mathbf{n}_f)\mathbf{w}^n,\mathbf{w}^n)_{\Gamma_N^f}$. Again, C_{11}, C_{12}, and C_{13} are positive constants. Now we have that

$$\begin{aligned}
\left\|\mathbf{w}^n\right\|^2_{0,\Omega^f_{t_n}}&\left[\frac{1}{\Delta t}-[C_{11}+C_{13}]\frac{{\rho^f}^4\left\|\mathbf{u}^n\right\|^4_{1,\Omega^f_{t_n}}}{C_9^3\nu_f^3}-\frac{\rho^f}{2}\left\|\nabla\cdot\mathbf{z}^n\right\|_{\mathbf{L}^\infty,\Omega^f_{t_n}}\right]\\
&+\frac{C_9\nu_f}{4}\left\|\mathbf{w}^n\right\|^2_{1,\Omega^f_{t_n}}\geq C_{10}\left\|\mathbf{w}^n\right\|_{1,\Omega^f_{t_n}},
\end{aligned}$$

where C_{10} is a positive constant. This result yields the coercivity of (4.52)–(4.53) when Δt is sufficiently small.

The operator for (4.52)–(4.53) is a time-discretized linearized Navier–Stokes operator with five additional terms: $c(\mathbf{w}^n,\mathbf{u}^n,\mathbf{v})_{\Omega^f_{t_n}}$, $((\nabla\cdot\mathbf{z}^n)\mathbf{w}^n,\mathbf{v})_{\Omega^f_{t_n}}$, $((\mathbf{w}^n\cdot\mathbf{n}_f)\mathbf{u}^n,\mathbf{v})_{\Gamma_N^f}$, $((\mathbf{u}^n\cdot\mathbf{n}_f)\mathbf{w}^n,\mathbf{v})_{\Gamma_N^f}$, and $(\mathbf{h}^n,\mathbf{v})_{\Gamma_{I_{t_n}}}$. We begin by noting that the linearized Navier–Stokes operator is continuous [65, p. 334] and now turn our attention to these five additional terms. For the first term, apply Hölder's inequality and the regularity of $\mathbf{u}^n$. For the second term, apply Hölder's inequality and use the regularity of $\mathbf{z}^n$ (see (4.16)). Then, apply the Sobolev imbedding of $\mathbf{W}^{\frac{1}{2},2}(\Gamma_{I_{t_n}})\subseteq\mathbf{W}^{0,4}(\Gamma_{I_{t_n}})$ and Hölder's inequality followed by the trace theorem along with the boundedness of $\mathbf{u}^n$ to the third and fourth terms. For the fifth term, apply Cauchy–Schwarz inequality. In this way, it can be shown that (4.52)–(4.53) is continuous at $(\mathbf{u}^n,p^n,\boldsymbol{\eta}^n,\dot{\boldsymbol{\eta}}^n,\mathbf{g}^n)$. Since (4.54)–(4.55) is linear, it retains the same continuity

as the system (4.6)–(4.7).

Using the Lax–Milgram theorem and the continuity, coercivity, and inf-sup condition satisfied by the operator (4.52)–(4.53), for each element in $\mathbf{Y}$, there is a unique solution in $\mathbf{X}$. Similarly, with $\mathbf{h}^n = \mathbf{0}$, (4.54)–(4.55) have the same properties of well-posedness as (4.50)–(4.51).

Since a unique solution to $M'(\mathbf{u}^n, p^n, \boldsymbol{\eta}^n, \dot{\boldsymbol{\eta}}^n, \mathbf{g}^n) \cdot (\mathbf{w}^n, r^n, \boldsymbol{\theta}^n, \boldsymbol{\varphi}^n, \mathbf{h}^n) = (\bar{\mathbf{f}}_f^n, \bar{\phi}_1, \bar{\mathbf{f}}_s^n, \bar{\boldsymbol{\phi}}_2)$ exists $\forall (\bar{\mathbf{f}}_f^n, \bar{\phi}_1^n, \bar{\mathbf{f}}_s^n, \bar{\boldsymbol{\phi}}_2^n) \in \mathbf{Y}$, $M'(\mathbf{u}^n, p^n, \boldsymbol{\eta}^n, \dot{\boldsymbol{\eta}}^n, \mathbf{g}^n)$ is onto $\mathbf{Y}$. □

Theorem 4.10. *Let* $(\mathbf{u}^n, p^n, \boldsymbol{\eta}^n, \dot{\boldsymbol{\eta}}^n, \mathbf{g}^n) \in \mathbf{X}$ *denote an optimal solution to Problem* (4.10). *Then there exists a nonzero Lagrange multiplier* $(\bar{\mathbf{u}}^n, \bar{p}^n, \bar{\boldsymbol{\eta}}^n, \bar{\dot{\boldsymbol{\eta}}}^n) \in \mathbf{Y}^*$ *such that*

$$
\begin{aligned}
-(\mathcal{J}_n^\delta)'(\mathbf{u}^n, p^n, \boldsymbol{\eta}^n, \dot{\boldsymbol{\eta}}^n, \mathbf{g}^n) \cdot (\mathbf{w}^n, r^n, \boldsymbol{\theta}^n, \boldsymbol{\varphi}^n, \mathbf{h}^n) \\
+ \langle M'(\mathbf{u}^n, p^n, \boldsymbol{\eta}^n, \dot{\boldsymbol{\eta}}^n, \mathbf{g}^n) \cdot (\mathbf{w}^n, r^n, \boldsymbol{\theta}^n, \boldsymbol{\varphi}^n, \mathbf{h}^n), (\bar{\mathbf{u}}^n, \bar{p}^n, \bar{\boldsymbol{\eta}}^n, \bar{\dot{\boldsymbol{\eta}}}^n) \rangle = 0 \\
\forall (\mathbf{w}^n, r^n, \boldsymbol{\theta}^n, \boldsymbol{\varphi}^n, \mathbf{h}^n) \in \mathbf{X}, \qquad (4.56)
\end{aligned}
$$

where $\mathbf{Y}^* = \boldsymbol{H}_D^1(\Omega_{t_n}^f) \times L^2(\Omega_{t_n}^f) \times \boldsymbol{H}_D^1(\Omega^s) \times \boldsymbol{L}^2(\Omega^s)$.

Proof. We have shown that M' is onto $\mathbf{Y}$, that M' exists and is continuous in a neighborhood about $(\mathbf{u}^n, p^n, \boldsymbol{\eta}^n, \dot{\boldsymbol{\eta}}^n, \mathbf{g}^n) \in \mathbf{X}$, and we also know that $\mathcal{J}_n^\delta$ is Fréchet differentiable. We now apply Lemma 4.7 to see that there exists a solution $(\bar{\mathbf{u}}^n, \bar{p}^n, \bar{\boldsymbol{\eta}}^n, \bar{\dot{\boldsymbol{\eta}}}^n) \in \mathbf{Y}^*$ satisfying (4.56). □

4.8 Lagrange Multiplier Rule

The optimality system will now be derived using the Lagrange multiplier rule. Again, we treat the deformation and velocity of Ω_t^f as known. For an example of performing such a derivation with the deformation and velocity of Ω_t^f treated as unknowns, see [63], where optimization was applied to a fluid-structure interaction problem for the purpose of parameter estimation.

Let us begin by defining the Lagrangian

$$
\begin{aligned}
&\mathcal{L}(\mathbf{u}^n, p^n, \boldsymbol{\eta}^n, \dot{\boldsymbol{\eta}}^n, \mathbf{g}^n, \bar{\mathbf{u}}^n, \bar{p}^n, \bar{\boldsymbol{\eta}}^n, \bar{\dot{\boldsymbol{\eta}}}^n) = \\
&\quad - \mathcal{J}_n^\delta(\mathbf{u}^n, p^n, \boldsymbol{\eta}^n, \dot{\boldsymbol{\eta}}^n, \mathbf{g}^n) + \rho^f[(\mathbf{u}^n, \bar{\mathbf{u}}^n)_{\Omega^f_{t_n}} - (\mathbf{u}^{n-1}, \mathcal{V}(\bar{\mathbf{u}}^n))_{\Omega^f_{t_{n-1}}}] \\
&\quad + \Delta t\ \rho^f[c(\mathbf{u}^n, \mathbf{u}^n, \bar{\mathbf{u}}^n)_{\Omega^f_{t_n}} + \frac{1}{2}((\mathbf{u}^n \cdot \mathbf{n}_f)\mathbf{u}^n, \bar{\mathbf{u}}^n)_{\Gamma^f_N} - \frac{1}{2}((\nabla \cdot \mathbf{z}^n)\mathbf{u}^n, \bar{\mathbf{u}}^n)_{\Omega^f_{t_n}} \\
&\quad - c(\mathbf{z}^n, \mathbf{u}^n, \bar{\mathbf{u}}^n)_{\Omega^f_{t_n}}] + \Delta t\ 2\nu_f a(\mathbf{u}^n, \bar{\mathbf{u}}^n)_{\Omega^f_{t_n}} + \Delta t\ b(\bar{\mathbf{u}}^n, p^n)_{\Omega^f_{t_n}} - \Delta t\ (\mathbf{f}^n_f, \bar{\mathbf{u}}^n)_{\Omega^f_{t_n}} \\
&\quad - \Delta t\ (\mathbf{u}^n_N, \bar{\mathbf{u}}^n)_{\Gamma^f_N} - \Delta t\ (\mathbf{g}^n, \bar{\mathbf{u}}^n)_{\Gamma_{I_{t_n}}} + \Delta t\ b(\mathbf{u}^n, \bar{p}^n)_{\Omega^f_{t_n}} + \rho^s[(\dot{\boldsymbol{\eta}}^n, \bar{\boldsymbol{\eta}}^n)_{\Omega^s} - (\dot{\boldsymbol{\eta}}^{n-1}, \bar{\boldsymbol{\eta}}^n)_{\Omega^s}] \\
&\quad + \Delta t\ \nu_s d(\boldsymbol{\eta}^n + \boldsymbol{\eta}^{n-1}, \bar{\boldsymbol{\eta}}^n)_{\Omega^s} + \frac{\Delta t}{2}\ \lambda e(\boldsymbol{\eta}^n + \boldsymbol{\eta}^{n-1}, \bar{\boldsymbol{\eta}}^n)_{\Omega^s} - \frac{\Delta t}{2}\ (\mathbf{f}^n_s + \mathbf{f}^{n-1}_s, \bar{\boldsymbol{\eta}}^n)_{\Omega^s} \\
&\quad - \frac{\Delta t}{2}\ (\boldsymbol{\eta}^n_N + \boldsymbol{\eta}^{n-1}_N, \bar{\boldsymbol{\eta}}^n)_{\Gamma^s_N} + \frac{\Delta t}{2}\ (\mathcal{V}(\mathbf{g}^n)J_{t_n} + \mathcal{V}(\mathbf{g}^{n-1})J_{t_{n-1}}, \bar{\boldsymbol{\eta}}^n)_{\Gamma_{I_{t_0}}} + \frac{\Delta t}{2}[(\dot{\boldsymbol{\eta}}^n, \bar{\dot{\boldsymbol{\eta}}}^n)_{\Omega^s} \\
&\quad + (\dot{\boldsymbol{\eta}}^{n-1}, \bar{\dot{\boldsymbol{\eta}}}^n)_{\Omega^s}] - [(\boldsymbol{\eta}^n, \bar{\dot{\boldsymbol{\eta}}}^n)_{\Omega^s} - (\boldsymbol{\eta}^{n-1}, \bar{\dot{\boldsymbol{\eta}}}^n)_{\Omega^s}]
\end{aligned}
$$

for any $(\mathbf{u}^n, p^n, \boldsymbol{\eta}^n, \dot{\boldsymbol{\eta}}^n, \mathbf{g}^n, \bar{\mathbf{u}}^n, \bar{p}^n, \bar{\boldsymbol{\eta}}^n, \bar{\dot{\boldsymbol{\eta}}}^n) \in \mathbf{X} \times \mathbf{Y}^*$. We will now seek to find stationary points of $\mathcal{L}$ over the product space $\mathbf{X} \times \mathbf{Y}^*$. Variations in the Lagrange multipliers $\bar{\mathbf{u}}^n, \bar{p}^n, \bar{\boldsymbol{\eta}}^n$, and $\bar{\dot{\boldsymbol{\eta}}}^n$ yield the state equations (4.4)–(4.7). Variations in the state variables $\mathbf{u}^n, p^n, \boldsymbol{\eta}^n$, and $\dot{\boldsymbol{\eta}}^n$ yield the adjoint equations

$$
\begin{aligned}
\rho^f(\bar{\mathbf{u}}^n, \mathbf{v})_{\Omega^f_{t_n}} &+ \Delta t\ \rho^f[c(\mathbf{u}^n, \mathbf{v}, \bar{\mathbf{u}}^n)_{\Omega^f_{t_n}} + c(\mathbf{v}, \mathbf{u}^n, \bar{\mathbf{u}}^n)_{\Omega^f_{t_n}} + \frac{1}{2}((\mathbf{u}^n \cdot \mathbf{n}_f)\mathbf{v}, \bar{\mathbf{u}}^n)_{\Gamma^f_N} \\
&+ \frac{1}{2}((\mathbf{v} \cdot \mathbf{n}_f)\mathbf{u}^n, \bar{\mathbf{u}}^n)_{\Gamma^f_N} - \frac{1}{2}((\nabla \cdot \mathbf{z}^n)\mathbf{v}, \bar{\mathbf{u}}^n)_{\Omega^f_{t_n}} \\
&- c(\mathbf{z}^n, \mathbf{v}, \bar{\mathbf{u}}^n)_{\Omega^f_{t_n}}] + \Delta t\ 2\nu_f a(\bar{\mathbf{u}}^n, \mathbf{v})_{\Omega^f_{t_n}} + \Delta t\ b(\mathbf{v}, \bar{p}^n)_{\Omega^f_{t_n}} \\
&= \left(\mathbf{u}^n - \frac{\mathcal{V}(\boldsymbol{\eta}^n) - \mathcal{V}(\boldsymbol{\eta}^{n-1})}{\Delta t}, \mathbf{v}\right)_{\Gamma_{I_{t_n}}} \qquad \forall \mathbf{v} \in \boldsymbol{H}^1_D(\Omega^f_{t_n}), \qquad (4.57)
\end{aligned}
$$

$$
b(\bar{\mathbf{u}}^n, q)_{\Omega^f_{t_n}} = 0 \quad q \in L^2(\Omega^f_{t_n}), \qquad (4.58)
$$

$$-(\bar{\dot{\boldsymbol{\eta}}}^n, \boldsymbol{\xi})_{\Omega^s} + \Delta t\ \nu_s d(\bar{\boldsymbol{\eta}}^n, \boldsymbol{\xi})_{\Omega^s} + \frac{\Delta t}{2}\ \lambda e(\bar{\boldsymbol{\eta}}^n, \boldsymbol{\xi})_{\Omega^s}$$
$$= -\frac{1}{\Delta t}\left(J_{t_n}\left[\mathcal{V}(\mathbf{u}^n) - \frac{\boldsymbol{\eta}^n - \boldsymbol{\eta}^{n-1}}{\Delta t}\right], \boldsymbol{\xi}\right)_{\Gamma_{I_{t_0}}} \quad \forall \boldsymbol{\xi} \in \boldsymbol{H}^1_D(\Omega^s), \tag{4.59}$$

$$\frac{\Delta t}{2}(\bar{\dot{\boldsymbol{\eta}}}^n, \boldsymbol{\gamma})_{\Omega^s} + \rho^s(\bar{\boldsymbol{\eta}}^n, \boldsymbol{\gamma})_{\Omega^s} = 0 \quad \forall \boldsymbol{\gamma} \in \boldsymbol{L}^2(\Omega^s). \tag{4.60}$$

Also, variations in the control $\mathbf{g}^n$ yield the necessary condition

$$\delta(\mathbf{g}^n, \mathbf{c})_{\Gamma_{I_{t_n}}} = -\Delta t\ (\mathbf{c}, \bar{\mathbf{u}}^n)_{\Gamma_{I_{t_n}}} + \frac{\Delta t}{2}\ (\mathcal{V}(\mathbf{c})J_{t_n}, \bar{\boldsymbol{\eta}}^n)_{\Gamma_{I_{t_0}}} \quad \forall \mathbf{c} \in \mathbf{L}^2(\Gamma_{I_{t_n}}). \tag{4.61}$$

The adjoint problem (4.57)–(4.60) is well-posed, similar to the linearized problem (4.52)–(4.55). Also, (4.56) can be rewritten as the adjoint equations (4.57)–(4.60) and the necessary condition (4.61). It is obvious that an optimal solution to (4.8) will satisfy the state equations (4.48)–(4.51), and therefore we see that an optimal solution satisfies the optimality system (4.4)–(4.7), (4.57)–(4.60), and (4.61).

4.9 Steepest Descent Approach

The optimality system is often large in practice, and so it is common practice to decouple the state equations, adjoint equations, and the necessary condition. This is referred to as a reduced space method [12]. As in [31], we will use a gradient method for minimizing the penalized function (4.9).

Accordingly, $\mathbf{g}^n_{(k)} = \mathbf{g}^n_{(k-1)} - \omega_k \frac{d\mathcal{J}^\delta_n}{d\mathbf{g}^n_{(k)}}$, where ω_k is a step-size appropriately chosen. The necessary condition (4.61) allows us to solve for $\frac{d\mathcal{J}^\delta_n}{d\mathbf{g}^n_{(k)}}$, yielding [39]

$\frac{d\mathcal{J}^\delta_n}{d\mathbf{g}^n_{(k)}} = \delta\mathbf{g}^n + \Delta t\bar{\mathbf{u}}^n|_{\Gamma_{I_{t_n}}} - \frac{\Delta t}{2}\ \bar{\boldsymbol{\eta}}^n \circ (\Psi^n_{(k)})^{-1}|_{\Gamma_{I_{t_n}}}$.

Let ω_k have the form $\frac{\alpha_k}{\delta}$, and now the algorithm has the form

$$\mathbf{g}^n_{(k+1)} = (1-\alpha_k)\mathbf{g}^n_{(k)} - \frac{\alpha_k}{\delta}(\Delta t\bar{\mathbf{u}}^n_{(k)}|_{\Gamma_{I_{t_n}}} - \frac{\Delta t}{2}\ \bar{\boldsymbol{\eta}}^n_{(k)} \circ (\Psi^n_{(k)})^{-1}|_{\Gamma_{I_{t_n}}}). \tag{4.62}$$

Algorithm 4.11. Steepest Descent Algorithm

1. Choose an initial control $\mathbf{g}^n_{(0)}$

2. For $k = 0, 1, \ldots$

   (a) Solve (4.4)–(4.7) for $(\mathbf{u}^n_{(k)}, p^n_{(k)}, \boldsymbol{\eta}^n_{(k)}, \dot{\boldsymbol{\eta}}^n_{(k)})$

   (b) If $\int_{\Gamma_{I_{t_n}}} \left| \mathbf{u}^n_{(k)} - \frac{\mathcal{V}(\boldsymbol{\eta}^n) - \mathcal{V}(\boldsymbol{\eta}^{n-1})}{\Delta t} \right|^2 \, d\Gamma < \epsilon_{tol}$, then break

   (c) Solve (4.57)–(4.60) for $(\bar{\mathbf{u}}^n_{(k)}, \bar{p}^n_{(k)}, \bar{\boldsymbol{\eta}}^n_{(k)}, \bar{\dot{\boldsymbol{\eta}}}^n_{(k)})$

   (d) Update the control using (4.62)

   (e) Solve (2.31), and then update $\mathbf{z}^n_{(k)}$ and the mesh deformation gradient

4.10 Numerical Results

An FSI problem using the ALE formulation for the moving fluid domain, reported in [54] and subsequently reproduced in Chapter 3, uses parameters that are consistent with blood flow in a human body.

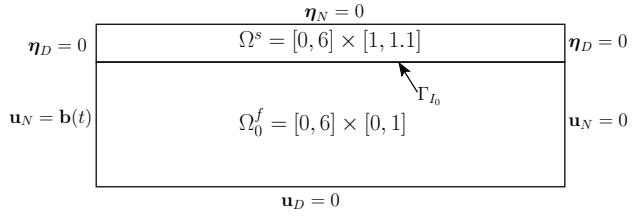

Figure 4.1: Domain and boundary conditions for numerical experiment

A force $\mathbf{b}(t)$ is applied to the left fluid boundary (Fig. 4.1) at t s where

$$\mathbf{b}(t) = \begin{cases} (-10^3(1 - \cos\frac{2\pi t}{.025}), 0) \ \text{ dyne/cm}^2, & t \leq 0.025 \\ (0,0), & 0.025 < t < T. \end{cases}$$

The function $\mathbf{b}(t)$ defines the stress on the inlet denoted by $\mathbf{u}_N$ in (2.4). For numerical tests, we impose the Neumann condition on both the inflow and outflow boundaries in order to use the same conditions and parameters as in the literature. The volume force for the fluid and structure are $\mathbf{f}(t) = (0,0)$ dyne/cm^2. The other boundary conditions on the domain

configuration are homogeneous Dirichlet or Neumann (Fig. 4.1), and the simulation begins at rest.

The reference domain for the fluid subsystem has height 1 cm and length 6 cm. The density of the fluid, ρ_f, is 1 g/cm^3 and the viscosity of the fluid, ν_f, is 0.035 g/cm·s. The structure domain has height 0.1 cm and length 6 cm. The density of the structure, ρ_s, is 1.1 g/cm^3. The Young's Modulus of the structure, E, is 3×10^6 dyne/cm^2 and its Poisson ratio, ν, is 0.3. The Lamé parameters λ and ν_s are defined as follows:

$$\lambda = \frac{\nu E}{(1-2\nu)(1+\nu)} \text{ dyne/cm}^2, \quad \nu_s = \frac{E}{2(1+\nu)} \text{ dyne/cm}^2.$$

In Figure 4.2, we compare the vertical displacement over time of three points along the interface. Comparison is made between the solution found using Aitken's relaxation [21] and the solution found using the optimization Algorithm 4.11. See Section 3.6.0.1 or [21] for more details on Aitken's relaxation.

The result using Aitken's relaxation is reliable and useful as a reference solution with which to compare. Spatial discretization was made in the x direction with $h_x = 0.2$ cm and in the y direction with $h_y = 0.1$ cm for both fluid and structure domains on a uniform mesh. The simulation was performed with $\Delta t = 10^{-4}$ s from $T = 0$ s to $T = 0.1$ s. Computations were performed in FreeFEM++ [41] using the triangular $(\mathbb{P}_1 + bubble, \mathbb{P}_1)$ finite element pair for the fluid and triangular $\mathbb{P}_1$ elements for the structure. The stopping criteria used for Aitken's relaxation was $\left(\int_{\Gamma_{I_{t_0}}} (\boldsymbol{\eta}^n_{(k)} - \boldsymbol{\eta}^n_{(k-1)})^2 \, d\Gamma\right)^{\frac{1}{2}} < 10^{-7}$, while $\delta = 10^{-15}$ and $\epsilon_{tol} = 10^{-4}$ for Algorithm 4.11.

There is strong agreement between the solution computed by Aitken's relaxation and the two solutions computed using Algorithm 4.11. The optimization algorithm has been implemented for both the first and second order formulations of the structure subsystem to demonstrate the similarity in result and that requiring a second order structure subsystem formulation is needed for analysis, but not necessarily for computation.

A study was also made of varying the Tikhonov regularization parameter δ in order

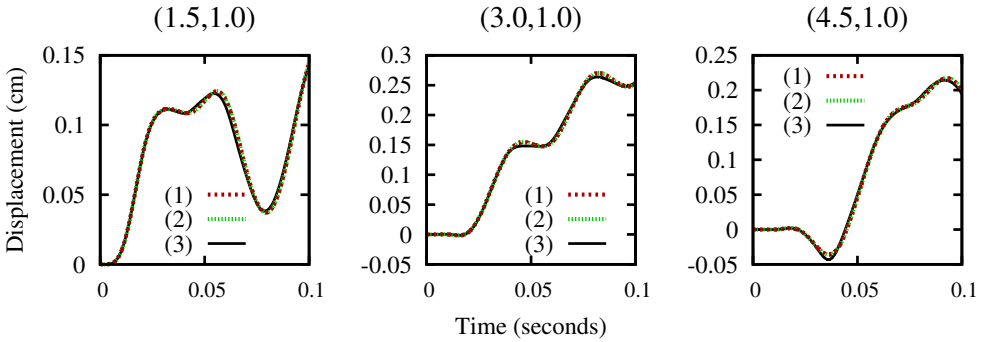

Figure 4.2: Vertical displacement at three points on the interface using (1) first and (2) second order formulations with the optimal control algorithm beside vertical displacement using (3) Aitken's relaxation

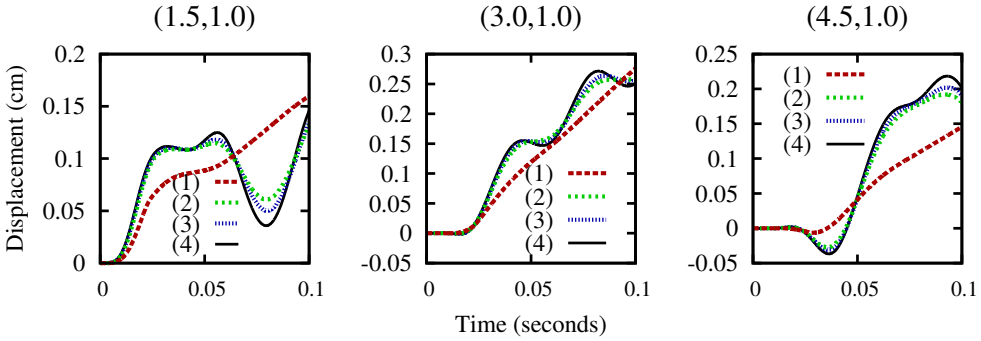

Figure 4.3: Vertical displacement at three points on the interface using (1) $\delta = 10^{-5}$, (2) $\delta = 10^{-6}$, (3) $\delta =$ 5e-7, and (4) $\delta = 10^{-10}$.

to see its effect on the solution. In Figure 4.3, the vertical displacement at three points along the interface are shown for $\delta = \{10^{-5}, 10^{-6}, \text{5e-7}, 10^{-10}\}$. It can be observed that with a larger penalty parameter, the optimization focuses more on minimizing the stress on the interface rather than minimizing the discontinuity of the velocities along the interface. For $\delta < 10^{-10}$, the results were indistinguishable. The computation times were similar for simulations made with $\delta < 10^{-6}$. For choices of δ larger than 10^{-6}, the step size for the steepest descent algorithm was required to be decreased in order for the algorithm not to diverge. This results in a less aggressive optimization, requiring more time to reach an optimal solution. When determining stopping criteria for each time step, it is obvious that

one should stop if the objective value is smaller than ϵ_{tol}. At an optimal solution for a larger δ value, the objective may still be larger than ϵ_{tol}. This requires an additional stopping criteria. An example of such a criteria could be to stop when more than a predetermined number of optimization iterations are executed without relative improvement of more than 1% in the objective.

4.11 Conclusion

We have introduced a control that has allowed the fluid-structure interaction problem to be decoupled into subsystems that may be solved in parallel. This control allowed us to demonstrate the uniform boundedness of each optimization variable in order to show the existence of an optimal solution for a given δ. Then, it was shown that as $\delta \to 0$, the optimal solutions for each given δ converge to an optimal solution with no penalty parameter, and that this optimal solution satisfies the constraint equations and minimizes the functional to within a $C\Delta t^{\frac{3}{2}}$ target tolerance.

The existence of Lagrange multipliers was proved, allowing us to derive the optimality system and to show that an optimal solution satisfies the optimality system. The steepest descent algorithm was then introduced for updating the control in order to decouple the optimality system.

The numerical results confirm that Algorithm 4.11 accurately simulates the fluid-structure interaction for a blood flow problem of great computational difficulty, due to the added mass effect. This computation was made over 1000 time steps while maintaining the correct solution profile, despite the analysis supporting only a single time step. In future work, we hope to provide an analytical framework for the optimal control problem over all time steps and then to extend this work to other fluid-structure configurations.

Chapter 5

THEORETICAL CONVERGENCE RATES

5.1 Introduction

Building off of previous analytical results showing the existence of an optimal solution and Lagrange multipliers in Chapter 4, an a priori error estimate is given for the optimality system by means of Brezzi–Rappaz–Raviart (BRR) [18] theory. The convergence of the steepest descent method is proven in a discrete setting for a sufficiently small time step and mesh size. A numerical study is included supporting the theoretical rate of convergence over a single time step. Additional numerical results demonstrate optimal convergence in space and time over several time steps.

5.2 Description of the Optimization Problem

By applying Green's theorem and replacing the term $(2\nu_f D(\mathbf{u}^n)\cdot\mathbf{n}_f - p\mathbf{n}_f - \frac{1}{2}((\mathbf{u}^n - \mathbf{z}^n)\cdot\mathbf{n}_f)\mathbf{u}^n, \mathbf{v})_{\Gamma_{I_{t_n}}}$ with $(\mathbf{g}^n, \mathbf{v})_{\Gamma_{I_{t_n}}}$ and $(2\nu_s D(\boldsymbol{\eta}^n)\cdot\mathbf{n}_s + \lambda(\nabla\cdot\boldsymbol{\eta}^n)\mathbf{n}_s, \boldsymbol{\xi})$ with $-(\mathcal{V}(\mathbf{g}^n)J_{t_n}, \boldsymbol{\xi})_{\Gamma_{I_{t_0}}}$ on the interface, we are left with seeking a $\mathbf{g}^n$ that will minimize the velocity jump on the interface between the fluid and structure subsystems. As explained in Chapter 3, the lack

of a $\mathbf{H}^1$ bound for the structure velocity requires us to minimize an objective function which uses some finite difference approximation of the structure velocity on the interface, e.g., we seek to minimize

$$\mathcal{J}_n^\delta(\mathbf{u}^n, p^n, \boldsymbol{\eta}^n, \dot{\boldsymbol{\eta}}^n, \mathbf{g}^n) = \frac{1}{2}\int_{\Gamma_{I_{t_n}}} \left|\mathbf{u}^n - \frac{\mathcal{V}(\boldsymbol{\eta}^n) - \mathcal{V}(\boldsymbol{\eta}^{n-1})}{\Delta t}\right|^2 d\Gamma_{I_{t_n}} + \frac{\delta}{2}\int_{\Gamma_{I_{t_n}}} |\mathbf{g}^n|^2 \, d\Gamma_{I_{t_n}} , \tag{5.1}$$

rather than

$$\mathcal{J}_n^\delta(\mathbf{u}^n, p^n, \boldsymbol{\eta}^n, \dot{\boldsymbol{\eta}}^n, \mathbf{g}^n) = \frac{1}{2}\int_{\Gamma_{I_{t_n}}} |\mathbf{u}^n - \mathcal{V}(\dot{\boldsymbol{\eta}}^n)|^2 \, d\Gamma_{I_{t_n}} + \frac{\delta}{2}\int_{\Gamma_{I_{t_n}}} |\mathbf{g}^n|^2 \, d\Gamma_{I_{t_n}} . \tag{5.2}$$

Therefore, we seek to

$$\begin{aligned} &\text{find } \mathbf{u}^n, p^n, \boldsymbol{\eta}^n, \dot{\boldsymbol{\eta}}^n, \text{ and } \mathbf{g}^n \text{ such that (5.1) is minimized} \\ &\text{for a given } \mathbf{u}^{n-1}, \boldsymbol{\eta}^{n-1}, \text{ and } \dot{\boldsymbol{\eta}}^{n-1}, \text{ subject to} \end{aligned} \tag{5.3}$$

$$\begin{aligned} \rho^f[(\mathbf{u}^n, \mathbf{v})_{\Omega^f_{t_n}} - (\mathbf{u}^{n-1}, \mathcal{V}(\mathbf{v}))_{\Omega^f_{t_{n-1}}}] + \Delta t\, \rho^f[c(\mathbf{u}^n, \mathbf{u}^n, \mathbf{v})_{\Omega^f_{t_n}} + \frac{1}{2}((\mathbf{u}^n \cdot \mathbf{n}_f)\mathbf{u}^n, \mathbf{v})_{\Gamma^f_N} \\ - \frac{1}{2}((\nabla \cdot \mathbf{z}^n)\mathbf{u}^n, \mathbf{v})_{\Omega^f_{t_n}} - c(\mathbf{z}^n, \mathbf{u}^n, \mathbf{v})_{\Omega^f_{t_n}}] \\ + \Delta t\, 2\nu_f a(\mathbf{u}^n, \mathbf{v})_{\Omega^f_{t_n}} + \Delta t\, b(\mathbf{v}, p^n)_{\Omega^f_{t_n}} \\ = \Delta t\, (\mathbf{f}^n_f, \mathbf{v})_{\Omega^f_{t_n}} + \Delta t\, (\mathbf{u}^n_N, \mathbf{v})_{\Gamma^f_N} + \Delta t\, (\mathbf{g}^n, \mathbf{v})_{\Gamma_{I_{t_n}}} \quad \forall \mathbf{v} \in \boldsymbol{H}^1_D(\Omega^f_{t_n}), \end{aligned} \tag{5.4}$$

$$b(\mathbf{u}^n, q)_{\Omega^f_{t_n}} = 0 \quad q \in L^2(\Omega^f_{t_n}), \tag{5.5}$$

and

$$\rho^s[(\dot{\boldsymbol{\eta}}^n, \boldsymbol{\xi})_{\Omega^s} - (\dot{\boldsymbol{\eta}}^{n-1}, \boldsymbol{\xi})_{\Omega^s}] + \Delta t\ \nu_s d(\boldsymbol{\eta}^n + \boldsymbol{\eta}^{n-1}, \boldsymbol{\xi})_{\Omega^s} + \frac{\Delta t}{2}\ \lambda e(\boldsymbol{\eta}^n + \boldsymbol{\eta}^{n-1}, \boldsymbol{\xi})_{\Omega^s}$$
$$= \frac{\Delta t}{2}\ (\mathbf{f}_s^n + \mathbf{f}_s^{n-1}, \boldsymbol{\xi})_{\Omega^s} + \frac{\Delta t}{2}\ (\boldsymbol{\eta}_N^n + \boldsymbol{\eta}_N^{n-1}, \boldsymbol{\xi})_{\Gamma_N^s}$$
$$- \frac{\Delta t}{2}\ (\mathcal{V}(\mathbf{g}^n) J_{t_n} + \mathcal{V}(\mathbf{g}^{n-1}) J_{t_{n-1}}, \boldsymbol{\xi})_{\Gamma_{I_{t_0}}} \quad \forall \boldsymbol{\xi} \in \boldsymbol{H}_D^1(\Omega^s), \tag{5.6}$$

$$\frac{\Delta t}{2}[(\dot{\boldsymbol{\eta}}^n, \boldsymbol{\gamma})_{\Omega^s} + (\dot{\boldsymbol{\eta}}^{n-1}, \boldsymbol{\gamma})_{\Omega^s}] = (\boldsymbol{\eta}^n, \boldsymbol{\gamma})_{\Omega^s} - (\boldsymbol{\eta}^{n-1}, \boldsymbol{\gamma})_{\Omega^s} \quad \forall \boldsymbol{\gamma} \in \boldsymbol{L}^2(\Omega^s). \tag{5.7}$$

For any choice of $\mathbf{g}^n$, (5.4)–(5.5) and (5.6)–(5.7) can be solved independently. Therefore, using $\mathbf{g}^n$ as a control at each time step permits the fluid and structure subsystems to be solved simultaneously using partitioned solvers.

5.3 Lagrange Multiplier Rule

With the existence of an optimal solution and Lagrange multipliers proven in Chapter 4, we may proceed in defining the Lagrangian and transforming our constrained optimization problem into an unconstrained one. The optimality system below is derived using the Lagrange multiplier rule, treating the deformation and velocity of Ω_t^f as known. Again, it should be noted that when the Fréchet derivative was taken to form the linearized operator in Theorem 4.8, the determinant of the deformation gradient and the deformation gradient are all implicitly defined by $\boldsymbol{\eta}^n$ and $\boldsymbol{\eta}^{n-1}$, but are treated as known.

We now define the Lagrangian as

$$
\begin{aligned}
&\mathcal{L}(\mathbf{u}^n, p^n, \boldsymbol{\eta}^n, \dot{\boldsymbol{\eta}}^n, \mathbf{g}^n, \bar{\mathbf{u}}^n, \bar{p}^n, \bar{\boldsymbol{\eta}}^n, \bar{\dot{\boldsymbol{\eta}}}^n) = \\
&\quad - \mathcal{J}_n^{\delta}(\mathbf{u}^n, p^n, \boldsymbol{\eta}^n, \dot{\boldsymbol{\eta}}^n, \mathbf{g}^n) + \rho^f[(\mathbf{u}^n, \bar{\mathbf{u}}^n)_{\Omega^f_{t_n}} - (\mathbf{u}^{n-1}, \mathcal{V}(\bar{\mathbf{u}}^n))_{\Omega^f_{t_{n-1}}}] \\
&\quad + \Delta t\ \rho^f[c(\mathbf{u}^n, \mathbf{u}^n, \bar{\mathbf{u}}^n)_{\Omega^f_{t_n}} + \frac{1}{2}((\mathbf{u}^n \cdot \mathbf{n}_f)\mathbf{u}^n, \bar{\mathbf{u}}^n)_{\Gamma^f_N} - \frac{1}{2}((\nabla \cdot \mathbf{z}^n)\mathbf{u}^n, \bar{\mathbf{u}}^n)_{\Omega^f_{t_n}} \\
&\quad - c(\mathbf{z}^n, \mathbf{u}^n, \bar{\mathbf{u}}^n)_{\Omega^f_{t_n}}] + \Delta t\ 2\nu_f a(\mathbf{u}^n, \bar{\mathbf{u}}^n)_{\Omega^f_{t_n}} + \Delta t\ b(\bar{\mathbf{u}}^n, p^n)_{\Omega^f_{t_n}} - \Delta t\ (\mathbf{f}^n_f, \bar{\mathbf{u}}^n)_{\Omega^f_{t_n}} \\
&\quad - \Delta t\ (\mathbf{u}^n_N, \bar{\mathbf{u}}^n)_{\Gamma^f_N} - \Delta t\ (\mathbf{g}^n, \bar{\mathbf{u}}^n)_{\Gamma_{I_{t_n}}} + \Delta t\ b(\mathbf{u}^n, \bar{p}^n)_{\Omega^f_{t_n}} + \rho^s[(\dot{\boldsymbol{\eta}}^n, \bar{\boldsymbol{\eta}}^n)_{\Omega^s} - (\dot{\boldsymbol{\eta}}^{n-1}, \bar{\boldsymbol{\eta}}^n)_{\Omega^s}] \\
&\quad + \Delta t\ \nu_s d(\boldsymbol{\eta}^n + \boldsymbol{\eta}^{n-1}, \bar{\boldsymbol{\eta}}^n)_{\Omega^s} + \frac{\Delta t}{2}\ \lambda e(\boldsymbol{\eta}^n + \boldsymbol{\eta}^{n-1}, \bar{\boldsymbol{\eta}}^n)_{\Omega^s} - \frac{\Delta t}{2}\ (\mathbf{f}^n_s + \mathbf{f}^{n-1}_s, \bar{\boldsymbol{\eta}}^n)_{\Omega^s} \\
&\quad - \frac{\Delta t}{2}\ (\boldsymbol{\eta}^n_N + \boldsymbol{\eta}^{n-1}_N, \bar{\boldsymbol{\eta}}^n)_{\Gamma^s_N} + \frac{\Delta t}{2}\ (\mathcal{V}(\mathbf{g}^n)J_{t_n} + \mathcal{V}(\mathbf{g}^{n-1})J_{t_{n-1}}, \bar{\boldsymbol{\eta}}^n)_{\Gamma_{I_{t_0}}} + \frac{\Delta t}{2}[(\dot{\boldsymbol{\eta}}^n, \bar{\dot{\boldsymbol{\eta}}}^n)_{\Omega^s} \\
&\quad + (\dot{\boldsymbol{\eta}}^{n-1}, \bar{\dot{\boldsymbol{\eta}}}^n)_{\Omega^s}] - [(\boldsymbol{\eta}^n, \bar{\dot{\boldsymbol{\eta}}}^n)_{\Omega^s} - (\boldsymbol{\eta}^{n-1}, \bar{\dot{\boldsymbol{\eta}}}^n)_{\Omega^s}]
\end{aligned}
$$

for any $(\mathbf{u}^n, p^n, \boldsymbol{\eta}^n, \dot{\boldsymbol{\eta}}^n, \mathbf{g}^n, \bar{\mathbf{u}}^n, \bar{p}^n, \bar{\boldsymbol{\eta}}^n, \bar{\dot{\boldsymbol{\eta}}}^n) \in \boldsymbol{H}^1_D(\Omega^f_{t_n}) \times L^2(\Omega^f_{t_n}) \times \boldsymbol{H}^1_D(\Omega^s) \times \boldsymbol{L}^2(\Omega^s) \times \mathbf{L}^2(\Gamma_{I_{t_n}}) \times \boldsymbol{H}^1_D(\Omega^f_{t_n}) \times L^2(\Omega^f_{t_n}) \times \boldsymbol{H}^1_D(\Omega^s) \times \boldsymbol{L}^2(\Omega^s)$. We will now seek to find stationary points of $\mathcal{L}$ over this product space.

Variations in the control $\mathbf{g}^n$ yield the necessary condition,

$$
\delta(\mathbf{g}^n, \mathbf{c})_{\Gamma_{I_{t_n}}} = -\Delta t\ (\mathbf{c}, \bar{\mathbf{u}}^n)_{\Gamma_{I_{t_n}}} + \frac{\Delta t}{2}\ (\mathcal{V}(\mathbf{c})J_{t_n}, \bar{\boldsymbol{\eta}}^n)_{\Gamma_{I_{t_0}}} \quad \forall \mathbf{c} \in \mathbf{L}^2(\Gamma_{I_{t_n}}). \tag{5.8}
$$

Since $\mathbf{H}^1(\Omega^f_{t_n})$ is compactly embedded in $\mathbf{L}^2(\Gamma_{I_{t_n}})$ and $\mathbf{H}^1(\Omega^s)$ is compactly embedded in $\mathbf{L}^2(\Gamma_{I_{t_n}})$, we can substitute the necessary condition (5.8) into the state equation (5.4) and (5.6) by considering $\mathbf{c} = \mathbf{v}|_{\Gamma_{I_{t_n}}}$ and $\mathbf{c} = \boldsymbol{\xi}|_{\Gamma_{I_{t_n}}}$ which can be substituted for any $\mathbf{v} \in \mathbf{H}^1(\Omega^f_{t_n})$ and $\boldsymbol{\xi} \in \mathbf{H}^1(\Omega^s)$, respectively.

Variations in the state variables, Lagrange multipliers, and the control $\mathbf{g}^n$ along

with the substitution just described yield the optimality system:

$$\begin{aligned}
\rho^f[(\mathbf{u}^n,\mathbf{v})_{\Omega^f_{t_n}} - (\mathbf{u}^{n-1},\mathcal{V}(\mathbf{v}))_{\Omega^f_{t_{n-1}}}] + \Delta t\ \rho^f[c(\mathbf{u}^n,\mathbf{u}^n,\mathbf{v})_{\Omega^f_{t_n}} + \frac{1}{2}((\mathbf{u}^n\cdot\mathbf{n}_f)\mathbf{u}^n,\mathbf{v})_{\Gamma^f_N} \\
- \frac{1}{2}((\nabla\cdot\mathbf{z}^n)\mathbf{u}^n,\mathbf{v})_{\Omega^f_{t_n}} - c(\mathbf{z}^n,\mathbf{u}^n,\mathbf{v})_{\Omega^f_{t_n}}] \\
+ \Delta t\ 2\nu_f a(\mathbf{u}^n,\mathbf{v})_{\Omega^f_{t_n}} + \Delta t\ b(\mathbf{v},p^n)_{\Omega^f_{t_n}} \\
= \Delta t\ (\mathbf{f}^n_f,\mathbf{v})_{\Omega^f_{t_n}} + \Delta t\ (\mathbf{u}^n_N,\mathbf{v})_{\Gamma^f_N} - \frac{\Delta t^2}{\delta}\ (\bar{\mathbf{u}}^n - \frac{\mathcal{V}(\bar{\boldsymbol{\eta}}^n)}{2},\mathbf{v})_{\Gamma_{I_{t_n}}} \\
\forall \mathbf{v}\in \boldsymbol{H}^1_D(\Omega^f_{t_n}), \quad (5.9)
\end{aligned}$$

$$b(\mathbf{u}^n,q)_{\Omega^f_{t_n}} = 0 \quad q\in L^2(\Omega^f_{t_n}), \tag{5.10}$$

$$\begin{aligned}
\rho^s[(\dot{\boldsymbol{\eta}}^n,\boldsymbol{\xi})_{\Omega^s} - (\dot{\boldsymbol{\eta}}^{n-1},\boldsymbol{\xi})_{\Omega^s}] + \Delta t\ \nu_s d(\boldsymbol{\eta}^n+\boldsymbol{\eta}^{n-1},\boldsymbol{\xi})_{\Omega^s} + \frac{\Delta t}{2}\ \lambda e(\boldsymbol{\eta}^n+\boldsymbol{\eta}^{n-1},\boldsymbol{\xi})_{\Omega^s} \\
= \frac{\Delta t}{2}\ (\mathbf{f}^n_s+\mathbf{f}^{n-1}_s,\boldsymbol{\xi})_{\Omega^s} + \frac{\Delta t}{2}\ (\boldsymbol{\eta}^n_N+\boldsymbol{\eta}^{n-1}_N,\boldsymbol{\xi})_{\Gamma^s_N} \\
+ \frac{\Delta t^2}{2\delta}\ (\mathcal{V}(\bar{\mathbf{u}}^n)J_{t_n} - \frac{1}{2}\bar{\boldsymbol{\eta}}^n J_{t_n},\boldsymbol{\xi})_{\Gamma_{I_{t_0}}} - \frac{\Delta t}{2}(\mathcal{V}(\mathbf{g}^{n-1})J_{t_{n-1}},\boldsymbol{\xi})_{\Gamma_{I_{t_0}}} \\
\forall \boldsymbol{\xi}\in \boldsymbol{H}^1_D(\Omega^s), \quad (5.11)
\end{aligned}$$

$$\frac{\Delta t}{2}[(\dot{\boldsymbol{\eta}}^n,\boldsymbol{\gamma})_{\Omega^s} + (\dot{\boldsymbol{\eta}}^{n-1},\boldsymbol{\gamma})_{\Omega^s}] = (\boldsymbol{\eta}^n,\boldsymbol{\gamma})_{\Omega^s} - (\boldsymbol{\eta}^{n-1},\boldsymbol{\gamma})_{\Omega^s} \quad \forall\boldsymbol{\gamma}\in\boldsymbol{L}^2(\Omega^s), \tag{5.12}$$

$$\begin{aligned}
\rho^f(\bar{\mathbf{u}}^n,\mathbf{w})_{\Omega^f_{t_n}} + \Delta t\ \rho^f[c(\mathbf{u}^n,\mathbf{w},\bar{\mathbf{u}}^n)_{\Omega^f_{t_n}} + c(\mathbf{w},\mathbf{u}^n,\bar{\mathbf{u}}^n)_{\Omega^f_{t_n}} + \frac{1}{2}((\mathbf{u}^n\cdot\mathbf{n}_f)\mathbf{w},\bar{\mathbf{u}}^n)_{\Gamma^f_N} \\
+ \frac{1}{2}((\mathbf{w}\cdot\mathbf{n}_f)\mathbf{u}^n,\bar{\mathbf{u}}^n)_{\Gamma^f_N} - \frac{1}{2}((\nabla\cdot\mathbf{z}^n)\mathbf{w},\bar{\mathbf{u}}^n)_{\Omega^f_{t_n}} \\
- c(\mathbf{z}^n,\mathbf{w},\bar{\mathbf{u}}^n)_{\Omega^f_{t_n}}] + \Delta t\ 2\nu_f a(\bar{\mathbf{u}}^n,\mathbf{w})_{\Omega^f_{t_n}} + \Delta t\ b(\mathbf{w},\bar{p}^n)_{\Omega^f_{t_n}} \\
= (\mathbf{u}^n - \frac{\mathcal{V}(\boldsymbol{\eta}^n)-\mathcal{V}(\boldsymbol{\eta}^{n-1})}{\Delta t},\mathbf{w})_{\Gamma_{I_{t_n}}} \quad \forall\mathbf{w}\in\boldsymbol{H}^1_D(\Omega^f_{t_n}),
\end{aligned} \tag{5.13}$$

$$b(\bar{\mathbf{u}}^n,r)_{\Omega^f_{t_n}} = 0 \quad r\in L^2(\Omega^f_{t_n}), \tag{5.14}$$

$$\begin{aligned}
-(\bar{\dot{\boldsymbol{\eta}}}^n,\boldsymbol{\phi})_{\Omega^s} + \Delta t\ \nu_s d(\bar{\boldsymbol{\eta}}^n,\boldsymbol{\phi})_{\Omega^s} + \frac{\Delta t}{2}\ \lambda e(\bar{\boldsymbol{\eta}}^n,\boldsymbol{\phi})_{\Omega^s} \\
= -\frac{1}{\Delta t}(J_{t_n}\left[\mathcal{V}(\mathbf{u}^n) - \frac{\boldsymbol{\eta}^n-\boldsymbol{\eta}^{n-1}}{\Delta t}\right],\boldsymbol{\phi})_{\Gamma_{I_{t_0}}} \quad \forall\boldsymbol{\phi}\in\boldsymbol{H}^1_D(\Omega^s),
\end{aligned} \tag{5.15}$$

$$\frac{\Delta t}{2}(\bar{\dot{\boldsymbol{\eta}}}^n,\boldsymbol{\theta})_{\Omega^s} + \rho^s(\bar{\boldsymbol{\eta}}^n,\boldsymbol{\theta})_{\Omega^s} = 0 \quad \forall\boldsymbol{\theta}\in\boldsymbol{L}^2(\Omega^s), \tag{5.16}$$

5.4 Finite Element Approximations

We select finite element spaces $\mathbf{W}^h$, Q^h, $\mathbf{D}^h$, and $\mathbf{V}^h$ such that $\mathbf{W}^h \subset \boldsymbol{H}^1_D(\Omega^f_{t_n})$, $Q^h \subset L^2(\Omega^f_{t_n})$, $\mathbf{D}^h \subset \boldsymbol{H}^1_D(\Omega^s)$, and $\mathbf{V}^h \subset \mathbf{H}^1(\Omega^s)$. We assume that the finite element spaces satisfy the standard approximation properties, i.e., there exists an integer k and a constant C such that

$$\inf_{\mathbf{v}^h \in \mathbf{W}^h} ||\mathbf{v} - \mathbf{v}^h||_{1,\Omega^f_{t_n}} \leq Ch^m \|\mathbf{v}\|_{m+1,\Omega^f_{t_n}} \quad \forall \mathbf{v} \in \boldsymbol{H}^1_D(\Omega^f_{t_n}),\ 1 \leq m \leq k, \tag{5.17}$$

$$\inf_{q^h \in \mathbf{Q}^h} ||q - q^h||_{0,\Omega^f_{t_n}} \leq Ch^m \|q\|_{m,\Omega^f_{t_n}} \quad \forall q \in L^2(\Omega^f_{t_n}),\ 1 \leq m \leq k, \tag{5.18}$$

$$\inf_{\boldsymbol{\eta}^h \in \mathbf{D}^h} ||\boldsymbol{\eta} - \boldsymbol{\eta}^h||_{1,\Omega^f_{t_0}} \leq Ch^m \|\boldsymbol{\eta}\|_{m+1,\Omega^f_{t_0}} \quad \forall \boldsymbol{\eta} \in \boldsymbol{H}^1_D(\Omega^f_{t_0}),\ 1 \leq m \leq k, \tag{5.19}$$

and

$$\inf_{\boldsymbol{\gamma}^h \in \mathbf{V}^h} ||\boldsymbol{\gamma} - \boldsymbol{\gamma}^h||_{0,\Omega^f_{t_0}} \leq Ch^m \|\boldsymbol{\gamma}\|_{m,\Omega^f_{t_0}} \quad \forall \boldsymbol{\gamma} \in \boldsymbol{H}^1_D(\Omega^f_{t_0}),\ 1 \leq m \leq k. \tag{5.20}$$

Additionally, we assume that the inf-sup condition holds, i.e.,

$$\inf_{0 \neq q^h \in Q^h} \sup_{0 \neq \mathbf{v}^h \in \mathbf{W}^h} \frac{(\mathbf{v}^h, q^h)_{\Omega^f_{t_n}}}{\|\mathbf{v}^h\|_{1,\Omega^f_{t_n}} \|q^h\|_{0,\Omega^f_{t_n}}} \geq C, \tag{5.21}$$

where C is a positive constant independent of h; see [4, 17, 36, 65].

The finite element approximations of solutions of the optimality system can now be defined as: find $(\mathbf{u}^{n,h}, p^{n,h}, \boldsymbol{\eta}^{n,h}, \dot{\boldsymbol{\eta}}^{n,h}, \bar{\mathbf{u}}^{n,h}, \bar{p}^{n,h}, \bar{\boldsymbol{\eta}}^{n,h}, \bar{\dot{\boldsymbol{\eta}}}^{n,h}) \in \mathbf{W}^h \times Q^h \times \mathbf{D}^h \times \mathbf{V}^h \times \mathbf{W}^h \times Q^h \times \mathbf{D}^h \times \mathbf{V}^H)$ such that

$$\rho^f[(\mathbf{u}^{n,h},\mathbf{v}^h)_{\Omega^f_{t_n}} - (\mathbf{u}^{n-1,h},\mathcal{V}(\mathbf{v}^h))_{\Omega^f_{t_{n-1}}}]$$
$$+\Delta t\ \rho^f[c(\mathbf{u}^{n,h},\mathbf{u}^{n,h},\mathbf{v}^h)_{\Omega^f_{t_n}} + \frac{1}{2}((\mathbf{u}^{n,h}\cdot\mathbf{n}_f)\mathbf{u}^{n,h},\mathbf{v}^h)_{\Gamma^f_N}$$
$$-\frac{1}{2}((\nabla\cdot\mathbf{z}^{n,h})\mathbf{u}^{n,h},\mathbf{v}^h)_{\Omega^f_{t_n}} - c(\mathbf{z}^{n,h},\mathbf{u}^{n,h},\mathbf{v}^h)_{\Omega^f_{t_n}}]$$
$$+\Delta t\ 2\nu_f a(\mathbf{u}^{n,h},\mathbf{v}^h)_{\Omega^f_{t_n}} + \Delta t\ b(\mathbf{v}^h,p^{n,h})_{\Omega^f_{t_n}}$$
$$=\Delta t\ (\mathbf{f}^n_f,\mathbf{v}^h)_{\Omega^f_{t_n}} + \Delta t\ (\mathbf{u}^n_N,\mathbf{v}^h)_{\Gamma^f_N}$$
$$-\frac{\Delta t^2}{\delta}\ (\bar{\mathbf{u}}^{n,h} - \frac{\mathcal{V}(\bar{\boldsymbol{\eta}}^{n,h})}{2},\mathbf{v}^h)_{\Gamma_{I_{t_n}}} \quad \forall\mathbf{v}^h\in\mathbf{W}^h, \tag{5.22}$$

$$b(\mathbf{u}^{n,h},q^h)_{\Omega^f_{t_n}} = 0 \quad q^h\in Q^h, \tag{5.23}$$

$$\rho^s[(\dot{\boldsymbol{\eta}}^{n,h},\boldsymbol{\xi}^h)_{\Omega^s} - (\dot{\boldsymbol{\eta}}^{n-1,h},\boldsymbol{\xi}^h)_{\Omega^s}]$$
$$+\Delta t\ \nu_s d(\boldsymbol{\eta}^{n,h}+\boldsymbol{\eta}^{n-1,h},\boldsymbol{\xi}^h)_{\Omega^s} + \frac{\Delta t}{2}\ \lambda e(\boldsymbol{\eta}^{n,h}+\boldsymbol{\eta}^{n-1,h},\boldsymbol{\xi}^h)_{\Omega^s}$$
$$=\frac{\Delta t}{2}\ (\mathbf{f}^n_s+\mathbf{f}^{n-1}_s,\boldsymbol{\xi}^h)_{\Omega^s} + \frac{\Delta t}{2}\ (\boldsymbol{\eta}^n_N+\boldsymbol{\eta}^{n-1}_N,\boldsymbol{\xi}^h)_{\Gamma^s_N} + \frac{\Delta t^2}{2\delta}\ (\mathcal{V}(\bar{\mathbf{u}}^{n,h})J_{t_n}$$
$$-\frac{1}{2}\bar{\boldsymbol{\eta}}^{n,h}J_{t_n},\boldsymbol{\xi}^h)_{\Gamma_{I_{t_0}}} - \frac{\Delta t}{2}(\mathcal{V}(\mathbf{g}^{n-1,h})J_{t_{n-1}},\boldsymbol{\xi}^h)_{\Gamma_{I_{t_0}}} \quad \forall\boldsymbol{\xi}^h\in\mathbf{D}^h, \tag{5.24}$$

$$\frac{\Delta t}{2}[(\dot{\boldsymbol{\eta}}^{n,h},\boldsymbol{\gamma}^h)_{\Omega^s} + (\dot{\boldsymbol{\eta}}^{n-1,h},\boldsymbol{\gamma}^h)_{\Omega^s}] = (\boldsymbol{\eta}^{n,h},\boldsymbol{\gamma}^h)_{\Omega^s} - (\boldsymbol{\eta}^{n-1,h},\boldsymbol{\gamma}^h)_{\Omega^s} \quad \forall\boldsymbol{\gamma}^h\in\mathbf{V}^h, \tag{5.25}$$

$$\rho^f(\bar{\mathbf{u}}^{n,h},\mathbf{w}^h)_{\Omega^f_{t_n}} + \Delta t\ \rho^f[c(\mathbf{u}^{n,h},\mathbf{w}^h,\bar{\mathbf{u}}^{n,h})_{\Omega^f_{t_n}} + c(\mathbf{w}^h,\mathbf{u}^{n,h},\bar{\mathbf{u}}^{n,h})_{\Omega^f_{t_n}}$$
$$+\frac{1}{2}((\mathbf{u}^{n,h}\cdot\mathbf{n}_f)\mathbf{w}^h,\bar{\mathbf{u}}^{n,h})_{\Gamma^f_N} + \frac{1}{2}((\mathbf{w}^h\cdot\mathbf{n}_f)\mathbf{u}^{n,h},\bar{\mathbf{u}}^{n,h})_{\Gamma^f_N}$$
$$-\frac{1}{2}((\nabla\cdot\mathbf{z}^{n,h})\mathbf{w}^h,\bar{\mathbf{u}}^{n,h})_{\Omega^f_{t_n}} - c(\mathbf{z}^{n,h},\mathbf{w}^h,\bar{\mathbf{u}}^{n,h})_{\Omega^f_{t_n}}]$$
$$+\Delta t\ 2\nu_f a(\bar{\mathbf{u}}^{n,h},\mathbf{w}^h)_{\Omega^f_{t_n}} + \Delta t\ b(\mathbf{w}^h,\bar{p}^{n,h})_{\Omega^f_{t_n}}$$
$$=(\mathbf{u}^{n,h} - \frac{\mathcal{V}(\boldsymbol{\eta}^{n,h})-\mathcal{V}(\boldsymbol{\eta}^{n-1,h})}{\Delta t},\mathbf{w}^h)_{\Gamma_{I_{t_n}}} \quad \forall\mathbf{w}^h\in\mathbf{W}^h, \tag{5.26}$$

$$b(\bar{\mathbf{u}}^{n,h},r^h)_{\Omega^f_{t_n}} = 0 \quad r^h\in Q^h, \tag{5.27}$$

$$-(\bar{\dot{\boldsymbol{\eta}}}^{n,h},\boldsymbol{\phi}^h)_{\Omega^s} + \Delta t\ \nu_s d(\bar{\boldsymbol{\eta}}^{n,h},\boldsymbol{\phi}^h)_{\Omega^s} + \frac{\Delta t}{2}\ \lambda e(\bar{\boldsymbol{\eta}}^{n,h},\boldsymbol{\phi}^h)_{\Omega^s}$$
$$=-\frac{1}{\Delta t}(J_{t_n}\left[\mathcal{V}(\mathbf{u}^{n,h}) - \frac{\boldsymbol{\eta}^{n,h}-\boldsymbol{\eta}^{n-1,h}}{\Delta t}\right],\boldsymbol{\phi}^h)_{\Gamma_{I_{t_0}}} \quad \forall\boldsymbol{\phi}^h\in\mathbf{D}^h, \tag{5.28}$$

$$\frac{\Delta t}{2}(\bar{\dot{\boldsymbol{\eta}}}^{n,h},\boldsymbol{\theta}^h)_{\Omega^s} + \rho^s(\bar{\boldsymbol{\eta}}^{n,h},\boldsymbol{\theta}^h)_{\Omega^s} = 0 \quad \forall\boldsymbol{\theta}^h\in\mathbf{V}^h. \tag{5.29}$$

We will now use BRR Theory to obtain error estimates for finite element approximation of the nonlinear optimality system [18].

Let X and Y denote Banach spaces and Λ a positive compact interval of $\mathbb{R}$ containing λ, $\lambda > 0$. We consider a nonlinear problem of the type

$$F(\lambda, \psi) = \psi + TG(\lambda, \psi) = 0, \tag{5.30}$$

where G is a C^2 mapping from $\Lambda \times X$ to Y and $T \in \mathcal{L}(Y, X)$. If $F(\lambda, \psi(\lambda)) = 0$ for $\lambda \in \Lambda$ and the mapping $\lambda \to \psi(\lambda)$ is a continuous function from Λ to X, then $\{(\lambda, \psi(\lambda)) : \lambda \in \Lambda\}$ is called a branch of solutions of (5.30). Additionally, if the Frèchet derivative $D_\psi F(\lambda, \psi(\lambda))$ is an isomorphism from X into X for all $\lambda \in \Lambda$, then the branch of solutions $\{(\lambda, \psi(\lambda)) : \lambda \in \Lambda\}$ are called a regular branch.

Let $X^h \in X$ be a finite element space and $T^h \in \mathcal{L}(Y, X^h)$ be a discretization of the operator T. The approximation problem for (5.30) seeks $\psi^h \in X^h$ such that

$$F^h(\lambda, \psi^h) = \psi^h + T^h G(\lambda, \psi^h) = 0. \tag{5.31}$$

Assume that there exists a Banach space Z continuously embedded in Y such that

$$D_\psi G(\lambda, \psi(\lambda)) \in \mathcal{L}(X, Z) \; \forall \lambda \in \Lambda, \; \psi \in X. \tag{5.32}$$

We also assume the following approximation properties for the operator T^h:

$$\lim_{h \to 0} \left\| (T^h - T) r \right\|_X = 0 \; \forall r \in Y \tag{5.33}$$

and

$$\lim_{h \to 0} \left\| T^h - T \right\|_{\mathcal{L}(Z,X)} = 0. \tag{5.34}$$

Under these assumptions, we now quote the following theorem of [18]:

Theorem 5.1. *Let X and Y be Banach spaces and Λ a compact interval of the real line $\mathbb{R}$.*

Assume that G is a C^2 mapping from $\Lambda \times X$ into Y and that D^2G is bounded on all bounded sets of $\Lambda \times X$. Assume that (5.32)–(5.34) hold and that $\{(\lambda, \psi(\lambda)) : \lambda \in \Lambda\}$ is a branch of regular solutions of (5.30). Then, there exists a neighborhood $\mathcal{O}$ of the origin in X and, for $h \leq h_0$ small enough, a unique C^2 function $\lambda \to \psi(\lambda) \in X^h$ such that $\{(\lambda, \psi^h(\lambda)) : \lambda \in \Lambda\}$ is a branch of regular solutions of (5.31) and $\psi^h(\lambda) - \psi(\lambda) \in \mathcal{O}$ for all $\lambda \in \Lambda$. Furthermore, there exists a positive constant C, independent of h and λ, such that

$$\left\| \psi(\lambda)^h - \psi(\lambda) \right\|_X \leq C \left\| (T^h - T) G(\lambda, \psi(\lambda)) \right\|_X \ \forall \lambda \in \Lambda. \tag{5.35}$$

We will use Theorem 5.1 to in order to obtain error estimates between the optimality system (5.9)–(5.16) and the discretized optimality system (5.22)–(5.29).

Let

$$\begin{aligned}
X &= (\boldsymbol{H}^1_D(\Omega^f_{t_n}) \times L^2(\Omega^f_{t_n}) \times \boldsymbol{H}^1_D(\Omega^s) \times \boldsymbol{L}^2(\Omega^s))^2, \\
Y &= \boldsymbol{H}^1_D(\Omega^f_{t_n})^* \times \mathbf{H}^{1/2}(\Gamma^f_N)^* \times \mathbf{H}^{1/2}(\Gamma_{I_{t_n}})^* \times \boldsymbol{H}^1_D(\Omega^s)^* \times \mathbf{H}^{1/2}(\Gamma^s_N)^* \times \mathbf{H}^{1/2}(\Gamma_{I_{t_0}})^* \\
&\quad \times \boldsymbol{H}^1_D(\Omega^s)^* \times \boldsymbol{H}^1_D(\Omega^f_{t_n})^* \times \mathbf{H}^{1/2}(\Gamma_{I_{t_n}})^* \times \boldsymbol{H}^1_D(\Omega^s)^* \times \mathbf{H}^{1/2}(\Gamma_{I_{t_0}})^* \times \boldsymbol{H}^1_D(\Omega^s)^* \\
Z &= \mathbf{L}^{3/2}(\Omega^f_{t_n}) \times \mathbf{L}^2(\Gamma^f_N) \times \mathbf{L}^2(\Gamma_{I_{t_n}}) \times \mathbf{L}^{3/2}(\Omega^s) \times \mathbf{L}^2(\Gamma^s_N) \times \mathbf{L}^2(\Gamma_{I_{t_0}}) \\
&\quad \times \mathbf{L}^{3/2}(\Omega^s) \times \mathbf{L}^{3/2}(\Omega^f_{t_n}) \times \mathbf{L}^2(\Gamma^f_N) \times \mathbf{L}^2(\Gamma_{I_{t_n}}) \times \mathbf{L}^{3/2}(\Omega^s) \times \mathbf{L}^2(\Gamma_{I_{t_0}}) \times \mathbf{L}^{3/2}(\Omega^s) \\
X^h &= (\mathbf{W}^h \times Q^h \times \mathbf{D}^h \times \mathbf{V}^h)^2.
\end{aligned}$$

Define the operator $T \in \mathcal{L}(Y, X)$ by $T(\sigma_{\mathbf{1}}, \sigma_{\mathbf{2}}, \sigma_{\mathbf{3}}, \boldsymbol{\Phi}_1, \boldsymbol{\Phi}_2, \boldsymbol{\Phi}_3, \boldsymbol{\Pi}, \varrho_{\mathbf{1}}, \varrho_{\mathbf{2}}, \varrho_{\mathbf{3}}, \boldsymbol{\Xi}_1, \boldsymbol{\Xi}_2, \boldsymbol{\Upsilon})$ $= (\mathbf{u}^n, p^n, \boldsymbol{\eta}^n, \dot{\boldsymbol{\eta}}^n, \bar{\mathbf{u}}^n, \bar{p}^n, \bar{\boldsymbol{\eta}}^n, \bar{\dot{\boldsymbol{\eta}}}^n)$ if and only if,

$$2\nu_f a(\mathbf{u}^n,\mathbf{v})_{\Omega^f_{t_n}} + b(\mathbf{v},p^n)_{\Omega^f_{t_n}} = (\sigma_{\mathbf{1}},\mathbf{v})_{\Omega^f_{t_n}} + (\sigma_{\mathbf{2}},\mathbf{v})_{\Gamma^f_N} + (\sigma_{\mathbf{3}},\mathbf{v})_{\Gamma_{I_{t_n}}} \quad \forall \mathbf{v} \in \boldsymbol{H}^1_D(\Omega^f_{t_n}), \tag{5.36}$$

$$b(\mathbf{u}^n,q)_{\Omega^f_{t_n}} = 0 \quad q \in L^2(\Omega^f_{t_n}), \tag{5.37}$$

$$\nu_s d(\boldsymbol{\eta}^n,\boldsymbol{\xi})_{\Omega^s} = (\boldsymbol{\Phi}_1,\boldsymbol{\xi})_{\Omega^s} + (\boldsymbol{\Phi}_2,\boldsymbol{\xi})_{\Gamma^s_N} + (\boldsymbol{\Phi}_3,\boldsymbol{\xi})_{\Gamma_{I_{t_0}}} \quad \forall \boldsymbol{\xi} \in \boldsymbol{H}^1_D(\Omega^s), \tag{5.38}$$

$$\frac{1}{2}(\dot{\boldsymbol{\eta}}^n,\boldsymbol{\gamma})_{\Omega^s} = (\boldsymbol{\Pi},\boldsymbol{\gamma})_{\Omega^s} \quad \forall \boldsymbol{\gamma} \in \boldsymbol{L}^2(\Omega^s), \tag{5.39}$$

$$2\nu_f a(\bar{\mathbf{u}}^n,\mathbf{w})_{\Omega^f_{t_n}} + b(\mathbf{w},\bar{p}^n)_{\Omega^f_{t_n}} = (\varrho_{\mathbf{1}},\mathbf{w})_{\Omega^f_{t_n}} + (\varrho_{\mathbf{2}},\mathbf{w})_{\Gamma^f_N} + (\varrho_{\mathbf{3}},\mathbf{w})_{\Gamma_{I_{t_n}}} \quad \forall \mathbf{w} \in \boldsymbol{H}^1_D(\Omega^f_{t_n}), \tag{5.40}$$

$$b(\bar{\mathbf{u}}^n,r)_{\Omega^f_{t_n}} = 0 \quad r \in L^2(\Omega^f_{t_n}), \tag{5.41}$$

$$\nu_s d(\bar{\boldsymbol{\eta}}^n,\boldsymbol{\phi})_{\Omega^s} = (\boldsymbol{\Xi}_1,\boldsymbol{\phi})_{\Omega^s} + (\boldsymbol{\Xi}_2,\boldsymbol{\phi})_{\Gamma_{I_{t_0}}} \quad \forall \boldsymbol{\phi} \in \boldsymbol{H}^1_D(\Omega^s), \tag{5.42}$$

$$\frac{1}{2}(\dot{\bar{\boldsymbol{\eta}}}^n,\boldsymbol{\theta})_{\Omega^s} = (\boldsymbol{\Upsilon},\boldsymbol{\theta})_{\Omega^s} \quad \forall \boldsymbol{\theta} \in \boldsymbol{L}^2(\Omega^s). \tag{5.43}$$

Likewise, the discrete operator $T^h \in \mathcal{L}(Y,X^h)$ is defined by: for $(\sigma_{\mathbf{1}},\sigma_{\mathbf{2}},\sigma_{\mathbf{3}},\boldsymbol{\Phi}_1,\boldsymbol{\Phi}_2,\boldsymbol{\Phi}_3,\boldsymbol{\Pi},\varrho_{\mathbf{1}},\varrho_{\mathbf{2}},\varrho_{\mathbf{3}},\boldsymbol{\Xi}_1,\boldsymbol{\Xi}_2,\boldsymbol{\Upsilon}) \in Y$ and $(\mathbf{u}^{n,h},p^{n,h},\boldsymbol{\eta}^{n,h},\dot{\boldsymbol{\eta}}^{n,h},\bar{\mathbf{u}}^{n,h},\bar{p}^{n,h},\bar{\boldsymbol{\eta}}^{n,h},\dot{\bar{\boldsymbol{\eta}}}^{n,h}) \in X^h$, $T^h(\sigma_{\mathbf{1}},\sigma_{\mathbf{2}},\sigma_{\mathbf{3}},\boldsymbol{\Phi}_1,\boldsymbol{\Phi}_2,\boldsymbol{\Phi}_3,\boldsymbol{\Pi},\varrho_{\mathbf{1}},\varrho_{\mathbf{2}},\varrho_{\mathbf{3}},\boldsymbol{\Xi}_1,\boldsymbol{\Xi}_2,\boldsymbol{\Upsilon}) = (\mathbf{u}^{n,h},p^{n,h},\boldsymbol{\eta}^{n,h},\dot{\boldsymbol{\eta}}^{n,h},\bar{\mathbf{u}}^{n,h},\bar{p}^{n,h},\bar{\boldsymbol{\eta}}^{n,h},\dot{\bar{\boldsymbol{\eta}}}^{n,h})$ if and only if,

$$2\nu_f a(\mathbf{u}^{n,h},\mathbf{v}^h)_{\Omega^f_{t_n}} + b(\mathbf{v}^h,p^{n,h})_{\Omega^f_{t_n}} = (\sigma_{\mathbf{1}},\mathbf{v}^h)_{\Omega^f_{t_n}} + (\sigma_{\mathbf{2}},\mathbf{v}^h)_{\Gamma^f_N} + (\sigma_{\mathbf{3}},\mathbf{v}^h)_{\Gamma_{I_{t_n}}} \quad \forall \mathbf{v}^h \in \mathbf{W}^h, \tag{5.44}$$

$$b(\mathbf{u}^{n,h},q^h)_{\Omega^f_{t_n}} = 0 \quad q^h \in Q^h, \tag{5.45}$$

$$\nu_s d(\boldsymbol{\eta}^{n,h},\boldsymbol{\xi}^h)_{\Omega^s} = (\boldsymbol{\Phi}_1,\boldsymbol{\xi}^h)_{\Omega^s} + (\boldsymbol{\Phi}_2,\boldsymbol{\xi}^h)_{\Gamma^s_N} + (\boldsymbol{\Phi}_3,\boldsymbol{\xi}^h)_{\Gamma_{I_{t_0}}} \quad \forall \boldsymbol{\xi}^h \in \mathbf{D}^h, \tag{5.46}$$

$$\frac{1}{2}(\dot{\boldsymbol{\eta}}^{n,h},\boldsymbol{\gamma}^h)_{\Omega^s} = (\boldsymbol{\Pi},\boldsymbol{\gamma}^h)_{\Omega^s} \quad \forall \boldsymbol{\gamma}^h \in \mathbf{V}^h, \tag{5.47}$$

$$2\nu_f a(\bar{\mathbf{u}}^{n,h}, \mathbf{w}^h)_{\Omega^f_{t_n}} + b(\mathbf{w}^h, \bar{p}^n)_{\Omega^f_{t_n}} = (\varrho_{\mathbf{1}}, \mathbf{w}^h)_{\Omega^f_{t_n}} + (\varrho_{\mathbf{2}}, \mathbf{w}^h)_{\Gamma^f_N} + (\varrho_{\mathbf{3}}, \mathbf{w}^h)_{\Gamma_{I_{t_n}}} \quad \forall \mathbf{w}^h \in \mathbf{W}^h, \tag{5.48}$$

$$b(\bar{\mathbf{u}}^{n,h}, r^h)_{\Omega^f_{t_n}} = 0 \quad r^h \in Q^h, \tag{5.49}$$

$$\nu_s d(\bar{\boldsymbol{\eta}}^{n,h}, \boldsymbol{\phi}^h)_{\Omega^s} = (\boldsymbol{\Xi}_1, \boldsymbol{\phi}^h)_{\Omega^s} + (\boldsymbol{\Xi}_2, \boldsymbol{\phi}^h)_{\Gamma_{I_{t_0}}} \quad \forall \boldsymbol{\phi}^h \in \mathbf{D}^h, \tag{5.50}$$

$$\frac{1}{2}(\bar{\dot{\boldsymbol{\eta}}}^{n,h}, \boldsymbol{\theta}^h)_{\Omega^s} = (\boldsymbol{\Upsilon}, \boldsymbol{\theta}^h)_{\Omega^s} \quad \forall \boldsymbol{\theta}^h \in \mathbf{V}^h. \tag{5.51}$$

Let Λ be a compact interval containing $\frac{1}{\delta}$. Let us define the nonlinear operator $G : \Lambda \times X \to Y$ by: for $(\sigma_{\mathbf{1}}, \sigma_{\mathbf{2}}, \sigma_{\mathbf{3}}, \boldsymbol{\Phi}_1, \boldsymbol{\Phi}_2, \boldsymbol{\Phi}_3, \boldsymbol{\Pi}, \varrho_{\mathbf{1}}, \varrho_{\mathbf{2}}, \varrho_{\mathbf{3}}, \boldsymbol{\Xi}_1, \boldsymbol{\Xi}_2, \boldsymbol{\Upsilon}) \in Y$ and $(\frac{1}{\delta}, (\mathbf{u}^n, p^n, \boldsymbol{\eta}^n, \dot{\boldsymbol{\eta}}^n, \bar{\mathbf{u}}^n, \bar{p}^n, \bar{\boldsymbol{\eta}}^n, \bar{\dot{\boldsymbol{\eta}}}^n)) \in \Lambda \times X$, $G(\frac{1}{\delta}, (\mathbf{u}^n, p^n, \boldsymbol{\eta}^n, \dot{\boldsymbol{\eta}}^n, \bar{\mathbf{u}}^n, \bar{p}^n, \bar{\boldsymbol{\eta}}^n, \bar{\dot{\boldsymbol{\eta}}}^n))$
$= (\sigma_{\mathbf{1}}, \sigma_{\mathbf{2}}, \sigma_{\mathbf{3}}, \boldsymbol{\Phi}_1, \boldsymbol{\Phi}_2, \boldsymbol{\Phi}_3, \boldsymbol{\Pi}, \varrho_{\mathbf{1}}, \varrho_{\mathbf{2}}, \varrho_{\mathbf{3}}, \boldsymbol{\Xi}_1, \boldsymbol{\Xi}_2, \boldsymbol{\Upsilon})$ if and only if,

$$\begin{aligned}
(\sigma_{\mathbf{1}}, \mathbf{v})_{\Omega^f_{t_n}} &= -\frac{\rho^f}{\Delta t}[(\mathbf{u}^n, \mathbf{v})_{\Omega^f_{t_n}} + (\mathbf{u}^{n-1}, \mathcal{V}(\mathbf{v}))_{\Omega^f_{t_{n-1}}}] + \rho^f [c(\mathbf{u}^n, \mathbf{u}^n, \mathbf{v})_{\Omega^f_{t_n}} \\
&\quad + \frac{1}{2}((\nabla \cdot \mathbf{z}^n)\mathbf{u}^n, \mathbf{v})_{\Omega^f_{t_n}} + c(\mathbf{z}^n, \mathbf{u}^n, \mathbf{v})_{\Omega^f_{t_n}}] - (\mathbf{f}^n_f, \mathbf{v})_{\Omega^f_{t_n}} \quad \forall \mathbf{v} \in \boldsymbol{H}^1_D(\Omega^f_{t_n}), \\
(\sigma_{\mathbf{2}}, \mathbf{v})_{\Gamma^f_N} &= \rho^f \frac{1}{2}((\mathbf{u}^n \cdot \mathbf{n}_f)\mathbf{u}^n, \mathbf{v})_{\Gamma^f_N} - (\mathbf{u}^n_N, \mathbf{v})_{\Gamma^f_N} \quad \forall \mathbf{v} \in \boldsymbol{H}^1_D(\Omega^f_{t_n}), \\
(\sigma_{\mathbf{3}}, \mathbf{v})_{\Gamma_{I_{t_n}}} &= -\frac{\Delta t}{\delta}\ (\bar{\mathbf{u}}^n - \frac{\mathcal{V}(\bar{\boldsymbol{\eta}}^n)}{2}, \mathbf{v})_{\Gamma_{I_{t_n}}} \quad \forall \mathbf{v} \in \boldsymbol{H}^1_D(\Omega^f_{t_n}), \\
(\boldsymbol{\Phi}_1, \boldsymbol{\xi})_{\Omega^s} &= -\frac{\rho^s}{\Delta t}[(\dot{\boldsymbol{\eta}}^n, \boldsymbol{\xi})_{\Omega^s} + (\dot{\boldsymbol{\eta}}^{n-1}, \boldsymbol{\xi})_{\Omega^s}] + \nu_s d(\boldsymbol{\eta}^{n-1}, \boldsymbol{\xi})_{\Omega^s} - \frac{1}{2}\ \lambda e(\boldsymbol{\eta}^n - \boldsymbol{\eta}^{n-1}, \boldsymbol{\xi})_{\Omega^s} \\
&\quad - \frac{1}{2}\ (\mathbf{f}^n_s + \mathbf{f}^{n-1}_s, \boldsymbol{\xi})_{\Omega^s} \quad \forall \boldsymbol{\xi} \in \boldsymbol{H}^1_D(\Omega^s), \\
(\boldsymbol{\Phi}_2, \boldsymbol{\xi})_{\Gamma^s_N} &= -\frac{1}{2}\ (\boldsymbol{\eta}^n_N + \boldsymbol{\eta}^{n-1}_N, \boldsymbol{\xi})_{\Gamma^s_N} \quad \forall \boldsymbol{\xi} \in \boldsymbol{H}^1_D(\Omega^s), \\
(\boldsymbol{\Phi}_3, \boldsymbol{\xi})_{\Gamma_{I_{t_0}}} &= \frac{\Delta t}{2\delta}\ (\mathcal{V}(\bar{\mathbf{u}}^n) J_{t_n} - \frac{1}{2}\bar{\boldsymbol{\eta}}^n J_{t_n}, \boldsymbol{\xi})_{\Gamma_{I_{t_0}}} + \frac{1}{2}(\mathcal{V}(\mathbf{g}^{n-1}) J_{t_{n-1}}, \boldsymbol{\xi})_{\Gamma_{I_{t_0}}} \quad \forall \boldsymbol{\xi} \in \boldsymbol{H}^1_D(\Omega^s), \\
(\boldsymbol{\Pi}, \boldsymbol{\gamma})_{\Omega^s} &= \frac{1}{2}(\dot{\boldsymbol{\eta}}^{n-1}, \boldsymbol{\gamma})_{\Omega^s} + \frac{1}{\Delta t}\left[(\boldsymbol{\eta}^n, \boldsymbol{\gamma})_{\Omega^s} + (\boldsymbol{\eta}^{n-1}, \boldsymbol{\gamma})_{\Omega^s}\right] \quad \forall \boldsymbol{\gamma} \in \boldsymbol{L}^2(\Omega^s),
\end{aligned}$$

$$
\begin{aligned}
(\varrho_{\mathbf{1}}, \mathbf{w})_{\Omega^f_{t_n}} &= -\frac{\rho^f}{\Delta t}(\bar{\mathbf{u}}^n, \mathbf{w})_{\Omega^f_{t_n}} + \rho^f [c(\mathbf{u}^n, \mathbf{w}, \bar{\mathbf{u}}^n)_{\Omega^f_{t_n}} + c(\mathbf{w}, \mathbf{u}^n, \bar{\mathbf{u}}^n)_{\Omega^f_{t_n}} + \frac{1}{2}((\nabla \cdot \mathbf{z}^n)\mathbf{w}, \bar{\mathbf{u}}^n)_{\Omega^f_{t_n}} \\
&\quad + c(\mathbf{z}^n, \mathbf{w}, \bar{\mathbf{u}}^n)_{\Omega^f_{t_n}}] \quad \forall \mathbf{w} \in \boldsymbol{H}^1_D(\Omega^f_{t_n}), \\
(\varrho_{\mathbf{2}}, \mathbf{w})_{\Gamma^f_N} &= \rho^f [\frac{1}{2}((\mathbf{u}^n \cdot \mathbf{n}_f)\mathbf{w}, \bar{\mathbf{u}}^n)_{\Gamma^f_N} + \frac{1}{2}((\mathbf{w} \cdot \mathbf{n}_f)\mathbf{u}^n, \bar{\mathbf{u}}^n)_{\Gamma^f_N}] \quad \forall \mathbf{w} \in \boldsymbol{H}^1_D(\Omega^f_{t_n}) \\
(\varrho_{\mathbf{3}}, \mathbf{w})_{\Gamma_{I_{t_n}}} &= \frac{1}{\Delta t}\left(\mathbf{u}^n - \frac{\mathcal{V}(\boldsymbol{\eta}^n) + \mathcal{V}(\boldsymbol{\eta}^{n-1})}{\Delta t}, \mathbf{w}\right)_{\Gamma_{I_{t_n}}} \quad \forall \mathbf{w} \in \boldsymbol{H}^1_D(\Omega^f_{t_n}) \\
(\boldsymbol{\Xi}_1, \boldsymbol{\phi})_{\Omega^s} &= \frac{1}{\Delta t}(\bar{\dot{\boldsymbol{\eta}}}^n, \boldsymbol{\phi})_{\Omega^s} - \frac{1}{2}\,\lambda e(\bar{\boldsymbol{\eta}}^n, \boldsymbol{\phi})_{\Omega^s} \quad \forall \boldsymbol{\phi} \in \boldsymbol{H}^1_D(\Omega^s), \\
(\boldsymbol{\Xi}_2, \boldsymbol{\phi})_{\Gamma_{I_{t_0}}} &= -\frac{1}{\Delta t^2}\left(J_{t_n}\left[\mathcal{V}(\mathbf{u}^n) - \frac{\boldsymbol{\eta}^n + \boldsymbol{\eta}^{n-1}}{\Delta t}\right], \boldsymbol{\phi}\right)_{\Gamma_{I_{t_0}}} \quad \forall \boldsymbol{\phi} \in \boldsymbol{H}^1_D(\Omega^s), \\
(\boldsymbol{\Upsilon}, \boldsymbol{\theta})_{\Omega^s} &= -\frac{\rho^s}{\Delta t}(\bar{\boldsymbol{\eta}}^n, \boldsymbol{\theta})_{\Omega^s} \quad \forall \boldsymbol{\theta} \in \boldsymbol{L}^2(\Omega^s).
\end{aligned}
$$

Now, the optimality system (5.9)–(5.16) is equivalent to

$$
\begin{aligned}
&(\mathbf{u}^n, p^n, \boldsymbol{\eta}^n, \dot{\boldsymbol{\eta}}^n, \bar{\mathbf{u}}^n, \bar{p}^n, \bar{\boldsymbol{\eta}}^n, \bar{\dot{\boldsymbol{\eta}}}^n) \\
&\qquad + TG(\frac{1}{\delta}, (\mathbf{u}^n, p^n, \boldsymbol{\eta}^n, \dot{\boldsymbol{\eta}}^n, \bar{\mathbf{u}}^n, \bar{p}^n, \bar{\boldsymbol{\eta}}^n, \bar{\dot{\boldsymbol{\eta}}}^n)) = 0,
\end{aligned}
$$

and the discrete optimality system (5.22)–(5.29) is equivalent to

$$
\begin{aligned}
&(\mathbf{u}^{n,h}, p^{n,h}, \boldsymbol{\eta}^{n,h}, \dot{\boldsymbol{\eta}}^{n,h}, \bar{\mathbf{u}}^{n,h}, \bar{p}^{n,h}, \bar{\boldsymbol{\eta}}^{n,h}, \bar{\dot{\boldsymbol{\eta}}}^{n,h}) \\
&\qquad + T^h G(\frac{1}{\delta}, (\mathbf{u}^{n,h}, p^{n,h}, \boldsymbol{\eta}^{n,h}, \dot{\boldsymbol{\eta}}^{n,h}, \bar{\mathbf{u}}^{n,h}, \bar{p}^{n,h}, \bar{\boldsymbol{\eta}}^{n,h}, \bar{\dot{\boldsymbol{\eta}}}^{n,h})) = 0.
\end{aligned}
$$

Now the optimality system and the discrete optimality system have the form of (5.30) and (5.31), respectively.

In the next theorem, we set $\lambda = \frac{1}{\delta}$ to simplify the notation.

Theorem 5.2. *Assume that* $\{(\lambda, \varphi(\lambda)) = (\mathbf{u}^n, p^n, \boldsymbol{\eta}^n, \dot{\boldsymbol{\eta}}^n, \bar{\mathbf{u}}^n, \bar{p}^n, \bar{\boldsymbol{\eta}}^n, \bar{\dot{\boldsymbol{\eta}}}^n) : \lambda \in \Lambda\}$ *is a branch of regular solutions of the optimality system (5.9)–(5.16), where* Λ *is a compact interval in* $\mathbb{R}$. *Assume that* $\mathbf{W}^h$, Q^h, $\mathbf{D}^h$, *and* $\mathbf{V}^h$ *satisfy (5.17)–(5.21). Then for* $h \leq h_0$ *small enough, there exists a unique branch of solutions of the discrete optimality system (5.22)–(5.29),* $\{(\lambda, \varphi^h(\lambda)) = (\mathbf{u}^{n,h}, p^{n,h}, \boldsymbol{\eta}^{n,h}, \dot{\boldsymbol{\eta}}^{n,h}, \bar{\mathbf{u}}^{n,h}, \bar{p}^{n,h}, \bar{\boldsymbol{\eta}}^{n,h}, \bar{\dot{\boldsymbol{\eta}}}^{n,h}) : \lambda \in \Lambda\}$, *such that*

$\phi - \phi^h \in \mathcal{O}$, a neighborhood about the origin in X. Additionally, as $h \to 0$ uniformly in X,

$$\begin{aligned}
&\left\|\varphi(\lambda) - \varphi^h(\lambda)\right\|_X \\
&\quad = \left\|\mathbf{u}^n(\lambda) - \mathbf{u}^{n,h}(\lambda)\right\|_{1,\Omega^f_{t_n}} + \left\|p^n(\lambda) - p^{n,h}(\lambda)\right\|_{0,\Omega^f_{t_n}} + \left\|\boldsymbol{\eta}^n(\lambda) - \boldsymbol{\eta}^{n,h}(\lambda)\right\|_{1,\Omega^s} \\
&\qquad + \left\|\dot{\boldsymbol{\eta}}^n(\lambda) - \dot{\boldsymbol{\eta}}^{n,h}(\lambda)\right\|_{0,\Omega^s} + \left\|\bar{\mathbf{u}}^n(\lambda) - \bar{\mathbf{u}}^{n,h}(\lambda)\right\|_{1,\Omega^f_{t_n}} + \left\|\bar{p}^n(\lambda) - \bar{p}^{n,h}(\lambda)\right\|_{0,\Omega^f_{t_n}} \\
&\qquad + \left\|\bar{\boldsymbol{\eta}}^n(\lambda) - \bar{\boldsymbol{\eta}}^{n,h}(\lambda)\right\|_{1,\Omega^s} + \left\|\bar{\dot{\boldsymbol{\eta}}}^n(\lambda) - \bar{\dot{\boldsymbol{\eta}}}^{n,h}(\lambda)\right\|_{0,\Omega^s} \to 0. \qquad (5.52)
\end{aligned}$$

With the additional assumption that $(\mathbf{u}^n(\lambda), p^n(\lambda), \boldsymbol{\eta}^n(\lambda), \dot{\boldsymbol{\eta}}^n(\lambda), \bar{\mathbf{u}}^n(\lambda), \bar{p}^n(\lambda), \bar{\boldsymbol{\eta}}^n(\lambda), \bar{\dot{\boldsymbol{\eta}}}^n(\lambda)) \in (\mathbf{H}^{m+1}(\Omega^f_{t_n}) \times \mathbf{H}^m(\Omega^f_{t_n}) \times \mathbf{H}^{m+1}(\Omega^s) \times \mathbf{H}^m(\Omega^s))^2$, there exists a constant C, independent of h, such that

$$\begin{aligned}
&\left\|\mathbf{u}^n(\lambda) - \mathbf{u}^{n,h}(\lambda)\right\|_{1,\Omega^f_{t_n}} + \left\|p^n(\lambda) - p^{n,h}(\lambda)\right\|_{0,\Omega^f_{t_n}} + \left\|\boldsymbol{\eta}^n(\lambda) - \boldsymbol{\eta}^{n,h}(\lambda)\right\|_{1,\Omega^s} \\
&\quad + \left\|\dot{\boldsymbol{\eta}}^n(\lambda) - \dot{\boldsymbol{\eta}}^{n,h}(\lambda)\right\|_{0,\Omega^s} + \left\|\bar{\mathbf{u}}^n(\lambda) - \bar{\mathbf{u}}^{n,h}(\lambda)\right\|_{1,\Omega^f_{t_n}} + \left\|\bar{p}^n(\lambda) - \bar{p}^{n,h}(\lambda)\right\|_{0,\Omega^f_{t_n}} \\
&\quad + \left\|\bar{\boldsymbol{\eta}}^n(\lambda) - \bar{\boldsymbol{\eta}}^{n,h}(\lambda)\right\|_{1,\Omega^s} + \left\|\bar{\dot{\boldsymbol{\eta}}}^n(\lambda) - \bar{\dot{\boldsymbol{\eta}}}^{n,h}(\lambda)\right\|_{0,\Omega^s} \\
&\quad \le Ch^m[\|\mathbf{u}^n(\lambda)\|_{m+1,\Omega^f_{t_n}} + \|p^n(\lambda)\|_{m,\Omega^f_{t_n}} + \|\boldsymbol{\eta}^n(\lambda)\|_{m+1,\Omega^s} + \|\dot{\boldsymbol{\eta}}^n(\lambda)\|_{m,\Omega^s} \\
&\qquad + \|\bar{\mathbf{u}}^n(\lambda)\|_{m+1,\Omega^f_{t_n}} + \|\bar{p}^n(\lambda)\|_{m,\Omega^f_{t_n}} + \|\bar{\boldsymbol{\eta}}^n(\lambda)\|_{m+1,\Omega^s} + \|\bar{\dot{\boldsymbol{\eta}}}^n(\lambda)\|_{m,\Omega^s}] \qquad (5.53)
\end{aligned}$$

Proof. Λ is compact and G is a C^∞ mapping from $\Lambda \times X$ into Y. Therefore D^2G is bounded on all bounded set of $\Lambda \times X$ by bound (2.16). G_φ, the Fréchet derivative of G, is defined by: for $(\tilde{\mathbf{v}}, \tilde{q}, \tilde{\boldsymbol{\xi}}, \tilde{\boldsymbol{\gamma}}, \tilde{\mathbf{w}}, \tilde{r}, \tilde{\boldsymbol{\phi}}, \tilde{\boldsymbol{\theta}}) \in X$, $G_\varphi(\lambda, (\mathbf{u}^n, p^n, \boldsymbol{\eta}^n, \dot{\boldsymbol{\eta}}^n, \bar{\mathbf{u}}^n, \bar{p}^n, \bar{\boldsymbol{\eta}}^n, \bar{\dot{\boldsymbol{\eta}}}^n)) \cdot (\tilde{\mathbf{v}}, \tilde{q}, \tilde{\boldsymbol{\xi}}, \tilde{\boldsymbol{\gamma}}, \tilde{\mathbf{w}}, \tilde{r}, \tilde{\boldsymbol{\phi}}, \tilde{\boldsymbol{\theta}}) = (\tilde{\sigma_1}, \tilde{\sigma_2}, \tilde{\sigma_3}, \tilde{\boldsymbol{\Phi}}_1, \tilde{\boldsymbol{\Phi}}_2, \tilde{\boldsymbol{\Phi}}_3, \tilde{\boldsymbol{\Pi}}, \tilde{\varrho_1}, \tilde{\varrho_2}, \tilde{\varrho_3}, \tilde{\boldsymbol{\Xi}}_1, \tilde{\boldsymbol{\Xi}}_2, \tilde{\boldsymbol{\Upsilon}})$ if and only if,

$$\begin{aligned}
(\tilde{\sigma_1}, \mathbf{v})_{\Omega^f_{t_n}} &= -\frac{\rho^f}{\Delta t}(\tilde{\mathbf{v}}, \mathbf{v})_{\Omega^f_{t_n}} + \rho^f[c(\tilde{\mathbf{v}}, \mathbf{u}^n, \mathbf{v})_{\Omega^f_{t_n}} + c(\mathbf{u}^n, \tilde{\mathbf{v}}, \mathbf{v})_{\Omega^f_{t_n}} \\
&\quad + \frac{1}{2}((\nabla \cdot \mathbf{z}^n)\tilde{\mathbf{v}}, \mathbf{v})_{\Omega^f_{t_n}} + c(\mathbf{z}^n, \tilde{\mathbf{v}}, \mathbf{v})_{\Omega^f_{t_n}}] \quad \forall \mathbf{v} \in \boldsymbol{H}^1_D(\Omega^f_{t_n}),
\end{aligned}$$

$$
\begin{aligned}
(\tilde{\sigma_{\mathbf{2}}}, \mathbf{v})_{\Gamma_N^f} &= \frac{\rho^f}{2}[((\tilde{\mathbf{v}} \cdot \mathbf{n}_f)\mathbf{u}^n, \mathbf{v})_{\Gamma_N^f} + ((\mathbf{u}^n \cdot \mathbf{n}_f)\tilde{\mathbf{v}}, \mathbf{v})_{\Gamma_N^f}] \quad \forall \mathbf{v} \in \boldsymbol{H}_D^1(\Omega_{t_n}^f),\\
(\tilde{\sigma_{\mathbf{3}}}, \mathbf{v})_{\Gamma_{I_{t_n}}} &= -\frac{\Delta t}{\delta}\,(\tilde{\mathbf{w}} - \frac{\mathcal{V}(\tilde{\boldsymbol{\phi}})}{2}, \mathbf{v})_{\Gamma_{I_{t_n}}} \quad \forall \mathbf{v} \in \boldsymbol{H}_D^1(\Omega_{t_n}^f),\\
(\tilde{\boldsymbol{\Phi}}_1, \boldsymbol{\xi})_{\Omega^s} &= -\frac{\rho^s}{\Delta t}(\tilde{\boldsymbol{\gamma}}, \boldsymbol{\xi})_{\Omega^s} - \frac{1}{2}\,\lambda e(\tilde{\boldsymbol{\xi}}, \boldsymbol{\xi})_{\Omega^s} \quad \forall \boldsymbol{\xi} \in \boldsymbol{H}_D^1(\Omega^s),\\
(\tilde{\boldsymbol{\Phi}}_2, \boldsymbol{\xi})_{\Gamma_N^s} &= 0 \quad \forall \boldsymbol{\xi} \in \boldsymbol{H}_D^1(\Omega^s),\\
(\tilde{\boldsymbol{\Phi}}_3, \boldsymbol{\xi})_{\Gamma_{I_{t_0}}} &= \frac{\Delta t}{2\delta}\,(\mathcal{V}(\tilde{\mathbf{w}})J_{t_n} - \frac{1}{2}\tilde{\boldsymbol{\phi}}J_{t_n}, \boldsymbol{\xi})_{\Gamma_{I_{t_0}}} \quad \forall \boldsymbol{\xi} \in \boldsymbol{H}_D^1(\Omega^s),\\
(\tilde{\boldsymbol{\Pi}}, \boldsymbol{\gamma})_{\Omega^s} &= \frac{1}{\Delta t}(\tilde{\boldsymbol{\xi}}, \boldsymbol{\gamma})_{\Omega^s} \quad \forall \boldsymbol{\gamma} \in \boldsymbol{L}^2(\Omega^s),\\
(\tilde{\varrho_{\mathbf{1}}}, \mathbf{w})_{\Omega_{t_n}^f} &= -\frac{\rho^f}{\Delta t}(\tilde{\mathbf{w}}, \mathbf{w})_{\Omega_{t_n}^f} + \rho^f[c(\tilde{\mathbf{v}}, \mathbf{w}, \bar{\mathbf{u}}^n)_{\Omega_{t_n}^f} + c(\mathbf{u}^n, \mathbf{w}, \tilde{\mathbf{w}})_{\Omega_{t_n}^f}\\
&\quad + c(\mathbf{w}, \tilde{\mathbf{v}}, \bar{\mathbf{u}}^n)_{\Omega_{t_n}^f} + c(\mathbf{w}, \mathbf{u}^n, \tilde{\mathbf{w}})_{\Omega_{t_n}^f}] + \frac{1}{2}((\nabla \cdot \mathbf{z}^n)\mathbf{w}, \tilde{\mathbf{w}})_{\Omega_{t_n}^f}\\
&\quad + c(\mathbf{z}^n, \mathbf{w}, \tilde{\mathbf{w}})_{\Omega_{t_n}^f}] \quad \forall \mathbf{w} \in \boldsymbol{H}_D^1(\Omega_{t_n}^f),\\
(\tilde{\varrho_{\mathbf{2}}}, \mathbf{w})_{\Gamma_N^f} &= \frac{\rho^f}{2}[((\tilde{\mathbf{v}} \cdot \mathbf{n}_f)\mathbf{w}, \bar{\mathbf{u}}^n)_{\Gamma_N^f} + ((\mathbf{u}^n \cdot \mathbf{n}_f)\mathbf{w}, \tilde{\mathbf{w}})_{\Gamma_N^f}\\
&\quad + ((\mathbf{w} \cdot \mathbf{n}_f)\tilde{\mathbf{v}}, \bar{\mathbf{u}}^n)_{\Gamma_N^f} + ((\mathbf{w} \cdot \mathbf{n}_f)\mathbf{u}^n, \tilde{\mathbf{w}})_{\Gamma_N^f}] \quad \forall \mathbf{w} \in \boldsymbol{H}_D^1(\Omega_{t_n}^f)\\
(\tilde{\varrho_{\mathbf{3}}}, \mathbf{w})_{\Gamma_{I_{t_n}}} &= \frac{1}{\Delta t}\left(\tilde{\mathbf{v}} - \frac{\mathcal{V}(\tilde{\boldsymbol{\xi}})}{\Delta t}, \mathbf{w}\right)_{\Gamma_{I_{t_n}}} \quad \forall \mathbf{w} \in \boldsymbol{H}_D^1(\Omega_{t_n}^f) \quad \forall \mathbf{w} \in \boldsymbol{H}_D^1(\Omega_{t_n}^f)\\
(\tilde{\boldsymbol{\Xi}}_1, \boldsymbol{\phi})_{\Omega^s} &= \frac{1}{\Delta t}(\tilde{\boldsymbol{\theta}}, \boldsymbol{\phi})_{\Omega^s} - \frac{1}{2}\,\lambda e(\tilde{\boldsymbol{\phi}}, \boldsymbol{\phi})_{\Omega^s} \quad \forall \boldsymbol{\phi} \in \boldsymbol{H}_D^1(\Omega^s),\\
(\tilde{\boldsymbol{\Xi}}_2, \boldsymbol{\phi})_{\Gamma_{I_{t_0}}} &= -\frac{1}{\Delta t^2}\left(J_{t_n}\left[\mathcal{V}(\tilde{\mathbf{v}}) - \frac{\tilde{\boldsymbol{\xi}}}{\Delta t}\right], \boldsymbol{\phi}\right)_{\Gamma_{I_{t_0}}} \quad \forall \boldsymbol{\phi} \in \boldsymbol{H}_D^1(\Omega^s),\\
(\tilde{\boldsymbol{\Upsilon}}, \boldsymbol{\theta})_{\Omega^s} &= -\frac{\rho^s}{\Delta t}(\tilde{\boldsymbol{\phi}}, \boldsymbol{\theta})_{\Omega^s} \quad \forall \boldsymbol{\theta} \in \boldsymbol{L}^2(\Omega^s).
\end{aligned}
$$

Therefore, $D_\varphi G(\lambda, (\mathbf{u}^n, p^n, \boldsymbol{\eta}^n, \dot{\boldsymbol{\eta}}^n, \bar{\mathbf{u}}^n, \bar{p}^n, \bar{\boldsymbol{\eta}}^n, \bar{\dot{\boldsymbol{\eta}}}^n)) \in \mathcal{L}(X, Y)$. By the Sobolev embedding theorem [1], $\mathbf{u}^n$, $\bar{\mathbf{u}^n}$, $\tilde{\mathbf{v}}$, and $\tilde{\mathbf{w}} \in \mathbf{L}^6(\Omega_{t_n}^f)$, and $\mathbf{u}^n|_{\Gamma_N^f}$, $\bar{\mathbf{u}^n}|_{\Gamma_N^f}$, $\tilde{\mathbf{v}}|_{\Gamma_N^f}$ and $\tilde{\mathbf{w}}|_{\Gamma_N^f} \in \mathbf{L}^4(\Gamma_N^f)$. Additionally, and $\nabla\mathbf{u}^n$, $\nabla\bar{\mathbf{u}^n}$, $\nabla\tilde{\mathbf{v}}$, and $\nabla\tilde{\mathbf{w}} \in \mathbf{L}^2(\Omega_{t_n}^f)$. As a result of these embeddings, $(\tilde{\sigma_{\mathbf{1}}}, \tilde{\sigma_{\mathbf{2}}}, \tilde{\sigma_{\mathbf{3}}}, \tilde{\boldsymbol{\Phi}}_1, \tilde{\boldsymbol{\Phi}}_2, \tilde{\boldsymbol{\Phi}}_3, \tilde{\boldsymbol{\Pi}}, \tilde{\varrho_{\mathbf{1}}}, \tilde{\varrho_{\mathbf{2}}}, \tilde{\varrho_{\mathbf{3}}}, \tilde{\boldsymbol{\Xi}}_1, \tilde{\boldsymbol{\Xi}}_2, \tilde{\boldsymbol{\Upsilon}}) \in Z$ and therefore we can write that $D_\varphi G(\lambda, (\mathbf{u}^n, p^n, \boldsymbol{\eta}^n, \dot{\boldsymbol{\eta}}^n, \bar{\mathbf{u}}^n, \bar{p}^n, \bar{\boldsymbol{\eta}}^n, \bar{\dot{\boldsymbol{\eta}}}^n)) \in \mathcal{L}(X, Z)$. Also, note that $Z \in Y$ is a compact embedding.

Considering the operators T and T^h, equations (5.36)–(5.37), (5.38), (5.39), (5.40)–

(5.41), (5.42), and (5.43) are all uncoupled from one another. This is likewise the case for (5.44)–(5.45), (5.46), (5.47), (5.48)–(5.49), (5.50), and (5.51). Using well known results for Stokes flow, Poisson's equation, and projections, the difference in solutions can be shown to be

$$\begin{aligned}
&\left\|\hat{\mathbf{u}}^n(\lambda)-\hat{\mathbf{u}}^{n,h}(\lambda)\right\|_{1,\Omega^f_{t_n}}+\left\|\hat{p}^n(\lambda)-\hat{p}^{n,h}(\lambda)\right\|_{0,\Omega^f_{t_n}}+\left\|\hat{\boldsymbol{\eta}}^n(\lambda)-\hat{\boldsymbol{\eta}}^{n,h}(\lambda)\right\|_{1,\Omega^s}\\
&\quad+\left\|\hat{\dot{\boldsymbol{\eta}}}^n(\lambda)-\hat{\dot{\boldsymbol{\eta}}}^{n,h}(\lambda)\right\|_{0,\Omega^s}+\left\|\hat{\bar{\mathbf{u}}}^n(\lambda)-\hat{\bar{\mathbf{u}}}^{n,h}(\lambda)\right\|_{1,\Omega^f_{t_n}}+\left\|\hat{\bar{p}}^n(\lambda)-\hat{\bar{p}}^{n,h}(\lambda)\right\|_{0,\Omega^f_{t_n}}\\
&\quad+\left\|\hat{\bar{\boldsymbol{\eta}}}^n(\lambda)-\hat{\bar{\boldsymbol{\eta}}}^{n,h}(\lambda)\right\|_{1,\Omega^s}+\left\|\hat{\bar{\dot{\boldsymbol{\eta}}}}^n(\lambda)-\hat{\bar{\dot{\boldsymbol{\eta}}}}^{n,h}(\lambda)\right\|_{0,\Omega^s}\to 0
\end{aligned}$$

as $h\to 0$ uniformly, where $(\hat{\mathbf{u}}^n,\hat{p}^n,\hat{\boldsymbol{\eta}}^n,\hat{\dot{\boldsymbol{\eta}}}^n,\hat{\bar{\mathbf{u}}}^n,\hat{\bar{p}}^n,\hat{\bar{\boldsymbol{\eta}}}^n,\hat{\bar{\dot{\boldsymbol{\eta}}}}^n)$ is a solution to (5.36)–(5.43) and $(\hat{\mathbf{u}}^{n,h},\hat{p}^{n,h},\hat{\boldsymbol{\eta}}^{n,h},\hat{\dot{\boldsymbol{\eta}}}^{n,h},\hat{\bar{\mathbf{u}}}^{n,h},\hat{\bar{p}}^{n,h},\hat{\bar{\boldsymbol{\eta}}}^{n,h},\hat{\bar{\dot{\boldsymbol{\eta}}}}^{n,h})$ is a solution to (5.44)–(5.51); see [65]. This means that (5.33) holds and we have already seen that $D_\varphi G(\lambda,(\mathbf{u}^n,p^n,\boldsymbol{\eta}^n,\dot{\boldsymbol{\eta}}^n,\bar{\mathbf{u}}^n,\bar{p}^n,\bar{\boldsymbol{\eta}}^n,\bar{\dot{\boldsymbol{\eta}}}^n))$ $\in\mathcal{L}(X,Z)$ where $Z\subset Y$ is compactly embedded, so (5.34) also holds. This satisfies all of the assumptions of Theorem 5.1. Also, we have the approximation result for the Stokes operator and projections, namely that

$$\begin{aligned}
&\left\|\hat{\mathbf{u}}^n(\lambda)-\hat{\mathbf{u}}^{n,h}(\lambda)\right\|_{1,\Omega^f_{t_n}}+\left\|\hat{p}^n(\lambda)-\hat{p}^{n,h}(\lambda)\right\|_{0,\Omega^f_{t_n}}+\left\|\hat{\boldsymbol{\eta}}^n(\lambda)-\hat{\boldsymbol{\eta}}^{n,h}(\lambda)\right\|_{1,\Omega^s}\\
&\quad+\left\|\hat{\dot{\boldsymbol{\eta}}}^n(\lambda)-\hat{\dot{\boldsymbol{\eta}}}^{n,h}(\lambda)\right\|_{0,\Omega^s}+\left\|\hat{\bar{\mathbf{u}}}^n(\lambda)-\hat{\bar{\mathbf{u}}}^{n,h}(\lambda)\right\|_{1,\Omega^f_{t_n}}+\left\|\hat{\bar{p}}^n(\lambda)-\hat{\bar{p}}^{n,h}(\lambda)\right\|_{0,\Omega^f_{t_n}}\\
&\quad+\left\|\hat{\bar{\boldsymbol{\eta}}}^n(\lambda)-\hat{\bar{\boldsymbol{\eta}}}^{n,h}(\lambda)\right\|_{1,\Omega^s}+\left\|\hat{\bar{\dot{\boldsymbol{\eta}}}}^n(\lambda)-\hat{\bar{\dot{\boldsymbol{\eta}}}}^{n,h}(\lambda)\right\|_{0,\Omega^s}\\
&\quad\le Ch^m[\|\hat{\mathbf{u}}^n(\lambda)\|_{m+1,\Omega^f_{t_n}}+\|\hat{p}^n(\lambda)\|_{m,\Omega^f_{t_n}}+\|\hat{\boldsymbol{\eta}}^n(\lambda)\|_{m+1,\Omega^s}+\left\|\hat{\dot{\boldsymbol{\eta}}}^n(\lambda)\right\|_{m,\Omega^s}\\
&\qquad+\left\|\hat{\bar{\mathbf{u}}}^n(\lambda)\right\|_{m+1,\Omega^f_{t_n}}+\left\|\hat{\bar{p}}^n(\lambda)\right\|_{m,\Omega^f_{t_n}}+\left\|\hat{\bar{\boldsymbol{\eta}}}^n(\lambda)\right\|_{m+1,\Omega^s}+\left\|\hat{\bar{\dot{\boldsymbol{\eta}}}}^n(\lambda)\right\|_{m,\Omega^s}]
\end{aligned}$$

for some constant C independent of h. If it is also true that
$(\mathbf{u}^n(\lambda),p^n(\lambda),\boldsymbol{\eta}^n(\lambda),\dot{\boldsymbol{\eta}}^n(\lambda),\bar{\mathbf{u}}^n(\lambda),\bar{p}^n(\lambda),\bar{\boldsymbol{\eta}}^n(\lambda),\bar{\dot{\boldsymbol{\eta}}}^n(\lambda))\in(\mathbf{H}^{m+1}(\Omega^f_{t_n})\times\mathbf{H}^m(\Omega^f_{t_n})\times$

$\mathbf{H}^{m+1}(\Omega^s) \times \mathbf{H}^m(\Omega^s))^2$, then

$$\begin{aligned}\left\|(T - T^h)G(\lambda, \varphi(\lambda)\right\|_X \\ &\leq Ch^m[\|\mathbf{u}^n(\lambda)\|_{m+1,\Omega^f_{t_n}} + \|p^n(\lambda)\|_{m,\Omega^f_{t_n}} + \|\boldsymbol{\eta}^n(\lambda)\|_{m+1,\Omega^s} + \|\dot{\boldsymbol{\eta}}^n(\lambda)\|_{m,\Omega^s} \\ &\quad + \|\bar{\mathbf{u}}^n(\lambda)\|_{m+1,\Omega^f_{t_n}} + \|\bar{p}^n(\lambda)\|_{m,\Omega^f_{t_n}} + \|\bar{\boldsymbol{\eta}}^n(\lambda)\|_{m+1,\Omega^s} + \|\bar{\dot{\boldsymbol{\eta}}}^n(\lambda)\|_{m,\Omega^s}].\end{aligned}$$

From this, the error estimate (5.53) follows.

□

5.5 Convergence of Steepest Descent

Using the steepest descent method described in Section 4.9, it will be shown that a sequence of solutions generated by this algorithm converge on an optimal solution if the time step is sufficiently small and the strong solution to the PDE is sufficiently smooth.

Theorem 5.3. *Let X be a Hilbert space equipped with the inner product $(\cdot,\cdot)_X$ and norm $\|\cdot\|_X$. Suppose $\mathcal{M}$ is a functional on X such that*

1. *$\mathcal{M}$ has a local minimum at $\hat{x}$ and is twice differentiable in an open ball B centered at $\hat{x}$;*
2. *$|\langle \mathcal{M}''(u), (x, y))\rangle| \leq m_a \|x\|_X \|y\|_X$, $\forall u \in B,\ x \in X,\ y \in X$;*
3. *$|\langle \mathcal{M}''(u), (x, x))\rangle| \geq m_b \|x\|_X^2$, $\forall u \in B,\ x \in X$,*

where m_a and m_b are positive constants. Let R denote the Riesz map, i.e. $\langle f, x\rangle = \langle Rf, x\rangle_X$ for all $x \in X$ and all $f \in X^*$. Choose $x^{(0)}$ sufficiently close to $\hat{x}$ and choose a sequence $\{\omega_n\}$ such that $0 < \omega_* \leq \omega_n \leq \omega^* < 2m_b/m_a^2$. Then, the sequence $\{x^{(n)}\}$ defined by

$$x^{(n)} = x^{(n-1)} - \omega_n R\mathcal{M}'(x^{(n-1)}), \quad for\ n = 1, 2, \ldots \tag{5.54}$$

converges to $\hat{x}$. Furthermore, if $B = X$ and $\hat{x}$ is a global minimum, then the sequence generated by (5.54) converges to $\hat{x}$ for any initial guess $x^{(0)}$.

Proof. See, e.g., [24]. □

Theorem 5.4. *Let* $(\mathbf{u}_{(m)}^{n,h}, p_{(m)}^{n,h}, \boldsymbol{\eta}_{(m)}^{n,h}, \dot{\boldsymbol{\eta}}_{(m)}^{n,h}, \bar{\mathbf{u}}_{(m)}^{n,h}, \bar{p}_{(m)}^{n,h}, \bar{\boldsymbol{\eta}}_{(m)}^{n,h}, \bar{\dot{\boldsymbol{\eta}}}_{(m)}^{n,h})$ *be a sequence obtained by Algorithm 4.11 and* $(\mathbf{u}^{n,h}, p^{n,h}, \boldsymbol{\eta}^{n,h}, \dot{\boldsymbol{\eta}}^{n,h}, \bar{\mathbf{u}}^{n,h}, \bar{p}^{n,h}, \bar{\boldsymbol{\eta}}^{n,h}, \bar{\dot{\boldsymbol{\eta}}}^{n,h})$ *be a solution of the optimality system (5.22)–(5.29), where* $\mathcal{M}$ *is functional (5.1) . If* $\alpha_m \leq \Delta t^4 \frac{\delta^2 - C\delta h^{\frac{1}{8}}}{2C}$, *h is sufficiently small, and* $\left\| \mathbf{g}_{(0)}^{n,h} - \mathbf{g}_*^{n,h} \right\|_{0,\Gamma_{I_{t_n}}} < 1$ *where* $\mathbf{g}_*^{n,h}$ *is a local minimum, then* $\mathbf{u}_{(m)}^{n,h} \to \mathbf{u}^{n,h}$, $p_{(m)}^{n,h} \to p^{n,h}$, $\boldsymbol{\eta}_{(m)}^{n,h} \to \boldsymbol{\eta}^{n,h}$, $\dot{\boldsymbol{\eta}}_{(m)}^{n,h} \to \dot{\boldsymbol{\eta}}^{n,h}$, $\bar{\mathbf{u}}_{(m)}^{n,h} \to \bar{\mathbf{u}}^{n,h}$, $\bar{p}_{(m)}^{n,h} \to \bar{p}^{n,h}$, $\bar{\boldsymbol{\eta}}_{(m)}^{n,h} \to \bar{\boldsymbol{\eta}}^{n,h}$, $\bar{\dot{\boldsymbol{\eta}}}_{(m)}^{n,h} \to \bar{\dot{\boldsymbol{\eta}}}^{n,h}$, *as* $m \to \infty$.

Proof. For a given $\tilde{\mathbf{g}}^n \in \mathbf{L}^2(\Gamma_{I_{t_n}})$, the second Fréchet derivative $D^2\mathcal{M}(\tilde{\mathbf{u}}^n(\tilde{\mathbf{g}}^n), \tilde{\boldsymbol{\eta}}^n(\tilde{\mathbf{g}}^n), \tilde{\mathbf{g}}^n)$ is defined by

$$D^2\mathcal{M}(\tilde{\mathbf{u}}^n(\tilde{\mathbf{g}}^n), \tilde{\boldsymbol{\eta}}^n(\tilde{\mathbf{g}}^n), \tilde{\mathbf{g}}^n) \cdot (\bar{\mathbf{g}}_1, \bar{\mathbf{g}}_2) = \left(\bar{\mathbf{u}}_1 - \frac{\bar{\boldsymbol{\eta}}_1}{\Delta t}, \bar{\mathbf{u}}_2 - \frac{\bar{\boldsymbol{\eta}}_2}{\Delta t} \right)_{\Gamma_{I_{t_n}}} + \left(\tilde{\mathbf{u}} - \frac{\tilde{\boldsymbol{\eta}} - \boldsymbol{\eta}^{n-1}}{\Delta t}, \bar{\tilde{\mathbf{u}}} - \frac{\bar{\tilde{\boldsymbol{\eta}}}}{\Delta t} \right)_{\Gamma_{I_{t_n}}} + \delta(\bar{\mathbf{g}}_1, \bar{\mathbf{g}}_2)_{\Gamma_{I_{t_n}}}, \tag{5.55}$$

where $\tilde{\mathbf{u}}$ is the solution of

$$\begin{cases} \rho^f [(\tilde{\mathbf{u}}, \mathbf{v})_{\Omega_{t_n}^f} - (\mathbf{u}^{n-1}, \mathbf{v})_{\Omega_{t_n}^f}] + \Delta t\, \rho^f [c(\tilde{\mathbf{u}}, \tilde{\mathbf{u}}, \mathbf{v})_{\Omega_{t_n}^f} + \frac{1}{2}((\tilde{\mathbf{u}} \cdot \mathbf{n}_f)\tilde{\mathbf{u}}, \mathbf{v})_{\Gamma_N^f} \\ \qquad\qquad - \frac{1}{2}((\nabla \cdot \mathbf{z}^n)\tilde{\mathbf{u}}, \mathbf{v})_{\Omega_{t_n}^f} - c(\mathbf{z}^n, \tilde{\mathbf{u}}, \mathbf{v})] + \Delta t\, 2\nu_f a(\tilde{\mathbf{u}}, \mathbf{v})_{\Omega_{t_n}^f} + \Delta t\, b(\mathbf{v}, \tilde{p})_{\Omega_{t_n}^f} \\ \qquad\qquad = \Delta t\, (\mathbf{f}_f^n, \mathbf{v})_{\Omega_{t_n}^f} + \Delta t\, (\mathbf{u}_N^n, \mathbf{v})_{\Gamma_N^f} + \Delta t\, (\tilde{\mathbf{g}}^n, \mathbf{v})_{\Gamma_{I_{t_n}}} \quad \forall \mathbf{v} \in \boldsymbol{H}_D^1(\Omega_{t_n}^f), \\ b(\tilde{\mathbf{u}}, q)_{\Omega_{t_n}^f} = 0 \quad q \in L^2(\Omega_{t_n}^f), \end{cases} \tag{5.56}$$

and $(\tilde{\boldsymbol{\eta}},\tilde{\dot{\boldsymbol{\eta}}})$ is the solution of

$$\begin{cases} \rho^s[(\tilde{\dot{\boldsymbol{\eta}}},\boldsymbol{\xi})_{\Omega^s}-(\dot{\boldsymbol{\eta}}^{n-1},\boldsymbol{\xi})_{\Omega^s}] & +\Delta t\ \nu_s d(\tilde{\boldsymbol{\eta}},\boldsymbol{\xi})_{\Omega^s}+\frac{\Delta t}{2}\ \lambda e(\tilde{\boldsymbol{\eta}},\boldsymbol{\xi})_{\Omega^s} \\ & =\frac{\Delta t}{2}\left(\mathbf{f}_s^n+\mathbf{f}_s^{n-1},\boldsymbol{\xi}\right)_{\Omega^s}+\frac{\Delta t}{2}\left(\boldsymbol{\eta}_N^n+\boldsymbol{\eta}_N^{n-1},\boldsymbol{\xi}\right)_{\Gamma_N^s} \\ & \quad -\frac{\Delta t}{2}\ (\mathcal{V}(\tilde{\mathbf{g}}^n)J_{t_n}+\mathcal{V}(\mathbf{g}^{n-1})J_{t_{n-1}},\boldsymbol{\xi})_{\Gamma_{I_{t_0}}} \quad \forall\boldsymbol{\xi}\in\boldsymbol{H}_D^1(\Omega^s), \\ \frac{\Delta t}{2}[(\tilde{\dot{\boldsymbol{\eta}}},\boldsymbol{\gamma})_{\Omega^s}+(\dot{\boldsymbol{\eta}}^{n-1},\boldsymbol{\gamma})_{\Omega^s}] & =(\tilde{\boldsymbol{\eta}},\boldsymbol{\gamma})_{\Omega^s}-(\boldsymbol{\eta}^{n-1},\boldsymbol{\gamma})_{\Omega^s} \quad \forall\boldsymbol{\gamma}\in\boldsymbol{H}_D^1(\Omega^s). \end{cases} \tag{5.57}$$

The first variations $\bar{\mathbf{u}}_i$, $i=1,2$, are the solutions of

$$\begin{cases} \rho^f(\bar{\mathbf{u}}_i,\mathbf{v})_{\Omega_{t_n}^f} & +\Delta t\ \rho^f[c(\bar{\mathbf{u}}_i,\tilde{\mathbf{u}}_i,\mathbf{v})_{\Omega_{t_n}^f}+c(\tilde{\mathbf{u}}_i,\bar{\mathbf{u}}_i,\mathbf{v})_{\Omega_{t_n}^f}+\frac{1}{2}((\bar{\mathbf{u}}_i\cdot\mathbf{n}_f)\tilde{\mathbf{u}}_i,\mathbf{v})_{\Gamma_N^f} \\ & +\frac{1}{2}((\tilde{\mathbf{u}}_i\cdot\mathbf{n}_f)\bar{\mathbf{u}}_i,\mathbf{v})_{\Gamma_N^f}-\frac{1}{2}((\nabla\cdot\mathbf{z}^n)\bar{\mathbf{u}}_i,\mathbf{v})_{\Omega_{t_n}^f}-c(\mathbf{z}^n,\bar{\mathbf{u}},\mathbf{v})] \\ & +\Delta t\ 2\nu_f a(\bar{\mathbf{u}},\mathbf{v})_{\Omega_{t_n}^f}+\Delta t\ b(\mathbf{v},\bar{p}_i)_{\Omega_{t_n}^f} \\ & =\Delta t\ (\bar{\mathbf{g}}_i,\mathbf{v})_{\Gamma_{I_{t_n}}} \quad \forall\mathbf{v}\in\boldsymbol{H}_D^1(\Omega_{t_n}^f), \\ b(\bar{\mathbf{u}}_i,q)_{\Omega_{t_n}^f} & =0 \quad q\in L^2(\Omega_{t_n}^f), \end{cases} \tag{5.58}$$

and the first variations $(\bar{\boldsymbol{\eta}}_i,\bar{\dot{\boldsymbol{\eta}}}_i)$, $i=1,2$, are the solutions of

$$\begin{cases} \rho^s(\bar{\dot{\boldsymbol{\eta}}}_i,\boldsymbol{\xi})_{\Omega^s}+\Delta t\ \nu_s d(\bar{\boldsymbol{\eta}}_i,\boldsymbol{\xi})_{\Omega^s} & +\frac{\Delta t}{2}\ \lambda e(\bar{\boldsymbol{\eta}}_i,\boldsymbol{\xi})_{\Omega^s} \\ & =-\frac{\Delta t}{2}\ (\mathcal{V}(\bar{\mathbf{g}}_i)J_{t_n},\boldsymbol{\xi})_{\Gamma_{I_{t_0}}} \quad \forall\boldsymbol{\xi}\in\boldsymbol{H}_D^1(\Omega^s), \\ \frac{\Delta t}{2}(\bar{\dot{\boldsymbol{\eta}}}_i,\boldsymbol{\gamma})_{\Omega^s}-(\bar{\boldsymbol{\eta}}_i,\boldsymbol{\gamma})_{\Omega^s} & =0 \quad \forall\boldsymbol{\gamma}\in\boldsymbol{H}_D^1(\Omega^s). \end{cases} \tag{5.59}$$

The second variation $\bar{\bar{\mathbf{u}}}$ is a solution of

$$\begin{cases} \rho^f(\bar{\bar{\mathbf{u}}},\mathbf{v})_{\Omega^f_{t_n}} & +\Delta t\ \rho^f[c(\bar{\bar{\mathbf{u}}},\tilde{\mathbf{u}},\mathbf{v})_{\Omega^f_{t_n}} + c(\tilde{\mathbf{u}},\bar{\bar{\mathbf{u}}},\mathbf{v})_{\Omega^f_{t_n}} + \frac{1}{2}((\bar{\bar{\mathbf{u}}}\cdot\mathbf{n}_f)\tilde{\mathbf{u}},\mathbf{v})_{\Gamma^f_N} \\ & +\frac{1}{2}((\tilde{\mathbf{u}}\cdot\mathbf{n}_f)\bar{\bar{\mathbf{u}}},\mathbf{v})_{\Gamma^f_N} - \frac{1}{2}((\nabla\cdot\mathbf{z}^n)\bar{\bar{\mathbf{u}}},\mathbf{v})_{\Omega^f_{t_n}} \\ & -c(\mathbf{z}^n,\bar{\bar{\mathbf{u}}},\mathbf{v})] + \Delta t\ 2\nu_f a(\bar{\bar{\mathbf{u}}},\mathbf{v})_{\Omega^f_{t_n}} + \Delta t\ b(\mathbf{v},\bar{\bar{p}})_{\Omega^f_{t_n}} \\ & = \Delta t\ \rho^f\Big[c(\bar{\mathbf{u}}_1,\bar{\mathbf{u}}_2,\mathbf{v})_{\Omega^f_{t_n}} + c(\bar{\mathbf{u}}_2,\bar{\mathbf{u}}_1,\mathbf{v})_{\Omega^f_{t_n}} \\ & \quad +\frac{1}{2}((\bar{\mathbf{u}}_1\cdot\mathbf{n}_f)\bar{\mathbf{u}}_2,\mathbf{v})_{\Gamma^f_N} + \frac{1}{2}((\bar{\mathbf{u}}_2\cdot\mathbf{n}_f)\bar{\mathbf{u}}_1,\mathbf{v})_{\Gamma^f_N}\Big] \quad \forall\mathbf{v}\in\boldsymbol{H}^1_D(\Omega^f_{t_n}), \\ b(\bar{\bar{\mathbf{u}}},q)_{\Omega^f_{t_n}} & = 0 \quad q\in L^2(\Omega^f_{t_n}), \end{cases} \tag{5.60}$$

and the second variation $(\bar{\bar{\boldsymbol{\eta}}},\bar{\bar{\dot{\boldsymbol{\eta}}}})$ is a solution of

$$\begin{cases} \rho^s(\bar{\bar{\dot{\boldsymbol{\eta}}}},\boldsymbol{\xi})_{\Omega^s} + \Delta t\ \nu_s d(\bar{\bar{\boldsymbol{\eta}}},\boldsymbol{\xi})_{\Omega^s} + \frac{\Delta t}{2}\ \lambda e(\bar{\bar{\boldsymbol{\eta}}},\boldsymbol{\xi})_{\Omega^s} = 0 \quad \forall\boldsymbol{\xi}\in\boldsymbol{H}^1_D(\Omega^s), \\ \frac{\Delta t}{2}(\bar{\bar{\dot{\boldsymbol{\eta}}}},\boldsymbol{\gamma})_{\Omega^s} - (\bar{\bar{\boldsymbol{\eta}}},\boldsymbol{\gamma})_{\Omega^s} = 0 \quad \forall\boldsymbol{\gamma}\in\boldsymbol{H}^1_D(\Omega^s). \end{cases} \tag{5.61}$$

Using Theorems 4.18–4.31 and making the same assumptions,

$$\|\tilde{\mathbf{u}}\|_{0,\Omega^f_{t_n}} \le C_{14}(\|\tilde{\mathbf{g}}^n\|_{0,\Gamma_{I_{t_n}}} + K_1), \tag{5.62}$$

$$\|\tilde{\mathbf{u}}\|_{1,\Omega^f_{t_n}} \le \Delta t^{-\frac{1}{2}} C_{14}(\|\tilde{\mathbf{g}}^n\|_{0,\Gamma_{I_{t_n}}} + K_1), \tag{5.63}$$

$$\|\tilde{\boldsymbol{\eta}}\|_{1,\Omega^s} \le C_{15}(\|\tilde{\mathbf{g}}^n\|_{0,\Gamma_{I_{t_n}}} + K_2), \tag{5.64}$$

$$\|\bar{\mathbf{u}}_i\|_{0,\Omega^f_{t_n}} \le \Delta t^{\frac{1}{2}} C_{16}\,\|\bar{\mathbf{g}}_i\|_{0,\Gamma_{I_{t_n}}} \quad for\ i=1,2, \tag{5.65}$$

$$\|\bar{\mathbf{u}}_i\|_{1,\Omega^f_{t_n}} \le C_{16}\,\|\bar{\mathbf{g}}_i\|_{0,\Gamma_{I_{t_n}}} \quad for\ i=1,2, \tag{5.66}$$

$$\|\bar{\boldsymbol{\eta}}_i\|_{1,\Omega^s} \le C_{17}\,\|\bar{\mathbf{g}}_i\|_{0,\Gamma_{I_{t_n}}} \quad for\ i=1,2, \tag{5.67}$$

and

$$\left\|\frac{\tilde{\boldsymbol{\eta}}-\boldsymbol{\eta}^{n-1}}{\Delta t}\right\|_{0,\Omega^s} \le \left\|\frac{\tilde{\dot{\boldsymbol{\eta}}}+\dot{\boldsymbol{\eta}}^{n-1}}{2}\right\|_{0,\Omega^s} \le C_{18}(\|\tilde{\mathbf{g}}^n\|_{0,\Gamma_{I_{t_n}}} + K_3). \tag{5.68}$$

For ease of notation, all trial and test functions that follow should be considered as

discrete finite element approximations. Use will be made of the inverse inequality, which requires a discrete setting.

Using the trace theorem and (5.68), we can now bound

$$
\begin{aligned}
&|D^2\mathcal{M}(\tilde{\mathbf{u}}^n(\tilde{\mathbf{g}}^n),\tilde{\boldsymbol{\eta}}^n(\tilde{\mathbf{g}}^n),\tilde{\mathbf{g}}^n)\cdot(\bar{\mathbf{g}}_1,\bar{\mathbf{g}}_2)| \leq \\
&\quad\Bigg[\delta\left\|\bar{\mathbf{g}}_1\right\|_{0,\Gamma_{I_{t_n}}}\left\|\bar{\mathbf{g}}_2\right\|_{0,\Gamma_{I_{t_n}}}+C_{19}^2\left\|\bar{\mathbf{u}}_1\right\|_{0,\Omega_{t_n}^f}^{\frac{1}{2}}\left\|\bar{\mathbf{u}}_1\right\|_{1,\Omega_{t_n}^f}^{\frac{1}{2}}\left\|\bar{\mathbf{u}}_2\right\|_{0,\Omega_{t_n}^f}^{\frac{1}{2}}\left\|\bar{\mathbf{u}}_2\right\|_{1,\Omega_{t_n}^f}^{\frac{1}{2}} \\
&\quad+C_{19}C_{20}\left\|\bar{\mathbf{u}}_1\right\|_{0,\Omega_{t_n}^f}^{\frac{1}{2}}\left\|\bar{\mathbf{u}}_1\right\|_{1,\Omega_{t_n}^f}^{\frac{1}{2}}\left\|\frac{\bar{\boldsymbol{\eta}}_2}{\Delta t}\right\|_{1,\Omega^s}+C_{19}C_{20}\left\|\bar{\mathbf{u}}_2\right\|_{0,\Omega_{t_n}^f}^{\frac{1}{2}}\left\|\bar{\mathbf{u}}_2\right\|_{1,\Omega_{t_n}^f}^{\frac{1}{2}}\left\|\frac{\bar{\boldsymbol{\eta}}_1}{\Delta t}\right\|_{1,\Omega^s}+C_{20}^2\left\|\frac{\bar{\boldsymbol{\eta}}_1}{\Delta t}\right\|_{1,\Omega^s}\left\|\frac{\bar{\boldsymbol{\eta}}_2}{\Delta t}\right\|_{1,\Omega^s} \\
&\quad+\left\|\bar{\tilde{\mathbf{u}}}\right\|_{0,\Omega_{t_n}^f}^{\frac{1}{2}}\left\|\bar{\tilde{\mathbf{u}}}\right\|_{1,\Omega_{t_n}^f}^{\frac{1}{2}}\Bigg[C_{19}^2\left\|\tilde{\mathbf{u}}\right\|_{0,\Omega_{t_n}^f}^{\frac{1}{2}}\left\|\tilde{\mathbf{u}}\right\|_{1,\Omega_{t_n}^f}^{\frac{1}{2}}+C_{19}C_{21}\left\|\frac{\tilde{\dot{\boldsymbol{\eta}}}+\dot{\boldsymbol{\eta}}^{n-1}}{2}\right\|_{0,\Omega^s}^{\frac{1}{2}}\left\|\frac{\tilde{\boldsymbol{\eta}}-\boldsymbol{\eta}^{n-1}}{\Delta t}\right\|_{1,\Omega^s}^{\frac{1}{2}}\Bigg]\Bigg]
\end{aligned}
$$

and

$$
\begin{aligned}
&|D^2\mathcal{M}(\tilde{\mathbf{u}}^n(\tilde{\mathbf{g}}^n),\tilde{\boldsymbol{\eta}}^n(\tilde{\mathbf{g}}^n),\tilde{\mathbf{g}}^n)\cdot(\bar{\mathbf{g}}_1,\bar{\mathbf{g}}_1)| \geq \\
&\quad\left[\delta\left\|\bar{\mathbf{g}}_1\right\|_{0,\Gamma_{I_{t_n}}}^2-\left\|\bar{\tilde{\mathbf{u}}}\right\|_{0,\Omega_{t_n}^f}^{\frac{1}{2}}\left\|\bar{\tilde{\mathbf{u}}}\right\|_{1,\Omega_{t_n}^f}^{\frac{1}{2}}\left[C_{19}^2\left\|\tilde{\mathbf{u}}\right\|_{0,\Omega_{t_n}^f}^{\frac{1}{2}}\left\|\tilde{\mathbf{u}}\right\|_{1,\Omega_{t_n}^f}^{\frac{1}{2}}+C_{19}C_{21}\left\|\frac{\tilde{\dot{\boldsymbol{\eta}}}+\dot{\boldsymbol{\eta}}^{n-1}}{2}\right\|_{0,\Omega^s}^{\frac{1}{2}}\left\|\frac{\tilde{\boldsymbol{\eta}}-\boldsymbol{\eta}^{n-1}}{\Delta t}\right\|_{1,\Omega^s}^{\frac{1}{2}}\right]\right],
\end{aligned}
$$

where C_{19}, C_{20}, and C_{21} are positive domain dependent constants which come from the trace theorem and Poincaré–Friedrich's inequality. Note that $\|\bar{\bar{\boldsymbol{\eta}}}\|_{0,\Gamma_{I_{t_n}}}=0$ by considering (5.61) with $\boldsymbol{\xi}=\bar{\bar{\dot{\boldsymbol{\eta}}}}$ and $\boldsymbol{\gamma}=\bar{\bar{\boldsymbol{\eta}}}$; this is why these terms do not appear in the inequality.

Substituting in (5.62)–(5.68) and using that $\left\|\boldsymbol{\eta}^{n-1}\right\|_{1,\Omega^s}\leq C_{22}$,

$$
\begin{aligned}
&|D^2\mathcal{M}(\tilde{\mathbf{u}}^n(\tilde{\mathbf{g}}^n),\tilde{\boldsymbol{\eta}}^n(\tilde{\mathbf{g}}^n),\tilde{\mathbf{g}}^n)\cdot(\bar{\mathbf{g}}_1,\bar{\mathbf{g}}_2)| \leq \\
&\qquad\Bigg[\Bigg[\delta+C_{16}^2C_{19}^2\Delta t^{\frac{1}{2}}+\frac{2\Delta t^{\frac{1}{4}}}{\Delta t}C_{16}C_{17}C_{19}C_{20}+\frac{1}{\Delta t^2}C_{17}^2C_{20}^2\Bigg]\left\|\bar{\mathbf{g}}_1\right\|_{0,\Gamma_{I_{t_n}}}\left\|\bar{\mathbf{g}}_2\right\|_{0,\Gamma_{I_{t_n}}} \\
&\qquad+\left\|\bar{\tilde{\mathbf{u}}}\right\|_{0,\Omega_{t_n}^f}^{\frac{1}{2}}\left\|\bar{\tilde{\mathbf{u}}}\right\|_{1,\Omega_{t_n}^f}^{\frac{1}{2}}\Big[\Delta t^{-\frac{1}{4}}C_{14}C_{19}^2(\|\tilde{\mathbf{g}}^n\|_{0,\Gamma_{I_{t_n}}}+K_1) \\
&\qquad+\Delta t^{-\frac{1}{2}}C_{19}C_{21}\Big[C_{18}(\|\tilde{\mathbf{g}}^n\|_{0,\Gamma_{I_{t_n}}}+K_3)(C_{15}(\|\tilde{\mathbf{g}}^n\|_{0,\Gamma_{I_{t_n}}}+K_2)+C_{22})\Big]^{\frac{1}{2}}\Big]\Bigg]
\end{aligned}
\tag{5.69}
$$

and

$$
\begin{aligned}
|D^2\mathcal{M}(\tilde{\mathbf{u}}^n(\tilde{\mathbf{g}}^n),\tilde{\boldsymbol{\eta}}^n(\tilde{\mathbf{g}}^n),\tilde{\mathbf{g}}^n)\cdot(\bar{\mathbf{g}}_1,\bar{\mathbf{g}}_1)| \geq &\Bigg[\delta\left\|\bar{\mathbf{g}}_1\right\|_{0,\Gamma_{I_{t_n}}}^2-\left\|\bar{\tilde{\mathbf{u}}}\right\|_{0,\Omega_{t_n}^f}^{\frac{1}{2}}\left\|\bar{\tilde{\mathbf{u}}}\right\|_{1,\Omega_{t_n}^f}^{\frac{1}{2}}\Big[\Delta t^{-\frac{1}{4}}C_{14}C_{19}^2(\|\tilde{\mathbf{g}}^n\|_{0,\Gamma_{I_{t_n}}}+K_1) \\
&+\Delta t^{-\frac{1}{2}}C_{19}C_{21}\Big[C_{18}(\|\tilde{\mathbf{g}}^n\|_{0,\Gamma_{I_{t_n}}}+K_3)(C_{15}(\|\tilde{\mathbf{g}}^n\|_{0,\Gamma_{I_{t_n}}}+K_2)+C_{22})\Big]^{\frac{1}{2}}\Big]\Bigg],
\end{aligned}
\tag{5.70}
$$

where $C_{14},\ldots,C_{17}$ are positive constants described above.

Now, supposing that we can find a bound for $\bar{\tilde{\mathbf{u}}}$ such that

$$\|\bar{\tilde{\mathbf{u}}}\|_{0,\Omega^f_{t_n}}^{\frac{1}{2}} \|\bar{\tilde{\mathbf{u}}}\|_{1,\Omega^f_{t_n}}^{\frac{1}{2}} < \Delta t^k C \|\bar{\mathbf{g}}_1\|_{0,\Gamma_{I_{t_n}}} \|\bar{\mathbf{g}}_2\|_{0,\Gamma_{I_{t_n}}} \text{ and } \|\bar{\tilde{\mathbf{u}}}\|_{0,\Omega^f_{t_n}}^{\frac{1}{2}} \|\bar{\tilde{\mathbf{u}}}\|_{1,\Omega^f_{t_n}}^{k} < \Delta t^{\frac{1}{2}} C \|\bar{\mathbf{g}}_1\|_{0,\Gamma_{I_{t_n}}}^2$$

for $k > \frac{1}{2}$, then we will have that $|D^2\mathcal{M}(\tilde{\mathbf{u}}^n(\tilde{\mathbf{g}}^n), \tilde{\boldsymbol{\eta}}^n(\tilde{\mathbf{g}}^n), \tilde{\mathbf{g}}^n)\cdot(\bar{\mathbf{g}}_1, \bar{\mathbf{g}}_2)| \leq C \|\bar{\mathbf{g}}_1\|_{0,\Gamma_{I_{t_n}}} \|\bar{\mathbf{g}}_2\|_{0,\Gamma_{I_{t_n}}}$ and $|D^2\mathcal{M}(\tilde{\mathbf{u}}^n(\tilde{\mathbf{g}}^n), \tilde{\boldsymbol{\eta}}^n(\tilde{\mathbf{g}}^n), \tilde{\mathbf{g}}^n)\cdot(\bar{\mathbf{g}}_1, \bar{\mathbf{g}}_1)| \geq C \|\bar{\mathbf{g}}_1\|_{0,\Gamma_{I_{t_n}}}^2$ for any choice of $\tilde{\mathbf{g}}^n$ in $\mathbf{L}^2(\Gamma_{I_{t_n}})$ and sufficiently small time step Δt.

Let us consider (5.60) with the choice of test functions $(\mathbf{v}, q) = (\bar{\tilde{\mathbf{u}}}, \bar{\tilde{p}})$ and immediately apply Young's inequality and use that $\mathbf{z}^n \in \mathbf{W}^{1,\infty}$:

$$\begin{aligned}
\|\bar{\tilde{\mathbf{u}}}\|_{0,\Omega^f_{t_n}}^2 \left[\rho^f - \Delta t \frac{\rho^f}{2} \|\nabla \cdot \mathbf{z}^n\|_{\infty,\Omega^f_{t_n}}\right] &+ \Delta t 2 C_{23} \nu_f \|\bar{\tilde{\mathbf{u}}}\|_{1,\Omega^f_{t_n}}^2 \\
&+ \Delta t\, \rho^f [c(\bar{\tilde{\mathbf{u}}}, \tilde{\mathbf{u}}, \bar{\tilde{\mathbf{u}}})_{\Omega^f_{t_n}} + \frac{1}{2}((\bar{\tilde{\mathbf{u}}} \cdot \mathbf{n}_f)\tilde{\mathbf{u}}, \bar{\tilde{\mathbf{u}}}_{\Gamma^f_N} + \frac{1}{2}((\tilde{\mathbf{u}} \cdot \mathbf{n}_f)\bar{\tilde{\mathbf{u}}}, \bar{\tilde{\mathbf{u}}})_{\Gamma^f_N}] \\
= \Delta t\, \rho^f \Big[&c(\bar{\mathbf{u}}_1, \bar{\mathbf{u}}_2, \bar{\tilde{\mathbf{u}}})_{\Omega^f_{t_n}} + c(\bar{\mathbf{u}}_2, \bar{\mathbf{u}}_1, \bar{\tilde{\mathbf{u}}})_{\Omega^f_{t_n}} \\
&+ \frac{1}{2}((\bar{\mathbf{u}}_1 \cdot \mathbf{n}_f)\bar{\mathbf{u}}_2, \bar{\tilde{\mathbf{u}}})_{\Gamma^f_N} + \frac{1}{2}((\bar{\mathbf{u}}_2 \cdot \mathbf{n}_f)\bar{\mathbf{u}}_1, \bar{\tilde{\mathbf{u}}})_{\Gamma^f_N}\Big] \quad \forall \mathbf{v} \in \boldsymbol{H}^1_D(\Omega^f_{t_n}).
\end{aligned}$$

Here, C_{23} is the constant based on Poincaré–Friedrich's inequality which bounds $C_{23} \|\bar{\tilde{\mathbf{u}}}\|_{1,\Omega^f_{t_n}} \leq \|\nabla \bar{\tilde{\mathbf{u}}}\|_{0,\Omega^f_{t_n}}$. For all terms of the form $c(\mathbf{u}, \mathbf{v}, \mathbf{w})_{\Omega^f_{t_n}}$, we can initially bound them from above by

$$\begin{aligned}
c(\mathbf{u}, \mathbf{v}, \mathbf{w})_{\Omega^f_{t_n}} \leq C_{24} \Big[&\|\mathbf{u}\|_{0,\Omega^f_{t_n}}^{\frac{1}{2}} \|\mathbf{u}\|_{1,\Omega^f_{t_n}}^{\frac{1}{2}} \|\mathbf{v}\|_{1,\Omega^f_{t_n}} \|\mathbf{w}\|_{0,\Omega^f_{t_n}}^{\frac{1}{2}} \|\mathbf{w}\|_{1,\Omega^f_{t_n}}^{\frac{1}{2}} \\
&+ \|\mathbf{u}\|_{0,\Omega^f_{t_n}}^{\frac{1}{2}} \|\mathbf{u}\|_{1,\Omega^f_{t_n}}^{\frac{1}{2}} \|\mathbf{w}\|_{1,\Omega^f_{t_n}} \|\mathbf{v}\|_{0,\Omega^f_{t_n}}^{\frac{1}{2}} \|\mathbf{v}\|_{1,\Omega^f_{t_n}}^{\frac{1}{2}} \Big].
\end{aligned} \tag{5.71}$$

On the left hand side of the inequality, using Holder's inequality with p=4, q=4, and r=2, the Sobolev imbedding of $\mathbf{W}^{\frac{1}{2},2}(\Gamma^f_N) \subset \mathbf{W}^{0,4}(\Gamma^f_N)$, and the trace theorem, we bound

$$((\bar{\tilde{\mathbf{u}}} \cdot \mathbf{n}_f)\tilde{\mathbf{u}}, \bar{\tilde{\mathbf{u}}})_{\Gamma^f_N} \leq C_{25} \|\bar{\tilde{\mathbf{u}}}\|_{0,\Omega^f_{t_n}}^{\frac{1}{2}} \|\bar{\tilde{\mathbf{u}}}\|_{1,\Omega^f_{t_n}}^{\frac{3}{2}} \|\tilde{\mathbf{u}}\|_{1,\Omega^f_{t_n}} \tag{5.72}$$

Additionally, noting that

$$c(\bar{\bar{\mathbf{u}}},\tilde{\mathbf{u}},\bar{\bar{\mathbf{u}}})_{\Omega^f_{t_n}} \leq C_{24}\left[\|\bar{\bar{\mathbf{u}}}\|_{0,\Omega^f_{t_n}}\|\tilde{\mathbf{u}}\|_{1,\Omega^f_{t_n}}\|\bar{\bar{\mathbf{u}}}\|_{1,\Omega^f_{t_n}} + \|\bar{\bar{\mathbf{u}}}\|^{\frac{1}{2}}_{0,\Omega^f_{t_n}}\|\tilde{\mathbf{u}}\|_{1,\Omega^f_{t_n}}\|\bar{\bar{\mathbf{u}}}\|^{\frac{3}{2}}_{1,\Omega^f_{t_n}}\right],$$
we can see that all trilinear terms on the left hand side of the inequality can be bounded above by

$$\begin{aligned}
&\Delta t\rho^f[c(\bar{\bar{\mathbf{u}}},\tilde{\mathbf{u}},\bar{\bar{\mathbf{u}}})_{\Omega^f_{t_n}} + \frac{1}{2}((\bar{\bar{\mathbf{u}}}\cdot\mathbf{n}_f)\tilde{\mathbf{u}},\bar{\bar{\mathbf{u}}})_{\Gamma^f_N} + \frac{1}{2}((\tilde{\mathbf{u}}\cdot\mathbf{n}_f)\bar{\bar{\mathbf{u}}},\bar{\bar{\mathbf{u}}})_{\Gamma^f_N}]\\
&\quad\leq \Delta t\rho^f\left[C_{24}\|\bar{\bar{\mathbf{u}}}\|_{0,\Omega^f_{t_n}}\|\bar{\bar{\mathbf{u}}}\|_{1,\Omega^f_{t_n}}\|\tilde{\mathbf{u}}\|_{1,\Omega^f_{t_n}} + (C_{24}+C_{25})\|\bar{\bar{\mathbf{u}}}\|^{\frac{1}{2}}_{0,\Omega^f_{t_n}}\|\bar{\bar{\mathbf{u}}}\|^{\frac{3}{2}}_{1,\Omega^f_{t_n}}\|\tilde{\mathbf{u}}\|_{1,\Omega^f_{t_n}}\right]\\
&\quad\leq \Delta t\left[\frac{(\rho^f C_{24})^2}{2C_{23}\nu_f}\|\tilde{\mathbf{u}}\|^2_{1,\Omega^f_{t_n}}\|\bar{\bar{\mathbf{u}}}\|^2_{0,\Omega^f_{t_n}} + \frac{(\rho^f(C_{24}+C_{25}))^4}{4(\frac{2}{3}C_{23}\nu_f)^3}\|\tilde{\mathbf{u}}\|^4_{1,\Omega^f_{t_n}}\|\bar{\bar{\mathbf{u}}}\|^2_{0,\Omega^f_{t_n}} + C_{23}\nu_f\|\bar{\bar{\mathbf{u}}}\|^2_{1,\Omega^f_{t_n}}\right]
\end{aligned}$$

using Young's inequality with p=2, q=2 and p=4, q=$\frac{4}{3}$, respectively. For the second application of Young's inequality, this also requires multiplying by 1 in the form of $\frac{\left(\frac{\frac{2}{3}C_{23}\nu_f}{\rho^f(C_{24}+C_{25})}\right)^{\frac{3}{4}}}{\left(\frac{\frac{2}{3}C_{23}\nu_f}{\rho^f(C_{24}+C_{25})}\right)^{\frac{3}{4}}}$. Next, we apply the inverse inequality and introduce the constant C_{26} under the assumption that the mesh is quasi-uniform, yielding

$$\begin{aligned}
&\Delta t\rho^f[c(\bar{\bar{\mathbf{u}}},\tilde{\mathbf{u}},\bar{\bar{\mathbf{u}}})_{\Omega^f_{t_n}} + \frac{1}{2}((\bar{\bar{\mathbf{u}}}\cdot\mathbf{n}_f)\tilde{\mathbf{u}},\bar{\bar{\mathbf{u}}})_{\Gamma^f_N} + \frac{1}{2}((\tilde{\mathbf{u}}\cdot\mathbf{n}_f)\bar{\bar{\mathbf{u}}},\bar{\bar{\mathbf{u}}})_{\Gamma^f_N}]\\
&\qquad\leq \Delta t\left[\frac{C^2_{26}h^{-2}(\rho^f C_{24})^2}{2C_{23}\nu_f}\|\tilde{\mathbf{u}}\|^2_{0,\Omega^f_{t_n}}\|\bar{\bar{\mathbf{u}}}\|^2_{0,\Omega^f_{t_n}}\right.\\
&\qquad\quad\left.+\frac{C^4_{26}h^{-4}(\rho^f(C_{24}+C_{25}))^3}{4(\frac{2}{3}C_{23}\nu_f)^3}\|\tilde{\mathbf{u}}\|^4_{0,\Omega^f_{t_n}}\|\bar{\bar{\mathbf{u}}}\|^2_{0,\Omega^f_{t_n}} + C_{23}\nu_f\|\bar{\bar{\mathbf{u}}}\|^2_{1,\Omega^f_{t_n}}\right].
\end{aligned}$$

For terms on the right hand side of the inequality, again using Holder's inequality with p=4, q=4, and r=2, the Sobolev imbedding of $\mathbf{W}^{\frac{1}{2},2}(\Gamma^f_N)\subset\mathbf{W}^{0,4}(\Gamma^f_N)$, and the trace theorem,

$$\begin{aligned}
&\frac{\Delta t\rho^f}{2}\left[((\bar{\mathbf{u}}_1\cdot\mathbf{n}_f)\bar{\mathbf{u}}_2,\bar{\bar{\mathbf{u}}})_{\Gamma^f_N} + ((\bar{\mathbf{u}}_2\cdot\mathbf{n}_f)\bar{\mathbf{u}}_1,\bar{\bar{\mathbf{u}}})_{\Gamma^f_N}\right]\\
&\qquad\qquad\leq \Delta t\rho^f C_{25}\|\bar{\mathbf{u}}_1\|_{1,\Omega^f_{t_n}}\|\bar{\mathbf{u}}_2\|_{1,\Omega^f_{t_n}}\|\bar{\bar{\mathbf{u}}}\|^{\frac{1}{2}}_{0,\Omega^f_{t_n}}\|\bar{\bar{\mathbf{u}}}\|^{\frac{1}{2}}_{1,\Omega^f_{t_n}}.
\end{aligned}$$

We apply Young's inequality with $p = \frac{4}{3}$ and $q = 4$, after multiplying by $\frac{\left(\frac{C_{23}\nu_f}{C_{25}\rho^f}\right)^{\frac{1}{4}}}{\left(\frac{C_{23}\nu_f}{C_{25}\rho^f}\right)^{\frac{1}{4}}}$, to get

$$\frac{\Delta t\rho^f}{2}\left[((\bar{\mathbf{u}}_1\cdot\mathbf{n}_f)\bar{\mathbf{u}}_2,\bar{\bar{\mathbf{u}}})_{\Gamma_N^f}+((\bar{\mathbf{u}}_2\cdot\mathbf{n}_f)\bar{\mathbf{u}}_1,\bar{\bar{\mathbf{u}}})_{\Gamma_N^f}\right]\leq\Delta t\frac{C_{23}\nu_f}{4}\left\|\bar{\bar{\mathbf{u}}}\right\|^2_{1,\Omega^f_{t_n}}$$
$$+\Delta t\frac{3(C_{25}\rho^f)^{\frac{4}{3}}}{4(C_{23}\nu_f)^{\frac{1}{3}}}\left\|\bar{\mathbf{u}}_1\right\|^{\frac{4}{3}}_{0,\Omega^f_{t_n}}\left\|\bar{\mathbf{u}}_2\right\|^{\frac{4}{3}}_{1,\Omega^f_{t_n}}\left\|\bar{\bar{\mathbf{u}}}\right\|^{\frac{2}{3}}_{0,\Omega^f_{t_n}}.$$

Now, we apply Young's inequality again with $p = \frac{3}{2}$ and $q = 3$, and multiply by unity in the form of $\frac{\Delta t^{\frac{1}{6}}}{\Delta t^{\frac{1}{6}}}$,

$$\frac{\Delta t\rho^f}{2}\left[((\bar{\mathbf{u}}_1\cdot\mathbf{n}_f)\bar{\mathbf{u}}_2,\bar{\bar{\mathbf{u}}})_{\Gamma_N^f}+((\bar{\mathbf{u}}_2\cdot\mathbf{n}_f)\bar{\mathbf{u}}_1,\bar{\bar{\mathbf{u}}})_{\Gamma_N^f}\right]\leq\Delta t\frac{C_{23}\nu_f}{4}\left\|\bar{\bar{\mathbf{u}}}\right\|^2_{1,\Omega^f_{t_n}}$$
$$+\Delta t\frac{3(C_{25}\rho^f)^{\frac{4}{3}}}{4(C_{23}\nu_f)^{\frac{1}{3}}}\left[\frac{\Delta t^{-\frac{1}{2}}}{3}\left\|\bar{\bar{\mathbf{u}}}\right\|^2_{0,\Omega^f_{t_n}}+\frac{2\Delta t^{\frac{1}{4}}}{3}\left\|\bar{\mathbf{u}}_1\right\|^2_{1,\Omega^f_{t_n}}\left\|\bar{\mathbf{u}}_2\right\|^2_{1,\Omega^f_{t_n}}\right].$$

Next we apply the inverse inequality, using $\left\|\bar{\mathbf{u}}_1\right\|_{1,\Omega^f_{t_n}}\leq C_{27}h^{-1}\left\|\bar{\mathbf{u}}_1\right\|_{0,\Omega^f_{t_n}}$, where C_{27} is the inverse inequality constant, to get

$$\frac{\Delta t\rho^f}{2}\left[((\bar{\mathbf{u}}_1\cdot\mathbf{n}_f)\bar{\mathbf{u}}_2,\bar{\bar{\mathbf{u}}})_{\Gamma_N^f}+((\bar{\mathbf{u}}_2\cdot\mathbf{n}_f)\bar{\mathbf{u}}_1,\bar{\bar{\mathbf{u}}})_{\Gamma_N^f}\right]\leq\Delta t\frac{C_{23}\nu_f}{4}\left\|\bar{\bar{\mathbf{u}}}\right\|^2_{1,\Omega^f_{t_n}}$$
$$+\Delta t\frac{(C_{25}\rho^f)^{\frac{4}{3}}}{4(C_{23}\nu_f)^{\frac{1}{3}}}\left[\Delta t^{-\frac{1}{2}}\left\|\bar{\bar{\mathbf{u}}}\right\|^2_{0,\Omega^f_{t_n}}+2C_{27}h^{-1}\Delta t^{\frac{1}{4}}\left\|\bar{\mathbf{u}}_1\right\|_{0,\Omega^f_{t_n}}\left\|\bar{\mathbf{u}}_1\right\|_{1,\Omega^f_{t_n}}\left\|\bar{\mathbf{u}}_2\right\|^2_{1,\Omega^f_{t_n}}\right].$$

Since $\Omega^f_{t_n}\in\mathbb{R}^2$, as in (5.71), we have that

$$\Delta t\rho^f c(\bar{\mathbf{u}}_i,\bar{\mathbf{u}}_j,\bar{\bar{\mathbf{u}}})_{\Omega^f_{t_n}}\leq\Delta t\rho^f C_{24}\left[\left\|\bar{\mathbf{u}}_i\right\|^{\frac{1}{2}}_{0,\Omega^f_{t_n}}\left\|\bar{\mathbf{u}}_i\right\|^{\frac{1}{2}}_{1,\Omega^f_{t_n}}\left\|\bar{\mathbf{u}}_j\right\|_{1,\Omega^f_{t_n}}\left\|\bar{\bar{\mathbf{u}}}\right\|^{\frac{1}{2}}_{0,\Omega^f_{t_n}}\left\|\bar{\bar{\mathbf{u}}}\right\|^{\frac{1}{2}}_{1,\Omega^f_{t_n}}\right.$$
$$\left.+\left\|\bar{\mathbf{u}}_i\right\|^{\frac{1}{2}}_{0,\Omega^f_{t_n}}\left\|\bar{\mathbf{u}}_i\right\|^{\frac{1}{2}}_{1,\Omega^f_{t_n}}\left\|\bar{\bar{\mathbf{u}}}\right\|_{1,\Omega^f_{t_n}}\left\|\bar{\mathbf{u}}_j\right\|^{\frac{1}{2}}_{0,\Omega^f_{t_n}}\left\|\bar{\mathbf{u}}_j\right\|^{\frac{1}{2}}_{1,\Omega^f_{t_n}}\right].$$

Next, for the first term we multiply by unity in the form of $\frac{\left(\frac{C_{23}\nu_f}{2C_{24}\rho^f}\right)^{\frac{1}{4}}}{\left(\frac{C_{23}\nu_f}{2C_{24}\rho^f}\right)^{\frac{1}{4}}}$ and apply Young's inequality with $p = \frac{4}{3}$ and $q = 4$, while for the second term we multiply by unity in the

form of $\frac{\left(\frac{C_{23}\nu_f}{4C_{24}\rho^f}\right)^{\frac{1}{2}}}{\left(\frac{C_{23}\nu_f}{4C_{24}\rho^f}\right)^{\frac{1}{2}}}$ and then apply Young's inequality with $p=2$ and $q=2$:

$$\begin{aligned}\Delta t\rho^f c(\bar{\mathbf{u}}_i,\bar{\mathbf{u}}_j,\bar{\bar{\mathbf{u}}})_{\Omega^f_{t_n}} \leq \\ \Delta t\left[\frac{3(C_{24}\rho^f)^{\frac{4}{3}}}{4(\frac{1}{2}C_{23}\nu_f)^{\frac{1}{3}}}\left\|\bar{\mathbf{u}}_i\right\|^{\frac{2}{3}}_{0,\Omega^f_{t_n}}\left\|\bar{\mathbf{u}}_i\right\|^{\frac{2}{3}}_{1,\Omega^f_{t_n}}\left\|\bar{\mathbf{u}}_j\right\|^{\frac{4}{3}}_{1,\Omega^f_{t_n}}\left\|\bar{\bar{\mathbf{u}}}\right\|^{\frac{2}{3}}_{0,\Omega^f_{t_n}}+\frac{C_{23}\nu_f}{8}\left\|\bar{\bar{\mathbf{u}}}\right\|^2_{1,\Omega^f_{t_n}}\right. \\ \left.+\frac{2(C_{24}\rho^f)^2}{C_{23}\nu_f}\left\|\bar{\mathbf{u}}_i\right\|_{0,\Omega^f_{t_n}}\left\|\bar{\mathbf{u}}_i\right\|_{1,\Omega^f_{t_n}}\left\|\bar{\mathbf{u}}_j\right\|_{0,\Omega^f_{t_n}}\left\|\bar{\mathbf{u}}_j\right\|_{1,\Omega^f_{t_n}}+\frac{C_{23}\nu_f}{8}\left\|\bar{\bar{\mathbf{u}}}\right\|^2_{1,\Omega^f_{t_n}}\right].\end{aligned}$$

Again we must apply Young's inequality with $p=\frac{3}{2}$ and $q=3$, multiplying by 1 in the form of $\frac{\Delta t^{\frac{1}{6}}}{\Delta t^{\frac{1}{6}}}$, to get

$$\begin{aligned}\Delta t\rho^f c(\bar{\mathbf{u}}_i,\bar{\mathbf{u}}_j,\bar{\bar{\mathbf{u}}})_{\Omega^f_{t_n}} \leq \\ \Delta t\left[\frac{(C_{24}\rho^f)^{\frac{4}{3}}}{4(\frac{1}{2}C_{23}\nu_f)^{\frac{1}{3}}}\left[2\Delta t^{\frac{1}{4}}\left\|\bar{\mathbf{u}}_i\right\|_{0,\Omega^f_{t_n}}\left\|\bar{\mathbf{u}}_i\right\|_{1,\Omega^f_{t_n}}\left\|\bar{\mathbf{u}}_j\right\|^2_{1,\Omega^f_{t_n}}+\Delta t^{-\frac{1}{2}}\left\|\bar{\bar{\mathbf{u}}}\right\|^2_{0,\Omega^f_{t_n}}\right]\right. \\ \left.+\frac{2(C_{24}\rho^f)^2}{C_{23}\nu_f}\left\|\bar{\mathbf{u}}_i\right\|_{0,\Omega^f_{t_n}}\left\|\bar{\mathbf{u}}_i\right\|_{1,\Omega^f_{t_n}}\left\|\bar{\mathbf{u}}_j\right\|_{0,\Omega^f_{t_n}}\left\|\bar{\mathbf{u}}_j\right\|_{1,\Omega^f_{t_n}}+\frac{C_{23}\nu_f}{4}\left\|\bar{\bar{\mathbf{u}}}\right\|^2_{1,\Omega^f_{t_n}}\right].\end{aligned}$$

Substituting in the inequalities for terms on the left hand side,

$$\begin{aligned}\left\|\bar{\bar{\mathbf{u}}}\right\|^2_{0,\Omega^f_{t_n}}\left[\rho^f-\Delta t\frac{\rho^f}{2}\left\|\nabla\cdot\mathbf{z}^n\right\|_{\infty,\Omega^f_{t_n}}-\frac{\Delta t}{h^2}\frac{C_{26}^2(\rho^f C_{24})^2}{2C_{23}\nu_f}\left\|\tilde{\mathbf{u}}\right\|^2_{0,\Omega^f_{t_n}}\right. \\ \left.-\frac{\Delta t}{h^4}\frac{C_{26}^4(\rho^f(C_{24}+C_{25}))^3}{4(\frac{2}{3}C_{23}\nu_f)^3}\left\|\tilde{\mathbf{u}}\right\|^4_{0,\Omega^f_{t_n}}\right]+\Delta t C_{23}\nu_f\left\|\bar{\bar{\mathbf{u}}}\right\|^2_{1,\Omega^f_{t_n}} \\ \leq \Delta t\ \rho^f\left[c(\bar{\mathbf{u}}_1,\bar{\mathbf{u}}_2,\bar{\bar{\mathbf{u}}})_{\Omega^f_{t_n}}+c(\bar{\mathbf{u}}_2,\bar{\mathbf{u}}_1,\bar{\bar{\mathbf{u}}})_{\Omega^f_{t_n}}\right. \\ \left.+\frac{1}{2}((\bar{\mathbf{u}}_1\cdot\mathbf{n}_f)\bar{\mathbf{u}}_2,\bar{\bar{\mathbf{u}}})_{\Gamma^f_N}+\frac{1}{2}((\bar{\mathbf{u}}_2\cdot\mathbf{n}_f)\bar{\mathbf{u}}_1,\bar{\bar{\mathbf{u}}})_{\Gamma^f_N}\right].\end{aligned}$$

Next, we make a substitution for terms on the right hand side,

$$\begin{aligned}
\|\bar{\tilde{\mathbf{u}}}\|^2_{0,\Omega^f_{t_n}} \Bigg[& \rho^f - \Delta t \frac{\rho^f}{2} \|\nabla \cdot \mathbf{z}^n\|_{\infty,\Omega^f_{t_n}} - \frac{\Delta t}{h^2} \frac{C_{26}^2 (\rho^f C_{24})^2}{2 C_{23} \nu_f} \|\tilde{\mathbf{u}}\|^2_{0,\Omega^f_{t_n}} \\
& - \frac{\Delta t}{h^4} \frac{C_{26}^4 (\rho^f (C_{24} + C_{25}))^3}{4 (\frac{2}{3} C_{23} \nu_f)^3} \|\tilde{\mathbf{u}}\|^4_{0,\Omega^f_{t_n}} - \Delta t^{\frac{1}{2}} \frac{(C_{24} \rho^f)^{\frac{4}{3}}}{2 (\frac{1}{2} C_{23} \nu_f)^{\frac{1}{3}}} - \Delta t^{\frac{1}{2}} \frac{(C_{25} \rho^f)^{\frac{4}{3}}}{4 (C_{23} \nu_f)^{\frac{1}{3}}} \Bigg] \\
& + \Delta t \frac{C_{23} \nu_f}{4} \|\bar{\tilde{\mathbf{u}}}\|^2_{1,\Omega^f_{t_n}} \\
& \leq \frac{\Delta t^{\frac{5}{4}}}{h} \frac{C_{27} (C_{25} \rho^f)^{\frac{4}{3}}}{2 (C_{23} \nu_f)^{\frac{1}{3}}} \|\bar{\mathbf{u}}_1\|_{0,\Omega^f_{t_n}} \|\bar{\mathbf{u}}_1\|_{1,\Omega^f_{t_n}} \|\bar{\mathbf{u}}_2\|^2_{1,\Omega^f_{t_n}} \\
& \quad + \sum_{i,j=1, i \neq j}^{2} \Bigg[\Delta t^{\frac{5}{4}} \frac{(C_{24} \rho^f)^{\frac{4}{3}}}{2 (\frac{1}{2} C_{23} \nu_f)^{\frac{1}{3}}} \|\bar{\mathbf{u}}_i\|_{0,\Omega^f_{t_n}} \|\bar{\mathbf{u}}_i\|_{1,\Omega^f_{t_n}} \|\bar{\mathbf{u}}_j\|^2_{1,\Omega^f_{t_n}} \\
& \qquad + \Delta t \frac{2 (C_{24} \rho^f)^2}{C_{23} \nu_f} \|\bar{\mathbf{u}}_i\|_{0,\Omega^f_{t_n}} \|\bar{\mathbf{u}}_i\|_{1,\Omega^f_{t_n}} \|\bar{\mathbf{u}}_j\|_{0,\Omega^f_{t_n}} \|\bar{\mathbf{u}}_j\|_{1,\Omega^f_{t_n}} \Bigg]
\end{aligned}$$

Finally, substituting in (5.62)–(5.63) and (5.65)–(5.66), we have

$$\begin{aligned}
\|\bar{\tilde{\mathbf{u}}}\|^2_{0,\Omega^f_{t_n}} \Bigg[& \rho^f - \Delta t \frac{\rho^f}{2} \|\nabla \cdot \mathbf{z}^n\|_{\infty,\Omega^f_{t_n}} - \frac{\Delta t}{h^2} \frac{C_{26}^2 (\rho^f C_{24})^2}{2 C_{23} \nu_f} C_{14}^2 (\|\tilde{\mathbf{g}}^n\|_{0,\Gamma_{I_{t_n}}} + K_1)^2 \\
& - \frac{\Delta t}{h^4} \frac{C_{26}^4 (\rho^f (C_{24} + C_{25}))^3}{4 (\frac{2}{3} C_{23} \nu_f)^3} C_{14}^4 (\|\tilde{\mathbf{g}}^n\|_{0,\Gamma_{I_{t_n}}} + K_1)^4 \\
& - \Delta t^{\frac{1}{2}} \frac{(C_{24} \rho^f)^{\frac{4}{3}}}{2 (\frac{1}{2} C_{23} \nu_f)^{\frac{1}{3}}} - \Delta t^{\frac{1}{2}} \frac{(C_{25} \rho^f)^{\frac{4}{3}}}{4 (C_{23} \nu_f)^{\frac{1}{3}}} \Bigg] + \Delta t \frac{C_{23} \nu_f}{4} \|\bar{\tilde{\mathbf{u}}}\|^2_{1,\Omega^f_{t_n}} \\
\leq C_{16}^4 \|\bar{\mathbf{g}}_1\|^2_{0,\Gamma_{I_{t_n}}} & \|\bar{\mathbf{g}}_2\|^2_{0,\Gamma_{I_{t_n}}} \left[\frac{\Delta t^{\frac{7}{4}}}{h} \frac{C_{27} (C_{25} \rho^f)^4}{2 (C_{23} \nu_f)^3} + \Delta t^{\frac{7}{4}} \frac{(C_{24} \rho^f)^{\frac{4}{3}}}{(\frac{1}{2} C_{23} \nu_f)^{\frac{1}{3}}} + \Delta t^2 \frac{4 (C_{24} \rho^f)^2}{C_{23} \nu_f} \right]
\end{aligned}$$

which yields the following inequalities for a sufficiently small Δt:

$$\|\bar{\tilde{\mathbf{u}}}\|^{\frac{1}{2}}_{0,\Omega^f_{t_n}} \leq \frac{C \Delta t^{\frac{7}{16}}}{h^{\frac{1}{4}}} (\|\bar{\mathbf{g}}_1\|_{0,\Gamma_{I_{t_n}}} \|\bar{\mathbf{g}}_2\|_{0,\Gamma_{I_{t_n}}})^{\frac{1}{2}} \tag{5.73}$$

$$\|\bar{\tilde{\mathbf{u}}}\|^{\frac{1}{2}}_{1,\Omega^f_{t_n}} \leq \frac{C \Delta t^{\frac{3}{16}}}{h^{\frac{1}{4}}} (\|\bar{\mathbf{g}}_1\|_{0,\Gamma_{I_{t_n}}} \|\bar{\mathbf{g}}_2\|_{0,\Gamma_{I_{t_n}}})^{\frac{1}{2}}. \tag{5.74}$$

Therefore,

$$\|\bar{\bar{\mathbf{u}}}\|^{\frac{1}{2}}_{0,\Omega^f_{t_n}} \|\bar{\bar{\mathbf{u}}}\|^{\frac{1}{2}}_{1,\Omega^f_{t_n}} \leq \frac{\Delta t^{\frac{5}{8}}}{h^{\frac{1}{2}}} C \tag{5.75}$$

and we have continuity and coercivity of the second Fréchet derivative of the penalized functional if $\Delta t < h^5$ and Δt is sufficiently small.

Let us make the assumption that the ball B from which we make our initial guess has a radius of one. In the context of Theorem 5.3, our $m_a \leq \delta + C\Delta t^{-2}$ and $m_b \geq \delta - C\frac{\Delta t^{\frac{1}{8}}}{h^{\frac{1}{2}}} \geq \delta - Ch^{\frac{1}{8}}$, based on (5.69), (5.70), and (5.75). Therefore, $\max\{2\delta, 2C\Delta t^{-2}\} \geq m_a$, which means that $\frac{2(\delta - Ch^{\frac{1}{8}})}{\max\{4\delta^2, 4C\Delta t^{-4}\}} \leq \frac{2m_b}{m_a^2}$. We consider small values of δ, which in general is the case of interest. Therefore we concern ourselves only with the case $\delta \leq C\Delta t^{-2}$. In the steepest descent algorithm, ω_n has the form $\frac{\alpha_m}{\delta}$. According to Theorem 5.3, the algorithm is guaranteed to converge if $\frac{\alpha_m}{\delta} \leq \frac{2(\delta - Ch^{\frac{1}{8}})}{4C\Delta t^{-4}}$, which implies that $\alpha_m \leq \Delta t^4 \frac{\delta^2 - C\delta h^{\frac{1}{8}}}{2C}$ is a sufficient condition for convergence if h is small enough and the initial guess is close enough to the optimal solution.

□

5.6 Numerical Results

For an FSI problem which was presented by Astorino and Grandmont in [3], we will perform computations and give rates of convergence to the true solution over a single time step. However, we use the Navier–Stokes operator for the fluid rather than the Stokes operator. As in [3], we make the assumption of infinitesimal displacement of the structure and also of the fluid domain, but with nonnegligible velocity of the interface. The densities of the fluid and structure are similar, which adds the complication of having the added mass effect [21, 34].

All terms including $\mathbf{z}$ will be dropped since $\mathbf{z} = 0$ and $\nabla \cdot \mathbf{z} = 0$ in the Eulerian framework. This also means that the control will not be able to absorb the $\frac{1}{2}(((\mathbf{u}^n - \mathbf{z}^n) \cdot \mathbf{n}_f) \cdot \mathbf{u}^n, \mathbf{v})_{\Gamma_{I_{t_n}}}$ term and so the term $\frac{1}{2}((\mathbf{u}^n \cdot \mathbf{n}_f) \cdot \mathbf{u}^n, \mathbf{v})_{\Gamma_{I_{t_n}}}$ will appear in the fluid state equations as well as its respective derivatives in the adjoint equations.

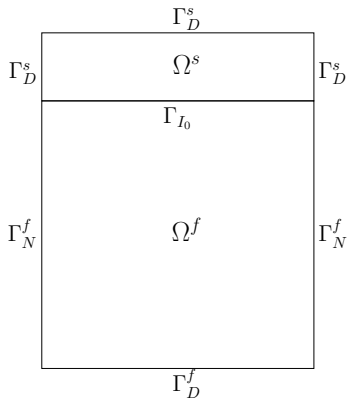

Figure 5.1: Computational domain for a manufactured solution.

Parameters for the problem are: $\rho_f = 1.0$ g/cm^3, $\nu_f = 0.013$ g/cm·s, $\rho_s = 1.9$ g/cm^3, $\nu_s = 3$ dyne/cm^2, and $\lambda = 4.5$ dyne/cm^2. Initial conditions, body forces, and boundary conditions are determined by the analytical solution according to the method of manufactured solutions:

On $\Omega_t^f = \Omega^f = [0,1] \times [0,1]$ and $\Omega^s = [0,1] \times [1,1.25]$ (Fig. 5.1),

$$\begin{aligned}
\mathbf{u}_1 &= \cos(x+t)\sin(y+t) + \sin(x+t)\cos(y+t), \\
\mathbf{u}_2 &= -\sin(x+t)\cos(y+t) - \cos(x+t)\sin(y+t), \\
p &= 2\nu_f(\sin(x+t)\sin(y+t) - \cos(x+t)\cos(y+t)) + 2\nu_s \cos(x+t)\sin(y+t), \\
\boldsymbol{\eta}_1 &= \sin(x+t)\sin(y+t), \\
\boldsymbol{\eta}_2 &= \cos(x+t)\cos(y+t).
\end{aligned} \tag{5.76}$$

We have used a uniform mesh. We fix $\Delta t = 10^{-6}$ s, and begin two simulations; one at $t_0 = 0.5$ s and the other at $t_0 = 0.8$ s. We perform the simulation over one time step in each case. The quadrilateral finite element pair, $(\mathbb{Q}_2, \mathbb{Q}_1)$, were used for solutions on the fluid domain, while $\mathbb{Q}_2$ finite elements were used to approximate the structure displacement and velocity. The FSI problem was repeatedly solved by Algorithm 4.11 using increasingly

fine spatial discretizations so as to see the rate at which the computed result converges upon the true solution (5.76). For Algorithm 4.11, $\delta = 10^{-24}$ and $\epsilon_{tol} = 10^{-10}$. All computations were made using the deal.II finite element library [7,8].

Table 5.1: Fluid velocity and pressure convergence results for a single time step using the steepest descent algorithm at $t = 0.5$ s.

h	$\left\|\mathbf{u}^n - \mathbf{u}^{true}\right\|_{\mathbf{L}^2}$	**Rate**	$\left\|\mathbf{u}^n - \mathbf{u}^{true}\right\|_{\mathbf{H}^1}$	**Rate**	$\left\|p^n - p^{true}\right\|_{\mathbf{L}^2}$	**Rate**
1/9	7.3904e-06	-	6.9480e-04	-	1.0303e-01	-
1/14	1.9413e-06	3.03	2.8502e-04	2.02	1.7667e-02	3.99
1/21	5.7139e-07	3.02	1.2612e-04	2.01	3.5218e-03	3.98
1/31	1.7694e-07	3.01	5.7724e-05	2.01	7.7002e-04	3.90
1/46	5.4076e-08	3.00	2.6185e-05	2.00	1.8383e-04	3.63
1/69	1.6069e-08	2.99	1.1653e-05	2.00	5.4785e-05	2.99

Table 5.2: Structure displacement and velocity convergence results for a single time step using the steepest descent algorithm at $t = 0.5$ s.

h_x	h_y	$\left\|\boldsymbol{\eta}^n - \boldsymbol{\eta}^{true}\right\|_{\mathbf{L}^2}$	Rate	$\left\|\boldsymbol{\eta}^n - \boldsymbol{\eta}^{true}\right\|_{\mathbf{H}^1}$	Rate	$\left\|\dot{\boldsymbol{\eta}}^n - \dot{\boldsymbol{\eta}}^{true}\right\|_{\mathbf{L}^2}$	Rate
1/9	1/36	2.0788e-06	-	1.9662e-04	-	4.3088e-06	-
1/14	1/56	5.4348e-07	3.04	7.9939e-05	2.04	1.1280e-06	3.03
1/21	1/84	1.5936e-07	3.03	3.5198e-05	2.02	3.3140e-07	3.02
1/31	1/124	4.9192e-08	3.02	1.6059e-05	2.01	1.0254e-07	3.01
1/46	1/184	1.4981e-08	3.01	7.2650e-06	2.01	3.1343e-08	3.00
1/69	1/276	4.4235e-09	3.01	3.2205e-06	2.01	9.3337e-09	2.99

It is observed in Tables 5.1–5.4 that we have full theoretical spatial convergence or better upon the true solution, cf. (5.53). Using $(\mathbb{Q}_2, \mathbb{Q}_1)$ for the fluid velocity and pressure, we expect second order convergence in the $\mathbf{H}^1$ norm of the fluid velocity and the L^2 norm of the pressure. With $\mathbb{Q}_2$ elements used for the structure displacement and velocity, we expect second order convergence in the $\mathbf{H}^1$ norm of the structure displacement and the $\mathbf{L}^2$ norm of the structure velocity.

Because we are unable to get an $\mathbf{H}^1$ bound on $\dot{\boldsymbol{\eta}}^n$, we were forced to minimize the

Table 5.3: Fluid velocity and pressure convergence results for a single time step using the steepest descent algorithm at $t = 0.8$ s.

h	$\left\|\mathbf{u}^n - \mathbf{u}^{true}\right\|_{\mathbf{L}^2}$	Rate	$\left\|\mathbf{u}^n - \mathbf{u}^{true}\right\|_{\mathbf{H}^1}$	Rate	$\left\|p^n - p^{true}\right\|_{\mathbf{L}^2}$	Rate
1/9	1.1474e-05	-	1.0856e-03	-	1.4352e-01	-
1/14	3.0366e-06	3.01	4.4687e-04	2.01	2.4530e-02	4.00
1/21	8.9572e-07	3.01	1.9800e-04	2.01	4.8644e-03	3.99
1/31	2.7770e-07	3.01	9.0689e-05	2.00	1.0397e-03	3.96
1/46	8.4869e-08	3.00	4.1143e-05	2.00	2.2699e-04	3.86
1/69	2.5150e-08	3.00	1.8283e-05	2.00	5.4895e-05	3.50

Table 5.4: Structure displacement and velocity convergence results for a single time step using the steepest descent algorithm at $t = 0.8$ s.

h_x	h_y	$\left\|\boldsymbol{\eta}^n - \boldsymbol{\eta}^{true}\right\|_{\mathbf{L}^2}$	Rate	$\left\|\boldsymbol{\eta}^n - \boldsymbol{\eta}^{true}\right\|_{\mathbf{H}^1}$	Rate	$\left\|\dot{\boldsymbol{\eta}}^n - \dot{\boldsymbol{\eta}}^{true}\right\|_{\mathbf{L}^2}$	Rate
1/9	1/36	1.7471e-06	-	1.6544e-04	-	4.8645e-06	-
1/14	1/56	4.5645e-07	3.04	6.7128e-05	2.04	1.2725e-06	3.04
1/21	1/84	1.3370e-07	3.03	2.9516e-05	2.03	3.7381e-07	3.02
1/31	1/124	4.1234e-08	3.02	1.3453e-05	2.02	1.1561e-07	3.01
1/46	1/184	1.2548e-08	3.01	6.0823e-06	2.01	3.5289e-08	3.01
1/69	1/276	3.7029e-09	3.01	2.6949e-06	2.01	1.0464e-08	3.00

functional (5.1) rather than (5.2). Despite not having the analytical support, in Tables 5.5–5.6 we compute the convergence rate using the penalized functional (5.2) and optimizing over all time steps. Here we use the conjugate gradient algorithm, as given in Section 3.5, to find the optimal solution at each time step. It is observed here that there is no loss of accuracy in space or time from using our approach by optimization.

5.7 Conclusion

After recasting the fluid-structure interaction problem into an optimal control problem, the optimality system was derived. The optimality system was then rewritten in terms of a linear and nonlinear operator to which the BRR theory was applied [18]. Finite element spaces were defined, and the existence of a solution to this system was shown along with

Table 5.5: Fluid velocity and pressure convergence results using the conjugate gradient algorithm from $t = 0.5$ to $t = 1.0$ s.

h	Δt	$\|\mathbf{u}^n - \mathbf{u}^{true}\|_{L^\infty(\mathbf{L}^2)}$	Rate	$\|\mathbf{u}^n - \mathbf{u}^{true}\|_{L^2(\mathbf{H}^1)}$	Rate	$\|p^n - p^{true}\|_{\mathbf{L}^2}$	Rate
1/6	1/15	1.1955e-02	-	1.0426e-01	-	8.9887e-03	-
1/9	1/27	2.6513e-03	3.71	3.9199e-02	2.41	3.5714e-03	2.28
1/14	1/53	5.0970e-04	4.07	1.2511e-02	2.82	1.5589e-03	2.04
1/21	1/97	8.6752e-05	4.01	3.5995e-03	2.82	6.4282e-04	2.00
1/31	1/173	2.3133e-05	3.26	1.2054e-03	2.70	2.8616e-04	2.00
1/46	1/312	6.5748e-06	3.23	4.3259e-04	2.63	1.3150e-04	2.00

Table 5.6: Structure displacement and velocity convergence results using the conjugate gradient algorithm from $t = 0.5$ to $t = 1.0$ s.

h_x	h_y	Δt	$\|\boldsymbol{\eta}^n - \boldsymbol{\eta}^{true}\|_{L^2(\mathbf{L}^2)}$	Rate	$\|\boldsymbol{\eta}^n - \boldsymbol{\eta}^{true}\|_{L^2(\mathbf{H}^1)}$	Rate	$\|\dot{\boldsymbol{\eta}}^n - \dot{\boldsymbol{\eta}}^{true}\|_{L^\infty(\mathbf{L}^2)}$	Rate
1/4	1/16	1/16	1.0642e-04	-	1.3550e-03	-	2.5272e-03	-
1/6	1/24	1/28	2.0519e-05	4.06	3.5795e-04	3.28	6.4563e-04	3.37
1/9	1/36	1/54	3.7975e-06	4.16	1.1056e-04	2.90	1.6216e-04	3.41
1/14	1/54	1/106	7.5280e-07	3.68	3.8761e-05	2.38	4.8158e-05	2.76
1/21	1/81	1/194	1.9953e-07	3.27	1.6277e-05	2.14	1.6575e-05	2.63
1/31	1/122	1/346	5.9897e-08	3.08	7.2861e-06	2.06	5.8173e-06	2.68

spatial approximation estimates to the discretized in time, continuous in space, solution.

Next, an algorithm for optimization by steepest descent was outlined along with a proof of convergence of the algorithm. A numerical study was made based on a known analytical solution. It assumed infinitesimal displacement of the fluid domain, with non-negligible velocity on the interface. Full spatial convergence was observed, demonstrating that there was no spatial degradation of the solution over a single time step.

Additional numerical results included show that using a functional lacking proofs of existence for an optimal solution and Lagrange multipliers, full order convergence was observable in both space and time over all simulations for the problem with a known analytical solution.

Chapter 6 extends this work by consider fluid-structure interaction in the case of a Newtonian fluid and a nonlinear elastic solid. This approach by optimization shows great promise of efficiently decoupling highly nonlinear FSI problems.

Part II

Navier-Stokes / Nonlinear St. Venant-Kirchhoff Elasticity

Chapter 6

APPLICATION TO NONLINEAR ELASTICITY

6.1 Introduction

An investigation is made of employing the optimization-based algorithm developed in this thesis to decouple and solve nonlinear nonsteady fluid-structure interaction. The constitutive equation for elasticity coupled with a Newtonian fluid in fluid-structure interaction is modeled here by the St. Venant–Kirchhoff hyperelastic model. Motivation is first given for the advantages of modeling FSI using a nonlinear elastic material. A derivation is next presented for relating the St. Venant–Kirchhoff constitutive equations to the familiar gradient of the elastic displacement field. The equations are transformed to the reference configuration, where appropriate. A linearization of the state equations are given which define the inner optimization problem to be solved as part of the Gauss–Newton iterations presented in Chapter 3.

Several numerical studies have been performed comparing the simulation results using the optimization-based algorithm against an implicit partitioned accelerated Aitken's approach. The first problem this has been applied to is a case of two dimensional FSI with nonlinear elasticity [54]. The second results are from a three dimensional pulsatile flow

through a straight cylinder [19] and they include a record of optimization iterations needed as the cylinder is refined. Using the number of Gauss–Newton and state solves, a study is made of the computational workload relative to a forward solve with a known traction force.

6.2 Nonlinear Elasticity

Remaining consistent with previous notation, let us denote the displacement of the elastic material as $\boldsymbol{\eta}$, and the rest configuration as $\mathbf{X}$. Therefore the physical configuration is $\mathbf{x} = \mathbf{X} + \boldsymbol{\eta}$.

The St. Venant–Kirchhoff model is an improvement over the linear elasticity model for modeling blood flow. The artery and vessel walls are soft tissue, which generally undergo large displacements. Large displacements obviously violate the small displacement assumption made in deriving the linear elasticity model. St. Venant–Kirchhoff is the most basic nonlinear elastic model, but is often used in numerical simulations using finite elements because of its ease of implementation relative to other nonlinear elastic models. In posing the linear elasticity equations, one makes the assumption that $\nabla\boldsymbol{\eta}^T\nabla\boldsymbol{\eta} \approx 0$ in the strain tensor, $\nabla_X\boldsymbol{\eta} \approx \nabla_x\boldsymbol{\eta}$, and that $J = \det(I + \nabla_x\boldsymbol{\eta}^T) \approx 1$. The St. Venant–Kirchhoff model makes none of these assumptions. It is often referred to as the "large displacement-small strain" model. Only partial existence results exist [23, p. 299] for this model primarily since nothing prevents $\det(\mathbf{F})$ from becoming zero or even negative.

The Jacobian that results from the displacement, generally denoted $\mathbf{F}$, is defined as:

$$\mathbf{F}_{i,j} = \frac{\partial \mathbf{x}_i}{\partial \mathbf{X}_j} = \mathbf{1}[i = j] + \frac{\partial \boldsymbol{\eta}_i}{\partial \mathbf{X}_j} = \mathbf{I}_{i,j} + \nabla\boldsymbol{\eta}_{j,i} = [\mathbf{I} + \nabla\boldsymbol{\eta}^T]_{i,j}$$

or

$$\mathbf{F} = \mathbf{I} + \nabla\boldsymbol{\eta}^T.$$

The deformation tensor locally characterizes the difference between current and reference

configuration. Strain should not take into account rotations and translations, i.e., rigid-body motions. George Green defined what has come to be known as the right Cauchy–Green deformation tensor:

$$\mathbf{C}_{i,j} = \sum_k \mathbf{F}_{k,i}\mathbf{F}_{k,j} \text{ or equivalently, } \mathbf{C} = \mathbf{F}^T\mathbf{F}.$$

This measure of strain is symmetric and positive definite and is invariant to rigid-body motions. The Green–St. Venant strain tensor is defined as:

$$\mathbf{E} = \frac{1}{2}[\mathbf{C} - \mathbf{I}], \text{ where } \mathbf{C} \text{ is the right Cauchy–Green deformation tensor,}$$

and is a measure difference between the deformed material modulo rigid-body motions and the reference configuration. This strain tensor is also symmetric and positive definite.

The strain-energy density function describes the energy per unit of volume stored by the elastic structure due to its deformation. For the St. Venant–Kirchhoff equations, this function is

$$W(\mathbf{E}) = \frac{\lambda}{2}\, Tr(\mathbf{E})^2 + \nu_s\, Tr(\mathbf{E}^2), \tag{6.1}$$

where $Tr(\cdot)$ is the trace operator, λ is Lamé's first parameter, and ν_s is the shear modulus. Differentiating this strain-energy density function (6.1) with respect to the strain tensor $\mathbf{E}$ gives the second Piola–Kirchhoff stress, also called the material stress:

$$\mathbf{\Sigma} = \frac{\partial W(\mathbf{E})}{\partial \mathbf{E}} = \lambda\, Tr(\mathbf{E})\mathbf{I} + 2\nu_s\, E$$

The second Piola–Kirchhoff stress is related to the Cauchy stress, also called the true stress, through the stress-strain relation

$$\boldsymbol{\sigma} = \frac{1}{J}\mathbf{F}\mathbf{\Sigma}\mathbf{F}^T. \tag{6.2}$$

With deformation, strain, and stress tensors defined, we are now prepared to present the

equations for nonlinear elasticity having derivatives in the deformed configuration and use appropriate substitutions to return them to the reference domain.

The equations for elasticity are

$$\rho \frac{d^2 \boldsymbol{\eta}}{dt^2}(\mathbf{X}) - J\nabla_{\mathbf{x}} \cdot \boldsymbol{\sigma} = J\mathbf{f}_s \ \ in\ \Omega^s$$

or equivalently,

$$\rho \frac{d\dot{\boldsymbol{\eta}}}{dt} - J\nabla_{\mathbf{x}} \cdot \boldsymbol{\sigma} = J\mathbf{f}_s \ \ in\ \Omega^s \tag{6.3}$$

$$\dot{\boldsymbol{\eta}} - \frac{d\boldsymbol{\eta}}{dt} = 0 \ \ in\ \Omega^s \tag{6.4}$$

The Piola transform [23, pp. 37–39] allows us to pull back the divergence operator for a tensor or vector as

$$J\nabla_{\mathbf{x}} \cdot \mathbf{v} = \nabla_{\mathbf{X}} \cdot (J\mathbf{F}^{-1}\mathbf{v}) \text{ and } J\nabla_{\mathbf{x}} \cdot \boldsymbol{\sigma} = \nabla_{\mathbf{X}} \cdot (J\boldsymbol{\sigma}\mathbf{F}^{-T}).$$

Using the Piola transform, we can rewrite the elasticity equations (6.3)–(6.4) as

$$\rho \frac{d\dot{\boldsymbol{\eta}}}{dt} - \nabla_{\mathbf{X}} \cdot (J\boldsymbol{\sigma}\mathbf{F}^{-T}) = J\mathbf{f}_s \ \ in\ \Omega^s$$

$$\dot{\boldsymbol{\eta}} - \frac{d\boldsymbol{\eta}}{dt} = 0 \ \ in\ \Omega^s.$$

Next, we apply the relationship between the Cauchy and Piola–Kirchhoff stress tensors (6.2) to get

$$\rho \frac{d\dot{\boldsymbol{\eta}}}{dt} - \nabla_{\mathbf{X}} \cdot (\mathbf{F}\boldsymbol{\Sigma}) = J\mathbf{f}_s \ \ in\ \Omega^s \tag{6.5}$$

$$\dot{\boldsymbol{\eta}} - \frac{d\boldsymbol{\eta}}{dt} = 0 \ \ in\ \Omega^s, \tag{6.6}$$

and $\mathbf{F}\boldsymbol{\Sigma}$ is the first Piola–Kirchhoff stress tensor.

In order to make connection with the Lagrangian mapping clear, here substitutions

are made into the stress tensor to the granularity of $\nabla\boldsymbol{\eta}$.

$$\begin{aligned}
\mathbf{F}\boldsymbol{\Sigma} &= \mathbf{F}[\lambda\, Tr(\mathbf{E})\mathbf{I} + 2\nu_s\, E] \\
&= \mathbf{F}\left[\lambda\, Tr\left(\frac{1}{2}[\mathbf{C}-\mathbf{I}]\right)\mathbf{I} + 2\nu_s\,\frac{1}{2}[\mathbf{C}-\mathbf{I}]\right] \\
&= \mathbf{F}\left[\lambda\, Tr\left(\frac{1}{2}[\mathbf{F}^T\mathbf{F}-\mathbf{I}]\right)\mathbf{I} + 2\nu_s\,\frac{1}{2}[\mathbf{F}^T\mathbf{F}-\mathbf{I}]\right] \\
&= [\mathbf{I}+\nabla_{\mathbf{x}}\boldsymbol{\eta}^T]\left[\lambda\, Tr\left(\frac{1}{2}[[\mathbf{I}+\nabla_{\mathbf{x}}\boldsymbol{\eta}^T]^T[\mathbf{I}+\nabla_{\mathbf{x}}\boldsymbol{\eta}^T]-\mathbf{I}]\right)\mathbf{I} + \right. \\
&\qquad\qquad \left. 2\nu_s\,\frac{1}{2}[[\mathbf{I}+\nabla_{\mathbf{x}}\boldsymbol{\eta}^T]^T[\mathbf{I}+\nabla_{\mathbf{x}}\boldsymbol{\eta}^T]-\mathbf{I}]\right] \qquad (6.7)
\end{aligned}$$

Temporal discretization of the fluid subsystem (2.34)–(2.35) by implicit Euler and of the variational formulation of the of the strong form of the structure subsystem (6.5)–(6.6) by a second order midpoint scheme yields: find $(\mathbf{u}^n, p^n, \boldsymbol{\eta}^n, \dot{\boldsymbol{\eta}}^n) \in \boldsymbol{H}^1_D(\Omega^f_{t_n}) \times L^2(\Omega^f_{t_n}) \times \boldsymbol{H}^1_D(\Omega^s) \times \mathbf{L}^2(\Omega^s)$ such that

$$\begin{aligned}
\rho_f\left[(\mathbf{u}^n,\mathbf{v})_{\Omega^f_{t_n}} - (\mathbf{u}^{n-1},\mathcal{V}(\mathbf{v}))_{\Omega^f_{t_{n-1}}}\right] &+ \Delta t\,\rho_f\left[((\mathbf{u}^n-\mathbf{z}^n)\cdot\nabla\mathbf{u}^n,\mathbf{v})_{\Omega^f_{t_n}} - ((\nabla\cdot\mathbf{z}^n)\mathbf{u}^n,\mathbf{v})_{\Omega^f_{t_n}}\right] \\
&+ \Delta t\left[2\nu_f a(\mathbf{u}^n,\mathbf{v})_{\Omega^f_{t_n}} + b(\mathbf{v},p^n)_{\Omega^f_{t_n}}\right] \\
&- \Delta t\,(2\nu_f D(\mathbf{u}^n)\cdot\mathbf{n}_f - p^n\mathbf{n}_f,\mathbf{v})_{\Gamma_{I_t}} \\
&= \Delta t\left[(\mathbf{f}^n_f,\mathbf{v})_{\Omega^f_{t_n}} + (\mathbf{u}^n_N,\mathbf{v})_{\Gamma^f_N}\right]\ \forall\mathbf{v}\in\boldsymbol{H}^1_D(\Omega^f_{t_n})\,, \quad (6.8) \\
b(\mathbf{u}^n,q)_{\Omega^f_{t_n}} &= 0 \quad \forall q\in L^2(\Omega^f_{t_n})\,, \qquad (6.9)
\end{aligned}$$

and

$$\begin{aligned}
\rho_s\left(\dot{\boldsymbol{\eta}}^n-\dot{\boldsymbol{\eta}}^{n-1},\boldsymbol{\xi}\right)_{\Omega^s} &+ \frac{\Delta t}{2}\left(\mathbf{F}^n\boldsymbol{\Sigma}^n + \mathbf{F}^{n-1}\boldsymbol{\Sigma}^{n-1},\nabla_{\mathbf{x}}\boldsymbol{\xi}\right) \\
&- \frac{\Delta t}{2}\left(\left[\mathbf{F}^n\boldsymbol{\Sigma}^n + \mathbf{F}^{n-1}\boldsymbol{\Sigma}^{n-1}\right]\cdot\mathbf{n}_s,\boldsymbol{\xi}\right)_{\Gamma_{I_{t_0}}} \\
&= \frac{\Delta t}{2}\left[\left(\mathbf{f}^n_s+\mathbf{f}^{n-1}_s,\boldsymbol{\xi}\right)_{\Omega^s} + \left(\boldsymbol{\eta}^n_N+\boldsymbol{\eta}^{n-1}_N,\boldsymbol{\xi}\right)_{\Gamma^s_N}\right]\forall\boldsymbol{\xi}\in\boldsymbol{H}^1_D(\Omega^s)\,, \quad (6.10) \\
\frac{\Delta t}{2}\left(\dot{\boldsymbol{\eta}}^n+\dot{\boldsymbol{\eta}}^{n-1},\boldsymbol{\gamma}\right)_{\Omega^s} &= \left(\boldsymbol{\eta}^n-\boldsymbol{\eta}^{n-1},\boldsymbol{\gamma}\right)_{\Omega^s}\ \forall\boldsymbol{\gamma}\in\boldsymbol{L}^2(\Omega^s)\,, \qquad (6.11)
\end{aligned}$$

and satisfying the interface continuity equations

$$\mathbf{u}^n \circ \Psi_{t_n} = \dot{\boldsymbol{\eta}}^n \text{ on } \Gamma_{I_{t_0}} \tag{6.12}$$

and

$$[[2\nu_f D(\mathbf{u}^n) - p^n\, \mathbf{I}] \cdot \mathbf{n}_f] \circ \Psi_{t_n} = -\mathbf{F}\boldsymbol{\Sigma} \cdot \mathbf{n}_s \text{ on } \Gamma_{I_{t_0}}. \tag{6.13}$$

6.3 Description of the Optimization Problem

Since $[[2\nu_f D(\mathbf{u}^n) - p^n\, \mathbf{I}] \cdot \mathbf{n}_f] \circ \Psi_{t_n} = -\mathbf{F}\boldsymbol{\Sigma} \cdot \mathbf{n}_s$ on $\Gamma_{I_{t_0}}$, these terms can be substituted from the variational formulation of the FSI problem in (6.8)–(6.11) with a control $\mathbf{g}^n$ defined on the reference domain $\Gamma_{I_{t_0}}$, ensuring the continuity of traction force for any choice of the control.

In order to find a choice of control in $\mathbf{L}^2(\Omega^f_{t_0})$ that enforces continuity of velocity, we seek to minimize the penalized functional

$$\mathcal{J}_n(\mathbf{u}^n, \dot{\boldsymbol{\eta}}^n, \mathbf{g}^n) = \frac{1}{2}\int_{\Gamma_{I_{t_n}}} |\mathbf{u}^n - \mathcal{V}(\dot{\boldsymbol{\eta}}^n)|^2 \, d\Gamma + \frac{\epsilon}{2}\int_{\Gamma_{I_{t_n}}} |\mathbf{g}^n|^2 \, d\Gamma\,, \tag{6.14}$$

subject to

$$\begin{aligned}
\rho_f \left[(\mathbf{u}^n, \mathbf{v})_{\Omega^f_{t_n}} \right. & \left. -(\mathbf{u}^{n-1}, \mathcal{V}(\mathbf{v}))_{\Omega^f_{t_{n-1}}}\right] + \Delta t\, \rho_f \left[((\mathbf{u}^n - \mathbf{z}^n)\cdot\nabla \mathbf{u}^n, \mathbf{v})_{\Omega^f_{t_n}} - ((\nabla\cdot\mathbf{z}^n)\mathbf{u}^n, \mathbf{v})_{\Omega^f_{t_n}}\right] \\
& + \Delta t \left[2\nu_f a(\mathbf{u}^n, \mathbf{v})_{\Omega^f_{t_n}} + b(\mathbf{v}, p^n)_{\Omega^f_{t_n}}\right] \\
& = \Delta t \left[(\mathcal{V}(\mathbf{g}^n), \mathbf{v})_{\Gamma_{I_{t_n}}} + (\mathbf{f}^n_f, \mathbf{v})_{\Omega^f_{t_n}} + (\mathbf{u}^n_N, \mathbf{v})_{\Gamma^f_N}\right] \ \forall \mathbf{v} \in \boldsymbol{H}^1_D(\Omega^f_{t_n})\,, \qquad (6.15) \\
b(\mathbf{u}^n, q)_{\Omega^f_{t_n}} & = 0 \quad \forall q \in L^2(\Omega^f_{t_n})\,, \qquad (6.16)
\end{aligned}$$

and

$$\rho_s \left(\dot{\boldsymbol{\eta}}^n - \dot{\boldsymbol{\eta}}^{n-1}, \boldsymbol{\xi}\right)_{\Omega^s} + \frac{\Delta t}{2} \left(\mathbf{F}^n \boldsymbol{\Sigma}^n + \mathbf{F}^{n-1} \boldsymbol{\Sigma}^{n-1}, \nabla_{\mathbf{x}}\right)$$
$$= \frac{\Delta t}{2} \left[- \left(\mathbf{g}^n + \mathbf{g}^{n-1}, \boldsymbol{\xi}\right)_{\Gamma_{I_{t_0}}} + \left(\mathbf{f}_s^n + \mathbf{f}_s^{n-1}, \boldsymbol{\xi}\right)_{\Omega^s} \right.$$
$$\left. + \left(\boldsymbol{\eta}_N^n + \boldsymbol{\eta}_N^{n-1}, \boldsymbol{\xi}\right)_{\Gamma_N^s} \right] \forall \boldsymbol{\xi} \in \boldsymbol{H}_D^1(\Omega^s)\,, \tag{6.17}$$

$$\frac{\Delta t}{2} \left(\dot{\boldsymbol{\eta}}^n + \dot{\boldsymbol{\eta}}^{n-1}, \boldsymbol{\gamma}\right)_{\Omega^s} = \left(\boldsymbol{\eta}^n - \boldsymbol{\eta}^{n-1}, \boldsymbol{\gamma}\right)_{\Omega^s} \ \forall \boldsymbol{\gamma} \in \boldsymbol{L}^2(\Omega^s)\,. \tag{6.18}$$

6.4 Linearization of the First Piola–Kirchhoff Stress Tensor

We now linearize the structure equations with respect to $\boldsymbol{\eta}$ in order to get each Newton iteration update to solve the nonlinear PDE. Solving this problem will have the form $\mathbf{K}'(\boldsymbol{\eta}) \cdot (\boldsymbol{\eta}_{(k)} - \boldsymbol{\eta}_{(k-1)}) = -\mathbf{K}(\boldsymbol{\eta}_{(k-1)})$, where $\mathbf{K}$ is the elasticity operator (6.5)–(6.6). Focus is first placed on linearizing the first Piola–Kirchhoff stress tensor (6.7), denoted $\mathbf{S}$, since all other terms in the structure equations are linear.

$$\mathbf{S}'(\boldsymbol{\eta}) \cdot (\boldsymbol{\phi}) = \frac{\partial(\mathbf{F}\boldsymbol{\Sigma})}{\partial \boldsymbol{\eta}} \cdot (\boldsymbol{\phi})$$
$$= [\mathbf{I} + \nabla_{\mathbf{x}} \boldsymbol{\eta}_{(k-1)}^T] \left[\frac{\lambda}{2}\, Tr\left(\nabla_{\mathbf{x}} \boldsymbol{\phi} [\mathbf{I} + \nabla_{\mathbf{x}} \boldsymbol{\eta}_{(k-1)}^T] + [\mathbf{I} + \nabla_{\mathbf{x}} \boldsymbol{\eta}_{(k-1)}^T]^T \nabla_{\mathbf{x}} \boldsymbol{\phi}^T\right) \mathbf{I} \right.$$
$$\left. + \nu_s \left[\nabla_{\mathbf{x}} \boldsymbol{\phi} [\mathbf{I} + \nabla_{\mathbf{x}} \boldsymbol{\eta}_{(k-1)}^T] + [\mathbf{I} + \nabla_{\mathbf{x}} \boldsymbol{\eta}_{(k-1)}^T]^T \nabla_{\mathbf{x}} \boldsymbol{\phi}^T\right] \right]$$
$$+ \nabla_{\mathbf{x}} \boldsymbol{\phi}^T \left[\lambda\, Tr\left(\frac{1}{2}[[\mathbf{I} + \nabla_{\mathbf{x}} \boldsymbol{\eta}_{(k-1)}^T]^T [\mathbf{I} + \nabla_{\mathbf{x}} \boldsymbol{\eta}_{(k-1)}^T] - \mathbf{I}]\right) \mathbf{I} \right.$$
$$\left. + 2\nu_s\, \frac{1}{2}[[\mathbf{I} + \nabla_{\mathbf{x}} \boldsymbol{\eta}_{(k-1)}^T]^T [\mathbf{I} + \nabla_{\mathbf{x}} \boldsymbol{\eta}_{(k-1)}^T] - \mathbf{I}] \right] \tag{6.19}$$

Using this definition for the linearized first Piola–Kirchhoff stress tensor, we can substitute $\boldsymbol{\eta}_{(k)} - \boldsymbol{\eta}_{(k-1)}$ in place of $\boldsymbol{\phi}$ to get the stress tensor's contribution for a Newton iteration.

$$
\begin{aligned}
&\mathbf{S}'(\boldsymbol{\eta}) \cdot (\boldsymbol{\eta}_{(k)} - \boldsymbol{\eta}_{(k-1)}) \\
&\qquad = [\mathbf{I} + \nabla_{\mathbf{x}} \boldsymbol{\eta}_{(k-1)}^T] \left[\frac{\lambda}{2}\, Tr \left([\nabla_{\mathbf{x}} \boldsymbol{\eta}_{(k)}^T - \nabla_{\mathbf{x}} \boldsymbol{\eta}_{(k-1)}^T]^T [\mathbf{I} + \nabla_{\mathbf{x}} \boldsymbol{\eta}_{(k-1)}^T] \right.\right. \\
&\qquad\qquad \left.\left. + [\mathbf{I} + \nabla_{\mathbf{x}} \boldsymbol{\eta}_{(k-1)}^T]^T [\nabla_{\mathbf{x}} \boldsymbol{\eta}_{(k)}^T - \nabla_{\mathbf{x}} \boldsymbol{\eta}_{(k-1)}^T] \right) \mathbf{I} \right. \\
&\qquad\qquad + \nu_s \left[[\nabla_{\mathbf{x}} \boldsymbol{\eta}_{(k)}^T - \nabla_{\mathbf{x}} \boldsymbol{\eta}_{(k-1)}^T]^T [\mathbf{I} + \nabla_{\mathbf{x}} \boldsymbol{\eta}_{(k-1)}^T] \right. \\
&\qquad\qquad \left. \left. + [\mathbf{I} + \nabla_{\mathbf{x}} \boldsymbol{\eta}_{(k-1)}^T]^T [\nabla_{\mathbf{x}} \boldsymbol{\eta}_{(k)}^T - \nabla_{\mathbf{x}} \boldsymbol{\eta}_{(k-1)}^T] \right] \right] \\
&\qquad + [\nabla_{\mathbf{x}} \boldsymbol{\eta}_{(k)}^T - \nabla_{\mathbf{x}} \boldsymbol{\eta}_{(k-1)}^T] \left[\lambda\, Tr \left(\frac{1}{2} [[\mathbf{I} + \nabla_{\mathbf{x}} \boldsymbol{\eta}_{(k-1)}^T]^T [\mathbf{I} + \nabla_{\mathbf{x}} \boldsymbol{\eta}_{(k-1)}^T] - \mathbf{I}] \right) \mathbf{I} \right. \\
&\qquad\qquad \left. + \, 2\nu_s\, \frac{1}{2} [[\mathbf{I} + \nabla_{\mathbf{x}} \boldsymbol{\eta}_{(k-1)}^T]^T [\mathbf{I} + \nabla_{\mathbf{x}} \boldsymbol{\eta}_{(k-1)}^T] - \mathbf{I}] \right]
\end{aligned}
$$

Adding the contribution of $-(\mathbf{F\Sigma})(\boldsymbol{\eta}_{(k-1)})$ from the right hand side to the left hand side gives that $(\mathbf{F\Sigma})'(\boldsymbol{\eta}) \cdot (\boldsymbol{\eta}_{(k)} - \boldsymbol{\eta}_{(k-1)}) = -(\mathbf{F\Sigma})(\boldsymbol{\eta}_{(k-1)})$ is equivalent to

$$
\begin{aligned}
&[\mathbf{I} + \nabla_{\mathbf{x}} \boldsymbol{\eta}_{(k-1)}^T] \left[\frac{\lambda}{2}\, Tr \left([\nabla_{\mathbf{x}} \boldsymbol{\eta}_{(k)}^T - \nabla_{\mathbf{x}} \boldsymbol{\eta}_{(k-1)}^T]^T [\mathbf{I} + \nabla_{\mathbf{x}} \boldsymbol{\eta}_{(k-1)}^T] \right.\right. \\
&\qquad\qquad \left.\left. + [\mathbf{I} + \nabla_{\mathbf{x}} \boldsymbol{\eta}_{(k-1)}^T]^T [\nabla_{\mathbf{x}} \boldsymbol{\eta}_{(k)}^T - \nabla_{\mathbf{x}} \boldsymbol{\eta}_{(k-1)}^T] \right) \mathbf{I} \right. \\
&\qquad\qquad + \nu_s \left[[\nabla_{\mathbf{x}} \boldsymbol{\eta}_{(k)}^T - \nabla_{\mathbf{x}} \boldsymbol{\eta}_{(k-1)}^T]^T [\mathbf{I} + \nabla_{\mathbf{x}} \boldsymbol{\eta}_{(k-1)}^T] \right. \\
&\qquad\qquad \left. \left. + [\mathbf{I} + \nabla_{\mathbf{x}} \boldsymbol{\eta}_{(k-1)}^T]^T [\nabla_{\mathbf{x}} \boldsymbol{\eta}_{(k)}^T - \nabla_{\mathbf{x}} \boldsymbol{\eta}_{(k-1)}^T] \right] \right] \\
&\qquad + [\mathbf{I} + \nabla_{\mathbf{x}} \boldsymbol{\eta}_{(k)}^T] \left[\lambda\, Tr \left(\frac{1}{2} [[\mathbf{I} + \nabla_{\mathbf{x}} \boldsymbol{\eta}_{(k-1)}^T]^T [\mathbf{I} + \nabla_{\mathbf{x}} \boldsymbol{\eta}_{(k-1)}^T] - \mathbf{I}] \right) \mathbf{I} \right. \\
&\qquad\qquad \left. + \, 2\nu_s\, \frac{1}{2} [[\mathbf{I} + \nabla_{\mathbf{x}} \boldsymbol{\eta}_{(k-1)}^T]^T [\mathbf{I} + \nabla_{\mathbf{x}} \boldsymbol{\eta}_{(k-1)}^T] - \mathbf{I}] \right] = \mathbf{0}. \qquad (6.20)
\end{aligned}
$$

Substituting the left hand side of (6.20) into the structure equation (6.17) in place of $\mathbf{F\Sigma}$ results in the Newton iteration operator for the structure subproblem.

For the linearized problem which is used for a linear least squares solve in the Gauss–Newton algorithm, the operator for (6.17)–(6.18) is linearized in the form of $\mathbf{K}'(\boldsymbol{\eta}) \cdot (\boldsymbol{\phi})$,

resulting in solving: find $(\mathbf{w}, r, \boldsymbol{\eta}, \boldsymbol{\varphi}) \in \boldsymbol{H}^1_D(\Omega^f_{t_n}) \times L^2(\Omega^f_{t_n}) \times \boldsymbol{H}^1_D(\Omega^s) \times \mathbf{L}^2(\Omega^s)$ such that

$$\begin{aligned}
\rho^f(\mathbf{w},\mathbf{v})_{\Omega^f_{t_n}} &+ \Delta t\ \rho^f[c(\mathbf{u}^n,\mathbf{w},\mathbf{v})_{\Omega^f_{t_n}} + c(\mathbf{w},\mathbf{u}^n,\mathbf{v})_{\Omega^f_{t_n}} + \frac{1}{2}((\mathbf{u}^n\cdot\mathbf{n}_f)\mathbf{w},\mathbf{v})_{\Gamma^f_N} \\
&+ \frac{1}{2}((\mathbf{w}\cdot\mathbf{n}_f)\mathbf{u}^n,\mathbf{v})_{\Gamma^f_N} - \frac{1}{2}((\nabla\cdot\mathbf{z}^n)\mathbf{w},\mathbf{v})_{\Omega^f_{t_n}} - c(\mathbf{z}^n,\mathbf{w},\mathbf{v})_{\Omega^f_{t_n}}] \\
&+ \Delta t\ 2\nu_f a(\mathbf{w},\mathbf{v})_{\Omega^f_{t_n}} + \Delta t\ b(\mathbf{v},r)_{\Omega^f_{t_n}} \\
&= \Delta t\ (\mathbf{h},\mathbf{v})_{\Gamma_{I_{t_n}}} \quad \forall \mathbf{v} \in \boldsymbol{H}^1_D(\Omega^f_{t_n}), \qquad (6.21)\\
b(\mathbf{w},q)_{\Omega^f_{t_n}} &= 0 \quad q \in L^2(\Omega^f_{t_n}), \qquad (6.22)
\end{aligned}$$

$$\rho^s(\boldsymbol{\varphi},\boldsymbol{\xi})_{\Omega^s} + \Delta t(\mathbf{S}'(\boldsymbol{\eta})\cdot(\boldsymbol{\theta}),\nabla_{\mathbf{x}}\boldsymbol{\xi})_{\Omega^s} = -\frac{\Delta t}{2}\ (\mathbf{h},\boldsymbol{\xi})_{\Gamma_{I_{t_0}}} \quad \forall \boldsymbol{\xi} \in \boldsymbol{H}^1_D(\Omega^s), \qquad (6.23)$$

$$\frac{\Delta t}{2}(\boldsymbol{\varphi},\boldsymbol{\gamma})_{\Omega^s} - (\boldsymbol{\theta},\boldsymbol{\gamma})_{\Omega^s} = 0 \quad \forall \boldsymbol{\gamma} \in \boldsymbol{L}^2(\Omega^s). \qquad (6.24)$$

where $\mathbf{h}$ is a function determined by the optimization routine selected, and $\mathbf{S}'(\boldsymbol{\eta})\cdot(\boldsymbol{\theta})$ is defined in (6.19).

6.5 Numerical Results

6.5.1 Haemodynamic Experiment

The first numerical experiment we study plots the vertical displacement of the structure at three locations on the interface. We revisit the problem that was described in Section 4.10, but this time using the St. Venant–Kirchhoff equations as the constitutive equation for the elastic structure. A comparison is made between a sequentially staggered Dirichlet–Neumann approach augmented by Aitken's relaxation and our optimization-based approach. For more details on sequentially staggered approaches, see [30]. The plots in Figure 6.2 demonstrate the contrast between using linear and the St. Venant–Kirchhoff constitutive equation for the elastic structure, in order to emphasize the significant difference in response between a linear and nonlinear elastic as well as the agreement between the optimization

approach and the relaxed sequentially staggered method.

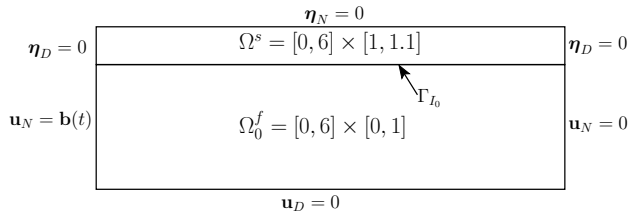

Figure 6.1: Domain and boundary conditions for numerical experiment

A force $\mathbf{b}(t)$ is applied to the left fluid boundary (Fig. 6.1) at t s where

$$\mathbf{b}(t) = \begin{cases} (-10^3(1-\cos\frac{2\pi t}{.025}),0) \ \text{ dyne/cm}^2, & t \leq 0.025 \\ (0,0), & 0.025 < t < T. \end{cases}$$

The function $\mathbf{b}(t)$ defines the stress on the inlet denoted by $\mathbf{u}_N$ in (2.4). The volume force for the fluid and structure are $\mathbf{f}(t) = (0,0)$ dyne/cm^2. The other boundary conditions on the domain configuration are homogeneous Dirichlet or Neumann (Fig. 6.1), and the simulation begins at rest.

The reference domain for the fluid subsystem has height 1 cm and length 6 cm. The density of the fluid, ρ_f, is 1 g/cm^3 and the viscosity of the fluid, ν_f, is 0.035 g/cm·s. The structure domain has height 0.1 cm and length 6 cm. The density of the structure, ρ_s, is 1.1 g/cm^3. The Young's Modulus of the structure, E, is 3×10^6 dyne/cm^2 and its Poisson ratio, ν, is 0.3. Spatial discretization in the x direction is $h_x = 0.2$ cm and in the y direction is $h_y = 0.1$ cm for both fluid and structure domains on a uniform quadrilateral mesh. The simulation was performed with $\Delta t = 10^{-4}$ s from $T = 0$ s to $T = 0.1$ s. Computations were performed in deal.II [7,8] using the tensor product $(\mathbb{Q}_2, \mathbb{Q}_1)$ finite element pair for the fluid, and tensor product $\mathbb{Q}_2$ elements for the structure. The stopping criteria used for Aitken's relaxation was $\left(\int_{\Gamma_{I_{t_0}}} (\boldsymbol{\eta}^n_{(k)} - \boldsymbol{\eta}^n_{(k-1)})^2 \, d\Gamma \right)^{\frac{1}{2}} < 10^{-14}$, while $\delta = 10^{-24}$ and $\epsilon_{tol} = 10^{-18}$ for the Gauss-Newton Algorithm 3.3 adapted to the state and linearized equations (6.15)–(6.18) and (6.21)–(6.24).

In Figure 6.1, close agreement can be observed between solutions computed using the

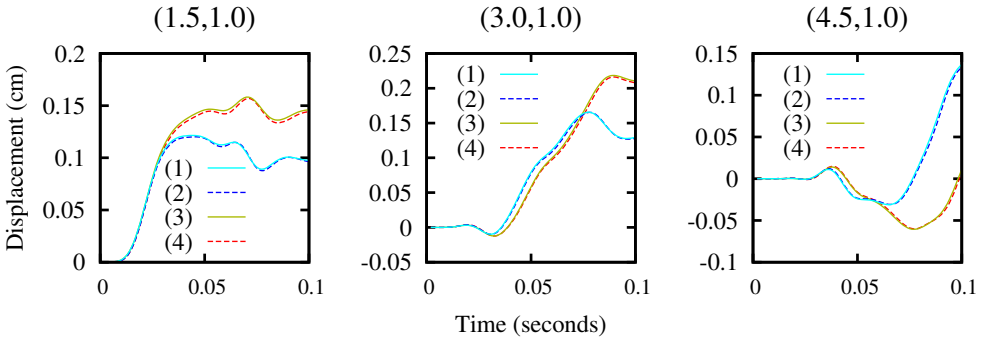

Figure 6.2: Vertical displacement at three points on the interface using (1) optimization and (2) Aitken's relaxation with the St. Venant–Kirchhoff constitutive equation and (3) optimization and (4) Aitken's relaxation with the linear elastic constitutive equation.

optimization-based approach presented in this thesis and the Aitken relaxed sequentially staggered Dirichlet–Neumann coupling approach. The difference in the response of the vertical displacement of the structure to the linear or nonlinear elastic physics is pronounced.

6.5.2 3D Pulsatile Flow Through a Cylinder

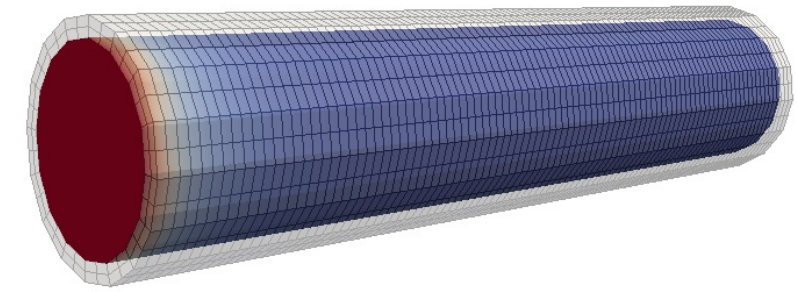

Figure 6.3: Computational domain for 3D pulsatile flow through a cylinder.

In three dimensions, a pressure driven flow through a cylinder is commonly simulated numerically [19, 29, 34, 49]. In this setting, a fluid modeled by the Navier–Stokes equations is in contact with an elastic solid modeled by the St. Venant–Kirchhoff equations. The fluid has parameters $\mu = 0.035$ poise, $\rho_f = 1$ g/cm^3, in an initially straight vessel of radius 0.5

cm and length 5 cm. The structure has parameters $\rho_s = 1.2$ g/cm^3, E = 3.0e+6 dynes/cm^2, and $\nu = 0.3$, with a surrounding structure thickness of 0.1 cm. There is an overpressure on the inlet boundary of 1.3332e+4 dynes/cm^2 for 0.005 s. The inlet and outlet boundaries are clamped, i.e., no displacement. The simulation step size is $\Delta t = 10^{-4}$ s. All parameters exactly match those used in [19].

In Figure 6.4, snapshots are taken of the fluid pressure on the moving fluid domain with the domain deformation scaled by a factor of 10. The enveloping elastic structure is clipped and the deformation is scaled by the same factor. Snapshots are included for four time steps using the tensor product, LBB deficient ($\mathbb{Q}_1, \mathbb{Q}_0^{DC}$) finite element pair for the fluid velocity and pressure, and using tensor product $\mathbb{Q}_1$ elements for the ALE mesh and structure velocity and displacement.

A quantity of interest when applying optimization to a problem is how the number of optimization iterations needed for convergence respond to increasingly refining the computational domain. For this sequence of computations performed on increasingly refined meshes, the tensor product $\mathbb{Q}_1$ elements are used for the fluid velocity, fluid pressure, mesh update, structure displacement, and structure velocity in the deal.II finite element library. This fluid velocity and pressure pair do not satisfy the Ladyzhenskaya–Babuska–Brezzi (LBB) condition, and so they are stabilized by a stabilization method for low-order mixed finite elements [13].

$$\text{Work Factor} = \frac{\text{Fluid Solves (Total)} + 2 \text{ Gauss–Newton Iterations}}{\text{Fluid Solves (Stress Determined)}} \tag{6.25}$$

In the case of CPU wall times, it is possible that certain accelerations may be added to a code and omitted from another, intentionally or unintentionally, so that when compared one will outperform the other. In order to prepare as fair of an estimate as possible for the computational complexity of our optimization-based algorithm, a metric is proposed which will compare the computational effort as a multiplier of the effort to perform a forward

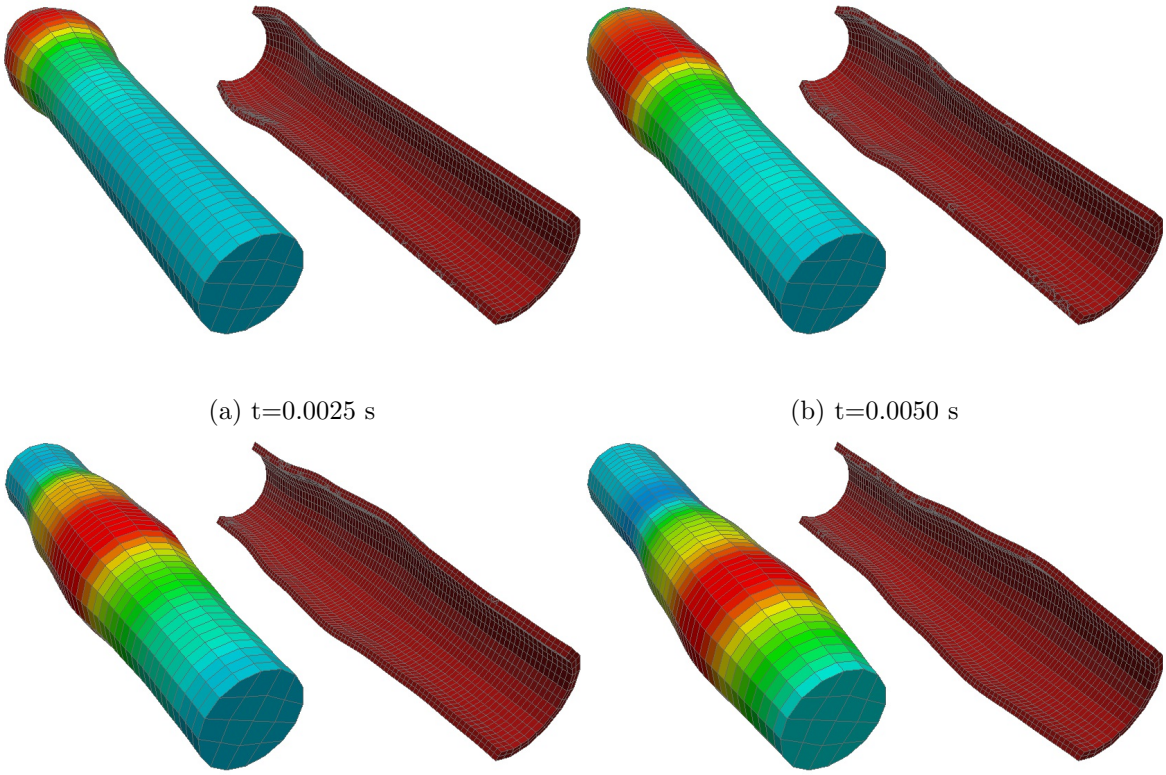

(a) t=0.0025 s (b) t=0.0050 s

(c) t=0.0075 s (d) t=0.0100 s

Figure 6.4: Snapshots of fluid pressure and scaled solid deformation (by a factor of 10) using $(\mathbb{Q}_1, \mathbb{Q}_0^{DC})$ elements for the fluid pressure and velocity, $\mathbb{Q}_1$ elements for structure and mesh updates.

solve, had the correct boundary conditions on the interface been known a priori. In Table 6.1, the average number of Gauss–Newton iterations per time step are listed along with the average number of GMRES solves needed per Gauss–Newton iteration. The work factor is determined using definition (6.25). The rationale for this metric is based on the fact that in every Gauss–Newton iteration, a sequence of GMRES iterations must be performed, but it is only the first iteration that requires matrix assembly and factorization. After this first iteration, the factorization can be cheaply reused and so the primary effort lies in the initial factorization which is approximately the same as one nonlinear state solve iteration. For this reason, the computational effort for the GMRES solves are represented in the Work Factor formula by two times the number of Gauss–Newton iterations.

Table 6.1: Iteration counts for Gauss–Newton, GMRES, and fluid state solves.

Refinement	h	DOFs	Gauss–Newton / Time Step	GMRES / Gauss–Newton	Fluid Solves (Total)	Fluid Solves (Stress Determined)	Work Factor
1	5/12	3975	3.807	11.54	14302	2570	8.53
2	5/24	17983	4.472	15.39	16608	2473	10.33
3	5/48	128790	5.185	24.84	20006	2791	10.88

While Table 6.1 is a limited amount of information to draw conclusions from, required solution times made additional refinements prohibitive. It can be observed through the Work Factor that the amount of computational work required relative to performing the forward solve, assuming a known traction, can be observed to grow very slowly with the refinement of the mesh or degrees of freedom. The number of Gauss–Newton iterations per time step appear to grow slightly with refinement of the mesh, but this is not expected to grow asymptotically. The total fluid solves appear to grow slightly as well, but this also should not be expected to grow asymptotically. Since the GMRES algorithm has a restart of 50 and is performed in double precision, it can not be guaranteed that the algorithm will converge. Despite this, the number of GMRES iterations per Gauss–Newton iteration are small. There is a dependence on the number of degrees of freedom, but this is mitigated by only needing to reassemble and factor the matrix once, namely on the first GMRES iteration.

6.6 Conclusion

An FSI problem modeling a nonlinear fluid in contact with a nonlinear elastic structure was described. The problem was recast as a PDE constrained optimization seeking an optimal control which enforces the continuity of traction and seeks to minimize violations of continuity of velocity on the interface.

The first Piola–Kirchhoff stress tensor was linearized and substituted back into the variational form. Using the state and linearized problems, Gauss–Newton in tandem with the GMRES algorithm were applied to problems having parameters consistent with blood

flow in a human body. Comparing vertical displacements at three points on the interface in the 2D problem by Murea and Sy [54], the difference in response between linear and nonlinear elastic structures is demonstrated. A 3D simulation is performed using the St. Venant–Kirchhoff elasticity combined with a fluid modeled by the Navier–Stokes equations. The computational work needed for solution of the FSI problem is calculated for a sequence of increasingly refined meshes, demonstrating that the overall computational complexity of the algorithm does not grow quickly with the increased number of degrees of freedom.

Chapter 7

Conclusions

A new framework has been presented for solving fluid-structure interaction problems. The method is an implicit partitioned scheme which can be constructed from existing solvers. Through the use of a common control between the fluid and structure subproblems, the need to iterate sequentially between subsystems is eliminated and with it the instability that accompanies many partitioned methods. The choice of control used in Chapter 4 has overcome a difficulty in analytically showing stability that would otherwise even be present in the Navier–Stokes variational formulation alone.

With the existence of optimal solutions and Lagrange multipliers proven to exist, there are now opportunities to apply many optimization algorithms to this class of problems with a strong theoretical basis. Additionally, since the method for implementing Gauss–Newton iterations has been provided, there are many algorithms that may be applied to the inner optimization loop.

We treated the deformation gradient, determinant of the deformation gradient, and velocity of the moving mesh as known when deriving the linearized and adjoint forms of the state equations. Had we not treated them as known, then it would provide a more robust approach to solving more sensitive problems. However, this would then entail an adjoint problem with coupling between the fluid and structure adjoint variables. In the approach detailed in this thesis, there is no coupling present between adjoint variables.

The fluids of interest in FSI problems may include blood, air in the bronchial passages, molten chocolate, paint, latex, or some industrial polymer. This adds the difficulty of simulating a fluid which is non-Newtonian in nature since the fluid's shear stress is not proportional to the rate of shear.

The largest motivation for this research has been the application to FSI blood flow simulation, and it is common to model the flow of blood through arteries by treating the fluid as Newtonian. However, it is known that blood is a non-Newtonian fluid, and therefore a more accurate and realistic model should take that into account [35, 47]. Extending this current work into the realm of non-Newtonian fluid-structure interaction would enrich this field, where relatively few analytical and numerical studies have been made.

Bibliography

[1] Robert Adams and John Fournier. *Sobolev spaces*, volume 140. Academic Press, 2003.

[2] Matteo Astorino, Franz Chouly, and Miguel A. Fernández. Robin based semi-implicit coupling in fluid-structure interaction: Stability analysis and numerics. *SIAM Journal on Scientific Computing*, 31(6):4041–4065, 2009.

[3] Matteo Astorino and Céline Grandmont. Convergence analysis of a projection semi-implicit coupling scheme for fluid–structure interaction problems. *Numerische Mathematik*, 116(4):721–767, 2010.

[4] Ivo Babuška. The finite element method with Lagrangian multipliers. *Numerische Mathematik*, 20(3):179–192, 1973.

[5] Santiago Badia, Fabio Nobile, and Christian Vergara. Fluid–structure partitioned procedures based on Robin transmission conditions. *Journal of Computational Physics*, 227(14):7027–7051, 2008.

[6] Santiago Badia, Annalisa Quaini, and Alfio Quarteroni. Splitting methods based on algebraic factorization for fluid-structure interaction. *SIAM Journal on Scientific Computing*, 30(4):1778–1805, 2008.

[7] Wolfgang Bangerth, Ralf Hartmann, and Guido Kanschat. deal.II – a general purpose object oriented finite element library. *ACM Transactions on Mathematical Software*, 33(4):24/1–24/27, 2007.

[8] Wolfgang Bangerth, Timo Heister, Luca Heltai, Guido Kanschat, Martin Kronbichler, Matthias Maier, Bruno Turcksin, and Toby D. Young. The `deal.II` library, version 8.2. *Archive of Numerical Software*, 3, 2015.

[9] Andrew T. Barker and Xiao-Chuan Cai. Scalable parallel methods for monolithic coupling in fluid–structure interaction with application to blood flow modeling. *Journal of Computational Physics*, 229(3):642–659, 2010.

[10] Yuri Bazilevs, Victor M. Calo, Thomas J.R. Hughes, and Yongjie Zhang. Isogeometric fluid-structure interaction: theory, algorithms, and computations. *Computational Mechanics*, 43(1):3–37, 2008.

[11] Yuri Bazilevs, Kenji Takizawa, and Tayfun E. Tezduyar. *Computational fluid-structure interaction: methods and applications*. John Wiley & Sons, 2013.

[12] George Biros and Omar Ghattas. Parallel Lagrange–Newton–Krylov–Schur methods for PDE-constrained optimization. Part I: The Krylov–Schur Solver. *SIAM Journal on Scientific Computing*, 27(2):687–713, 2005.

[13] Pavel B. Bochev, Clark R. Dohrmann, and Max D. Gunzburger. Stabilization of low-order mixed finite elements for the Stokes equations. *SIAM Journal on Numerical Analysis*, 44(1):82–101, 2006.

[14] Daniele Boffi, Nicola Cavallini, and Lucia Gastaldi. Finite element approach to immersed boundary method with different fluid and solid densities. *Mathematical Models and Methods in Applied Sciences*, 21(12):2523–2550, 2011.

[15] Daniele Boffi and Lucia Gastaldi. Stability and geometric conservation laws for ALE formulations. *Computer Methods in Applied Mechanics and Engineering*, 193(42):4717–4739, 2004.

[16] Jacqueline Boujot. Mathematical formulation of fluid–structure interaction problems. *Modélisation Mathématique et Analyse Numérique*, 21(2):239–260, 1987.

[17] Franco Brezzi. On the existence, uniqueness and approximation of saddle-point problems arising from Lagrangian multipliers. *ESAIM: Mathematical Modelling and Numerical Analysis-Modélisation Mathématique et Analyse Numérique*, 8(R2):129–151, 1974.

[18] Franco Brezzi, Jacques Rappaz, and Pierre-Arnaud Raviart. Finite dimensional approximation of nonlinear problems. *Numerische Mathematik*, 36(1):1–25, 1980.

[19] Erik Burman and Miguel A. Fernández. Stabilization of explicit coupling in fluid–structure interaction involving fluid incompressibility. *Computer Methods in Applied Mechanics and Engineering*, 198(5):766–784, 2009.

[20] Sunčica Čanić, Andro Mikelić, and Josip Tambača. A two-dimensional effective model describing fluid–structure interaction in blood flow: analysis, simulation and experimental validation. *Comptes Rendus Mécanique*, 333(12):867–883, 2005.

[21] Paola Causin, Jean-Frédéric Gerbeau, and Fabio Nobile. Added-mass effect in the design of partitioned algorithms for fluid–structure problems. *Computer Methods in Applied Mechanics and Engineering*, 194(42):4506–4527, 2005.

[22] John Chrispell and Lisa Fauci. Peristaltic pumping of solid particles immersed in a viscoelastic fluid. *Mathematical Modelling of Natural Phenomena*, 6(05):67–83, 2011.

[23] Philippe G. Ciarlet. *Three-dimensional elasticity*, volume 1. Elsevier, 1988.

[24] Philippe G. Ciarlet. *Introduction to numerical linear algebra and optimisation*. Cambridge University Press, 1989.

[25] Simone Deparis, Marco Discacciati, Gilles Fourestey, and Alfio Quarteroni. Fluid–structure algorithms based on Steklov–Poincaré operators. *Computer Methods in Applied Mechanics and Engineering*, 195(41):5797–5812, 2006.

[26] Jean Donea, S. Giuliani, and Jean-Pierre Halleux. An arbitrary Lagrangian–Eulerian finite element method for transient dynamic fluid-structure interactions. *Computer Methods in Applied Mechanics and Engineering*, 33(1):689–723, 1982.

[27] Qiang Du, Max D. Gunzburger, and Steven L. Hou. Analysis and finite element approximation of optimal control problems for a Ladyzhenskaya model for stationary, incompressible, viscous flows. *Journal of Computational and Applied Mathematics*, 61(3):323–343, 1995.

[28] Vincent J. Ervin, Eleanor Jenkins, and Hyesuk Lee. Approximation of the Stokes–Darcy system by optimization. *Journal of Scientific Computing*, 59(3):775–794, 2014.

[29] Luca Formaggia, Jean-Frédéric Gerbeau, Fabio Nobile, and Alfio Quarteroni. On the coupling of 3D and 1D Navier–Stokes equations for flow problems in compliant vessels. *Computer Methods in Applied Mechanics and Engineering*, 191(6):561–582, 2001.

[30] Christiane Förster, Wolfgang A Wall, and Ekkehard Ramm. Artificial added mass instabilities in sequential staggered coupling of nonlinear structures and incompressible viscous flows. *Computer Methods in Applied Mechanics and Engineering*, 196(7):1278–1293, 2007.

[31] Keith Galvin and Hyesuk Lee. Analysis and approximation of the Cross model for quasi-Newtonian flows with defective boundary conditions. *Applied Mathematics and Computation*, 222:244–254, 2013.

[32] Lucia Gastaldi. A priori error estimates for the Arbitrary Lagrangian Eulerian formulation with finite elements. *Journal of Numerical Mathematics*, 9(2):123–156, 2001.

[33] Michael W. Gee, Ulrich Küttler, and Wolfgang A. Wall. Truly monolithic algebraic multigrid for fluid–structure interaction. *International Journal for Numerical Methods in Engineering*, 85(8):987–1016, 2011.

[34] Jean-Frédéric Gerbeau and Marina Vidrascu. A quasi-Newton algorithm based on a reduced model for fluid-structure interaction problems in blood flows. *ESAIM: Mathematical Modelling and Numerical Analysis*, 37(04):631–647, 2003.

[35] Frank J.H. Gijsen, Frans N. van de Vosse, and J.D. Janssen. The influence of the non-Newtonian properties of blood on the flow in large arteries: steady flow in a carotid bifurcation model. *Journal of Biomechanics*, 32(6):601–608, 1999.

[36] Vivette Girault and Pierre-Arnaud Raviart. Finite element approximation of the Navier-Stokes equations. *Lecture Notes in Mathematics, Berlin Springer Verlag*, 749, 1979.

[37] Gene H. Golub and Charles F. van Loan. *Matrix computations*. The John Hopkins University Press, 1989.

[38] Charles W. Groetsch. *Generalized inverses of linear operators*. Dekker, 1977.

[39] Max D. Gunzburger and Hyesuk Kwon Lee. An optimization-based domain decomposition method for the Navier–Stokes equations. *SIAM Journal on Numerical Analysis*, 37(5):1455–1480, 2000.

[40] Nicholas Haritos. Introduction to the analysis and design of offshore structures–an overview. *Electronic Journal of Structural Engineering*, 7:55–65, 2007.

[41] F. Hecht. New development in freefem++. *Journal of Numerical Mathematics*, 20(3-4):251–265, 2012.

[42] Matthias Heil. An efficient solver for the fully coupled solution of large-displacement fluid–structure interaction problems. *Computer Methods in Applied Mechanics and Engineering*, 193(1):1–23, 2004.

[43] Jeffrey J. Heys, Thomas A. Manteuffel, Stephen F. McCormick, and J.W. Ruge. First-order system least squares (FOSLS) for coupled fluid–elastic problems. *Journal of Computational Physics*, 195(2):560–575, 2004.

[44] John G. Heywood and Rolf Rannacher. Finite-element approximation of the nonstationary Navier-Stokes problem. Part IV: Error analysis for second-order time discretization. *SIAM Journal on Numerical Analysis*, 27(2):353–384, 1990.

[45] Jaroslav Hron and Stefan Turek. *A monolithic FEM/multigrid solver for an ALE formulation of fluid-structure interaction with applications in biomechanics*, volume 53. Springer, 2006.

[46] Thomas J.R. Hughes, Wing Kam Liu, and Thomas K. Zimmermann. Lagrangian-Eulerian finite element formulation for incompressible viscous flows. *Computer Methods in Applied Mechanics and Engineering*, 29(3):329–349, 1981.

[47] Barbara M. Johnston, Peter R. Johnston, Stuart Corney, and David Kilpatrick. Non-Newtonian blood flow in human right coronary arteries: steady state simulations. *Journal of Biomechanics*, 37(5):709–720, 2004.

[48] Ramji Kamakoti and Wei Shyy. Fluid–structure interaction for aeroelastic applications. *Progress in Aerospace Sciences*, 40(8):535–558, 2004.

[49] Ulrich Küttler and Wolfgang A. Wall. Fixed-point fluid–structure interaction solvers with dynamic relaxation. *Computational Mechanics*, 43(1):61–72, 2008.

[50] William Layton. *Introduction to the numerical analysis of incompressible viscous flows*, volume 6. Siam, 2008.

[51] Patrick Le Tallec and Saloua Mani. Numerical analysis of a linearised fluid-structure interaction problem. *Numerische Mathematik*, 87(2):317–354, 2000.

[52] Hyesuk Lee. Numerical approximation of Quasi-Newtonian flows by ALE-FEM. *Numerical Methods for Partial Differential Equations*, 28(5):1667–1695, 2012.

[53] Randall J. Leveque and Zhilin Li. The immersed interface method for elliptic equations with discontinuous coefficients and singular sources. *SIAM Journal on Numerical Analysis*, 31(4):1019–1044, 1994.

[54] Cornel M. Murea and Soyibou Sy. A fast method for solving fluid–structure interaction problems numerically. *International Journal for Numerical Methods in Fluids*, 60(10):1149–1172, 2009.

[55] Fabio Nobile. *Numerical approximation of fluid-structure interaction problems with application to haemodynamics*. PhD thesis, Politecnico di Milano, 2001.

[56] Fabio Nobile and Luca Formaggia. A stability analysis for the Arbitrary Lagrangian Eulerian formulation with finite elements. *East-West Journal of Numerical Mathematics*, 7(EPFL-ARTICLE-176278):105–132, 1999.

[57] Fabio Nobile and Christian Vergara. An effective fluid-structure interaction formulation for vascular dynamics by generalized Robin conditions. *SIAM Journal on Scientific Computing*, 30(2):731–763, 2008.

[58] Robert G. Owens and Timothy N. Phillips. *Computational rheology*, volume 2. World Scientific, 2002.

[59] Christopher C Paige and Michael A Saunders. LSQR: An algorithm for sparse linear equations and sparse least squares. *ACM Transactions on Mathematical Software*, 8(1):43–71, 1982.

[60] Charles S. Peskin. The immersed boundary method. *Acta Numerica*, 11:479–517, 2002.

[61] Alfio Quarteroni, Massimiliano Tuveri, and Alessandro Veneziani. Computational vascular fluid dynamics: problems, models and methods. *Computing and Visualization in Science*, 2(4):163–197, 2000.

[62] Alfio Quarteroni and Alberto Valli. *Domain decomposition methods for partial differential equations*. Number CMCS-BOOK-2009-019. Oxford University Press, 1999.

[63] Thomas Richter and Thomas Wick. Optimal control and parameter estimation for stationary fluid–structure interaction problems. *SIAM Journal on Scientific Computing*, 35(5):B1085–B1104, 2013.

[64] Kiril P. Selverov and Howard A. Stone. Peristaltically driven channel flows with applications toward micromixing. *Physics of Fluids*, 13(7):1837–1859, 2001.

[65] Roger Temam. *Navier–Stokes Equations. Theory and numerical analysis*. North-Holland Publishing Company, 1977.

[66] Thomas Wick. Fluid-structure interactions using different mesh motion techniques. *Computers & Structures*, 89(13):1456–1467, 2011.

[67] Thomas Wick. Solving monolithic fluid-structure interaction problems in arbitrary lagrangian eulerian coordinates with the deal.II library. *Archive of Numerical Software*, 1(1):1–19, 2013.

[68] Jinchao Xu and Kai Yang. Well-posedness and robust preconditioners for discretized fluid–structure interaction systems. *Computer Methods in Applied Mechanics and Engineering*, 2014.

[69] Eberhard Zeidler. *Nonlinear functional analysis: Part I.* Springer Verlag, 1985.